



UNIVERSITY OF LEEDS

PATH INTEGRAL TECHNIQUES FOR
CLASSICAL STOCHASTIC PROCESSES

Thomas Jacob Ward Honour

Submitted in accordance with the
requirements for the degree of
Doctor of Philosophy

School of Mathematics
University of Leeds

School of Mathematics

April 2023

The candidate confirms that the work submitted is his own and that appropriate credit has been given where reference has been made to the work of others.

This copy has been supplied on the understanding that it is copyright material and that no quotation from the thesis may be published without proper acknowledgement.

The right of Thomas Jacob Ward Honour to be identified as Author of this work has been asserted by him in accordance with the Copyright, Designs and Patents Act 1988.

The undertaking of this PhD has been a fantastic experience and would not have been possible without the support of a few important people.

Firstly, I would like to express my thanks to my supervisor, Dr Steve Fitzgerald, for his support in this journey over the past four years. His continuous advice and guidance throughout this project have kept my interest in this project at such a high level it has been a joy completing this PhD.

Secondly, to my co-supervisor, Professor Daniel Read, for his ideas and contributions throughout the past 4 years, and his invaluable contributions to the drafts of this work.

Massive thanks to my family for their continuous support and encouragement in this endeavour.

And finally, to my wife for your love and comfort throughout this remarkable journey. Being by my side whilst the world went crazy around us, keeping me grounded and reassured me that I am doing what I love. On to the next adventure.



At nonzero temperature, thermal fluctuations play a role in the behaviour of any physical, chemical, or biological system. The use of *stochastic processes* to model such systems dates back over 100 years, to the work of Einstein, Langevin, and Smoluchowski. Modern computer simulation techniques, in particular kinetic Monte Carlo, are built on these foundations, and a whole field of mathematical research has grown from these seeds.

Conventionally, two approaches are used in their study: 1) stochastic differential equations, where a random component is explicitly included in the forces acting on the system, and 2) deterministic partial differential equations for the system's probability density function. In this work, we will investigate a third, less widely known, approach: *path* or *functional* integrals [1] [2]. This technique expresses the probability density as a sum over system trajectories, with a statistical weight attached to each one.

Inspired by *semiclassical* quantum-mechanical path integrals, which allows certain quantities to be expressed in closed form as $\hbar \rightarrow 0$, we develop a weak noise approximate theory for classical stochastic processes. This reveals a remarkable correspondence between the most probable stochastic paths and Hamiltonian mechanics in an effective potential. We investigate several previously overlooked subtleties, such as the role played by the functional Jacobian, and the necessity of turning paths, to correctly treat the long-time limit.

Armed with these tools, we derive, for the first time, closed-form expressions for the first passage density in a one-dimensional stochastic system subject to a general, nontrivial potential, and investigate simple potentials in detail. We revisit the ubiquitous problem of fluctuation-driven escape over an energy barrier, and derive the full first passage density, where only the mean was previously available. The extension to higher dimensions is then briefly explored, with the simplest free diffusion results returned to demonstrate the technique's validity beyond one dimension.

Contents

List of Figures	xi
List of Tables	xv
1 Introduction	1
1.1 What is a stochastic process?	3
1.2 First Passage Times	12
1.2.1 Mean First Passage Time	21
2 Introduction to Path Integrals	26
2.1 An analytical path integral solution	30
2.1.1 Flat potential: $V(x) = 0$	47
2.1.2 Linear Potential: $V(x) = bx$	49
2.1.3 The long time limit	50
3 Numerical Solution using Path Integrals	56
3.1 The method	57
3.2 Reducing the computation time	63
3.2.1 Diagonalising the matrix	64
3.2.2 Only calculating nearest neighbours	65
3.3 Initial results	68
3.4 Further one-dimensional investigations	75
3.4.1 Finding a PDF for the initial position	75
3.4.2 Diffusion Constant	77
3.5 Two-dimensional numerical solution	79
4 The introduction of the Jacobian	85
5 The concept of the turning path	94
5.1 Using time to introduce the turn	95

5.2	The appearance of a second peak	98
5.3	Looking at the long time limit	102
6	The Harmonic Oscillator	109
6.1	The Eigenfunction expansion	110
6.2	Transformation and separation of variables	119
6.3	The WKB approximation	123
6.4	Using Path Integrals	126
7	The use of the Laplace Transform	138
7.1	Introduction of Boundary Conditions	144
8	First Passage Times	150
8.1	The flat potential	151
8.2	Linear potential	161
8.2.1	Two absorbing boundaries	161
8.2.2	A mixture of boundaries	164
8.3	General potential	173
8.4	A Barrier Escape problem	176
8.5	Numerical solution	183
8.5.1	Boundary conditions	183
8.5.2	Calculation of the flux at the boundaries	186
8.6	Moments of the FPT density	189
9	Multi Dimensional Path Integrals	194
9.1	Three-dimensional free diffusion	197
9.2	Three-dimensional Harmonic oscillator	202
	Conclusion	205
	Bibliography	209

List of Figures

1.1	A 1-D model of diffusion from random motion [37]	10
1.2	A diffusing particle in a given region B with boundary ∂B	12
1.3	FPT example system with two boundaries at the edge of the system for a generic potential $V(x)$	13
1.4	Idealised model of diffusion over a barrier	17
1.5	An example of the “shells” drawn around the particles, with which the FPT density is calculated to, with only particle 7 moving at the current timestep [48]	19
1.6	Comparison of a general FPT density and the exponential distribution with the same mean value	20
1.7	Domain graph for the integrals	24
2.1	A “practical” example of multiple gates path [1]	28
2.2	An example of the Potential $V(x)$ for a tilted double well vs the corresponding Ito prescription effective potential $\mathcal{V}(x) = -V(x)^2$	36
2.3	Showing an approximation of the complex potential on the left to the Harmonic potential on the right for x_i positions near the minimum at x_m	42
2.4	A path in the effective potential for a cubic potential, spending infinite time at the peaks of the effective potential, $H \rightarrow 0$	51
2.5	Path example on only the positive portion of the potential	52
2.6	Path example on only the negative portion of the potential	53
2.7	Paths in the effective potential, $\mathcal{V}(x)$, for the harmonic potential, graphically illustrating the issues that the paths have in reaching infinite time.	54
3.1	The linear approximation discretisation	57
3.2	Showing a few of the possibilities of paths between the initial and final position for two timesteps	59
3.3	n possible time segmentations with possible paths	60

3.4	A straight line approximation showing it can miss the potential barrier, not taking into account the crucial element of the system.	65
3.5	Comparison between the full probability density function, in blue —, overlain with the nearest neighbour probability, in black ·, showing no difference between the two results. $dt = 0.0005$, $dx = 0.01$, $D = 0.1$	67
3.6	Symmetric double well potential	69
3.7	The probability density function $P(X, T x_0)$ as a function of position. Snapshots taken at different times, (A) $T=0.08$, (B) $T=0.86$, (C) $T = 10.24$. $dt = 0.001$, $dx = 0.01$, $x_i = -1$, $D = 1$	70
3.8	Tilted double well potential	71
3.9	The probability density function $P(X, T x_0)$ as a function of position. Snapshots taken at different times, (A) $T=0.08$, (B) $T=0.86$, (C) $T = 14.80$. $dt = 0.001$, $dx = 0.05$, $x_i = -1$, $D = 1$	72
3.10	The probability density function as it evolves over time until equilibrium. With initial position $x_i = -2$ and a diffusion value, $dt = 0.001$, $dx = 0.05$, $D = 1$	73
3.11	PDF comparison to the Matlab PDE solver for small T , an intermediate T , and large T for the symmetric double well potential and the tilted double well potential	74
3.12	Probability density function of initial positions, in blue, over time, for a final position of $x_f = 2$. $dt = 0.001$, $dx = 0.01$ and $D = 1$	76
3.13	Probability density function of initial positions, in blue, over time, for a final position of $x_f = 0.75$. $dt = 0.001$, $dx = 0.01$ and $D = 1$	77
3.14	How the probability of moving from $x_i = -2$ to $x_f = 2$ changes as the diffusion increases for a tilted potential.	78
3.15	Probability density function over time for a flat potential, $dx = 0.1$, $dy = 0.1$, $dt = 0.0001$, $D = 0.01$	82
3.16	Probability density function over time for a sloped potential, $dx = 0.1$, $dy = 0.1$, $dt = 0.0607$ $D = 0.01$	83
4.1	Example path that portrays the unintuitive path of ending on a downhill slope for infinite time in both the potential, top in red, and effective potential, bottom in blue.	92
5.1	An example of the maximum direct path, if H is greater than this critical value, a turning path must exist	95
5.2	The Ito effective potential $\mathcal{V} = -V'(x)^2$, in green —, vs the Stratonovich effective potential $\mathcal{V} = -V'(x)^2 + 2DV''(x)$, in blue —, with the corresponding titled double well potential, in red —.	99

5.3	Probability density function at timesteps either side of the critical time, showing the beginning of the appearance of the second peak, only once the critical time has passed.	100
5.4	Probability density function at timesteps either side of the critical time, showing the beginning of the appearance of the second peak, only once the critical time has passed.	101
5.5	A direct path example for $x_i < 0 < x_f$ in the harmonic potential . . .	103
5.6	The direct path (black) and turning path extra segments (purple), for $x_i < x_f < 0$ in the harmonic potential	105
6.1	Graphs showing the elements for the path integral formalism over time with the time constraint imposed, detailing the change between the direct path and the turning path at the critical time.	132
7.1	Bromwich Contour to calculate the inverse Laplace transform [97], deformed around the poles on the real axis.	142
8.1	The four “base” paths for this flat potential system.	154
8.2	PDF at different time steps for the flat potential with double absorbing boundaries, $x_i = 0.5$, $D = 0.25$	155
8.3	FPT density for the double absorbing boundary in the flat potential, for $D = 0.25$	158
8.4	PDF at different timesteps for a sloped potential, $V(x) = \frac{x}{10}$ with two absorbing boundaries	162
8.5	FPT density for the sloped potential, $V(x) = \frac{x}{10}$, with two absorbing boundaries, $D = 0.25$	163
8.6	The “base” paths for the linear potential	168
8.7	PDF over time for the sloped potential $V = 0.1x$ with diffusion $D = 0.1$ and mixed boundaries, reflecting on the left, absorbing on the right	169
8.8	FPT density for the sloped potential $y = x$ with mixed boundaries, meaning only one curve with the one absorbing barrier, $D = 0.1$	172
8.9	A generic barrier escape potential	176
8.10	An example path, that travels to the peak multiple times before crossing	181
8.11	Kramers Exponential Distribution, in blue, vs the path integral FPT density, in red, with $D = 1$ and $V(x) = -\frac{x^3}{3} + x^2$	182
8.12	Comparison between the natural logarithm of the FPT density and the Kramers exponential approximation, with $D = 1$	182
8.13	The probability density function for a tilted potential for $T = 2.5$, showing the probability being 0 outside the boundaries.	184

8.14 The probability density function for a tilted potential for $T = 10$, showing the probability being 0 outside the boundaries. 184

8.15 A surface plot of the f_{ij} matrix for a tilted potential for $T = 6$, showing the hard boundaries imposed cuts forces 0 outside the boundaries. . . 185

8.16 Matlab partial differential equation solver vs the numerical path integral with hard boundary conditions, showing the comparable nature of the numerical path integral technique. 186

8.17 The flux over time, calculated using the gradient of the probabilities and the change in the cumulative density function over time. 189

8.18 FPT density comparison between the exponential distribution and the full FPT solution for a sloped potential with a mixture of boundaries. Showing the discrepancy at short time, with the path integral technique providing a fuller solution. 190

8.19 Comparison between second and third moments for the exponential distribution (*) and the full FPT solution (-) 192

9.1 Two paths from 0 to $r \in B$: one direct and the other bouncing off R at r' , with a mirror direct path from B' 201

List of Tables

- 3.1 Table showing the effect of reducing nearest neighbours on the normalisation of the probability curve - $dt = 0.0005$, $dx = 0.01$, $D = 0.1$. 66

Chapter 1

Introduction

In this chapter, we will begin the journey of finding a semi-closed form solution for a stochastic process using *path integrals*. To begin with, we will explore what a stochastic process is and how it relates to the specific equation we will be solving throughout this work, the *Smoluchowski equation*. This will entail deriving the Smoluchowski equation from the stochastic differential equation and then discussing some possible applications of the *first passage time density* and *mean first passage time*, deriving the known equations for both of these quantities. Within this, we will explore some of the current techniques and discuss some of the limitations that occur and the possibility of the path integral in tackling these issues.

The use of stochastic processes is integral to research in many areas of science because of the range of systems they can model. Due to the random variable elements of stochastic processes, they can model almost any natural phenomenon with a random nature in its evolution [3][4]. This can range from bacterial growth [5] to particle movement through materials [6], from financial systems [7][8] to population dynamics [9], even including telecommunications [10]. The range of applications means that this area of mathematics has been widely researched, and several techniques have been formulated to tackle these problems over the years. These techniques can be used for a variety of systems, for example, the Bernoulli process [11], used for binary systems, such as the flipping of a coin; Brownian motion [12], used for particles in a medium; or a Poisson process [13], used for random events modelled in time. This type of mathematics has rapidly come to the forefront in recent years due to the increase in demand for knowing how these processes act over time and the range of possible systems to which this technique can be applied.

A second method, classical mechanics, is still used in many areas of science and engineering, for example, using Newton's equations of motion to determine the evolution of a system, such as the movement of celestial models, which also exposes more applied and sophisticated mathematics theories, Hamiltonian systems [14], Lagrangians [15], and Hamilton-Jacobi equations [16], all of which govern the movement of physical systems due to their equations of motion.

The third major dynamical system paradigm is Quantum dynamics, which describes systems that play by an entirely different set of rules in quantum mechanics but have a basis in classical mechanics, for example, Feynman's path integral formulation which uses classical actions and Lagrangian mechanics [17][18].

An excellent quote from Ge and Qian's paper "Analytical mechanics in Stochastic dynamics" [19] ties all three together:

“Classical dynamics has trajectories but only singular distributions; quantum dynamics has distributions but no trajectories due to Heisenberg’s uncertainty principle; stochastic requires both perspectives.”

In this work, we will combine elements from all three areas of dynamics in an attempt to solve the overarching problem of formulating a semi-analytical probability density function (PDF) for a stochastic process. First, we explore some existing mathematical techniques used to solve a particular type of stochastic process which is applicable to particles diffusing under the influence of a given potential and explain some of the limitations that occur due to computational constraints. We will also briefly describe techniques that are used to work around this limitation, for example, forward flux sampling [20] [21]. We will then introduce the use of path integral techniques from quantum mechanics [22] and find a remarkable correspondence between stochastic dynamics in a potential to a classical Hamiltonian system with an effective potential to find a semi-analytical solution which may be able to provide more complete understanding for both probability and first passage time densities of the system. We will find these densities both numerically and analytically and discuss how this path integral technique could solve some of the current problems of computational techniques arising from computational limits in both power and time [23] [24].

1.1 What is a stochastic process?

First, we must define a stochastic process and the mathematics governing its properties and uses. There are many different ways to model a stochastic process, and in this section, we will concentrate on two standard methods. The first is a stochastic differential equation (SDE) called the *Langevin equation* [25]. The second is a partial differential equation (PDE) called the *Fokker-Planck equation* [26].

A SDE is a differential equation with a stochastic force, a term with a random element, allowing the SDE to model random phenomena. Typically for the Langevin equation, this random element is a Gaussian white noise variable, z , which is described by a probability density function,

$$P(z) = \frac{1}{\sigma\sqrt{2\pi}} \exp\left(-\frac{(z-\mu)^2}{2\sigma^2}\right),$$

$$E[z] = \mu,$$

$$SD[z] = \sigma,$$

where $E[z]$ is the mean and $SD[z]$ is the standard deviation. One of the famous realisations of the Langevin equation is the use for Brownian motion, the random motion of particles in a fluid due to collisions with the fluids particles [1]. To derive the Langevin equation, the first step is to appeal to known classical dynamics representations, i.e. Newton's Law, and then introduce a random element to the system to move the derivation into stochastic dynamics. This is an example of the crossover between classical and stochastic dynamics and how easily they can be used to describe similar systems. To find the governing Langevin equation, we begin by writing the classical mechanics Newton's equation, $F = ma$, as a sum of forces,

$$m\dot{v} = F(t) + f(t), \tag{1.1}$$

where $F(t)$ represents the forces due to some external field, for example, a potential gradient, and $f(t)$ is the force produced by collisions of fluid particles against the particle of interest. What was seen experimentally in the system is that there are rapid fluctuations in the particle's velocity v , which comes from the random contribution of the impacts of the fluid particle occurring when the mass of the particle of interest is much larger than the fluid particles. These random fluctuations that are experimentally observed mean that the dynamical system can be described using a stochastic equation by writing the collision force $f(t)$ as proportional to the velocity and including a random element to account for the fluctuations through a

fluid. This means that we can write,

$$\frac{1}{m}f(t) = -\gamma v + \xi(t), \quad (1.2)$$

where γ is the friction coefficient of the fluid which opposes the particle's motion, hence the minus sign. $\xi(t)$ is the white noise term that governs the random contributions of the force, which averages to zero, $E[\xi(t)] = 0$, and is required to be independent of previous time values, with the correlation function

$$\langle \xi(t)\xi(t') \rangle = 2D\delta(t - t').$$

$\langle \dots \rangle$ is defined as the average over the fluctuations of the noise. The use of the Dirac delta function means that there is no correlation between timesteps and this is called uncorrelated noise, meaning the function has no memory of previous timesteps normally applied to Markov processes [27]. Some systems have correlated noise, meaning the variance of the noise function has some memory of previous timesteps with work having been done with correlated noise for calculating escape rates in the weak-noise limit [28][29]. In this work, we will stick with uncorrelated noise keeping the timestep independent. Combining (1.1) and (1.2) without an external force, $F(t) = 0$, gives

$$\dot{v} = -\gamma v + \xi(t),$$

the simplest stochastic differential equation. We can go one step more complicated by reintroducing the external field and remembering that the velocity is the derivative of position; we have a pair of equations

$$\dot{x} = v, \quad (1.3)$$

$$\dot{v} = \frac{1}{m}F(x) - \gamma v + \xi(t). \quad (1.4)$$

Differentiating (1.3) and substituting into (1.4) we arrive at a second order differential equation,

$$\ddot{x} = \frac{1}{m}F(x) - \gamma\dot{x} + \xi(t). \quad (1.5)$$

Restricting the system to high friction, γ large, which means particles are instantly at terminal velocity, $\ddot{x} \approx 0$, as the friction in the system dominates $|\gamma\dot{x}| \gg |\ddot{x}|$. This is an observed phenomenon and an assumption of a Markovian process, because in a highly viscous fluid inertia will be lost instantaneously, an approximation that we can make on the timescales that we are interested in, and that means there is no acceleration on the particle [19]. We can rewrite equation (1.5) as

$$\dot{x} = -\frac{d}{dx}V(x) + \xi(t), \quad (1.6)$$

where $\frac{d}{dx}V(x) = -F(x)$, and m and γ are constants that can be set equal to 1 without loss of generality. This final equation (1.6) is the Langevin equation corresponding to the problem of diffusion in a potential field $V(x)$, the specific system that we will be tackling throughout this work.

The actual specific problem we will investigate begins with a Fokker-Planck (F-P) equation which requires derivation from the Langevin equation (1.6) that we have just found. A Fokker-Planck equation is a deterministic partial differential equation as opposed to a stochastic differential equation, that will also describe the evolution of a particle in a given potential but explicitly describes the time evolution of the probability of position of the particle under the influence of a given potential and diffusion value and removes the dependency of the random element $\xi(t)$. To find this F-P equation, we begin with a general version of the Langevin equation (1.6), using $\dot{x} = \frac{dx}{dt}$ we can rearrange to,

$$dx = \mu(x)dt + \sigma(x)dW(t), \quad (1.7)$$

where $dW = \xi(t)dt$ is a *Wiener process*, a tool used in stochastic calculus to relate

the given noise term to a differential, and dW is the increment of a Wiener process. It is a process that holds the random nature of the stochastic process and is famously used for Brownian motion, with its independent increments detailing the random nature of movement very well. $\mu(x)$ in (1.7) is defined as the drift velocity, here it is related to the gradient of the potential, and $\sigma(x)$ is the diffusivity term.

Several useful properties are used in Brownian motion, but here we will use it for the fact that in one dimension it follows a normal distribution with mean $E[W(t)] = 0$ and variance $\text{Var}(W(t)) = t$ [30]. In order to find the Fokker-Planck equation we can define a general form for a function by using stochastic calculus rules, Ito's Lemma [31]. We begin with the understanding that we are describing a system that obeys the Langevin equation (1.7). If we have a generic function, $f(x, t)$, that is twice differentiable it will have the following Taylor expansion,

$$df = \frac{\partial f}{\partial t} dt + \frac{\partial f}{\partial x} dx + \frac{1}{2} \frac{\partial^2 f}{\partial x^2} dx^2 + \mathcal{O}(t^2) + \mathcal{O}(x^3)$$

We do not need any higher-order terms as they become zero when we will take a limit in the next steps. Substituting in the Langevin equation for dx (1.7) we find,

$$df = \frac{\partial f}{\partial t} dt + \frac{\partial f}{\partial x} (\mu dt + \sigma dW) + \frac{1}{2} \frac{\partial^2 f}{\partial x^2} (\mu^2 dt^2 + 2\mu\sigma dt dW + \sigma^2 dW^2).$$

We wish to have the most continuous system possible in time, meaning we find the limit $dt \rightarrow 0$ and only concentrate on the most dominant terms, the ones proportional to dt . One of the characteristics of the Wiener process we can use is that dW^2 is proportional to dt . Collecting like terms, and replacing dW^2 for dt we obtain Ito's Lemma [31],

$$df = \left(\frac{\partial f}{\partial t} + \mu \frac{\partial f}{\partial x} + \frac{\sigma^2}{2} \frac{\partial^2 f}{\partial x^2} \right) dt + \sigma \frac{\partial f}{\partial x} dW. \quad (1.8)$$

This is an example of the extra mathematics that arises from using stochastic dynamics, as we gain an additional term from dW^2 than we would in normal calculus because of the choice of using the Ito prescription in this derivation. There is also the

Stratonovich prescription which does not have the additional term and preserves the normal calculus chain rule but has differing properties elsewhere. For the majority of this work, we will be consistent and work with the Ito prescription of stochastic integrals. We can use this Lemma and other properties of the Wiener process W to find the F-P equation. First of all, as f is an arbitrary function, we can choose to drop the time dependence of the function, $f(x, t) = f(x)$, meaning that $\frac{\partial f}{\partial t} = 0$. Next, we will take the average value of both sides of the equation. This step is taken to introduce a probability density function (PDF) into the representation by introducing the average value of a density [32] defined as;

$$\langle G(x) \rangle = \int_{-\infty}^{\infty} G(x)P(x, t)dx.$$

Taking these steps with (1.8) we end up with the equation, remembering $dW = \xi dt$,

$$\left\langle \frac{df}{dt} \right\rangle = \left\langle \left[\mu \frac{\partial f}{\partial x} + \frac{\sigma^2}{2} \frac{\partial^2 f}{\partial x^2} \right] \right\rangle + \left\langle \sigma \frac{\partial f}{\partial x} \xi \right\rangle$$

Using the fact that, $\langle \xi \rangle = 0$

$$\frac{d}{dt} \int_{-\infty}^{\infty} f(x)P(x, t)dx = \int_{-\infty}^{\infty} \left[\mu(x) \frac{\partial f}{\partial x} + \frac{\sigma^2}{2} \frac{\partial^2 f}{\partial x^2} \right] P(x, t)dx.$$

We can calculate a couple of lines of integration by parts to find a usable form, using the fact that there are boundary conditions for the probability density function. The conditions are that at $\pm\infty$ the probability equals zero, $P(x \rightarrow \pm\infty, t) = 0$. This condition will be relaxed in later chapters when we begin to introduce hard boundaries to confine the potential when looking at particular systems. The infinite boundary conditions mean that only the integral terms are left during integration by parts as all the evaluations that occur at the boundaries equal zero. This leaves,

$$\int_{-\infty}^{\infty} f(x) \frac{dP(x, t)}{dt} dx = \int_{-\infty}^{\infty} f(x) \frac{\partial}{\partial x} \left[-\mu(x)P(x, t) + \frac{\partial}{\partial x} \left(\frac{\sigma(x)^2}{2} P(x, t) \right) \right] dx.$$

As $f(x)$ is an arbitrary function this equation holds for all $f(x)$, meaning we can

extract the general form for the Fokker-Planck equation,

$$\frac{\partial P}{\partial t} = \frac{\partial}{\partial x} \left[-\mu(x)P(x, t) + \frac{\partial}{\partial x} \left(\frac{\sigma(x)^2}{2} P(x, t) \right) \right]. \quad (1.9)$$

So, we have found the general over-damped Fokker-Planck equation, but to relate it to our particular area of interest, we do one more transformation to the Smoluchowski equation [33] by relating μ and σ to a potential and diffusivity function,

$$\begin{aligned} \mu(x) &= \frac{\partial D(x)}{\partial x} - \frac{dV}{dx}, \\ \sigma(x) &= \sqrt{2D(x)}, \\ \Rightarrow \frac{\partial P}{\partial t} &= \frac{\partial}{\partial x} \left[\frac{dV}{dx} P + D(x) \frac{\partial P}{\partial x} \right]. \end{aligned}$$

The diffusivity $D(x)$ is the function that governs the diffusion effect of the particle through the potential $V(x)$. The diffusion value is a measure of the noise for a given system, and in this work, it is non-specific to a particular system as we apply the techniques to generic potentials. For physical systems, it may be that D is related to the temperature in a thermal system through fluctuation-dissipation theory [34] [35] $D = \mu k_B T$, or it may be related to the volatility of stocks in a financial system. For the duration of this work, we will be dealing with a constant diffusion value so we have the form of the Smoluchowski equation,

$$\frac{\partial P(x, t)}{\partial t} = \frac{\partial}{\partial x} \left[\frac{dV(x)}{dx} P(x, t) + D \frac{\partial P(x, t)}{\partial x} \right]. \quad (1.10)$$

$$\text{In 3-D} \quad \frac{\partial P(\underline{x}, t)}{\partial t} = \nabla \cdot [\nabla V(\underline{x}) P(\underline{x}, t) + D \nabla P(\underline{x}, t)] \quad (1.11)$$

This is the specific partial differential equation that we will explore throughout this work and investigate the possibility of using path integral techniques to solve for the probability density function in a given potential $V(x)$ with diffusion value D . There is a need in many areas of science to investigate the time evolution of the

probability of the position of a given particle of interest. Under certain conditions, the Smoluchowski equation will return simpler equations that are used in specific areas.

In the case that the potential does not change, $V(x) = 0 \Rightarrow \frac{dV(x)}{dx} = 0$, we return the diffusion equation,

$$\frac{\partial P}{\partial t} = D \frac{\partial^2 P}{\partial x^2}.$$

This famous equation is used in various areas, specifically in physics, where it relates to the random movements of particles under Brownian motion with no external force. It also is closely related to the heat equation [36], a PDE in which instead of D for diffusion, we have a constant proportional to the thermal diffusivity of a material, κ . The heat equation then describes the transference of heat over time in a material.

We can show how this diffusion equation can come from first principle arguments instead of using the Smoluchowski equation to highlight the dynamics of what is happening in a flat potential system [37]. If we consider a region of space containing particles at some concentration $c(x, t)$ where $c(x, t)$ is the number of particles per unit length, we can discretise the space into boxes of width Δx , the number of particles in each box is $c(x, t)\Delta x$, figure (1.1).

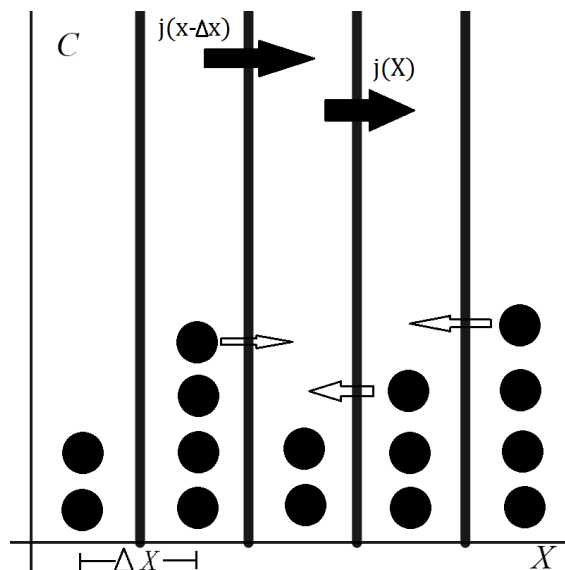


Figure 1.1: A 1-D model of diffusion from random motion [37]

Defining the rule of motion for each particle, we also discretise time into steps Δt . At each time step, we suppose that a fraction of the particles ϵ hop into a neighbouring box ($\frac{\epsilon}{2}$ jump left, $\frac{\epsilon}{2}$ jump right). We now obtain the diffusive particle current $j_D(x, t)$, defined as the net number of particles crossing a boundary at position x per unit of time. Finding this current is done by summing the number of particles jumping left to right minus the number of particles jumping right to the left,

$$j_D(x, t)\Delta t = \left[c\left(x - \frac{\Delta x}{2}, t\right) - c\left(x + \frac{\Delta x}{2}, t\right) \right] \Delta x \frac{\epsilon}{2},$$

which in the limit of small Δx becomes,

$$j_D(x, t) = -D \frac{\partial c}{\partial x}, \quad (1.12)$$

which is Fick's law of diffusion, with $D = \frac{\epsilon \Delta x^2}{2\Delta t}$ [38]. Next, we want to find an expression for how the concentration changes over time, which is the sum of the concentration in the prior timestep, plus the net number flowing in from the left, minus the net number flowing in from the right;

$$\begin{aligned} c(x, t + \Delta t)\Delta x &= c(x, t)\Delta x + j_D\left(x - \frac{\Delta x}{2}, t\right)\Delta t - j_D\left(x + \frac{\Delta x}{2}, t\right)\Delta t \\ \Rightarrow \frac{c(x, t + \Delta t) - c(x, t)}{\Delta t} &= -\frac{j_D\left(x + \frac{\Delta x}{2}, t\right) - j_D\left(x - \frac{\Delta x}{2}, t\right)}{\Delta x}. \end{aligned}$$

In the small Δx and Δt limit this becomes the continuity equation, and when combined with (1.12) becomes,

$$\begin{aligned} \frac{\partial c}{\partial t} &= -\frac{\partial j_D}{\partial x}, \\ (1.12) \Rightarrow \frac{\partial c}{\partial t} &= D \frac{\partial^2 c}{\partial x^2} \end{aligned}$$

1.2 First Passage Times

Alongside the probability density function, another primarily used quantity in the scientific investigation of stochastic systems and the other major investigation of this work is the first passage time density (FPT). The FPT density is a probability density function describing the probability for the interested “particle” of the system to interact with a boundary for the first time at time t [39]. For example, as shown in figure 1.2, the FPT density $f(t)$ will be the probability density function in time t of when a diffusing particle will diffuse through region B and touch the boundary ∂B for the first time.

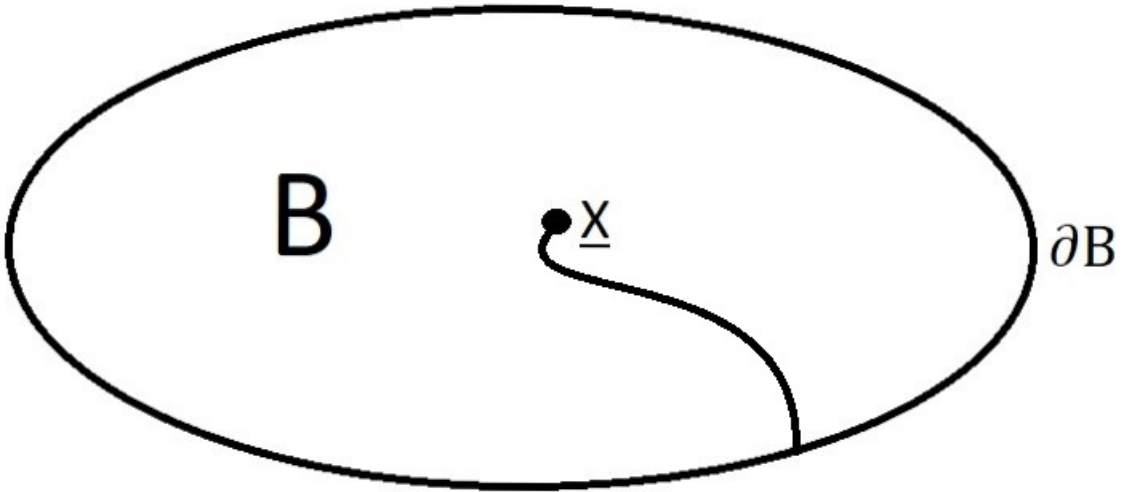


Figure 1.2: A diffusing particle in a given region B with boundary ∂B

To find the FPT density, we begin with a generic system that has a probability density function that will solve the multidimensional Smoluchowski equation with the given boundary condition,

$$\dot{P} = \nabla \cdot [\nabla V(x)P + D\nabla P]; \quad P(\underline{x} \in \partial B) = 0.$$

The boundary condition at ∂B exists as particles are removed from the system as soon as they interact with the boundary. To calculate the first passage time density,

we measure the total flux out of the region B over the barrier ∂B , i.e. how much has escaped out of the system at a given time,

$$f(t|\underline{x}, 0) = -D \int_{\partial B} \nabla P \cdot \hat{n} dS. \quad (1.13)$$

In a one-dimensional case with a system of two absorbing boundaries, like the one shown in figure 1.3, with relevant boundary conditions, $P(x = a) = 0 = P(x = b)$ we can derive the first passage time density from the survival probability of the system.

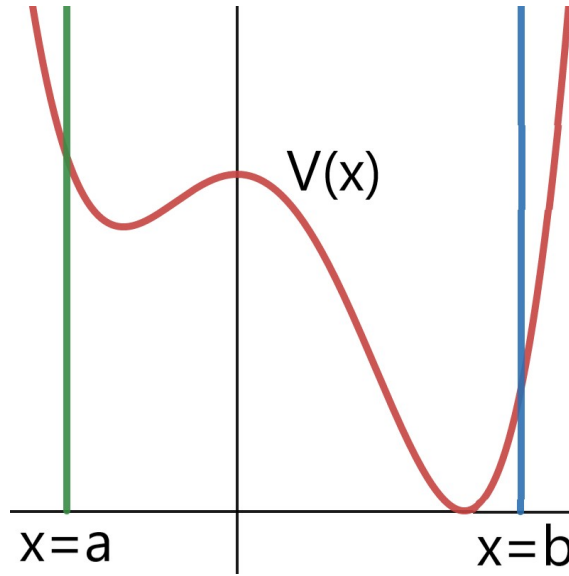


Figure 1.3: FPT example system with two boundaries at the edge of the system for a generic potential $V(x)$

The survival probability (SP) is the probability that the particle has remained within the boundaries and is given by,

$$SP(t) = \int_a^b P(x, t) dx.$$

It is related to the FPT density by the fact that the FPT density describes the probability that the particle has reached the absorption point between time t and $t + dt$, so $f(t)dt = SP(t) - SP(t + dt)$. Giving the relationship,

$$f(t) = -\frac{\partial SP(t)}{\partial t},$$

which by using the Smoluchowski equation, we can find the explicit FPT density.

$$\begin{aligned}
 f(t) &= - \int_a^b \frac{\partial P(x, t)}{\partial t} dx \\
 &= - \int_a^b \frac{\partial}{\partial x} \left[V'(x)P(x, t) + D \frac{\partial P(x, t)}{\partial x} \right] \\
 &= - \left[V'(x)P(x, t) + D \frac{\partial P(x, t)}{\partial x} \right] \Big|_a^b
 \end{aligned}$$

Then using the boundary conditions that the probability vanishes on the boundary means the first term in the bracket is 0, leaving us with the FPT density,

$$\begin{aligned}
 f(t) &= -D P'(x, t) \Big|_a^b, \\
 f(t) &= -D [P'(x = b) - P'(x = a)]. \tag{1.14}
 \end{aligned}$$

Equation (1.13) is the most common form of the FPT density and will be the representation that we will continue to use in this work as it has the most versatility for various systems, and will return (1.14) in one dimension. The majority of systems have some form of barrier that is being investigated, so a formalism dependent on the barriers is the most useful for our purposes.

We can also find a second representation for the probability that the system first reaches \underline{x} at time t , given that it started at 0 at time 0. There are no restrictions on the path the system may take, other than it may not visit \underline{x} before t . The FPT density must satisfy,

$$P(\underline{x}, t|0, 0) = \int_0^t f(\underline{x}, t|0, \tau) P(0, \tau|0, 0) d\tau, \tag{1.15}$$

where the transition probability satisfies the Smoluchowski equation

$$\frac{\partial P}{\partial t} = \nabla \cdot (P \nabla V + D \nabla P); \quad P(\underline{x}, 0) = \delta(\underline{x} - \underline{x}_0); \quad P(\underline{x}, t) \rightarrow 0 \text{ as } |\underline{x}| \rightarrow \infty.$$

What this representation means is that the probability of starting from position 0 at time 0 and arriving at \underline{x} in time t , $P(\underline{x}, t|0, 0)$, is the integral over all time of the probability of not moving for a time τ , $P(0, \tau|0, 0)$, then reaching the final position \underline{x} for the first time in the remaining time $t - \tau$, remembering that $f(t)$ is itself a PDF density. This can also be written more concisely by assuming that the stochastic process is stationary [40], meaning that for an unconditional probability, it is unaffected by a shift in time, so equation (1.15) becomes

$$P(\underline{x}, t) = \int_0^t f(\underline{x}, t - \tau)P(0, \tau)d\tau. \quad (1.16)$$

However, we are after a representation of the FPT density, so we wish to remove the integral and rearrange it to find $f(\underline{x}, t)$. To do this, we use Laplace transforms to find the representation for the FPT density by using the convolution identity [41], leading to a Laplace domain form for the FPT density

$$\begin{aligned} \bar{P}(\underline{x}; s) &= \bar{f}(\underline{x}; s)\bar{P}(0; s) \\ \bar{f}(\underline{x}; s) &= \frac{\bar{P}(\underline{x}; s)}{\bar{P}(0; s)}. \end{aligned} \quad (1.17)$$

Where \bar{P} is the Laplace transformed P with Laplace parameter s . For a single exit point x in one dimension, the two definitions (1.13) and (1.16) are equivalent as the system cannot “go around” the final position x , but in all other cases, they differ. The two definitions have different applications, with (1.16) applying to situations concerning the time taken for a system to find a certain point and (1.13) in situations concerning escape from a specific region. For both, we require a solution to the Smoluchowski equation, which we will find the approximation in the weak-noise limit in this work. Primarily we are interested in a system in which escape from a region is the interesting dynamics, meaning that we concentrate on (1.13) for the duration of this work.

The first representation, equations (1.13) and (1.14), is what is widely used in various fields of science to find when a system triggers an important event for the first time and provides essential information about that system. These systems and the knowledge of the FPT density are in all areas and for a variety of reasons, for example:

- In finance, you may want to know when a stock price might reach a certain price for the first time to know when best to exercise an option to sell or buy [42][43]
- In chemical dynamics, the knowledge of knowing when reactants may reach a certain energy which activates a reaction can be useful when setting up experiments to capture the resultant products [44]
- In material science, the movement of defects through a solid-state material and when they may interact with each other for the first time, possibly gaining knowledge in how long materials may last for under certain strains [45]
- In neuroscience, with integrate-and-fire models for neurons and when they may fire for the first time after a certain voltage is reached, meaning the time when an event occurs in the body can be approximated [46]
- Or reaction-diffusion systems where particles diffuse independently through a zero potential and interact with each other when they make contact, whether coalescing or annihilating [47] [48]

We can explore a couple of the more common techniques commonly used to calculate an FPT density and also look at why there are issues with these techniques in certain situations and then discuss how the path integral approach may be able to provide some missing information or help speed up numerical simulations.

First is the standard idealised model for many systems, diffusion over a potential barrier, figure 1.4 [49] [50]. In this system, we have a group of particles that begin in a potential well and are near equilibrium. The particles then make independent attempts to cross over the barrier into the other potential well. Independent because the assumption made is that the system does not remember previous tries, so the probability density can become unconditional on previous attempts as the process is Markovian in nature.

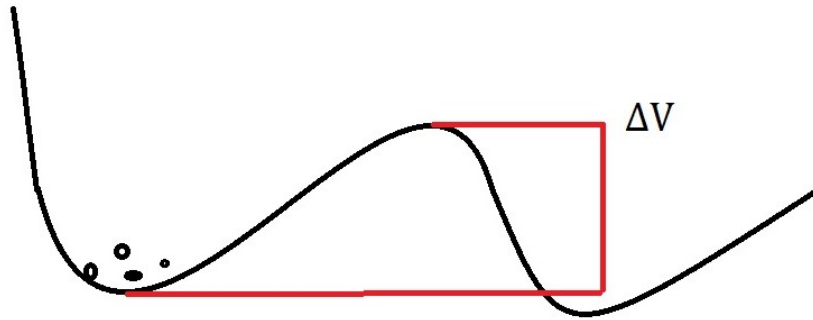


Figure 1.4: Idealised model of diffusion over a barrier

What is calculated is the rate of the system, Γ , which comes from the attempt frequency A of the attempts made by the particles to cross the barrier and the escape probability exponential, called an Arrhenius equation, [51]

$$\Gamma = A \exp\left(-\frac{\Delta V}{kT}\right),$$

where k is the Boltzmann constant and T is the temperature for the system. This result is based on the Poisson process, with wait times exponentially distributed and describes the fraction of particles that make it over the barrier with each attempt. This rate value can then be used in Monte Carlo (MC) methods to simulate particles moving over potential barriers, with the likelihood of an attempt succeeding depending on the rate. This exponential approximation means that only the mean or long-time limit of the FPT density is used to calculate the rate of the system, leading to much information about what happens at short time being discarded by the FPT density curve, along with not being able to model non-equilibrated sys-

tems correctly. See later in section 8.4 for a fuller comparison between Kramer’s rate approximation and a full FPT density from path integrals.

Further, the assumptions made may only hold for some systems, and if, for example, the system has multiple potential barriers the calculations may work for one of the barriers and not the others. This is called the “small-barrier” problem, where due to the MC algorithm being iterated with respect to rates, the barriers with the higher rates will always be preferential. These higher rates will be where the potential difference between the bottom and the top of the barrier is the smallest because of the exponential relationship. This can result in larger barriers being missed, and in a particular system, the largest barrier is the most interesting one. In this work, we will hopefully show that this is a potential advantage of the path integral technique that will be introduced. In a system with multiple peaks and troughs in the potential, for example, a crystal structure, there would have to be multiple Monte Carlo simulations for each potential barrier, with each simulation having further assumptions and issues with the event occurring in a computationally allowed timeframe and with the “small-barrier” issue. The path integral technique, however, could be quicker as we will see that it will be possible to incorporate all the energy wells into a single potential and allow the larger barriers to be taken into account as if in the timeframe, the largest barrier is the most likely the path integral should pick this up [52].

Another issue can occur alongside the “small-barrier” issue when there are multiple particles in a potential with multiple wells. For this system, what is being looked for is when two particles come close enough together to interact with each other to have an interesting reaction. The issue lies in systems where the density of particles is so low that the particles take too many hops over a number of potential barriers to find each other, and much of the computational work is wasted with particles exploring blank space, and the interesting reactions occur very infrequently. One advancement to help combat this issue is given in a paper by Ooppelstrup and colleagues [48].

This technique uses the whole first passage time density instead of just the mean first passage time or rate to evolve a system of multiple particles through time, with all the movements assumed to occur at equilibrium. It is typically applied to systems that evolve through collisions among random walkers or “reaction-diffusion” systems, and at present, is only valid for a zero potential. The system is set up with each particle having a “protective shell”, as shown in figure 1.5. The arrival time

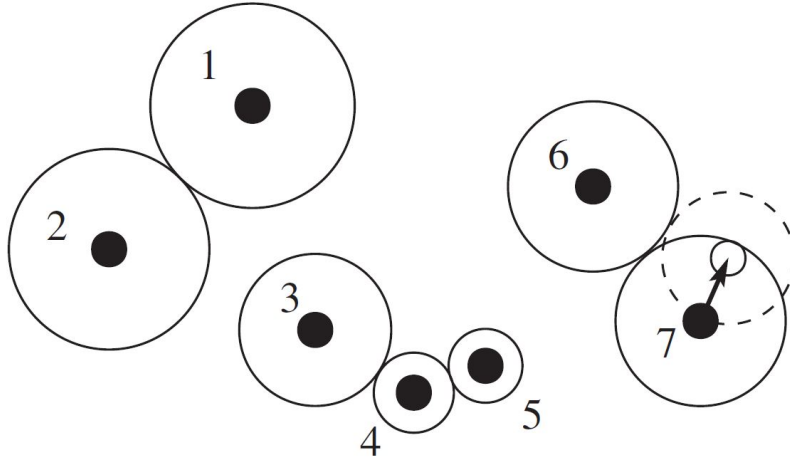


Figure 1.5: An example of the “shells” drawn around the particles, with which the FPT density is calculated to, with only particle 7 moving at the current timestep [48]

at the protective shell for all particles is then calculated based on a first passage time density function for free diffusion which is calculable for a system with no potential. The particle with the shortest time, in this case particle 7, is then the only one that is moved and the system evolves and the shells are redrawn around particle 7. This negates the need to move all the particles for each timestep and reduces the computational requirement, increasing the applications of the technique. However, as with diffusion over the barrier, some assumptions may only hold for some situations. In this kinetic Monte Carlo (kMC) technique, the FPT is assumed to follow an exponential distribution, where τ is the mean FPT value, the inverse of the rate,

$$f(t) = \Gamma e^{-\Gamma t}; \quad \Gamma = \frac{1}{\tau}.$$

This FPT density approximation does agree with the known shape of a density curve in the long time limit, $T \rightarrow \infty$, as both will tend to 0 but does not agree at

short times, as shown in figure (1.6). The short-time disagreement comes from the fact that the mode of the exponential distribution is zero, whereas the short-time limit of an FPT density is itself zero. This is because, at short times, you would expect particles to have no time to travel to the boundary, meaning $\lim_{t \rightarrow 0} f(t) = 0$. Typically the exponential distribution is a good approximation and can be used in a wide variety of FPT applications as equilibrium is an assumption made it is therefore valid in the long-time limit when $T \rightarrow \infty$; it is just the short-time limit which disagrees with the known shape of an FPT density curve. This disagreement may be negligible for specific systems or never come into question as the reactions all happen on a long enough time limit that it does not produce a large enough error to be significant. For the purpose of figure (1.6), it was manufactured to show a considerable divergence at a short time to highlight the possibility of disagreement.

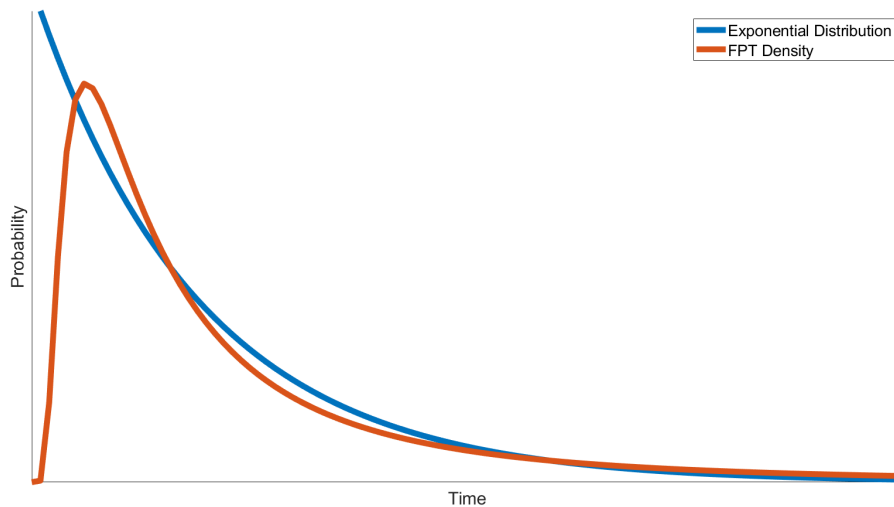


Figure 1.6: Comparison of a general FPT density and the exponential distribution with the same mean value

This is a possible advantage of the path integral technique to find a fuller description of the FPT density negating the need for an approximation at all, or only the need for a weak-noise approximation, along with the ability to allow the calculation of non-equilibrated systems. The possibility of being able to calculate the full FPT density for a non-zero potential is another path integral improvement.

These are a couple of the significant limitations of using current FPT density techniques, namely computational limits of running the simulation long enough for something to happen or that assumptions for one system may not hold for all. The hope for the path integral that we will explore throughout this work is that there will be the introduction of the full FPT density, see chapter 8, which will provide more information for all times and also allow a generalisation to non-zero potentials in multiple dimensions. We will also find a closed-form solution in a semi-analytical approximation for more complete information about the given system.

1.2.1 Mean First Passage Time

The mean first passage time is a useful result from the FPT density that provides important information about a system. This gives the mean time that an event will occur and can be derived from either the first passage time or first principles. This value is used in the kMC simulations, τ , as the inverse of the transition rate, Γ . Here we will derive the value from first principles following lecture notes from an Advanced Entropy course [37] by solving the Smoluchowski equation directly, but with an extra element to incorporate the effect of injecting particles at the position $x = x_0$ at a rate r , this injection will add an additional term to the Smoluchowski equation, $r\delta(x - x_0)$. We impose a boundary condition at $x = b$ as an absorbing barrier $P(x = b) = 0$, where particles are removed from the system, and then allow the system to reach a steady state and calculate the number of particles in the system n allowing the calculation of the mean FPT, $\tau = \frac{n}{r}$. We begin with the Smoluchowski equation with the relevant initial and boundary condition,

$$\frac{\partial P}{\partial t} = \frac{\partial}{\partial x} [V'(x)P + DP'(x)] + r\delta(x - x_0), \quad P(x = b) = 0.$$

If we allow the system to reach a steady state, equilibrium $\frac{\partial P}{\partial t} = 0$, then we can find the number of particles within the system

$$n = \int_a^b P(x)dx, \tag{1.18}$$

where a is a reflecting barrier, $a < x_0 < b$.

To find $P(x)$ we need another value called the flux of the system, $\frac{dj}{dx} = -\frac{\partial P}{\partial t}$. Flux is a measure of what travels through a particular point or barrier. In this system, we only have an absorbing barrier to the right of the initial position, meaning all the particles will escape the system to the right. This means that nothing will escape to the left, meaning no flux over $x = a$. As $j(x) = -V'(x)P - DP'$ the flux of the system has the value

$$j(x) = r \quad x > x_0$$

$$0 \quad x < x_0,$$

where r is the magnitude of the flux over the barrier at $x = b$ and is the injection rate of the particles into the system, meaning what goes in must come out. Due to everything escaping from the system to the right, we can define it as a constant value because it has no dependence on position. So we have a differential equation for P and there are two different flux equations that we can solve for P on either side of the initial position due to the different barriers,

$$\text{For } \underline{x < x_0} \quad V'(x)P + DP' = 0,$$

$$P(x < x_0) = A \exp\left(-\frac{V(x)}{D}\right), \tag{1.19}$$

$$\text{and for } \underline{x > x_0} \quad V'(x)P + DP' = -r,$$

$$\frac{d}{dx} \left[P \exp\left(\frac{V(x)}{D}\right) \right] = -\frac{r}{D} \exp\left(\frac{V(x)}{D}\right),$$

$$\int_x^b \frac{d}{dx'} \left[P \exp\left(\frac{V(x')}{D}\right) \right] dx' = -\frac{r}{D} \int_x^b \exp\left(\frac{V(y)}{D}\right) dy,$$

$$P(b) \exp\left(\frac{V(b)}{D}\right) - P(x) \exp\left(\frac{V(x)}{D}\right) = -\frac{r}{D} \int_x^b \exp\left(\frac{V(y)}{D}\right) dy,$$

$$P(b) = 0; \quad P(x > x_0) = \frac{r}{D} \exp\left(-\frac{V(x)}{D}\right) \int_x^b \exp\left(\frac{V(y)}{D}\right) dy. \quad (1.20)$$

We can find the constant A in (1.19) by using the fact that the probability is continuous across the entire system meaning that the probabilities on either side of x_0 must equal each other at x_0 ,

$$\begin{aligned} P(x < x_0; x_0) &= P(x > x_0; x_0) \\ A \exp\left(-\frac{V(x_0)}{D}\right) &= \frac{r}{D} \exp\left(-\frac{V(x_0)}{D}\right) \int_{x_0}^b \exp\left(\frac{V(y)}{D}\right) dy \\ A &= \frac{r}{D} \int_{x_0}^b \exp\left(\frac{V(y)}{D}\right) dy. \end{aligned}$$

We can now calculate the mean first passage time τ , using the fact that the mean first passage time is defined as $\tau = \frac{n}{r}$, where we have n from equation (1.18) which we split due to two PDF expressions,

$$n = \int_a^{x_0} P(x < x_0) dx + \int_{x_0}^b P(x > x_0) dx,$$

$$\tau = \frac{1}{D} \int_a^{x_0} \exp\left(-\frac{V(x)}{D}\right) \int_{x_0}^b \exp\left(\frac{V(y)}{D}\right) dy dx \quad (1.21)$$

$$+ \frac{1}{D} \int_{x_0}^b \exp\left(-\frac{V(x)}{D}\right) \int_x^b \exp\left(\frac{V(y)}{D}\right) dy dx. \quad (1.22)$$

This integral can be rewritten by combining the integral domains into one integral,

$$\tau = \frac{1}{D} \int_{x_0}^b \exp\left(\frac{V(y)}{D}\right) \int_a^y \exp\left(-\frac{V(x)}{D}\right) dx dy \quad (1.23)$$

This combination can be shown using a domain graph 1.7. The first integral in (1.21) is highlighted in green, while the second is in red. The change into one

integral changes the integral limits meaning the whole domain is brought under one integral. We have derived an integral form of the mean first passage time for a

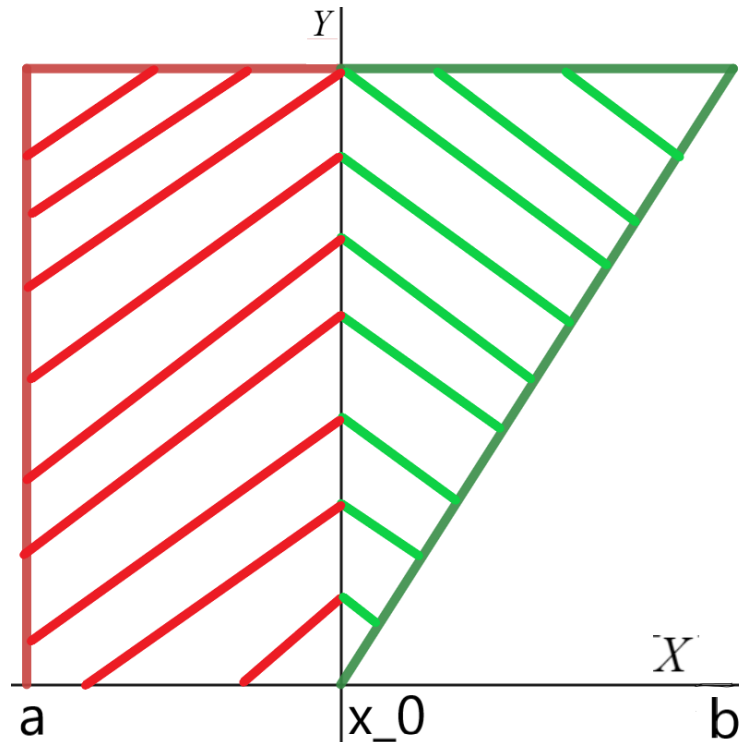


Figure 1.7: Domain graph for the integrals

general $V(x)$, which we will utilise later to confirm our results when we use the path integral technique on simple potentials.

In this introductory chapter, we have looked at the basic principles of stochastic dynamics and how the fundamental equations that will be investigated throughout this work are found. We have briefly looked at some of the current techniques that are being used to describe dynamical systems and have explored some of the limitations of these techniques due to computational requirements. Throughout the rest of this work, we will further explore a specific technique in solving for the key information of a system, namely by using the path integral formulation to find the probability density function, first passage time density, and mean first passage time. The use of path integrals to the extent in this work has yet to be fully understood concisely in a single result, and we will be exploring how different elements of the path integral form provides differing information to the classically known solutions.

Work has been done using path integrals for the calculation of the mean first passage time as that is the important element in Monte Carlo methods.

Path integrals are the “third way” to look at solving the Smoluchowski equation and what we will explore in the rest of this work. It is still an approximate solution, only exact for quadratic potentials and simpler, much like solutions to the Schrödinger equation in quantum mechanics [53]. However, we will see that it can begin to provide some of the currently discarded information and provide possibly useful insights into the interesting dynamics of a system.

We will explore how these path integrals are defined in chapter 2, then look at how they can be implemented numerically to provide fast solutions to complex systems in chapter 3. We will then explore the key ingredients to provide the full picture of the system in chapters 4 and 5 before applying the knowledge to one of the more well-known systems, the Harmonic oscillator chapter 6. Finally, we will explore how the first passage time densities and mean first passage times can be calculated using techniques of the Laplace domain, chapters 7 and 8 before finishing off with a brief look as to how the path integral might work in higher dimensions 9.

Chapter 2

Introduction to Path Integrals

In this chapter, we will begin to explore the use of the path integral formulation in solving the Smoluchowski equation, beginning by deriving the general form of a stochastic dynamic path in the potential $V(x)$. We look at building a probability density function form for the most dominant paths in the system, working in the weak noise limit. Then, making a handy comparison to the dynamics of a *classical path* in a fictitious potential allows the use of Hamiltonian mechanics and Euler-Lagrange equations to help provide a full insight into the dynamics of the paths. We will then form a full probability density function for the classical path and show that it solves the simplest of problems, the flat and sloped potential. Finally, we will end by looking at a long time-limit exploration and wondering whether the solution will return the correct equilibrated solution or whether more pieces are needed to provide the complete information about the system at all times.

The first step of introducing the concept of the path integral, and how it can be used to solve the Smoluchowski equation (1.10) for a given potential, is to use techniques previously used to find an integral representation of the path's specific weight by using more characteristics of Wiener processes. We will then specifically look at the most *dominant* paths using Hamiltonian mechanics, revealing a relationship between stochastic most probable paths in the potential $V(x)$ and Hamiltonian trajectories in a virtual potential $\mathcal{V}(x)$, allowing more information about the paths to be determined.

To begin finding the path integral representation, we will follow a derivation of the general path integral for a Markov Stochastic process from Horatio Wio's book "Path Integrals for Stochastic Processes" [1] in one dimension. Initially, we are finding a probability density function in the time domain using known techniques, which we will apply specifically to the systems we wish to investigate. To begin trying to find this probability density function, we start by looking at the probability that at a given time t , the process takes a value between a and b having been at q_0 at time t_0 ,

$$P(a < x < b, t|q_0, t_0) = \int_a^b dq P(q, t|q_0, t_0).$$

The integrand is the probability density value for a path that began at (q_0, t_0) and finished at (q, t) . What this expression achieves is to "sum" over all possible final positions between a and b with each probability $P(q, t|q_0, t_0)$. We can take this a step further, and to represent a path that travels from (q_0, t_0) to (q_N, t_N) , we splice the journey up and end up with an expression that utilises *short-time propagators* $P(q_{i+1}, t_{i+1}|q_i, t_i)$. This means that we can build a probability that the process, starting at (q_0, t_0) , has a value between a_1 and b_1 at t_1 , a value between a_2 and b_2 at time t_2 , ..., a value between a_{N-1} and b_{N-1} at t_{N-1} , and reaching q_N at t_N , is given by:

$$\begin{aligned}
 P(q_N, t_N | q_0, t_0) &\approx \\
 \int_{a_1}^{b_1} \int_{a_2}^{b_2} \dots \int_{a_{N-1}}^{b_{N-1}} &dq_1 dq_2 \dots dq_{N-1} P(q_N, t_N | q_{N-1}, t_{N-1}) \dots P(q_2, t_2 | q_1, t_1) P(q_1, t_1 | q_0, t_0).
 \end{aligned}
 \tag{2.1}$$

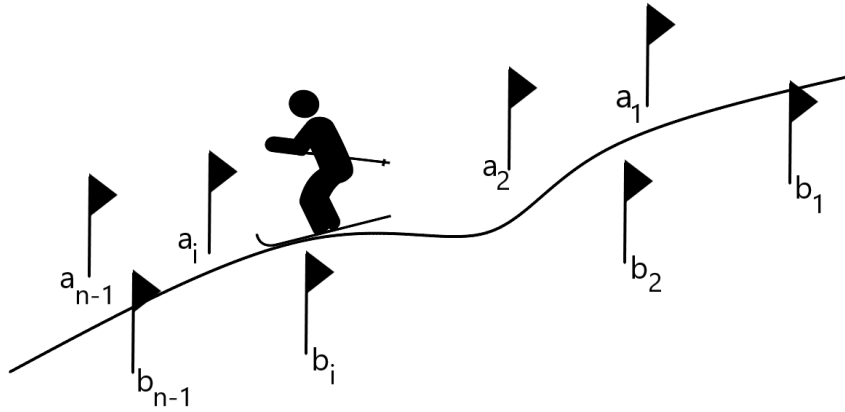


Figure 2.1: A “practical” example of multiple gates path [1]

Subsequently, suppose we increase the number of time segmentations we use and narrow the spatial windows around the path. In that case, we can increase the accuracy of the final probability value by increasing the number of propagators representing how we can partition up a single path trajectory into multiple smaller segments. We can then appeal to known solutions to find an expression for these short-time propagators, thus finding an expression for the full probability density function. To find an integral form for the probability density function that will be calculable, we need to know how the whole integral will form when we use known results, namely, the Wiener process [54]. Appealing to this known solution for a small t propagator means that we can find a full probability integral form which allows a comparison to the Langevin equation resulting in a more usable form for the stochastic probability density function.

The Wiener process has a probability density function for travelling from W_1 to W_2 in time $(t_2 - t_1)$:

$$P(W_2, t_2 | W_1, t_1) = \frac{1}{\sqrt{2\pi D(t_2 - t_1)}} \exp \left[-\frac{1}{2D(t_2 - t_1)} (W_2 - W_1)^2 \right]. \quad (2.2)$$

If then we split the path into infinitely many segments (2.1), $N \rightarrow \infty$, we can define a *Wiener measure* [2] by substituting the short-time propagator (2.2) into the full probability form (2.1). This substitution, along with the discretisation allows a transformation of the integral form to a product of the Wiener processes. The Wiener measure is then defined as;

$$P(W, T | W_0, t_0) = \prod_{j=1}^N \left(\frac{dW_j}{\sqrt{4\pi\epsilon D}} \right) \exp \left[-\frac{1}{4D\epsilon} \sum_j (W_j - W_{j-1})^2 \right],$$

where ϵ is our time gap which becomes uniform as $N \rightarrow \infty$ after the time discretisation. As $N \rightarrow \infty$ and $\epsilon \rightarrow 0$, we can transform the exponent from a sum to an integral and write the probability as

$$P(W, T | W_0, t_0) \propto \exp \left[-\frac{1}{4D} \int_{t_0}^T d\tau \left(\frac{dW}{d\tau} \right)^2 \right]. \quad (2.3)$$

So we now have a probability form, minus some normalisation, for a single path between two points (W_0, t_0) and (W, T) . To then recover a full probability density function, we extended to a full probability by integrating this value over all possible paths between (W_0, t_0) and (W, T) to get a *Wiener integral* [55]

$$P(W, T | W_0, t_0) = \int \mathcal{D}[W(\tau)] \exp \left[-\frac{1}{4D} \int_{t_0}^T d\tau \left(\frac{dW}{d\tau} \right)^2 \right], \quad (2.4)$$

where $\mathcal{D}[W(\tau)]$ represents the integral over all the paths and is a concise version of $dW_0 dW_1 dW_2 \dots dW$, condensing the multiple integral representation into an integral over all possible paths taken by the Wiener process. It also holds the normalisation constant, which can be found using standard techniques, ensuring that the proba-

bility density function satisfies the correct initial and final value limits for the given system.

So this represents a Wiener process probability using known short-time propagator results, which is valid for Brownian motion. However, can we use other known results from Stochastic processes to find a more usable and calculable form for general systems and potentials?

2.1 An analytical path integral solution

We have from Wio [1] a form for the probability as the integral over all possible paths (2.4), and in this section, we will begin to piece together a more calculable and closed-form representation for the probability density function of a system, not just a Wiener process. We can begin with a noise probability functional for a single path, which arises from the relationship between white noise and the Wiener process, $dW(t) \approx \xi(t)dt$. The single path expression we found earlier (2.3) can be transformed by this relationship to find a form for the probability density function that relates to the white noise functional instead,

$$P[\xi] \propto \exp \left[-\frac{1}{4D} \int |\xi(t)|^2 dt \right] \quad (2.5)$$

This is a probability density functional for the Gaussian white noise term, which is the same found in the general Langevin equation, which we can use to find a more usable form of the PDF for the general system that we are investigating in this work. Using the Langevin equation (1.6) to substitute in for the noise term,[25]

$$m\ddot{x} + \Gamma\dot{x} = -\nabla V(x) + \xi(t), \quad (2.6)$$

where m is the mass of the particle and Γ is the friction coefficient. Substituting (2.6) into (2.5) and subsequently into the (2.4) form we can write down the transition

probability for all paths from $(x_i, 0)$ to (x_f, T) ,

$$P(x_f, T|x_i, 0) = \int \mathcal{D}x \mathcal{J}[x] \exp \left[-\frac{1}{4D} \int_0^T |m\ddot{x} + \Gamma\dot{x} + \nabla V(x)|^2 dt \right].$$

What this integral represents is the sum of the probability of each individual path from the initial position x_i to the final position x_f in time T . The $\mathcal{J}[x]$ term is the *Jacobian* that arises from the change in variables $\xi \rightarrow x$. It is defined in the infinite-dimensional limit as the Jacobian functional $\mathcal{J} = |\mathcal{D}\xi/\mathcal{D}x|$, and in the case of the path integral, its value is dependent on when the noise term in the system is applied. For now, this value for a single path propagator can be taken to be unit, $\mathcal{J} = 1$, which arises from what is called the Ito prescription when the noise is added before the particle moves in Langevin simulations. It transpires, as we will see in chapter 4, that the Jacobian term does not become relevant until the potential is of quadratic order or higher. Still, we will explore it thoroughly in chapter 4.

The time integral in the exponential can be interpreted as the stochastic action $\mathcal{S}[x]$, with corresponding Lagrangian $L = |m\ddot{x} + \Gamma\dot{x} + \nabla V(x)|^2$, much like the work done by Onsager and Machlup [56], however, in this case, it was restricted to a linear Gaussian process. This can be expanded to give a more useful form,

$$\begin{aligned} L &= 2\Gamma\dot{x} (m\ddot{x} + \nabla V) + \Gamma^2\dot{x}^2 + (m\ddot{x} + \nabla V)^2, \\ &= 2\Gamma \frac{d}{dt} \left(\frac{1}{2}m\dot{x}^2 + V \right) + \Gamma^2\dot{x}^2 + (m\ddot{x} + \nabla V)^2, \end{aligned}$$

so P can now be written as

$$\begin{aligned} P(x_f, T|x_i, 0) &= \int \mathcal{D}x \mathcal{J}[x] \exp \left[-\frac{1}{4D} \int_0^T 2\Gamma \frac{d}{dt} \left(\frac{1}{2}m\dot{x}^2 + V \right) + \Gamma^2\dot{x}^2 + (m\ddot{x} + \nabla V)^2 dt \right] \\ &= \left(\exp \left[-\frac{\Gamma\Delta E}{2D} \right] \right) \int \mathcal{D}x \exp \left[-\frac{1}{4D} \int_0^T (\Gamma^2\dot{x}^2 + (m\ddot{x} + \nabla V)^2) dt \right] \end{aligned}$$

where $\Delta E = [\frac{1}{2}m\dot{x} + V]_{\text{initial}}^{\text{final}}$. As this is the non-overdamped system, this is for the full Fokker-Planck non-Markovian solution due to the inclusion of the \ddot{x} term. An

interesting thing to note is because the terms in the time integral are symmetric under time reversal, an immediate result is Crook's fluctuation theorem [57],

$$\frac{P(x_f, T|x_i, 0)}{P(x_i, T|x_f, 0)} = \exp \left[\frac{-\Delta E}{k_B T} \right] = \exp \left[-\frac{\left[-\frac{1}{2}m\dot{x} + V \right]_{x_i}^{x_f}}{kT} \right],$$

meaning the trajectory from x_i to x_f in time T with negative ΔE is exponentially more likely than its reverse, x_f to x_i in time T , where we have used the Einstein relation to relate temperature with the diffusion value, $D = \Gamma k_B T$ [34], an example of how the generic noise term D can be related to a specific system. This has comparisons with the Metropolis Monte Carlo algorithm [58] whose derivation begins with the principle of detailed balance [59], where the ratio between two probabilities which are time reversals of each other is a ratio of the relevant stationary distributions π ,

$$\frac{P(x_f|x_i)}{P(x_i|x_f)} = \frac{\pi(x_f)}{\pi(x_i)}.$$

Where the stationary distribution is recovered from the Boltzmann distribution [60], the long-time solution to the Smoluchowski equation, $\exp \left(-\frac{\Delta V}{k_B T} \right)$. This can be seen as similar to our ΔE , by the fact that at equilibrium the energy will reduce to $\Delta E = \Delta V|_{\text{initial}}^{\text{final}}$ as the particle has zero velocity, $\dot{x} = 0$, and the full probability density function that we have is for the Fokker-Planck equation which keeps the kinetic terms. This also shows a time invariance of our probability density function, meaning the probability of travelling in one direction is proportional to the probability of travelling in the opposite direction, with the proportionality factor being the Boltzmann distribution.

We can then restrict this problem to the overdamped limit, where the inertia term, \ddot{x} , in (2.6) equals zero as we assume the particles have reached terminal velocity immediately. We can then find a path integral expression (with $\Gamma = 1$ without loss of generality) that reads:

$$P(x_f, T|x_i, 0) = \int \mathcal{D}x \mathcal{J}[x] \exp \left[-\frac{1}{4D} \mathcal{S}[x] \right], \quad \mathcal{S}[x] = 2\Delta V + \int_0^T (\dot{x}^2 + V'^2) dt, \quad (2.7)$$

where the $\Delta V = V(x_f) - V(x_i)$ term comes from integrating the time derivative term in the Lagrangian and, due to being only dependent on the endpoints, can be removed from the path integral. $\mathcal{S}[x]$ can be called a *stochastic action* term, similar to what appears in Lagrangian dynamics. So starting from a stochastic differential equation, we have arrived at a form for the probability density function that has a form similar to that of classical mechanics actions, more specifically those of Hamiltonian mechanics which we may be able to use to understand the dynamics of the original stochastic system fully. This representation is an integral over all possible paths between the initial and final positions in time T .

What the action $\mathcal{S}[x]$ quantifies is how many fluctuations are needed to make the path occur as if no fluctuations occur we will have $\mathcal{S} = 0$ which results in sliding downhill under friction. Some of these fluctuations deviate so far from the classical path that the action is large, meaning the probability is extremely small, so they will not have a relevant contribution to the final solution. What this describes is the path of least resistance which is preferable and when doing stochastic simulations of a system, will be the most likely. For example, if we think about escape over a barrier, this event in itself is a rare event in which nothing happens at all as the particle wobbles at the bottom of the well. When the time is right all the fluctuations add up in the correct direction to allow the particle to jump over the barrier, a probabilistically unlikely event with a large action. Another way to think in terms of path integrals is in a similar situation with a potential barrier to overcome, if a particle travels halfway up the barrier and stays there for a period of time, it will take many fluctuations being in balance to keep the particle there, and then subsequently over the barrier, meaning this is probabilistically unlikely. What is more likely is that the fluctuations move the particle back to the bottom of the well,

and the probabilistically more likely event is for the particle to make it over the barrier all in one go, which also makes more physical sense. Considering this, we can concentrate on these paths that dominate the probability and provide the most dominant contributions to the solution [61] by having the smallest fluctuations from the classical path.

To do this, we can look at the paths that minimise the action term, subsequently maximising the probability which we can do by appealing to Euler-Lagrange equations and Hamiltonian dynamics [62]. This means that the comparison we are drawing is that stochastic dynamics in the potential $V(x)$ corresponds to classical conservative trajectories in a “virtual” *effective potential*, $\mathcal{V}(x)$, which we will find by using Euler-Lagrange equations [63]. As we are looking for the minimums of the stochastic action \mathcal{S} , we are after the stationary points of the integrand, which we can relate to the Lagrangian and use a combination of Euler-Lagrange equations and Hamiltonian mechanics. Using the Euler-Lagrange equations, we can find the equations of motion that the classical trajectories satisfy in the “virtual” potential. The Euler-Lagrange equation in one dimension is defined as,

$$\mathcal{S}(x) = \int_0^T L[\dot{x}, x, t] dt = \int_0^T (\dot{x} + V'(x))^2 dt,$$

$$\frac{\partial L}{\partial x} - \frac{d}{dt} \frac{\partial L}{\partial \dot{x}} = 0.$$

Solving this equation, we can find the equation of motion,

$$L = \dot{x}^2 + 2\dot{x}V'(x) + V'(x)^2,$$

$$\frac{\partial L}{\partial x} = 2\dot{x}V''(x) + 2V'(x)V''(x),$$

$$\frac{d}{dt} \frac{\partial L}{\partial \dot{x}} = \frac{d}{dt} [2\dot{x} + 2V'(x)] = 2\ddot{x} + 2V''(x)\dot{x},$$

$$\frac{\partial L}{\partial x} - \frac{d}{dt} \frac{\partial L}{\partial \dot{x}} = 2V'(x)V''(x) - 2\ddot{x} = 0,$$

$$\ddot{x} = V'(x)V''(x).$$

Note that in mechanics we can always add a total time derivative to the Lagrangian without changing the Euler-Lagrange equations. This is what the middle term in the L expansion is; without it, the equations of motion will be the same. So, the Euler-Lagrange equation returns an equation of motion for the trajectories in the “virtual” effective potential. Relating this to Newton’s second law of motion for a particle in a potential, $F = ma = -\nabla\mathcal{V}(x)$ we find that the potential is,

$$\begin{aligned} ma &= 2\ddot{x} = 2V'(x)V''(x), \\ 2V'(x)V''(x) &= -\frac{d}{dx}(-V'(x)^2) = -\frac{d}{dx}(\mathcal{V}(x)), \\ \mathcal{V}(x) &= -V'(x)^2. \end{aligned}$$

This means that by minimising the stochastic action in our representation of the path integral probability, we can relate the most probable, dominant stochastic paths that occur in the potential $V(x)$ to classical paths that obey Hamiltonian mechanics in the effective potential $\mathcal{V}(x) = -V'(x)^2$. An example of these two potentials is shown in figure 2.2 for an asymmetric double well potential. The knowledge of this comparison will be apparent throughout this work as we use the effective potential to show a complete picture of what happens to these paths as they travel through the potential $V(x)$.

As we are appealing to Hamiltonian mechanics for the trajectories in the effective potential, we can use other definitions to provide a useful piece of the puzzle. The other expression we can find using Hamiltonian mechanics is an “energy” value using the energy function,

$$\begin{aligned} H &= \frac{\partial L}{\partial \dot{x}} \dot{x} - L, \\ &= (2\dot{x} + 2V'(x)) \dot{x} - L, \\ H &= \dot{x}^2 - V'(x)^2. \end{aligned} \tag{2.8}$$

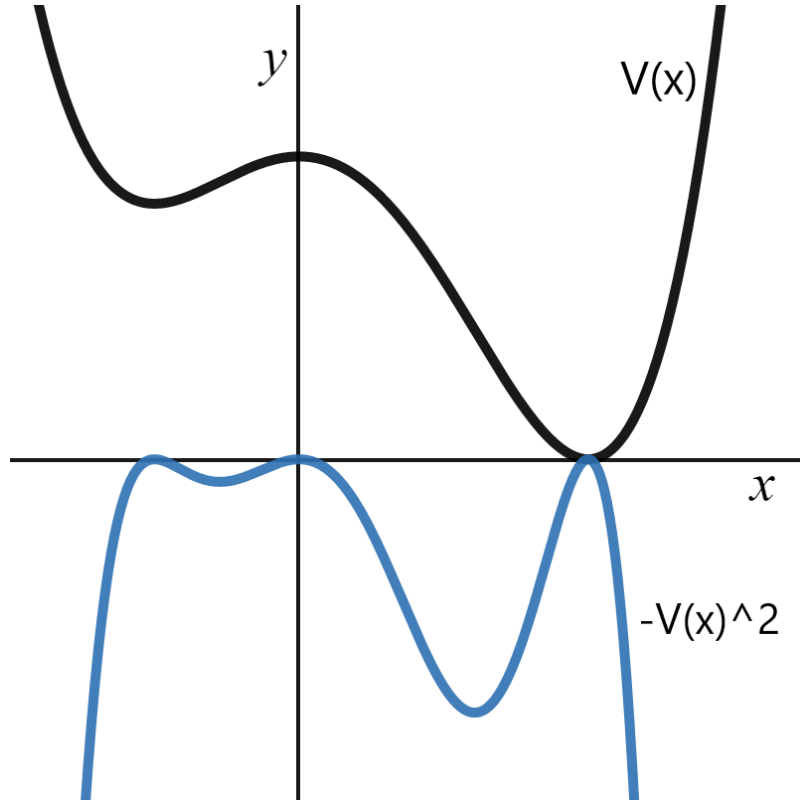


Figure 2.2: An example of the Potential $V(x)$ for a tilted double well vs the corresponding Ito prescription effective potential $\mathcal{V}(x) = -V(x)^2$

This quantity describes the energy that a particle possesses along a path in the effective potential and is analogous to the addition of kinetic and potential energy for the given system. For a small H value, the paths will spend most of their time near the peaks of the effective potential when $V'(x) = 0$, just like the weak-noise stochastic paths do in the real potential when they spend a lot of their time at the bottom of the wells or the top of the peak. Substituting this energy equation into our expression for $\mathcal{S}[x]$ (2.7) we return Hamilton's principal function [64], the action of the path evaluated down the extremal,

$$\begin{aligned}
 S(x) &= 2(V(x_f) - V(x_i)) + \int_0^T (2\dot{x}^2 - H)dt, \\
 &= 2(V(x_f) - V(x_i)) - HT + 2 \int_0^T \dot{x} \frac{dx}{dt} dt, \\
 &= 2(V(x_f) - V(x_i)) - HT + 2 \int_{x_i}^{x_f} \sqrt{H + V'(y)^2} dy, \quad (2.9)
 \end{aligned}$$

where we chose the + square root from the $\dot{x} = \pm\sqrt{H + V'^2}$ as the velocity is positive

when arriving at the given endpoint from the same direction as the initial position. In this system, we have the fact that $x_f > x_i$ so the particle will be travelling from left to right in the potential, and as the velocity \dot{x} has a direction it is positive as we take naturally that left to right is positive. Later we will consider paths that will arrive at x_f from the other side, opposite to x_i , which results in a turning path.

We can solve the equation of motion for the Hamiltonian system in order to find a relationship between time and “energy”. We have from Hamiltonian mechanics the “energy” equation which we can rearrange to find the velocity of the classical path particle,

$$H = \dot{x}^2 - V'(x)^2,$$

$$\dot{x} = \sqrt{H + V'(x)^2}.$$

Note that if we still had the friction coefficient and had not set it equal to 1, this “energy” term would actually have dimensions of power instead. Integrating this equation on both sides between the beginning and end point yields the relationship we are after,

$$\frac{dx}{dt} = \sqrt{H + V'(x)^2},$$

$$\int_0^T dt = \int_{x_i}^{x_f} \frac{dx}{\sqrt{H + V'^2}},$$

$$T = \int_{x_i}^{x_f} \frac{dx}{\sqrt{H + V'^2}}. \tag{2.10}$$

This representation derived from Hamiltonian mechanics methods describes the time taken for a path to travel from the initial position to the final position in the real potential, undergoing stochastic diffusion. This equation can also be found by the stationary action principle to return equations of motion and calculating the partial derivative $\frac{\partial S}{\partial H}$ and setting it equal to 0, $\frac{\partial S}{\partial H} = 0$ [65]. To find this action and time, we have used the Euler-Lagrange equation to find the classical path, the most

probable path. However, there may be more paths that are highly probable and will contribute to the full probability density function. These paths fluctuate around the most probable path, meaning what we want to calculate is the probability that a path is in a “tube” around the most probable path, but how do we take these into account? [66][2] To find this factor, we can look at the next term, the quadratic, in the expansion of the action around the classical path trajectory, S_* ,

$$\mathcal{S}[x] = S_* + \left. \frac{\delta \mathcal{S}}{\delta x} \right|_{x_*} + \frac{1}{2} y(t) \left. \frac{\delta^2 \mathcal{S}}{\delta x^2} \right|_{x_*} y(t) + \dots,$$

where $x(t) = x_*(T) + y(t)$, with $y(t)$ being the fluctuations. The second term in the expansion is what we have already used in order to find the classical path and what returns the Euler-Lagrange equations, so $\left. \frac{\delta \mathcal{S}}{\delta x} \right|_{x_*} = 0$. The next term is from the Taylor expansion of L to the second order and is defined as,

$$\delta^2 \mathcal{S} = \int_0^T \left(\left. \frac{\partial^2 L}{\partial \dot{x}^2} \right|_{x_*} \dot{y}^2 + 2 \left. \frac{\partial^2 L}{\partial x \partial \dot{x}} \right|_{x_*} y \dot{y} + \left. \frac{\partial^2 L}{\partial x^2} \right|_{x_*} y^2 \right) dt,$$

Using the Lagrangian $L = (\dot{x} + V'(x))^2$,

$$\begin{aligned} \frac{1}{2} y(t) \left. \frac{\delta^2 \mathcal{S}}{\delta x^2} \right|_{x_*} y(t) &= \int_0^T \left(\dot{y}^2 + (V'(x)V''(x))' \Big|_{x_*} y^2 \right) dt, \\ \Rightarrow \mathcal{S}[x] &= S_* + \int_0^T \left(-y \dot{y} + (V'V'')' \Big|_{x_*} y^2 \right) dt, \end{aligned}$$

where we have used the fact that during integration by parts, the fluctuation function $y(t)$ does not deviate at the beginning or the end of the path, $y(0) = y(T) = 0$.

This final expression can be written more concisely by using an operator \hat{M}

$$\begin{aligned} \mathcal{S}[x] &= S_* + \int_0^T y \left(\hat{M} y \right) dt, \\ &= S_* + \langle y | \hat{M} y \rangle; \\ \hat{M} &= -\frac{d^2}{dt^2} + (V'V'')' \Big|_{x_*}. \end{aligned}$$

We wish to integrate over “all” $y(t)$ to calculate the quadratic fluctuations around the classical path $x_*(t)$ in order to take these paths into account. To do this, we use the fact that the matrix \hat{M} is positive and self-adjoint, meaning its eigenfunctions form a complete set and are defined as $\hat{M}y_n = \lambda_n y_n$. This means that “any” $y(t)$ can be expanded as $y = \sum_n a_n y_n$. So, our operator equation becomes,

$$\begin{aligned} \langle y | \hat{M} y \rangle &= \sum_n \sum_m \langle a_n y_n | \hat{M} a_m y_m \rangle, \\ &= \sum_n \sum_m a_n a_m \langle y_n | \lambda_m y_m \rangle, \\ &= \sum_n a_n^2 \lambda_n, \end{aligned}$$

where we have chosen the eigenfunctions to be orthonormal, $\langle y_n | y_m \rangle = \delta_{nm}$, as we are integrating over all the values of a_n this is equivalent to integration over all functions $y(t)$. So we now have a second-order expansion of the action around the classical path, but how does this act when inputted into our general form for the probability density function? By now, we have a general form for the PDF to be,

$$P = \mathcal{N} \int \mathcal{D}x \mathcal{J}[x] \exp\left(-\frac{\mathcal{S}}{4D}\right),$$

and we can now use our expansion to reduce this to a multiple of the classical path, noting that \mathcal{N} is the normalisation constant and is non-dependent on x .

$$\begin{aligned} P &= \mathcal{N} \int (\mathcal{D}x_* + \mathcal{D}y) \mathcal{J}[x_* + y] \exp\left(-\frac{S_* + \sum_n a_n^2 \lambda_n}{4D}\right), \\ &= \mathcal{N} \mathcal{J}[x_*] \exp\left(-\frac{S_*}{4D}\right) \int \mathcal{D}a_n \exp\left(-\frac{\sum_n a_n^2 \lambda_n}{4D}\right), \\ &= \mathcal{N} \mathcal{J}[x_*] \exp\left(-\frac{S_*}{4D}\right) \prod_n \sqrt{\frac{4\pi D}{\lambda_n}}, \\ &= \mathcal{N} \mathcal{J}[x_*] \exp\left(-\frac{S_*}{4D}\right) \frac{(4\pi D)^{\frac{N}{2}}}{\sqrt{\det M}}, \end{aligned} \tag{2.11}$$

Furthermore, it is the term $\det M$ that we wish to find to include these quadratic fluctuations around the classical path. There is the possibility that there occurs

a zero mode in this representation when there is a zero eigenvalue, which would cause a divergent portion of the probability. This problem is something that occurs in quantum mechanics when solving the time-independent Schrödinger equation, corresponding to the zero mode solution that arises when looking at using path integrals in quantum mechanics [2]. We will investigate this divergence thoroughly when we have another piece of the puzzle in the Jacobian term in chapter 4.

The normalisation constant \mathcal{N} can be found using a comparison to the Ornstein-Uhlenbeck solution, the probability density function for the quadratic potential system [67], and returns $\mathcal{N} = (4\pi D)^{-\frac{N+1}{2}}$. To do this, we solve the simplest case, when $x_f = x_i$, to find $\det M$ and then compare to known solutions to find \mathcal{N} . For the probability of the particle staying still, $P_i(T) = P(x_i, T|x_i, 0)$, the action $S_* = 0$, and $J_* = \exp\left(\frac{1}{2} \int_0^T V''(x_i) dt\right) = \exp\left(\frac{1}{2} V_i'' T\right)$, see chapter 4 to see where this comes from explicitly. Finding $\det M_i$ for this system is done by solving the initial value problem,

$$M\psi(t) = 0; \quad \psi(0) = 0; \quad \dot{\psi}(0) = 1; \rightarrow \det M = \psi(T). \quad (2.12)$$

This amazing result is a trick from Gelfand and Yaglom [68]. For further derivation and explanation see the paper from Gelfand and Yaglom, or Schulman's path integral book [2].

In this specific system,

$$\begin{aligned} M_i &= -\frac{d^2}{dt^2} + (V'V'')' \Big|_{x_i} \\ &= -\frac{d^2}{dt^2} + \omega^2; \quad \text{as } V_i''^2 + V_i'V_i'' \text{ is constant} \\ M_i\Psi &= -\Psi'' + \omega^2\Psi = 0 \\ \Rightarrow \Psi &= A \sinh(\omega t) + B \cosh(\omega t) \end{aligned}$$

Using the initial conditions yields the solution,

$$\begin{aligned}\Psi &= \frac{1}{\omega} \sinh(\omega t) \\ \Rightarrow \det M_i &= \frac{\sinh(\omega T)}{\omega} \\ P_i(T) &= \frac{\mathcal{N}(4\pi D)^{\frac{N}{2}} \exp\left(\frac{V_i'' T}{2}\right)}{\sqrt{\frac{\sinh(\omega T)}{\omega}}}\end{aligned}$$

Now we say that this has to be equal to the Ornstein-Uhlenbeck solution for the harmonic approximation for the potential well that x_i is in, as we are after the probability of staying in the same place we only care about the potential around the initial position and can approximate it to be harmonic, as demonstrated in figure 2.3. If we say that x_i is near the minimum at $x = x_m$ then if $z = x - x_m$, the potential is $U = \frac{1}{2}V_m''z^2$, and

$$P_{O-U} = \sqrt{\frac{V_m''}{2\pi D(1 - \exp(-2V_m''T))}} \exp\left(-\frac{V_m''(z - z_i \exp(-V_m''T))^2}{1 - \exp(-2V_m''T)}\right).$$

This approximation allows us to equate between the Ornstein-Uhlenbeck solution and the representation that we have gained for full probability density function, in order to find constants. This equation to a specific representation is similar in methodology as when we find normalisation constants by integrating probability density functions overall space and equating to 1.

To find \mathcal{N} we equate this to $P_i(T)$ and evaluate it at $z = z_i = x_i - x_m$. If we simplify this and evaluate this at the bottom of the potential well, i.e. $x_i = x_m$, then $V_i' = 0$, meaning that $\omega = V_i''$ and then we can simplify even further.

$$\begin{aligned}P_{O-U}(x_i = x_m) &= P_i(T) \\ \sqrt{\frac{\omega}{2\pi D(1 - \exp(-2\omega T))}} &= \frac{\mathcal{N}(4\pi D)^{\frac{N}{2}} \exp\left(\frac{\omega T}{2}\right)}{\sqrt{\frac{\sinh(\omega T)}{\omega}}}\end{aligned}$$

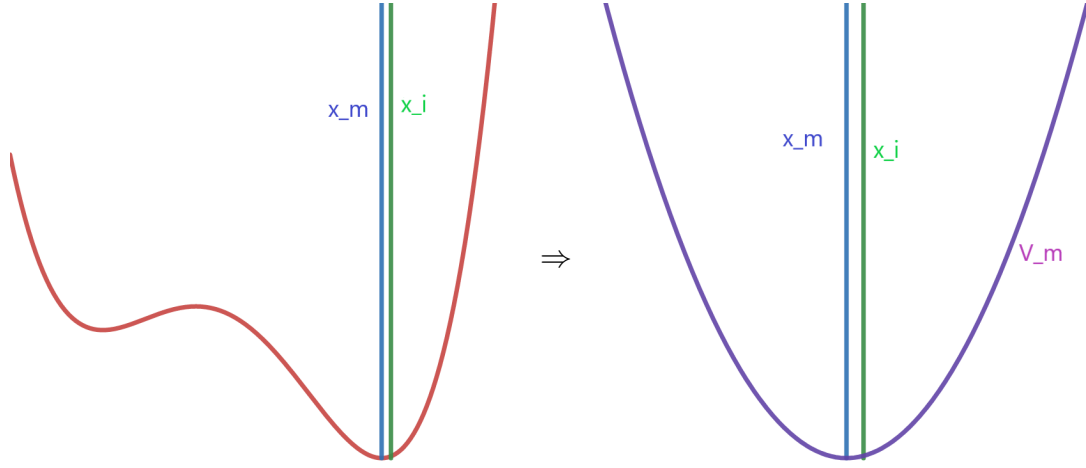


Figure 2.3: Showing an approximation of the complex potential on the left to the Harmonic potential on the right for x_i positions near the minimum at x_m

$$\sqrt{\frac{\omega}{4\pi D \exp(-\omega T) \sinh \omega T}} = \frac{\mathcal{N} (4\pi D)^{\frac{N}{2}} \exp\left(\frac{\omega T}{2}\right)}{\sqrt{\frac{\sinh(\omega T)}{\omega}}}$$

$$\begin{aligned} \frac{\exp\left(\frac{\omega T}{2}\right)}{\sqrt{4\pi D}} &= \mathcal{N} (4\pi D)^{\frac{N}{2}} \exp\left(\frac{\omega T}{2}\right) \\ \Rightarrow \mathcal{N} &= (4\pi D)^{-\frac{N+1}{2}} \end{aligned}$$

This means that the $(4\pi D)^{\frac{N}{2}}$ will cancel in the general solution (2.11) leaving a $\frac{1}{\sqrt{4\pi D}}$, which feels right as in most general solutions there is a term of this form to satisfy the normalisation as terms arise from Gaussian integrals.

Back to the general solution for $\det M$ (2.12), we actually already know one solution to the operator equation by the fact that from the Hamiltonian mechanics $\ddot{x} = V'V''$, which means that one of the solutions is $\psi = \dot{x}_*$, shown below,

$$\begin{aligned} M\psi &= M\dot{x}_*, \\ &= -\ddot{x}_* + (V'V'')' \dot{x}_*, \\ &= -(V'V'')' \dot{x}_* + (V'V'')' \dot{x}_* = 0. \end{aligned}$$

Finding the first solution is useful as with second-order ODEs we can find the second

solution from the first by using the Wronskian, W .

This is defined as,

$$W = \dot{y}_2 y_1 - y_2 \dot{y}_1,$$

and we can show that this is a constant by the fact that $\frac{dW}{dt} = 0$,

$$\begin{aligned} \frac{dW}{dt} &= \ddot{y}_2 y_1 + \dot{y}_2 \dot{y}_1 - \dot{y}_2 \dot{y}_1 - y_2 \ddot{y}_1 \\ M y_i = 0 &\Rightarrow = (V' V'')' y_2 y_1 - y_2 (V' V'')' y_1 \\ &= 0. \end{aligned}$$

This means that we can write the solution to $\psi(t)$ as a linear sum of the two solutions, and use the W equation to find the y_2 relationship;

$$\begin{aligned} \psi(t) &= A y_1 + B y_2, \\ y_1 &= \dot{x}_*, \\ y_2 &= y_1(t) \int_0^t \frac{W}{y_1^2} dt. \end{aligned}$$

So, we have our $\psi(t)$ solution in terms of some functions and constants, but to find these constants, we remember that we have initial values for $\psi(t)$ (2.12). As $\psi(0) = 0$ we can see that $y_2(0) = 0$ as the integral = 0 meaning that we require $A = 0$ as $y_1(0) \neq 0$. For the second constant, we have,

$$\begin{aligned} \dot{\psi}(t) &= B \dot{y}_2(t) \\ &= BW \left(\dot{y}_1 \int_0^t \frac{1}{y_1^2} dt + \frac{1}{y_1(t)} \right) \\ \dot{\psi}(0) = 1 &= BW \frac{1}{y_1(0)} \\ \Rightarrow BW &= \dot{x}_*(0). \end{aligned}$$

Giving a full solution for $\psi(t)$ and resultant form for our determinant,

$$\det M = \psi(T) = \dot{x}_*(0)\dot{x}_*(T) \int_0^T \frac{dt}{\dot{x}_*(t)}.$$

$$\begin{aligned} \text{Remember } H = \dot{x}_*^2 - V'(x_*)^2; &= \sqrt{H + V'(x_i)^2} \sqrt{H + V'(x_f)^2} \int \frac{1}{\dot{x}_*^2} dx_*, \\ &= \sqrt{H + V'(x_i)^2} \sqrt{H + V'(x_f)^2} \int_{x_i}^{x_f} \frac{dx_*}{\dot{x}_*^2}, \\ &= \sqrt{H + V'(x_i)^2} \sqrt{H + V'(x_f)^2} \int_{x_i}^{x_f} \frac{dx_*}{(H + V'(x_*)^2)^{\frac{3}{2}}}. \end{aligned}$$

This $\det M$ term can be combined with the \mathcal{N} term to form the prefactor term that encodes the classical path's *quadratic fluctuations*,

$$A = \left(4\pi D \left| \sqrt{H + V'(x_i)^2} \sqrt{H + V'(x_f)^2} \int_{x_i}^{x_f} \frac{dx}{(H + V'(x)^2)^{\frac{3}{2}}} \right| \right)^{-\frac{1}{2}}.$$

We now have included the second-order fluctuations in our solution, meaning that our probability density function expression will be more accurate and return a fuller solution for a given system. There is a second technique to find this prefactor term by appealing to a quantum mechanical analogy, and also arrives from integrating over the quadratic fluctuations about the most probable path. What we wish to find is a measure of how much two nearby extrema paths deviate from each other, and this can be expressed in terms of the derivative of the classical path's endpoints [1][16]. It arises as a term called a Van-Vleck determinant which originally occurs as a prefactor in the WKB approximation to the quantum time evolution operator as a solution to the Schrödinger equation. In our classical picture, it is the derivative of the final endpoint with respect to the momentum at the beginning, a measure of how much the end point shifts if the momentum at the beginning changes, combining the possible fluctuations. This is the appearance of the semi-classical nature of the path integral technique, where one portion of the system is described quantum mechanically, these quadratic fluctuations, whilst the other portion of the system is

described classically, the classical path that these fluctuations exist around. For a fuller description, see books such as Schulman [2] and Goldstein [16], but here we will show that this technique returns the same solution by looking at the classical expansion of the action to the second term. This is to show that a quantum mechanical equivalence can be made between the quantum mechanical path integral technique and the classical version that this work investigates. This prefactor term has the form;

$$P(x_f, T|x_i, 0) = A \exp[-S(x_f, x_i, T)/4D]; \quad A = \left(4\pi D \left| \frac{\partial x_f}{\partial \dot{x}_i} \right| \right)^{-\frac{1}{2}}.$$

To find the prefactor A , we can use the chain rule to split the partial derivative into ones that we know or can find from equations already found. Beginning with,

$$\frac{\partial}{\partial \dot{x}_i} = \frac{\partial H}{\partial \dot{x}_i} \frac{\partial}{\partial H} = 2\dot{x}_i \frac{\partial}{\partial H} = 2\sqrt{H + V'(x_i)^2} \frac{\partial}{\partial H}.$$

To find the partial derivative with respect to H we can vary H in the T relationship and hold t constant ($\delta t = 0$):

$$\begin{aligned} t + \delta t &= \int_{x_i}^{x_f + \delta x_f} \frac{dx}{\sqrt{H + \delta H + V'^2}} \\ &= \int_{x_i}^{x_f + \delta x_f} \frac{dx}{\sqrt{H + V'^2}} \left(1 - \frac{1}{2} \frac{\delta H}{H + V'^2} \dots \right) \quad \text{expanding the square root} \\ &\approx t + \delta x_f \frac{1}{\sqrt{H + V'(x_f)^2}} - \frac{\delta H}{2} \int_{x_i}^{x_f} \frac{dx}{(H + V'^2)^{3/2}}, \end{aligned}$$

so to keep t constant, we require

$$\begin{aligned} \frac{\delta H}{2} \int_{x_i}^{x_f} \frac{dx}{(H + V'^2)^{3/2}} &\approx \delta x_f \frac{1}{\sqrt{H + V'(x_f)^2}} \\ \frac{\delta x_f}{\delta H} &= \sqrt{H + V'(x_f)^2} \cdot \frac{1}{2} \int_{x_i}^{x_f} \frac{dx}{(H + V'^2)^{3/2}}. \end{aligned}$$

Combining this into the prefactor term returns,

$$\frac{\partial x_f}{\partial \dot{x}_i} = 2\sqrt{H + V'(x_i)^2} \frac{\partial x_f}{\partial H} = \sqrt{H + V'(x_i)^2} \sqrt{H + V'(x_f)^2} \int_{x_i}^{x_f} \frac{dx}{(H + V'^2)^{3/2}}$$

Since this returns the same solution we found starting with the next term in the classical action expansion, we are on the right lines. Some may notice that in the limit $H \rightarrow 0$ if the path travels across a turning point meaning that $V' = 0$ this integral will diverge. This relates to the zero mode energy from the eigenfunction, and we will solve this divergence issue in a later chapter when we introduce the Jacobian term in chapter 4.

In conclusion, we have the following analytical equations for the probability density function using the dominant path integral formulation with the extremal action with a unit Jacobian term,

$$T = \int_{x_i}^{x_f} \frac{dy}{\sqrt{H + V'^2(y)}}$$

$$S(x_f, x_i, T) = 2(V(x_f) - V(x_i)) - HT + 2 \int_{x_i}^{x_f} \sqrt{H + V'^2(y)} dy$$

$$A = \left(4\pi D \left| \sqrt{(H + V'(x_i)^2)(H + V'(x_f)^2)} \int_{x_i}^{x_f} \frac{dy}{(H + V'(y)^2)^{3/2}} \right| \right)^{-\frac{1}{2}}$$

$$P(x_f, T|x_i, 0) = A \exp \left[-\frac{S(x_f, x_i, T)}{4D} \right] \quad (2.13)$$

These analytical solutions give the probability density function exactly for potentials up to the level of quadratic; however, for higher degree potentials the integrals are unsolvable analytically and must be numerically calculated or done approximately. To show how this representation returns the known results for simple potentials, we can solve the two simplest potentials, $V(x) = 0$, $V(x) = bx$.

2.1.1 Flat potential: $V(x) = 0$

The simplest system that exists is a flat potential meaning that $V'(x) = 0$. First, we can find the time taken in relation to the initial and final positions along with the energy,

$$T = \int_{x_i}^{x_f} \frac{dx}{\sqrt{H}} = \frac{(x_f - x_i)}{\sqrt{H}}.$$

This can then be rearranged for the energy H ,

$$H = \frac{(x_f - x_i)^2}{T^2}.$$

This can be seen to be analogous to the energy due to kinetic energy, $E = \frac{1}{2}mv^2$, as there is no potential energy with the flat potential and $v = \frac{\Delta x}{\Delta t}$. Now looking at the expression for the action S ,

$$\begin{aligned} S &= -HT + 2 \int_{x_i}^{x_f} \sqrt{H} dx, \\ &= -\frac{(x_f - x_i)^2}{T} + 2\sqrt{H}(x_f - x_i), \\ &= \frac{(x_f - x_i)^2}{T}. \end{aligned}$$

Then calculating the prefactor term

$$A = \left(4\pi D \sqrt{H} \sqrt{H} \int_{x_i}^{x_f} \frac{dy}{H^{\frac{3}{2}}} \right)^{-\frac{1}{2}} = \left(\frac{4\pi D(x_f - x_i)}{\sqrt{H}} \right)^{-\frac{1}{2}} = \frac{1}{\sqrt{4\pi DT}},$$

which, when combined gives the probability density function as

$$P(x_f, T | x_i, 0) = \sqrt{\frac{1}{4\pi DT}} \exp \left[-\frac{(x_f - x_i)^2}{4DT} \right].$$

In this system, the Jacobian term that arises from the change in variables in the original derivation is still 1, so it does not affect the solution, but it will be needed when we step up the complexity of the potential. This is the standard Gaussian

result [69], and is the Green's function for the heat equation, $\frac{\partial P}{\partial t} = D \frac{\partial^2 P}{\partial x^2}$. We can solve this heat equation using standard methods to show that the path integral technique returns the correct result. Using the Fourier transform,

$$\begin{aligned} \frac{\partial P}{\partial t} &= D \frac{\partial^2 P}{\partial x^2}, \\ \text{Fourier transform } \dot{\bar{P}} &= -Dk^2 \bar{P}, \\ \bar{P} &= A \exp(-Dk^2 t). \end{aligned}$$

We can calculate A by using the initial condition of the probability, $P(x, t = 0) = \delta(x - x_i)$, which in Fourier becomes,

$$\begin{aligned} \bar{P}(t = 0) &= \frac{1}{\sqrt{2\pi}} \int_{-\infty}^{\infty} \delta(x - x_i) \exp(ikx) dx \\ \Rightarrow A &= \frac{1}{\sqrt{2\pi}} \exp(ikx_i) \\ \bar{P} &= \frac{1}{\sqrt{2\pi}} \exp(-Dtk^2 + ikx_i) \end{aligned}$$

Doing the inverse transform can calculate the probability density function, using standard Gaussian integral identities along with completing the square,

$$\begin{aligned} P &= \frac{1}{\sqrt{2\pi}} \int_{-\infty}^{\infty} \bar{P} \exp(-ikx) dk \\ &= \frac{1}{\sqrt{2\pi}} \int_{-\infty}^{\infty} \frac{1}{\sqrt{2\pi}} \exp(-Dtk^2 - ik(x - x_0)) dk, \\ &= \frac{1}{2\pi} \sqrt{\frac{\pi}{Dt}} \exp\left(\frac{(-i(x - x_0))^2}{4Dt}\right), \end{aligned}$$

$$P(x_f, T | x_i, 0) = \sqrt{\frac{1}{4\pi DT}} \exp\left[-\frac{(x_f - x_0)^2}{4DT}\right].$$

This shows that the path integral technique agrees with the standard methods.

2.1.2 Linear Potential: $V(x) = bx$

The next complication level is adding some potential to the system; in this case, it will have a non-zero gradient, $V'(x) = b$. Again beginning with the time integral to find the relationship between energy and time,

$$T = \int_{x_i}^{x_f} \frac{dx}{\sqrt{H + b^2}} = \frac{(x_f - x_i)}{\sqrt{H + b^2}}.$$

Rearranging for H ,

$$H = \frac{(x_f - x_i)^2}{T^2} - b^2.$$

Substituting into the action equation S and calculating the integral

$$\begin{aligned} S &= 2b(x_f - x_i) - \frac{(x_f - x_i)^2}{T} + b^2T + 2 \int_{x_i}^{x_f} \sqrt{H + b^2} dx, \\ &= 2b(x_f - x_i) - \frac{(x_f - x_i)^2}{T} + b^2T + 2(x_f - x_i)\sqrt{H + b^2}, \\ &= 2b(x_f - x_i) + \frac{(x_f - x_i)^2}{T} + b^2T. \end{aligned}$$

Last but not least, the prefactor calculation,

$$\begin{aligned} A &= \left(4\pi D \sqrt{(H + b^2)(H + b^2)} \int_{x_i}^{x_f} \frac{dy}{(H + b^2)^{3/2}} \right)^{-\frac{1}{2}}, \\ &= \frac{1}{\sqrt{4\pi D \frac{(x_i - x_f)}{\sqrt{H + b^2}}}} \\ &= \frac{1}{\sqrt{4\pi DT}}, \end{aligned}$$

which, when all substituted into the probability density function equation gives,

$$\begin{aligned} P(x_f, T | x_i, 0) &= \sqrt{\frac{1}{4\pi DT}} \exp \left[-\frac{(x_f - x_i)^2 + 2b(x_f - x_i)T + b^2T^2}{4DT} \right], \\ &= \sqrt{\frac{1}{4\pi DT}} \exp \left[-\frac{((x_f - x_i) + bT)^2}{4DT} \right]. \end{aligned}$$

This is the drifting Gaussian and the solution for a linear potential from solving the Smoluchowski equation directly [33]. This shows that the path integral formalism does solve the simplest of potentials; anything more complicated we will need another piece of the puzzle, the Jacobian term, which we will investigate in chapter 4.

2.1.3 The long time limit

So we have shown that our analytical form of the probability returns the correct result for both the flat and linear potentials. Does this form also return the correct long-time limit? This is because many systems are interested in the dynamics of the equilibrated state. The expected behaviour of the system would be that at equilibrium the probability density function will be proportional to the Boltzmann distribution $\exp\left(-\frac{V(x_f)}{D}\right)$ [60], so, does our probability density function also return the correct proportionality?

The long time limit, $T \rightarrow \infty$, corresponds to our energy value tending towards zero, $H \rightarrow 0$. This is due to the integral relationship that we have found previously between time T and the energy H , (2.10), and for a particle to take an infinite amount of time to travel a distance it must have infinitesimally small amounts of energy in the effective potential. To show that this is true, we can look at (2.10) and see what happens when $H \rightarrow 0$, where γ is the path taken;

$$T = \int_{\gamma} \frac{dy}{\sqrt{H + V'(y)^2}} \Rightarrow_{H \rightarrow 0} \int_{\gamma} \frac{dy}{|V'(y)|}$$

and $T \rightarrow \infty$ for all paths that cross a maximum or minimum of the potential, which will happen for equilibrated systems as the particles will “settle” at the base of a potential well at a long time, “ $H \rightarrow 0 \Rightarrow T \rightarrow \infty$ ”.

What figure 2.4 shows is for $H \rightarrow 0$ ($T \rightarrow \infty$), the particle will spend infinite time in the real potential diffusing in the wells or peaks of the potential which maps to the particle spending infinite time at the peaks of the effective potential. In terms

of Hamiltonian mechanics, this means that the path will only have enough energy to travel over the peaks accumulating infinite time at the peaks shown.

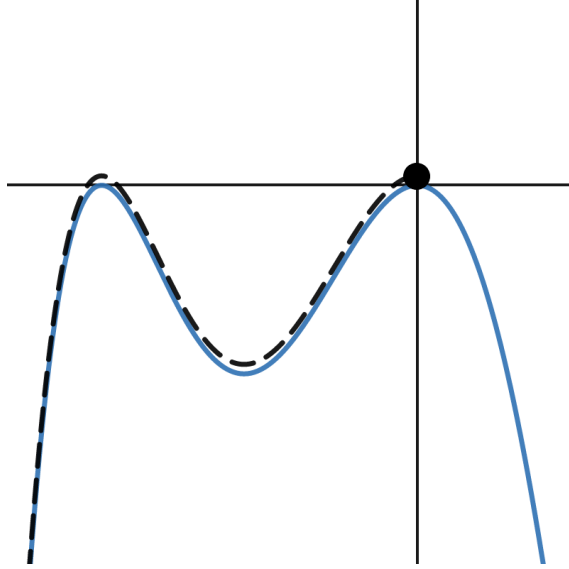


Figure 2.4: A path in the effective potential for a cubic potential, spending infinite time at the peaks of the effective potential, $H \rightarrow 0$

To see whether a given path returns the proportional long-time limit exponential relationship, we only need to look at the action as that is the exponential form and the prefactor A will not affect the exponent proportionality. First, we need to know what happens to the HT term in the action, as in the $H \rightarrow 0$ limit, it will become $0 \cdot \infty$ and we need to discern what the limit will be. Looking at HT ,

$$\begin{aligned}
 HT &= \int_{\gamma} \frac{H dy}{\sqrt{H + V'(y)^2}}, \\
 &= \sqrt{H} \int_{\gamma} \frac{dy}{\sqrt{1 + \frac{V'(y)^2}{H}}}, \\
 \lim_{H \rightarrow 0} \frac{V'(y)^2}{H} &= \infty \\
 \Rightarrow \lim_{H \rightarrow 0} HT &= 0.
 \end{aligned}$$

In the case that $V'(y)^2 = 0$ meaning $\lim_{H \rightarrow 0} \frac{V'(y)^2}{H} = 0$ HT still tends to 0 due to

the factor of \sqrt{H} out front of the expression. The long time limit for the action is,

$$S_{H \rightarrow 0} = 2V(x_f) - 2V(x_i) + 2 \int_{x_i}^{x_f} |V'(y)| dy.$$

Therefore, the long time limit depends on the potential gradient at the beginning and end points. If we have a system that starts and ends on an uphill portion of a potential, then $|V'(y)| = V'(y)$ for the entire integral, e.g. figure (2.5).

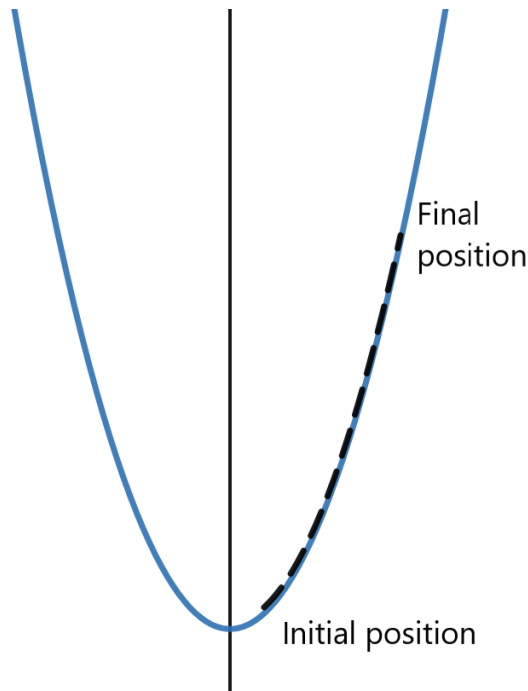


Figure 2.5: Path example on only the positive portion of the potential

Calculating the action for this system,

$$\begin{aligned} S_{H \rightarrow 0} &= 2V(x_f) - 2V(x_i) + 2 \int_{x_i}^{x_f} V'(y) dy \\ &= 2V(x_f) - 2V(x_i) + 2V(x_f) - 2V(x_i) \\ &= 4V(x_f) - 4V(x_i). \end{aligned}$$

This means that the probability will have a long time limit

$$P_{H \rightarrow 0} \propto \exp\left(-\frac{V(x_f) - V(x_i)}{D}\right).$$

This situation recovers the correct long-time limit, which is proportional to Boltzmann distribution, but what happens if we begin and end on the downhill portion of the potential? Figure (2.6) shows in this situation $|V'(y)| = -V'(y)$.

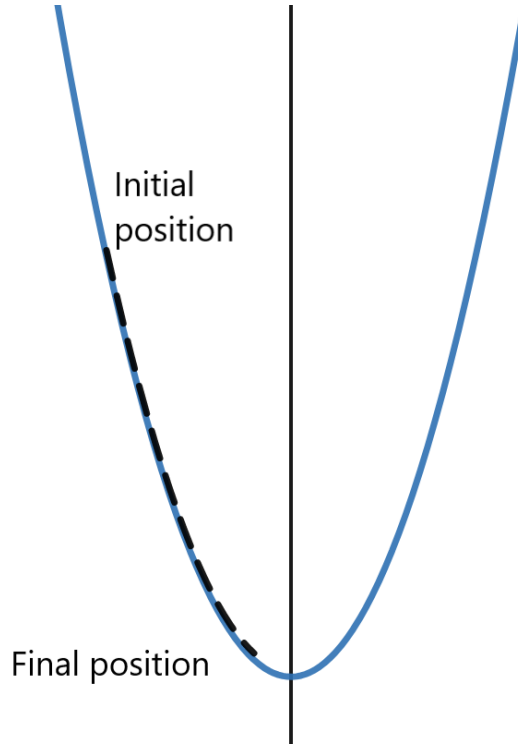


Figure 2.6: Path example on only the negative portion of the potential

Calculating the action for this system,

$$\begin{aligned}
 S_{H \rightarrow 0} &= 2V(x_f) - 2V(x_i) - 2 \int_{x_i}^{x_f} V'(y) dy \\
 &= 2V(x_f) - 2V(x_i) - 2V(x_f) + 2V(x_i) \\
 &= 0.
 \end{aligned}$$

This means that the long time limit does not return the correct equilibrium distribution. This makes physical sense, as for the longest finite time solution, the particle descends the potential under the influence of $V(x)$ meaning no fluctuations. However, in terms of the infinite-time solution, this does not make physical sense. How can a particle “hover” near the final position when what the potential wants to do is “pull” the particle to the bottom of the hill? So there must be something

else going on to give an infinite-time solution! This mystery is shown further in the effective potential plots of the above systems. Figures 2.7a and 2.7b show the corresponding paths in the effective potential. These graphs show that for particles in the effective potential, which obey Hamiltonian mechanics, there will not be an energy value that will allow the particle to reach an infinite time limit, as there will be a maximum energy for this path when the particle comes to rest at the final position, $H_{max} = -V'(x_f)^2$. For the uphill path, to return the maximum time, the particle is released at rest from the initial position, whereas for the downhill path, the particle is released with enough energy to reach the final position at rest. This allows the longest time to be reached, but what if we want a time longer than this?

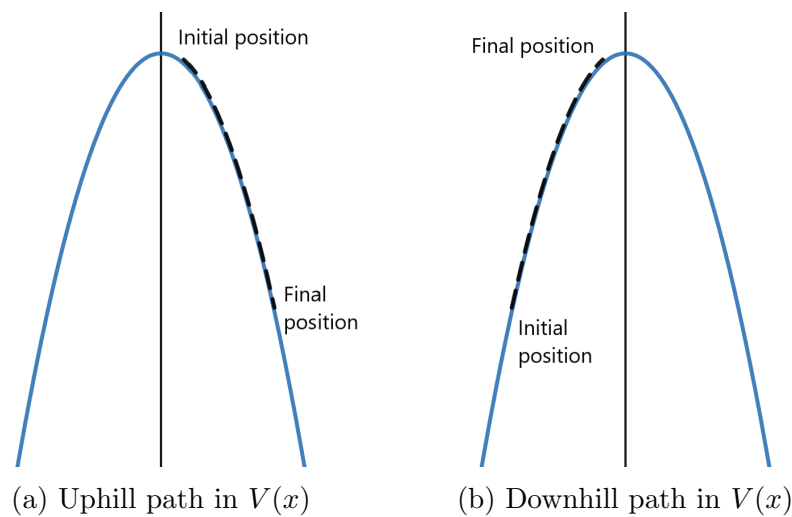


Figure 2.7: Paths in the effective potential, $\mathcal{V}(x)$, for the harmonic potential, graphically illustrating the issues that the paths have in reaching infinite time.

Whereas if we compare this system to the quadratic potential, there is an infinite time solution for the harmonic potential, the Ornstein-Uhlenbeck solution, which is valid for all times and initial and final positions. Does this mean that there is information about how the system works that is being missed in the standard Ornstein-Uhlenbeck solution that the path integral formulation may be able to provide? Will the path integral provide the solution to how initial and final positions we have just explored can survive in the long time limit and make intuitive sense? This

is a question that we will ponder for now and revisit in chapter 5 when we resolve this flaw in the representation after concentrating on another major element of the puzzle, the Jacobian in chapter 4, which will also be affected by the introduction of the *turning path*.

We have seen the introduction of the path integral and the first few pieces needed to understand the dynamics of a given system fully. We have used an effective potential to find information about the dominant paths in the transition and their corresponding energies for a given time to traverse the path and used the equivalent solution to solve the flat and sloped potential systems. These derivations return the known solutions for these systems. This interpretation has been investigated previously in works such as “Path integrals and non-Markov processes” by Luckock and McKane [70], or in “Path integrals for stochastic processes” by Wio [1]. However, they stop short of a full interpretation of a given system and focus on calculating rates for systems to be subsequently used in simulations. What this work has begun to show and will continue to is the use of this interpretation to provide a more physical sense of how paths interact in a given system, and the following chapters show how each element is used to calculate complete expressions for general potentials. At the end of this chapter, we discovered that our formulation only sometimes produces the full solution in certain situations, namely the long time limit. This inconsistency and the mystery of the Jacobian term, which we have not investigated fully, will be explored in chapter 4 and chapter 5 with a more in-depth discussion and exploration. But first, we will look at how the path integral can provide a numerical solution for the probability density function. This useful tool will be used in later chapters to compare results with visual representations of worded arguments, showing the versatility of the path integral technique.

Chapter 3

Numerical Solution using Path Integrals

As stated in chapter 2, there are exact solutions to the Smoluchowski equation up to quadratic potential. The difficulty comes in increasing this to cubic potentials or more complicated potentials as there are no exact solutions. Whilst we will endeavour to find a full general potential solution for the PDF, we can also use numerical techniques to use the path integral to explore these more complicated potentials. There are already a few techniques to do this, but what follows is the introduction of another technique, first developed in Baibuz's et al. paper "Diffusion in a potential field: Path-Integral approach" [71] in 1980, which uses the concept of paths to construct a matrix equation that can be iterated for a given time frame to solve for a PDF. In this chapter, we will follow this derivation and recreate the results from the original paper, then we extend it to more complicated potentials and look at methods to speed up the technique and other interesting applications of the technique. We then briefly explore whether this technique can be extended to two dimensions and provide preliminary proof of concept results.

3.1 The method

The method outlined in [71] finds a numerical path integral representation for the probability density function, which solves the Smoluchowski equation,

$$\frac{\partial P(x, t|x_i, 0)}{\partial t} = \frac{\partial}{\partial x} \left[\frac{dV(x)}{dx} P(x, t|x_i, 0) + D(x) \frac{\partial P(x, t|x_i, 0)}{\partial x} \right], \quad (3.1)$$

$$P(x, 0|x_i, 0) = \delta(x - x_i),$$

where $P(x, T|x_i, 0)$ is the probability that a particle travels from position x_i to position x in time T , $V(x)$ is the one-dimensional potential that the particle is travelling in and $D(x)$ is the diffusion coefficient, which for simplicity is a constant in our systems $D(x) = D$, with the initial condition being a delta function at x_i .

In order to solve higher-order systems, above the quadratic, the Smoluchowski equation can be solved using matrices, which involves discretising both the spatial coordinates and the time steps. Slicing up the journey in this way, into smaller and smaller jumps, means that we can treat each jump as a journey in a linear system, $V(x_i + \epsilon) \approx V(x_i) + \epsilon V'(x_i)$, for which an analytical solution can be found 3.1.

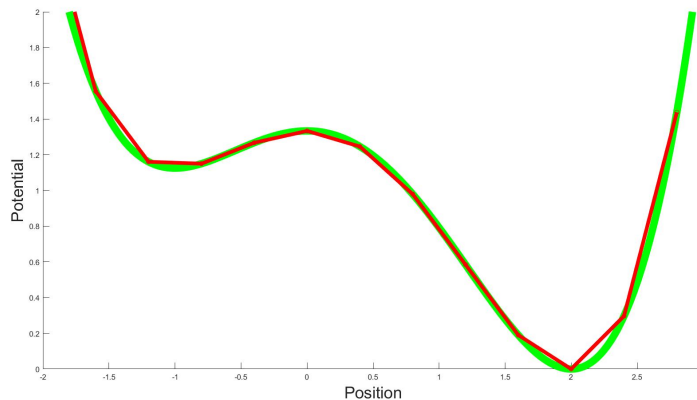


Figure 3.1: The linear approximation discretisation

The technique begins with a transformation of the Smoluchowski equation,

$$P(x, t|x_i, 0) = \exp \left[-\frac{V(x) - V(x_i)}{2D} \right] Q(x, t|x_i, 0), \quad (3.2)$$

when substituted into (3.1), this gives

$$-\frac{\partial Q}{\partial t} = \left[-D \frac{\partial^2}{\partial x^2} + \frac{V_{\text{Baibeff}}(x)}{2D} \right] Q, \quad (3.3)$$

where V_{Baibeff} is the effective potential from [71] defined as,

$$V_{\text{Baibeff}}(x) = \frac{[V'(x)]^2}{2} - DV''(x). \quad (3.4)$$

This “effective” potential is different to the one we have defined previously in the analytical path integral solution. However, it is only different by a factor of 2 along with the additional term from the second derivative of the potential. (3.3) is a partial differential equation, similar in form to a Schrödinger equation again showing the semi-classical nature of path integrals in which there are comparisons that can be made between quantum mechanic techniques and stochastic processes. It is easier to solve than the full Smoluchowski equation and has a solution which satisfies (3.3) in the small time limit, $t \rightarrow 0$,

$$Q(x, t|x_i) = \frac{1}{\sqrt{4\pi Dt}} \exp \left[-\frac{(x - x_i)^2}{4Dt} - \frac{t(V_{\text{Baibeff}}(x) + V_{\text{Baibeff}}(x_i))}{4D} \right]. \quad (3.5)$$

Note that this quantity is time reversible, meaning that we can switch the initial and final position and return the same value of Q . This useful property will prove helpful and be used later in this chapter. We only require the above equation to satisfy the transformed Smoluchowski equation (3.3) in the small time limit, because when we discretise both time and space, we are treating each jump over a small distance and a small time. This jump can be thought of as being approximated by a linear potential in which this representation of the probability returns the correct form, the Gaussian drift solution [72].

We can do a check to see whether this form does return the correct solution if the potential itself was linear, $V(x) = \alpha x$, meaning that $V_{\text{Baibeff}} = \frac{\alpha^2}{2}$ giving,

$$Q(x, t|x_i) = \frac{1}{\sqrt{4\pi Dt}} \exp \left[-\frac{(x - x_i)^2}{4Dt} - \frac{t\alpha^2}{4D} \right],$$

$$P(x, t|x_i) = \exp \left[-\frac{\alpha(x - x_i)}{2D} \right] Q(x, t|x_i),$$

$$P(x, t|x_i) = \frac{1}{\sqrt{4\pi Dt}} \exp \left[-\frac{(x - x_i + \alpha t)^2}{4Dt} \right].$$

Returning to how it will act with a general potential, we need to spatially discretise, and we can use a probability identity,

$$P(x, 2t|x_i) = \int_{-\infty}^{\infty} P(x, t|y)P(y, t|x_i)dy,$$

which describes the fact that we can split up a path into all possible paths between two points by integrating over all intermediate points to find a full probability.

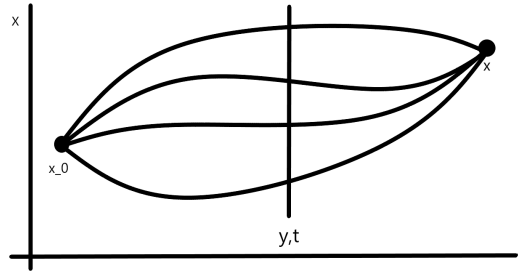


Figure 3.2: Showing a few of the possibilities of paths between the initial and final position for two timesteps

This identity makes sense as it integrates over all possible positions that a path goes through at the midpoint in terms of time. We can then substitute in our transformation (3.2) to see if the identity holds for Q ,

$$\exp\left(\frac{V(x_i) - V(x)}{2D}\right) Q(x, 2t|x_i) = \int_{-\infty}^{\infty} \exp\left(\frac{V(y) - V(x)}{2D}\right) Q(x, t|y) \exp\left(\frac{V(x_i) - V(y)}{2D}\right) Q(y, t|x_i) dy,$$

The cancellation of $V(y)$ in the exponential is apparent as is the $\Delta V = V(x) - V(x_i)$, leading to the identity

$$Q(x, 2t|x_i) = \int_{-\infty}^{\infty} Q(x, t|y) Q(y, t|x_i) dy. \tag{3.6}$$

This identity can then be extended to n time steps and integrated over all possible positions for every timestep, $T = t * n$ 3.3,

$$Q(x, T|x_i) = \int \dots \int Q(x, t|x_{n-1}) Q(x_{n-1}, t|x_{n-2}) \dots Q(x_1, t|x_i) dx_1 \dots dx_{n-2} dx_{n-1}. \tag{3.7}$$

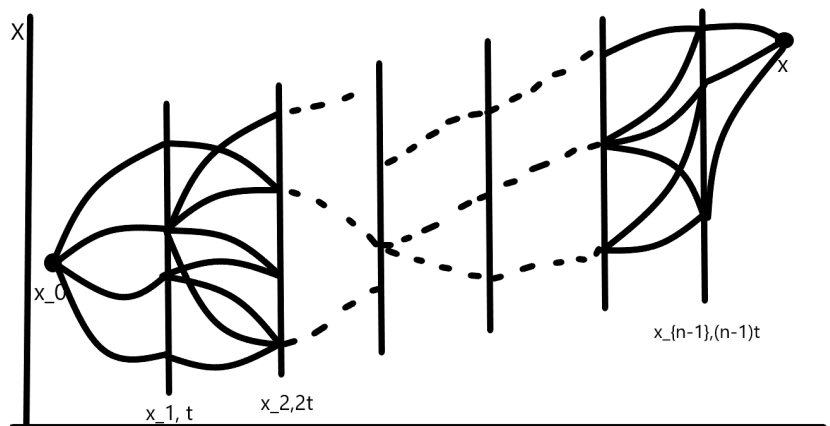


Figure 3.3: n possible time segmentations with possible paths

To evaluate this integral numerically within a reasonable computational time, we need to truncate the x values that the integrals, are bounded by as infinite limits would lead to infinite computation time. For example, we only have to evaluate

between $x = \pm 3$ if the potential wells of the potential are at $x = \pm 1$ as the density $Q(x, t|x_i)$ becomes negligible far away from the potential wells. This is because far away from the bottom of the wells the potential gradient becomes steeper and steeper, so it becomes unlikely that particles will diffuse up the potential that far. As we can set limits to the variable x , we can make it discrete by segmenting it into M equal steps of width Δ , within the range $x \in (-\frac{M\Delta}{2}, \frac{M\Delta}{2})$. The effect of making x discrete means that the continuous function $Q(x, t|x_0)$ becomes a discrete matrix $Q(x_j, t|x_k)$. We can then rewrite the integrals using the Riemann sum[73], for example equation (3.6) becomes

$$Q(x, 2t|x_0) = \sum_{j=-\frac{M}{2}}^{\frac{M}{2}} Q(x, t|j\Delta)Q(j\Delta, t|x_0)\Delta.$$

This sum is just the integrand evaluated at a discrete set of points with even spacing, Δ , cut off at $\pm\frac{M\Delta}{2}$ where $Q(x_j, t|x_k) = Q_{jk}$ is small enough to be neglected. This sum can also be thought of as a product of two vectors, $\underline{a} \cdot \underline{b} = \sum_j a_j b_j$, [74] with

$$Q(x, 2t|x_0) = \underline{a} \cdot \underline{b}\Delta \tag{3.8}$$

$$\underline{a} = \begin{pmatrix} Q(x, t|\frac{M\Delta}{2}) \\ Q(x, t|(\frac{M}{2}-1)\Delta) \\ \vdots \\ Q(x, t|-\frac{M\Delta}{2}) \end{pmatrix} \quad \underline{b} = \begin{pmatrix} Q(\frac{M\Delta}{2}, t|x_0) \\ Q((\frac{M}{2}-1)\Delta, t|x_0) \\ \vdots \\ Q(-\frac{M\Delta}{2}, t|x_0) \end{pmatrix}.$$

This can be extended, and the time segmentation split into three parts in order to see how the matrix structure starts to unfold:

$$\begin{aligned} Q(x, 3t|x_i) &= \int \int Q(x, t|y_2)Q(y_2, t|y_1)Q(y_1, t|x_0)dy_1dy_2 \\ &= \sum_{k=-\frac{M}{2}}^{\frac{M}{2}} Q(x, t|k\Delta) \left[\sum_{j=-\frac{M}{2}}^{\frac{M}{2}} Q(k\Delta, t|j\Delta)Q(j\Delta, t|x_i) \right] \cdot \Delta^2 \end{aligned}$$

$$\begin{aligned}
 &= \begin{pmatrix} Q(x, t | \frac{M\Delta}{2}) \\ Q(x, t | (\frac{M}{2} - 1)\Delta) \\ \vdots \\ Q(x, t | -\frac{M\Delta}{2}) \end{pmatrix}^T \begin{pmatrix} \sum_{i=-\frac{M}{2}}^{\frac{M}{2}} Q(\frac{M\Delta}{2}, t | i\Delta) Q(i\Delta, t | x_i) \\ \vdots \\ \sum_{i=-\frac{M}{2}}^{\frac{M}{2}} Q(-\frac{M\Delta}{2}, t | i\Delta) Q(i\Delta, t | x_i) \end{pmatrix} \cdot \Delta^2. \\
 &= \begin{pmatrix} Q(x, t | \frac{M\Delta}{2}) \\ Q(x, t | (\frac{M}{2} - 1)\Delta) \\ \vdots \\ Q(x, t | -\frac{M\Delta}{2}) \end{pmatrix}^T \begin{pmatrix} Q(\frac{M\Delta}{2}, t | \frac{M\Delta}{2}) & \dots & Q(\frac{M\Delta}{2}, t | -\frac{M\Delta}{2}) \\ \vdots & \vdots & \vdots \\ Q(-\frac{M\Delta}{2}, t | \frac{M\Delta}{2}) & \dots & Q(-\frac{M\Delta}{2}, t | -\frac{M\Delta}{2}) \end{pmatrix} \\
 &\cdot \begin{pmatrix} Q(\frac{M\Delta}{2}, t | x_i) \\ Q((\frac{M}{2} - 1)\Delta, t | x_i) \\ \vdots \\ Q(-\frac{M\Delta}{2}, t | x_i) \end{pmatrix} \cdot \Delta^2.
 \end{aligned}$$

This shows that segmenting the time into three steps results in the multiplication of two vectors and a matrix. The matrix is not dependent on the initial and final positions, meaning it only needs to be calculated once, helping reduce computation time. Extending this further to the full n segments in time results in the final representation being defined as

$$\begin{aligned}
 &Q(x_f, T | x_i, 0) = \\
 &\begin{pmatrix} 0 & \dots & 1 & \dots & 0 \end{pmatrix} \begin{pmatrix} Q(\frac{M\Delta}{2}, t | \frac{M\Delta}{2}) & \dots & Q(\frac{M\Delta}{2}, t | -\frac{M\Delta}{2}) \\ \vdots & \vdots & \vdots \\ Q(-\frac{M\Delta}{2}, t | \frac{M\Delta}{2}) & \dots & Q(-\frac{M\Delta}{2}, t | -\frac{M\Delta}{2}) \end{pmatrix}^n \begin{pmatrix} 0 \\ \vdots \\ 1 \\ \vdots \\ 0 \end{pmatrix} \cdot \Delta^{n-1}
 \end{aligned}$$

where $\begin{pmatrix} 0 \\ \vdots \\ 1 \\ \vdots \\ 0 \end{pmatrix}$ and $\begin{pmatrix} 0 & \dots & 1 & \dots & 0 \end{pmatrix}$ are projections onto the initial and final states.

We can write this more concisely as $Q(x_f, T|x_i, 0) = \frac{1}{\Delta} \underline{x}_f R^n \underline{x}_i$, where R is equal to the central matrix multiplied by Δ .

3.2 Reducing the computation time

One of our reasons for wanting to use path integrals to solve the Smoluchowski equation numerically is speed. Other approaches to studying stochastic processes, e.g. Monte Carlo methods, have issues with getting the simulation to run long enough for the rare interesting events to occur. This issue has meant that methods have been formulated to allow a rare event to be calculated within a realistic computational timeframe. For example, a technique called forward flux sampling can be used to artificially insert intermediate states and allow incremental progress towards the rare event, in which the relevant properties of the system can be found [20][21]. Other techniques may artificially enhance different aspects of the system, making the rare events more likely to occur in the given time frame and computational limitations then relevant properties are found using these enhanced systems, for example temperature-accelerated dynamics [75] or artificially modifying the potential [76]. The speed issue will become apparent for the numerical path integral technique as the number of dimensions increases.

For every increase in dimension, the matrix calculations become larger and larger, as the matrix size is taken to the dimensional power. Also, the off-diagonal elements become more numerous due to the increase of possible jumps in a single timestep.

Reducing the computation cost now when it is not too great will mean the benefits are magnified in higher dimensions. We will now look at a couple of techniques that can decrease the computation time for the calculations.

3.2.1 Diagonalising the matrix

The first technique is that of diagonalisation. As the equation to find $Q(x_f, T|x_0, 0) = \frac{1}{\Delta} \underline{x}_f R^n \underline{x}_i$ is taking a fixed matrix to the power of n the technique of diagonalising the matrix will allow the computing language to reduce its computation capacity needed to calculate such a large matrix multiplication [77]. The ability to use the languages built in eigenvalue finder means that we can utilise the fact that the matrix R is diagonalisable as it is symmetric, meaning we can use the fact that

$$R = PDP^{-1}$$

$$R^n = PD^nP^{-1}$$

where \mathcal{D} is the matrix of eigenvalues on the diagonal and P is a matrix of the corresponding eigenvectors. Using this technique means there is no need to compute a large matrix multiplication instead, take the eigenvalues to the power n and then a simpler matrix multiplication. This is because of the properties of a diagonal matrix,

$$D = \begin{pmatrix} a & 0 & 0 & \dots \\ 0 & b & 0 & \dots \\ 0 & 0 & c & \dots \\ \vdots & \vdots & \vdots & \vdots \end{pmatrix}, \Rightarrow D^n = \begin{pmatrix} a^n & 0 & 0 & \dots \\ 0 & b^n & 0 & \dots \\ 0 & 0 & c^n & \dots \\ \vdots & \vdots & \vdots & \vdots \end{pmatrix}.$$

To compare how this diagonalisation technique reduces the computational time, we run the calculations twice, once taking the matrix to the power n and the other with the diagonalisation technique. Doing this for a probability density function

for a tilted double-well potential, returning five different timesteps to see how the PDF evolves over time, gives 3.9s for the brute force method compared to 2.4s for the diagonalisation technique. This shows that this technique does reduce the computational time by a significant amount for this specific system in one dimension, however, it should be a valid technique for all systems due to the underlying structure of the matrix which is always symmetric no matter the potential or the parameters.

3.2.2 Only calculating nearest neighbours

A second technique to reduce computation time is using only the most relevant nearest neighbours. As the timesteps used tend to be very small, the probability for the particle to travel more than a relatively small number of positions in either direction tends towards zero quickly as we get further away from the relevant initial position. Secondly, some of the pairings of initial and final positions in the jumps do not always make physical sense. For example, if they are on separate sides of an energy barrier, the $Q(x_f, t|x_i)$ calculation will not consider the presence of the barrier, leading to errors in the probability value, figure (3.4).

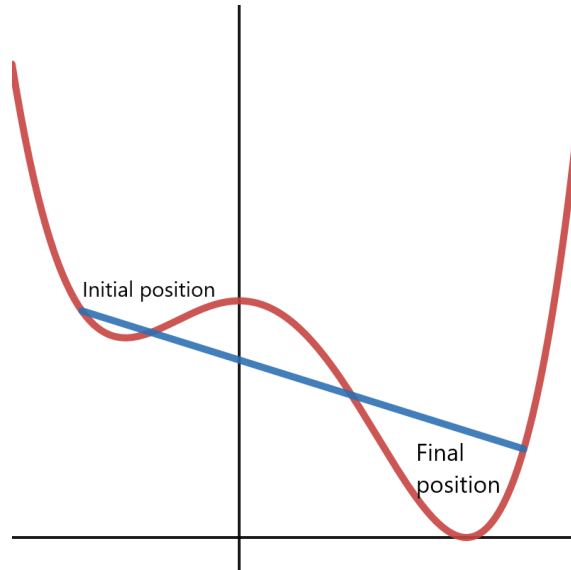


Figure 3.4: A straight line approximation showing it can miss the potential barrier, not taking into account the crucial element of the system.

This means that we may not need to calculate the transition probability between every pair of points, thus reducing the number of calculations required to build

the R matrix, and subsequently the diagonalisation method. To find the critical value of nearest neighbours, we keep reducing the number of entries calculated in the matrix, which represents the possible jumps in a one-time step that the particle could take. Initially, this was done for a single time and single initial position and compared each number of nearest neighbours with the density calculated with the full matrix. Through these calculations, the minimum number of nearest neighbours needed to conserve both the shape and the area under the curve for the probability in a double well potential is 8. The solution found using eight nearest neighbours was checked against the full solution, and table (3.1) shows the comparison between the number of nearest neighbours less than eight and the area underneath the probability curve at the same time. This indicates that it takes the known eight neighbours to conserve the normalisation of the probability density function up to four decimal places. We can also visually compare the probability density functions at different timesteps for the full matrix vs the reduced matrix which only calculated the eight nearest neighbours. This is shown in figure 3.5, and it shows that there is no visible difference for this system at these timesteps between the full probability and the use of just the 8 nearest neighbours. The choice of parameters and discretization was so that the probability density function was normalised and the simulation ran in a reasonable time. If D was smaller then more timesteps would be needed to reach equilibrium, whilst a larger D would lead to some transient states being missed as the probability evolves too quickly.

Number of nearest neighbours	Area under the graph
1	2.6202×10^{-142}
2	1.2814×10^{-32}
3	9.9420×10^{-6}
4	0.3149
5	0.9307
6	0.9973
7	0.9999
8	1.0000

Table 3.1: Table showing the effect of reducing nearest neighbours on the normalisation of the probability curve - $dt = 0.0005$, $dx = 0.01$, $D = 0.1$

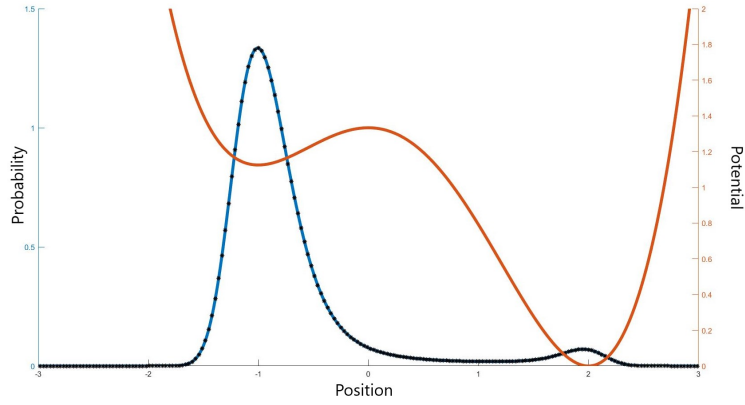
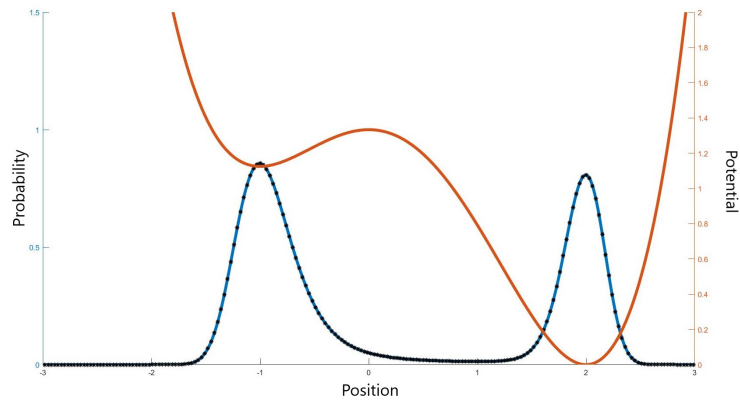
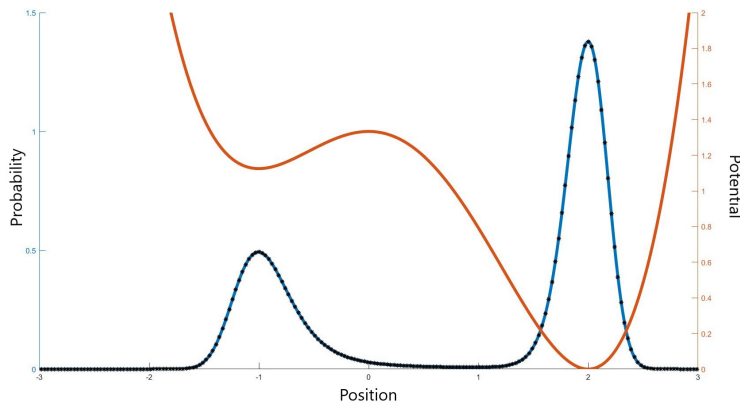

 (a) $T = 5$

 (b) $T = 25$

 (c) $T = 50$

Figure 3.5: Comparison between the full probability density function, in blue —, overlain with the nearest neighbour probability, in black ·, showing no difference between the two results. $dt = 0.0005$, $dx = 0.01$, $D = 0.1$

Both of these results show that for the tilted double well potential, $V(x) = \frac{x^4}{8} - \frac{x^3}{6} - \frac{x^2}{2} + \frac{4}{3}$, it is possible to reduce the number of necessary calculations and include only 17 non-zero entries per row in the matrix instead of M . The reduction in the number of nearest neighbours will, in turn, make diagonalisation quicker and

more straightforward, as the number of calculations needed to find eigenvalues and eigenvectors is reduced in Matlab's algorithms. This number of nearest neighbours is only valid for the titled double well potential. Other potentials may need more or less to retain the necessary accuracy needed for an accurate representation of the probability density function.

Both of these techniques, diagonalisation and nearest neighbours, make a reasonable reduction of computation time for this specific set of parameters and potential which is only slightly noticeable in one dimension, but the mechanisms should work for general parameters and potentials. This is because the diagonalisation technique is always valid due to the structure of the matrix, whilst the nearest neighbour technique would need to be investigated for each specific system, and the corresponding number found. For a single time step, there was a reduction in running time from 2.3s down to 0.95s, which is a good improvement but the effect should be amplified in higher dimensions. This is because an increase of dimension will increase the power of the matrix size, $M \times M$ in one dimension to $M^2 \times M^2$ in two dimensions, where M is the number of spatial discretisations calculated, a line in one dimension and a square in two. We will discuss these possibilities of computational reduction in section 3.5 where we consider the two-dimensional case.

3.3 Initial results

Using the equation for the probability density function, and a quicker algorithm, a Matlab code was written to handle the matrix calculations and subsequent plotting of the results. The potentials and analytical solutions we will compare against are the same used in the original Baibuz paper [71], to get a direct comparison. First of all, is the comparison to a symmetric double well potential, figure (3.6) with analytical solutions derived for initial and final probability density functions. The system has potential

$$V(x) = \frac{x^4}{4} - \frac{x^2}{2} + \frac{1}{4}, \quad (3.9)$$

with a diffusion value of $D = 1$ and an initial position $x_0 = -1$.

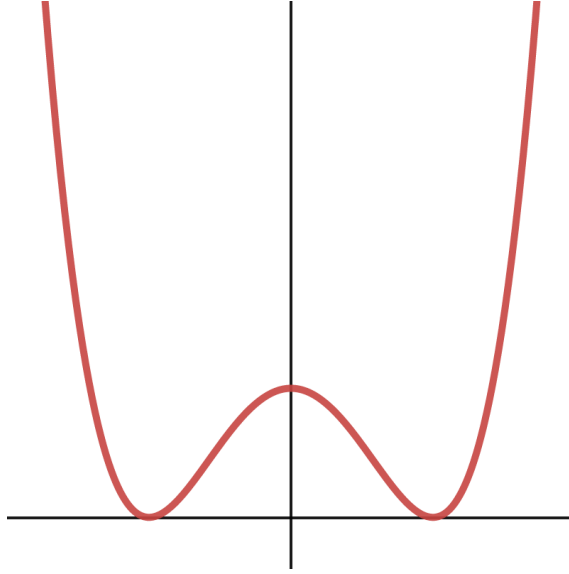


Figure 3.6: Symmetric double well potential

The two-time points we can find an analytical solution, to compare the numerical results with are the small time and long time limits. The small time approximation is achieved by approximating the potential to a quadratic potential expanded around the initial position, as very little density will have crossed the barrier, so we can act as if the second well does not exist.

We use the known Ornstein-Uhlenbeck solution [67] to find the probability,

$$V(x) \approx (x + 1)^2$$

$$P_{T_{\text{small}}}(X, T|x_0) \approx \left(\frac{1}{\pi D(1 - e^{-4T})} \right)^{\frac{1}{2}} \exp \left[-\frac{(x + 1)^2}{D(1 - e^{-4T})} \right]. \quad (3.10)$$

The long-time stationary solution is obtained by setting the left-hand side of the Smoluchowski equation (3.1) to zero, i.e. $\frac{\partial}{\partial t} P_{\text{eq}} = 0$, which satisfies the equation,

$$0 = \frac{d}{dx} [V'(x)P_{\text{eq}}(x) + DP'_{\text{eq}}(x)],$$

$$A = V'(x)P_{\text{eq}}(x) + DP'_{\text{eq}}(x),$$

$$\frac{A}{D} = P'_{\text{eq}}(x) + \frac{V'(x)}{D} P_{\text{eq}}(x),$$

leading to the equilibrium probability density function,

$$P_{\text{eq}}(x) = C \exp \left[-\frac{2V(x)}{D} \right], \quad C^{-1} = \int_{-\infty}^{\infty} \exp \left[-\frac{2V(x)}{D} \right] dx, \quad (3.11)$$

where the constant C comes from the normalisation of the probability density function at the long time limit, $\int P_{\text{eq}} dx = 1$.

Figure (3.7) shows the comparison between the numerical path integral solution against both the small time approximation (A) (3.10) and the stationary solution (C) (3.11). What curve (B) shows is an intermediate time showing how the probability will spread in the initial potential well before starting to spill over the potential barrier into the secondary potential well. This is an advantage of the path integral technique, the ability to calculate *transient states*.

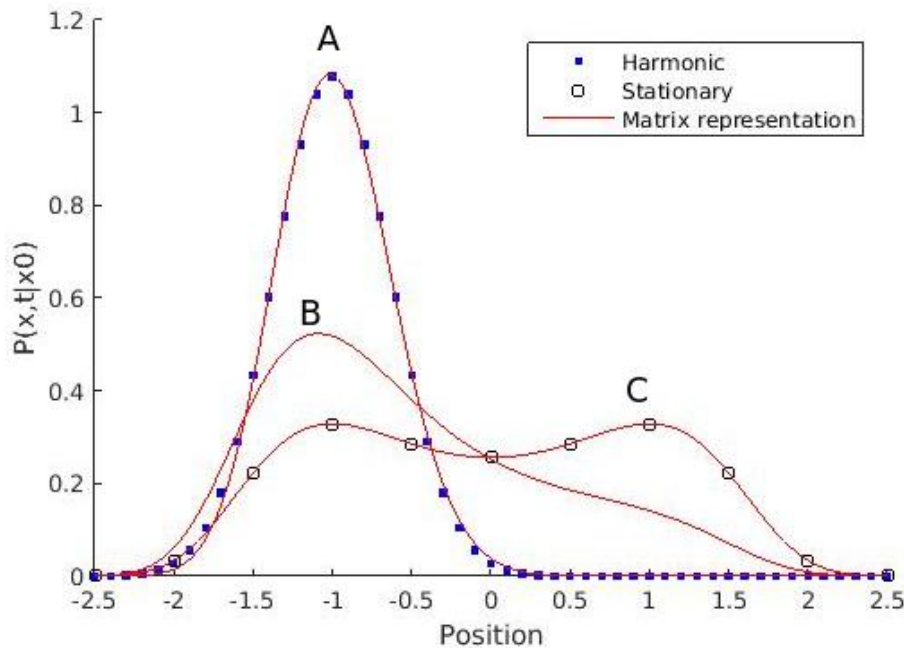


Figure 3.7: The probability density function $P(X, T|x_0)$ as a function of position. Snapshots taken at different times, (A) $T=0.08$, (B) $T=0.86$, (C) $T = 10.24$. $dt = 0.001$, $dx = 0.01$, $x_i = -1$, $D = 1$

This shows that the numerical path integral solution is accurate for both short and long time analytical solutions. What about more complicated potentials? The next

example is a non-symmetric double well potential.

$$V(x) = \frac{x^4}{8} - \frac{x^3}{6} - \frac{x^2}{2} + \frac{4}{3}. \quad (3.12)$$

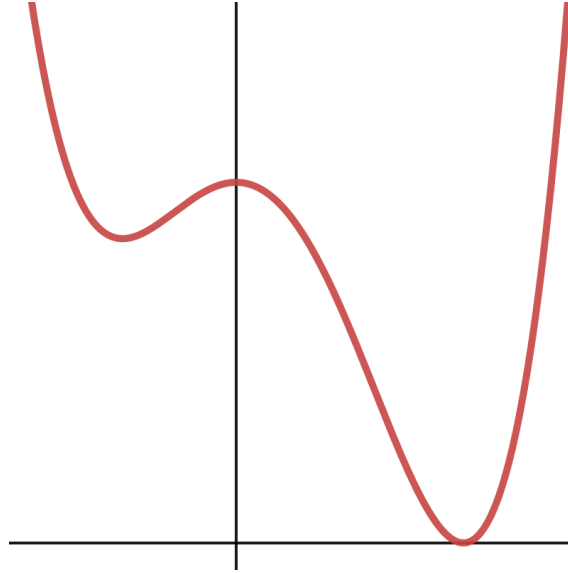


Figure 3.8: Tilted double well potential

The starting potential well is shallower than the second well, meaning intuitively the probability should spill over the potential barrier earlier but take longer to reach equilibrium and be more likely to end up in the deeper well at long-time. The analytical solutions are calculated the same way as for the symmetric double well, (3.10),(3.11). The results in figure (3.9) show again that the numerical solution matches up with analytical solutions at both small and large times. For the small time case, there is a slight difference between the analytical solution and the matrix representation, which is because the peak of the potential barrier is located at $x = 0$, meaning that the approximation that the potential is harmonic starts to break down for x close to 0. The intermediate time (B) shows the correct behaviour, in spreading out and starting to spill over into the second deeper potential well. The only difference in input parameters when compared to the symmetric potential was a minor alteration in the time discretisation, as there was the need for a finer

Δt in order to get a better comparison and to get to the stationary solution, the numerical path integral solution T was set at a larger value, as it took longer for particles to get over the peak and more ended in the right hand well.

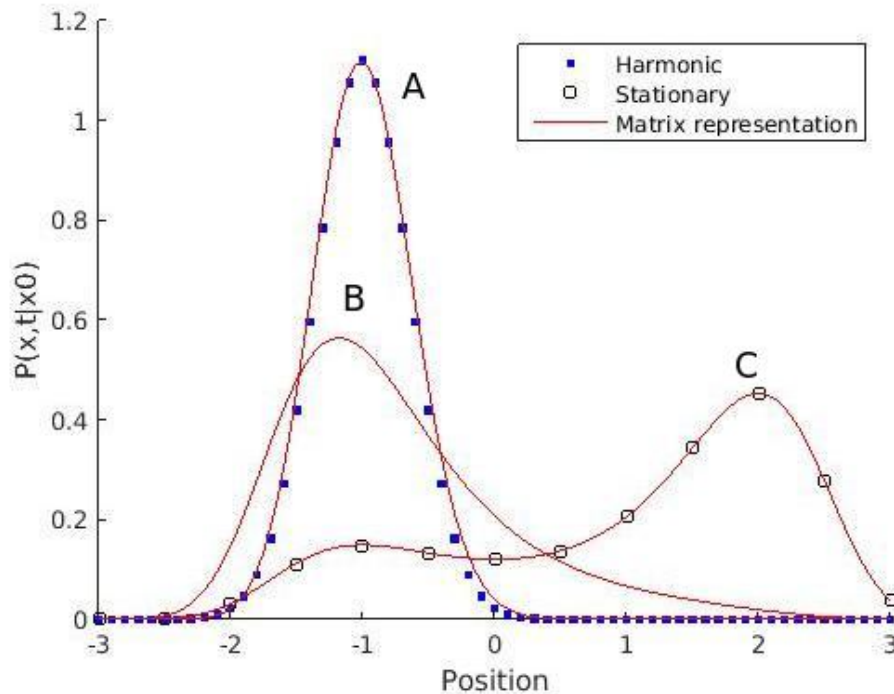
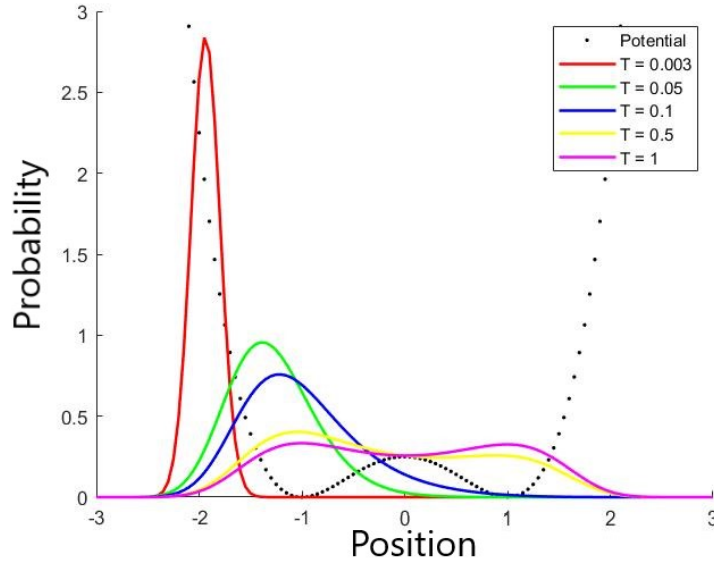


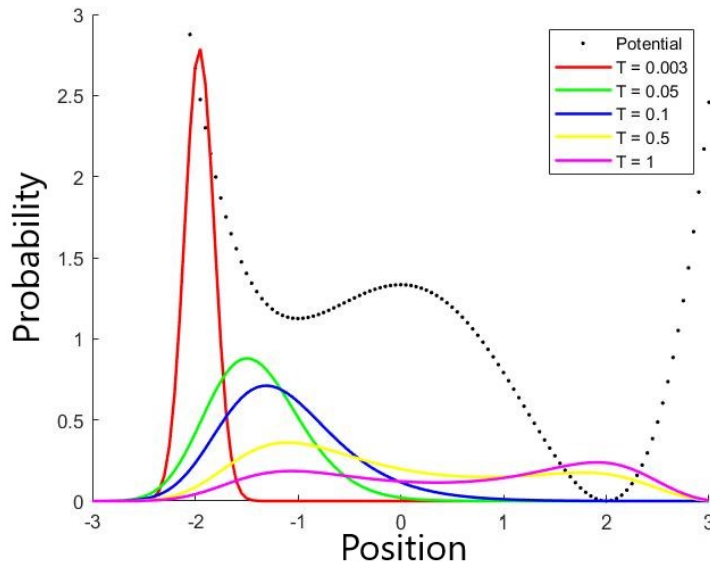
Figure 3.9: The probability density function $P(X, T|x_0)$ as a function of position. Snapshots taken at different times, (A) $T=0.08$, (B) $T=0.86$, (C) $T = 14.80$. $dt = 0.001$, $dx = 0.05$, $x_i = -1$, $D = 1$

A major advantage of using path integrals to get a numerical solution is that the transient states are possible to show. However, how do we know these transient states behave as expected? One way is to see if intuitively, the behaviour of the probability density function acts as we would expect. The probability begins as a delta function at the initial position and spreads out in the initial potential well. Then it begins to slowly spill over the potential barrier into the other potential well before settling into the relevant stationary distribution, for which we have a definite solution. This is how we expect the probability density function to act over time, so the solution gained from the numerical iteration lines up with intuition. In order to check if the behaviour is logical we can use the numerical path integral solution for different values of n to find the probability density function over time. This is

what figures 3.10a and 3.10b show, the behaviour we expect.



(a) Symmetric potential, $V(x) = \frac{x^4}{4} - \frac{x^2}{2} + \frac{1}{4}$.

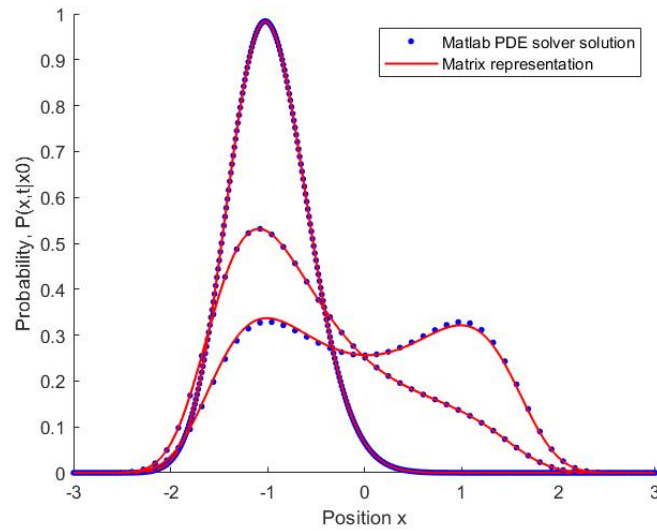


(b) Tilted potential, $V(x) = \frac{x^4}{8} - \frac{x^3}{6} - \frac{x^2}{2} + \frac{4}{3}$.

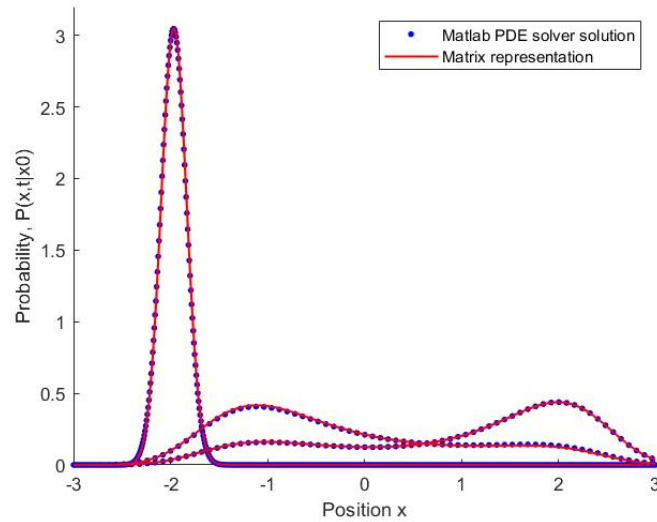
Figure 3.10: The probability density function as it evolves over time until equilibrium. With initial position $x_i = -2$ and a diffusion value, $dt = 0.001$, $dx = 0.05$, $D = 1$.

Another way we can check the transient state solutions is to use Matlab's built-in partial differential equation solver. This will solve the Smoluchowski equation approximately and give a solution for a specific time. Matching these times with the relevant times in the numerical path integral solution gives figures (3.11a) and

(3.11b). These figures show the accuracy of the path integral technique, including the transient state solutions. Other numerical techniques are available to solve time-dependent solutions, for example, finite-difference time-domain or spectral methods, that can be used to solve specific differential equation systems [78] [79]. However, Matlab's PDE solver provides excellent agreement with the path integral technique that it is sufficient to compare with this one technique.



(a) Symmetric potential



(b) Tilted potential

Figure 3.11: PDF comparison to the Matlab PDE solver for small T , an intermediate T , and large T for the symmetric double well potential and the tilted double well potential

The advantages of the path integral technique, however, is one of speed and adaptability. The PDE solver takes more time to run for a specific timestep, meaning that if we wish to find solutions over time, it will take much longer to run and is more awkward to construct the code. For example, to find the titled potential plot it took 4.5s to solve for the three timesteps only, whereas to solve using the matrix representation, it takes 1.5s to calculate and plot the three timesteps. This is a significant improvement, and the versatility of the matrix representation makes it quicker and easier to build a complete solution, switch initial positions, or even construct visualisations.

The fact that we have a matrix propagator R which is non-dependent on the initial or final positions means that we can solve for all initial conditions simultaneously; another important attribute of the numerical path integral technique being able to change conditions very quickly and return quick results for the relevant system.

3.4 Further one-dimensional investigations

3.4.1 Finding a PDF for the initial position

An interesting investigation to look at is to look at finding the probability density function in reverse. If we know the final position of the particle, can we find out where it started for a given time T ? Using the numerical path integral solution, this is an easy change; instead of extracting the relevant column from the final probability matrix for a given initial position, we extract the relevant row for the given final position. What figures (3.12a) through (3.12d) show is the progression of the probability density function as the simulation is run for a longer time. It begins as expected as a tall peak at the final position $x_f = 2$ as there has not been long enough for the particles to get from very far to finish in a short t . As time progresses, the probability spreads out, and after a long enough time period, the probability density function becomes flat, meaning that we cannot gain any information about where the particle has started from.

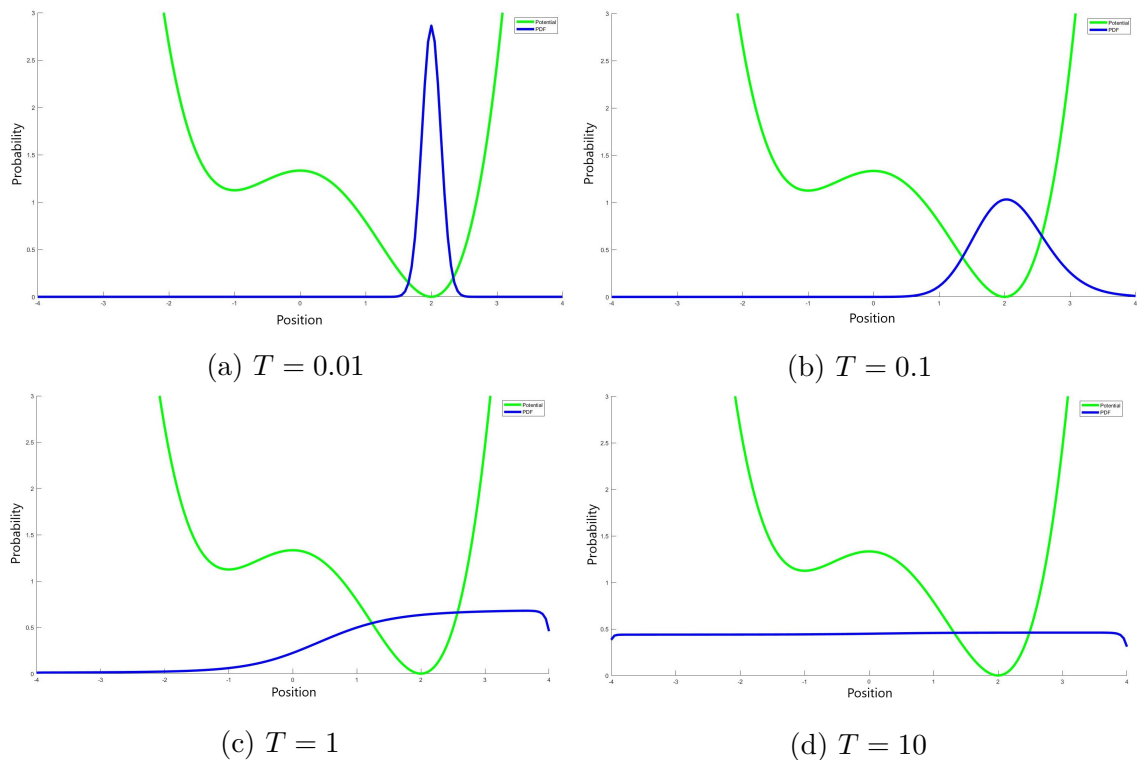


Figure 3.12: Probability density function of initial positions, in blue, over time, for a final position of $x_f = 2$. $dt = 0.001$, $dx = 0.01$ and $D = 1$.

This shows the possible initial positions for the most likely final position at the bottom of the deeper well, but what happens if we want to investigate when the probability ends at an unlikely final position? This is what figures (3.13a) through (3.13d) show, when the final position in question is on the side of the larger potential well, $x_f = 0.75$. At short times it follows similar behaviour to the most likely position, figure (3.12a), but as we look further back from the final position, the initial position is skewed by an earlier possibility of starting in the left-hand well. Shown in the fact that at $T = 0.5$, figure (3.13c), the particle already has the possibility of starting in the left-hand well, whilst for the most likely position, this possibility was minimal at $T = 1$, figure (3.12c). This is because travelling over the potential peak takes time, but once a particle is over, it will reach the side of the well before it reaches the bottom, which means that this does make physical sense as well.

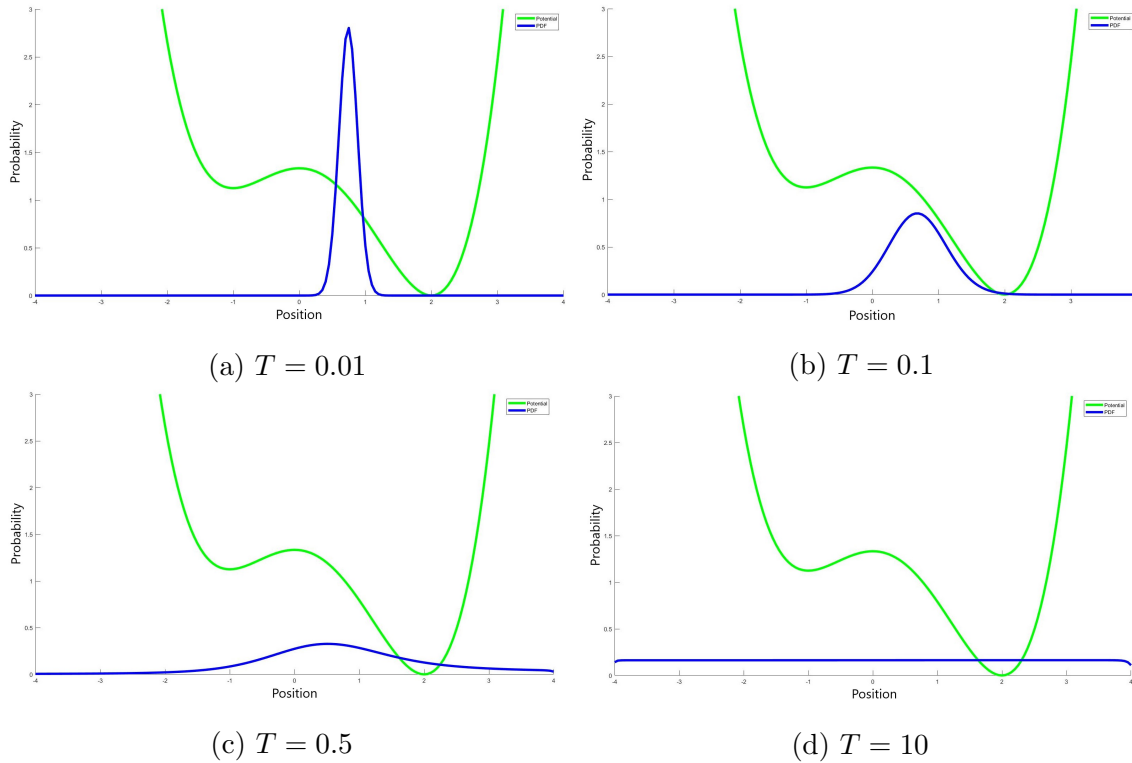


Figure 3.13: Probability density function of initial positions, in blue, over time, for a final position of $x_f = 0.75$. $dt = 0.001$, $dx = 0.01$ and $D = 1$.

3.4.2 Diffusion Constant

Another valuable and interesting investigation is to find the most likely diffusion constant for a given initial, final position and time. If we know both endpoints and the given time, then we might want to know the diffusion value of the system D . Fixing the initial position to $x_i = -2$ for a tilted double well potential (3.12), and the final position to $x_f = 2$, we can calculate the probability of travelling from the initial to the final position in $T = 8$ for a range of diffusion constants.

Figure 3.14 shows how the probability changes as the diffusion value increases. It has some interesting properties that do line up with intuition. The initial portion is a low probability value, as the diffusion value is not high enough to climb over the potential barrier between the initial and final position, so traversing this in the given timeframe is probabilistically unlikely. This will then peak just after a diffusion value similar to the height of the potential barrier. It then plateaus for higher diffusion values as the diffusion value becomes too overpowered, meaning

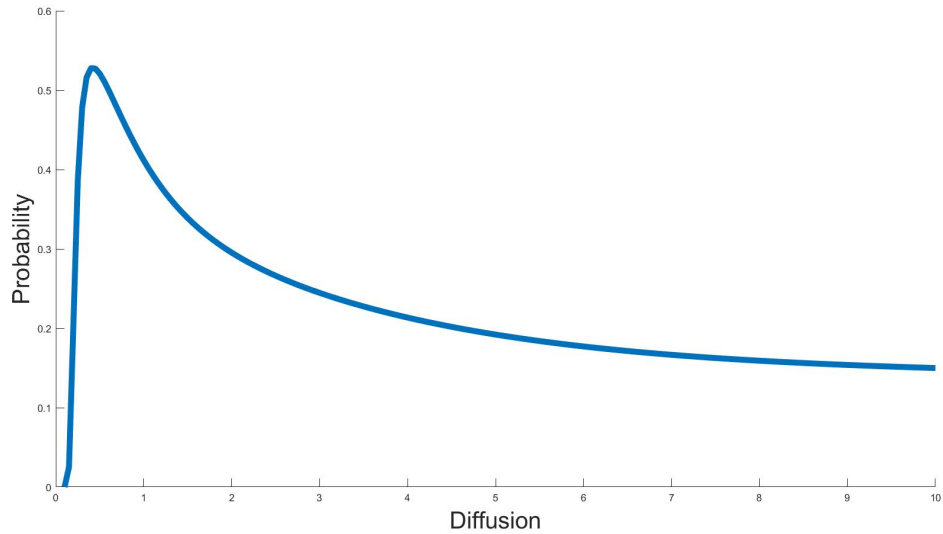


Figure 3.14: How the probability of moving from $x_i = -2$ to $x_f = 2$ changes as the diffusion increases for a tilted potential.

the probability of the path essentially takes no notice of the potential barrier, and the probability density function becomes constant for the higher diffusion range. Something to take into consideration is that the higher value of diffusion also means that there will be more possible neighbours for the particle to travel to in a single timestep requiring a finer grid of discretisation of both time and space, meaning that a separate set of initial discretisations is required to return this result. A reminder here that the diffusion value in this work is not explicitly related to a characteristic, like temperature, of a specific system; it is just a measure of the noise strength of the system, which we relate solely to the height of the barrier in a given potential as the major contributor of how a system acts over time.

3.5 Two-dimensional numerical solution

After complicated potentials in one dimension, the next logical step is to see how the numerical path integral solution handles being used in two dimensions. This solves a very similar problem just now the multidimensional version of the Smoluchowski equation;

$$\begin{aligned} \frac{\partial P(\underline{x}, t)}{\partial t} &= \nabla \cdot [\nabla V(\underline{x})P(\underline{x}, t) + D\nabla P(\underline{x}, t)], \\ P(\underline{x}, 0|\underline{x}_i) &= \delta(\underline{x} - \underline{x}_i). \end{aligned} \quad (3.13)$$

Doing a similar transformation as in the one-dimensional case, we also have a similar function that, in the small time limit, solves the two-dimensional Smoluchowski equation. $\underline{x} = (x, y)$.

$$\begin{aligned} P(\underline{x}, t|\underline{x}_i) &= \exp\left[-\frac{V(\underline{x}) - V(\underline{x}_i)}{2D}\right] Q(\underline{x}, t|\underline{x}_i), \\ Q(\underline{x}, t|\underline{x}_i) &= \frac{1}{\sqrt{4\pi Dt^2}} \exp\left[-\frac{(\underline{x} - \underline{x}_i)^2 + t^2 (V_{\text{Baibeff}}(\underline{x}) + V_{\text{Baibeff}}(\underline{x}_i))}{4Dt}\right], \end{aligned} \quad (3.14)$$

$$V_{\text{Baibeff}} = \frac{1}{2} (\nabla V) \cdot (\nabla V) - D\nabla \cdot (\nabla V).$$

This representation of the probability density function solves, in the small time limit $t \rightarrow 0$, the two-dimensional Smoluchowski equation with a similar derivation to the one-dimensional version (3.5).

Now that we have a two-dimensional version of the jump probability, we need to form the matrices. In the one-dimensional version, the central matrix has a change in the initial position along the rows and the change in the final position along the columns. So, how does this change when we have two coordinate systems?

We can follow a similar technique as in the one-dimensional case. For two time steps, we discretise twice as there are two coordinates, in this case for y_1 and y_2 , and we have a double integral,

$$Q(\underline{x}, 2t|\underline{x}_i) = \int \int Q(\underline{x}, 2t|(y_1, y_2), t)Q((y_1, y_2), t|\underline{x}_i, 0)dy_1dy_2,$$

$$\text{discretising; } = \delta y_1 \delta y_2 \sum_j \sum_k Q(\underline{x}, 2t|y_{jk}, t)Q(y_{jk}, t|\underline{x}_i, 0).$$

This gives a similar representation as in one dimension (3.8), with two vectors

$$Q(\underline{x}, 2t|\underline{x}_i) = \delta y_1 \delta y_2 \underline{xy} \cdot \underline{yx}_i,$$

$$\underline{xy} = \begin{pmatrix} Q(\underline{x}, t|y_{11}) \\ Q(\underline{x}, t|y_{21}) \\ \vdots \\ Q(\underline{x}, t|y_{(M+1)(M+1)}) \end{pmatrix}; \quad \underline{yx}_i = \begin{pmatrix} Q(y_{11}, t|\underline{x}_i) \\ Q(y_{21}, t|\underline{x}_i) \\ \vdots \\ Q(y_{(M+1)(M+1)}, t|\underline{x}_i) \end{pmatrix},$$

$$y_{jk} = \left(\left(\frac{M - 2(j - 1)}{2} \right) \Delta, \left(\frac{M - 2(k - 1)}{2} \right) \Delta \right).$$

The main difference with the one-dimensional case is the size of the vectors. In the 1-D case, we had vectors with $M + 1$ entries; in the 2-D case, we have $(M + 1)^2$ entries. This increase in the size of the vectors, and as we will see the size of the matrices, leads to a significant increase in computational time. The representation can, in a similar way to the one-dimensional case, be extended through to n time steps, giving a final numerical path integral solution where we define the matrix elements as;

$$xy_{jk} = Q(\underline{x}, t|y_{jk}) \quad y_{jk}z_{jk} = Q(y_{jk}, t|z_{jk}) \quad z_{jk}x_i = Q(z_{jk}, t|\underline{x}_i)$$

$$Q(\underline{X}, T | \underline{x}_i) = \begin{pmatrix} xy_{11} & xy_{12} & \dots & xy_{NM} \end{pmatrix} \begin{pmatrix} y_{11}z_{11} & y_{11}z_{12} & \dots & y_{11}z_{NM} \\ y_{12}z_{11} & y_{12}z_{12} & \dots & y_{12}z_{NM} \\ \vdots & \vdots & \ddots & \vdots \\ y_{NM}z_{11} & y_{NM}z_{12} & \dots & y_{NM}z_{NM} \end{pmatrix}^n \begin{pmatrix} z_{11}x_i \\ z_{12}x_i \\ \vdots \\ z_{NM}x_i \end{pmatrix} \cdot \Delta^{2(n-1)}$$

Here the matrix is again constant as it was in the one-dimensional case, but it is now size $(M + 1)(N + 1)$ where M and N are the number of spatial discretisations of the x and y axis respectively. This dramatically increases the computational time required for one timestep calculation. In one dimension it took a couple of seconds, and with the diagonalisation and nearest neighbours techniques was reduced to a single second. However, in two dimensions for the flat potential, we will now look at a single calculation that took 274 seconds to calculate the full probability for $dx = dy = 0.1$, $dt = 0.0607$ and $n = 7$. This is a considerable increase in computational time, with 20% of that time being taken up with taking the matrix to the power of n and the other major calculation being calculating each element of the matrix, which for a grid being for $-3 < x < 3$, $-3 < y < 3$, there are 3600 elements.

The process of diagonalisation of the matrix should still be possible in two dimensions, since the matrix itself is symmetric, meaning that it equals its own transpose. This is possible because the probability density function for the linear approximation Q is spatially invariant, meaning $Q(y, t | z) = Q(z, t | y)$. This means there is the possibility of using the diagonalisation technique to speed up the numerical calculations. For the process of using the nearest neighbours, this is trickier to see if it would be possible. In one dimension we had a band diagonal matrix. In contrast, in two dimensions some elements may not be negligible due to the positioning of peaks and troughs of the potential, and it may not be possible to constrict the band in the diagonal as in one dimension. This property makes it more challenging to see whether the use of the nearest neighbours is possible. Still, it may be possible to

exclude the negligible probabilities and only take forward the matrix calculation of the more dominant probabilities, which is, in essence, what the nearest neighbour technique in one dimension was doing. This problem has yet to be thoroughly investigated here. This area could be investigated further to reduce computation time in two dimensions, and then make the three-dimension jump easier.

Now that we have a representation for the probability, does it give correct results for a two-dimensional potential? The computational limitations of the increase in dimension mean that, for now, we will only be able to investigate the behaviour of the solution. The most straightforward potential to look at is the flat potential.

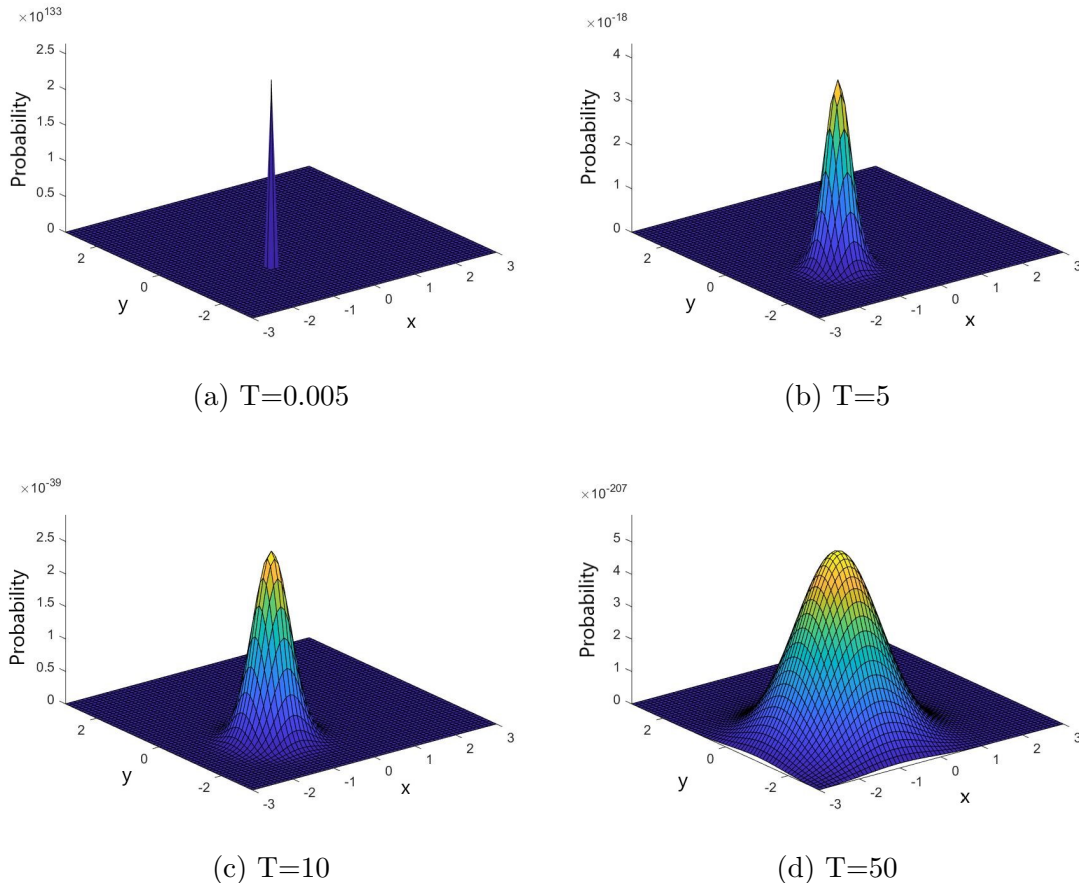


Figure 3.15: Probability density function over time for a flat potential, $dx = 0.1$, $dy = 0.1$, $dt = 0.0001$, $D = 0.01$

In this situation, the expected behaviour is that the probability will expand out from the initial position and spread out to a symmetric probability density function peak. This is what figure (3.15) shows. The PDF begins as a spike at the initial position and slowly flattens over time. For reference, these plots are not normalised due to computational limits, so this is to give an idea about the correct behaviour of the technique. What about something a bit more complicated? The linear potential is the obvious next step; intuitively, the probability density function would again start as a peak but as it expands over time it would also “slide down” the potential. This is what figure 3.16 shows.

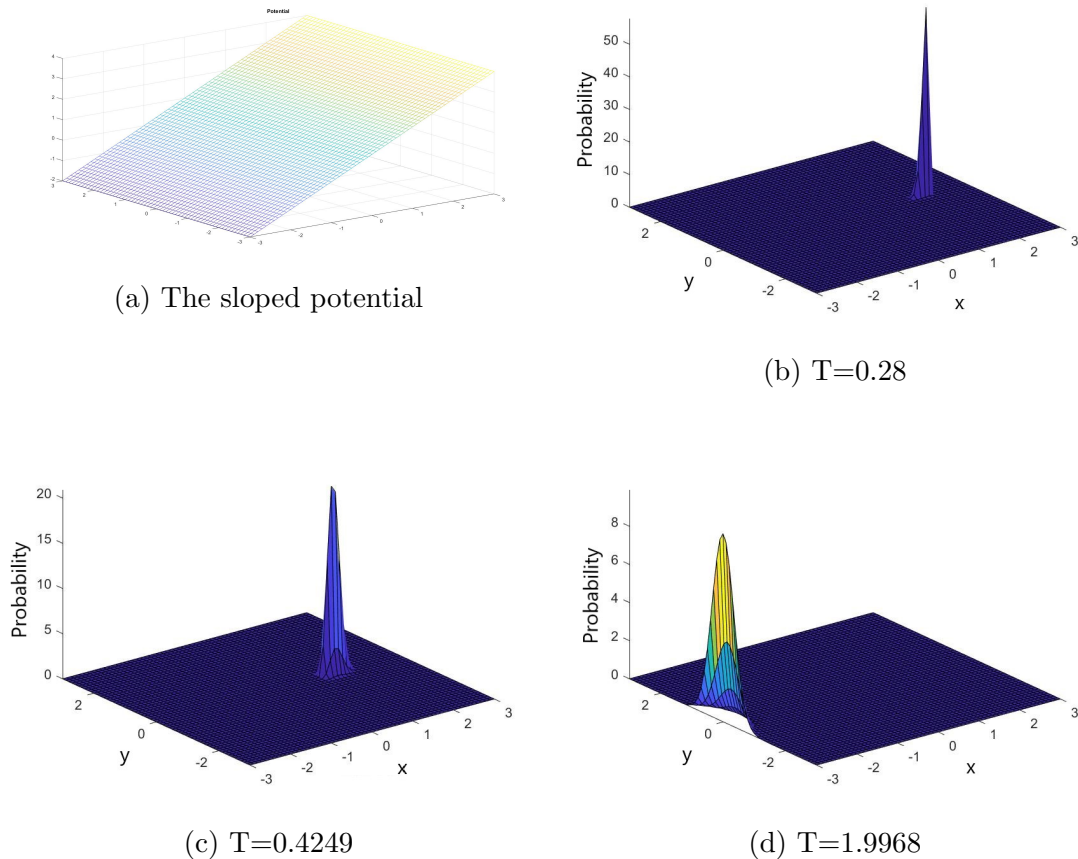


Figure 3.16: Probability density function over time for a sloped potential, $dx = 0.1$, $dy = 0.1$, $dt = 0.0607$ $D = 0.01$

We can see that the representation derived mechanically behaves correctly using these two simple cases. The primary issue that the jump to two dimensions gives is

the increased computational power needed. This has so far limited the investigation into two dimensions to just these two most straightforward cases because for these systems there is a reduction in the number of terms as they are either 0 or constant; they were the easiest to code and simulate a reasonable time frame compared to one dimension and the easiest to know the intuitive behaviour. The possibility of diagonalisation and nearest neighbours as time reduction methods does look possible as the central matrix is symmetric, but this work concentrates on one dimension, so we will leave the two-dimensional argument for now.

In this chapter, we have explored the use of a path integral formalism in solving the Smoluchowski equation numerically. We have recreated results from Baibuz's paper [71] with the initial results but have taken it further by comparing more results to Matlab's own PDE solver. Then we have been able to reduce the computation time of the technique by using properties of matrices and which paths make physical sense in the system with diagonalisation and nearest neighbours. Further, we have looked at more potential uses of the one-dimensional numerical solution for reverse engineering the initial position and calculating the most probable diffusion value for a given system. Finally, we looked at how the numerical technique could be translated into two dimensions, showing results for the simplest of systems to prove proof of concept and that the solution makes physical sense. The computational complexity goes up very fast as the dimensions increase, so whilst it is very efficient in one dimension, something else will be needed for higher dimensional investigations. The technique will become infeasible for very high-dimensional systems, for example, 3×10^3 dimensions for a million atom system. However, as we will see later there is the hope that the analytical approach will allow progress in using the path integral in higher dimensions. So, although only an incremental advancement of the original Baibuz method, it extends the possibility of path integral formalisms being used in numerical calculations, and the comparisons to Matlab PDE solvers, the engineering of the initial position and diffusion constant are all new elements to this technique.

Chapter 4

The introduction of the Jacobian

In this chapter, we will introduce the Jacobian term. This is another key piece of information that arises from the change of variables in the original path integral derivation (2.7). We have not needed it up to now as it only becomes non-unit when the system has a potential of quadratic order or higher. This additional term will provide more information on how the path integral acts over time and will potentially solve some of the issues at long time limits that we have been having, along with intuitive errors when it comes to how a path should act. We will derive a usable form for the Jacobian, represented using time and space, and look at how it solves some of the long-time issues.

In chapter 2, we mentioned the introduction of the Jacobian term, which arises from the change in variables from $d\xi$ to dx (2.7). The Jacobian term [80] is given by,

$$\mathcal{J} = \det \left(\frac{d\xi_i}{dx_j} \right),$$

with the subscripts indicating that the derivative is a matrix, and subsequently, we will need to calculate a determinant. In the limit of $N \rightarrow \infty$ of the variable discretisation, it will become a functional Jacobian, $|\frac{\partial \xi}{\partial x}|$. The method to calculate the determinant is to first of all return to the general Langevin equation (1.6) and discretise the equation by multiplying each side by dt ,

$$dx_i = -(\lambda V'(x_i) + (1 - \lambda)V'(x_{i-1})) dt + d\xi_i.$$

The difference here is the introduction of the value λ , which governs the choice of different techniques and when to calculate the gradient of the potential. $\lambda = 0$ [81] relates to the *Ito* prescription of the Langevin equation, which is the one that we use in chapter 2 in the substitution into the ξ integral (2.5). $\lambda = \frac{1}{2}$ [82] relates to the *Stratonovich* prescription, where for time evolution, the average is taken between the beginning and end points. The $\lambda = 0$ value is typically used in mathematics, whilst the $\lambda = \frac{1}{2}$ is typically used in physics. This choice of λ governs when the random element is added when the system is simulated like the Langevin equation. In the *Ito* prescription, the noise term is added at the beginning of the timestep and then the effect from the forces is taken into account. Whilst in the *Stratonovich* prescription, we move the particle under the forces for half the timestep, then calculate the noise term before finishing the timestep with the remaining elements of the force term. Typically this choice between prescriptions is only when the system has white noise, as it can make elements of the mathematics easier depending on which prescription is used. In the case of correlated noise, the choice is always *Stratonovich* due to the nature of the mathematics encountered when the noise function is not a delta function as it is for uncorrelated (white) noise.

Calculating the derivative of ξ_i leads to,

$$\begin{aligned} d\xi_i &= dx_i + (\lambda V'(x_i) + (1 - \lambda)V'(x_{i-1})) dt, \\ \frac{d\xi_i}{dx_j} &= 1 \cdot \delta_{ij} + (\lambda V''(x_i)\delta_{ij} + (1 - \lambda)V''(x_{i-1})\delta_{i-1,j}) dt. \end{aligned}$$

This then forms an upper triangular matrix in which the only non-zero elements are the leading diagonal and the first off-diagonal from the δ_{ij} terms,

$$\begin{pmatrix} (1 + \lambda V''_i) dt & (1 - \lambda) V''_{i-1} dt & 0 & 0 & \dots \\ 0 & (1 + \lambda V''_i) dt & (1 - \lambda) V''_{i-1} dt & 0 & \dots \\ 0 & 0 & (1 + \lambda V''_i) dt & (1 - \lambda) V''_{i-1} dt & \dots \\ \vdots & \vdots & \vdots & \dots & \dots \end{pmatrix}$$

Finally, we then need to calculate the determinant of this matrix, and a bonus of a triangular matrix is that the determinant is just the product of the diagonal elements, as most of the entries are zero.

$$\det \left(\frac{d\xi_i}{dx_j} \right) = \prod_i (1 + \lambda V''(x_i) \delta t)$$

Using the Taylor expansion, δt small,

$$\begin{aligned} &= \prod_i \exp(\lambda V''(x_i) \delta t) \\ &= \exp \left(\lambda \delta t \sum_i V''(x_i) \right) \\ &\rightarrow \exp \left(\lambda \int_0^T V''(x(t)) dt \right). \end{aligned}$$

This means that for the Ito prescription, $\lambda = 0$, the Jacobian will be a unit transformation, while the Stratonovich prescription will have a factor $\exp \left(\frac{1}{2} \int_0^T V''(x(t)) dt \right)$. The Ito prescription does return the same factor as Stratonovich; however, it is found from the cross-term total derivative in the action derivation (2.7) in chapter 2 when we expand the Lagrangian $(\dot{x} + V'(x))^2$.

The total derivative in action integral in (2.7) becomes an *Ito integral* [83],

$$\begin{aligned} 2 \int_0^T V' \dot{x} dt &\rightarrow 2 \int_0^T V' dX_t, \\ &= 2 \int_0^T dV(X_t) - 2D \int_0^T V''(X_t) dt, \\ &= 2\Delta V(x) - 2D \int_0^T V''(x(t)) dt, \end{aligned}$$

where we have also used Ito's lemma [31], $df(X_t) = f'(X_t)dX_t + \frac{1}{2}\sigma^2(t)f''(X_t)dt$ and remembering that $\frac{1}{2}\sigma^2(t) = D$ from our derivation of the Smoluchowski equation (1.10). The extra integral can be extracted from the action definition as an extra term to what we currently have in S , and when divided by $-\frac{1}{4D}$, returns the same expression as the Stratonovich prescription.

Both prescriptions return the same factor, and from now on the term ‘‘Jacobian’’ will refer to the integral form in the exponent that arises from both prescriptions, albeit from different routes. This form is only in one-dimension as that is what we will be concentrating on for now, but we will look at the three-dimensional case in chapter 9 and how it is constructed for free diffusion and harmonic potential cases. We have a time-dependent representation of the Jacobian, but we can recover a spatial-dependent form via a transformation. To do this we transform via $y = x(t)$,

$$\begin{aligned} \mathcal{J} &= \exp\left(\frac{1}{2} \int_0^T V''(x(t)) dt\right), \\ \frac{dy}{dt} = \dot{x}(t); &= \exp\left(\frac{1}{2} \int_{\gamma} V''(y) \frac{dy}{|\dot{x}|}\right), \\ \text{Using (2.8)} &= \exp\left(\frac{1}{2} \int_{\gamma} \frac{V''(y)}{\sqrt{H + V'(y)^2}} dy\right). \end{aligned}$$

Now that we have found the Jacobian term in full, we can write down a full probability density function weight in one dimension for a path γ , from $(x_i, 0)$ to (x_f, T) ;

$$\begin{aligned}
P[x_f, T|x_i, 0] &= A[x] \mathcal{J}[x] \exp\left(-\frac{S[x]}{4D}\right) \\
S &= 2\Delta V - HT + 2 \int_{\gamma} \sqrt{H + V'^2(x)} |dx| \\
A &= \left(4\pi D \sqrt{H + V'(x_0)^2} \sqrt{H + V'(x_1)^2} \int_{\gamma} \frac{|dx|}{(H + V'^2)^{3/2}}\right)^{-1/2} \\
\mathcal{J} &= \exp\left(\frac{1}{2} \int_{\gamma} \frac{V''(x) |dx|}{\sqrt{H + V'(x)^2}}\right) \\
T &= \int_{\gamma} \frac{|dx|}{\sqrt{H + V'(x)^2}}
\end{aligned}$$

To build the full probability density function, we have to calculate the integral over all possible path weights, $P(x_f, T|x_i, 0) = \int \mathcal{D}x P[x_f, T|x_i, 0]$. The Jacobian term is not relevant for the simplest of integrals that we have already looked at, as $V''(x) = 0$ for both the flat and sloped potential, meaning $\mathcal{J} = 1$, but does this Jacobian term provide more information to the system, and fix some of the issues that we have been having at long times? We can investigate our Jacobian term further by evaluating the integral immediately. By noting that $V''(x)dx = d(V'(x))$ we can transform our integral

$$\int_{\gamma} \frac{V''(x)}{\sqrt{H + V'(x)^2}} dx = \int_{\gamma} \frac{1}{\sqrt{H + V'(x)^2}} d(V'(x)).$$

This integral can be done by using trigonometric substitutions, and it results in a logarithmic solution

$$\int_{\gamma} \frac{1}{\sqrt{H + V'(x)^2}} d(V'(x)) = \frac{1}{2} \log \left[\frac{\sqrt{H + V'(x)^2} + V'(x)}{\sqrt{H + V'(x)^2} - V'(x)} \right] \Big|_{\gamma}$$

Inserting this into the Jacobian and evaluating this for a path for which $x_i < x_f$,

$$\mathcal{J}[x] = \exp\left(\frac{1}{4} \log \left[\frac{\sqrt{H + V'(x_f)^2} + V'(x_f)}{\sqrt{H + V'(x_f)^2} - V'(x_f)} \frac{\sqrt{H + V'(x_i)^2} - V'(x_i)}{\sqrt{H + V'(x_i)^2} + V'(x_i)} \right]\right),$$

$$\begin{aligned}
 &= \left[\frac{\sqrt{H + V'(x_f)^2} + V'(x_f)}{\sqrt{H + V'(x_f)^2} - V'(x_f)} \frac{\sqrt{H + V'(x_i)^2} - V'(x_i)}{\sqrt{H + V'(x_i)^2} + V'(x_i)} \right]^{\frac{1}{4}}, \\
 &= \left[\frac{\left(\sqrt{H + V'(x_f)^2} + V'(x_f) \right) \left(\sqrt{H + V'(x_i)^2} - V'(x_i) \right)}{H} \right]^{\frac{1}{2}}.
 \end{aligned}$$

We now have the Jacobian term in full for a default direct right-moving path. Right-moving due to the choice in the sign of the \dot{x} term in the derivation as we take the right-moving direction to have positive velocity. We can now show that this form will solve one of the divergent issues that the path integral representation has previously had. The form of the Jacobian we have will fix the divergent portion of the prefactor integral, which we can see by extracting the divergence. For a path between x_i and x_f that travels through a turning point at $x = \alpha$, $V'(\alpha) = 0$, we can split the prefactor integral into constituents parts,

$$\begin{aligned}
 \int_{x_i}^{x_f} (H + V'(y)^2)^{-\frac{3}{2}} dy &= \int_{x_i}^{\alpha-\epsilon} (H + V'(y)^2)^{-\frac{3}{2}} dy \\
 &\quad + \int_{\alpha-\epsilon}^{\alpha+\epsilon} (H + V'(y)^2)^{-\frac{3}{2}} dy + \int_{\alpha+\epsilon}^{x_f} (H + V'(y)^2)^{-\frac{3}{2}} dy.
 \end{aligned}$$

We can then expand the middle integral around α by substituting in $y = z + \alpha$,

$$\begin{aligned}
 V'(z + \alpha)^2 &= [V'(\alpha) + zV''(\alpha) + \mathcal{O}(z^2)]^2 = z^2V''(\alpha)^2 + \mathcal{O}(z^3), \\
 \int_{\alpha-\epsilon}^{\alpha+\epsilon} (H + V'(y)^2)^{-\frac{3}{2}} dy &= \int_{-\epsilon}^{\epsilon} (H + z^2V''(\alpha)^2)^{-\frac{3}{2}} dz, \\
 &= \left[\frac{z}{H\sqrt{H + z^2V''(\alpha)^2}} \right] \Big|_{-\epsilon}^{\epsilon}, \\
 &= \frac{2\epsilon}{H\sqrt{H + \epsilon^2V''(\alpha)^2}}.
 \end{aligned}$$

We have a form now for the divergent portion of the integral, which in the limit $H \rightarrow 0$ means that the prefactor becomes,

$$\lim_{H \rightarrow 0} A = \left[|V'(x_f)| |V'(x_i)| \int_{x_i}^{\alpha-\epsilon} (H + V'(y)^2)^{-\frac{3}{2}} dy \right]$$

$$+ \int_{\alpha+\epsilon}^{x_f} (H + V'(y)^2)^{-\frac{3}{2}} dy + \frac{2}{H|V''(\alpha)|} \Big]^{-\frac{1}{2}}.$$

Then looking at the Jacobian term, in the same limit, it returns the form,

$$\lim_{H \rightarrow 0} = \left[\frac{4|V'(x_f)||V'(x_i)|}{H} \right]^{\frac{1}{2}}.$$

Combining these two limits we see the cancellation of the $|V'(x_f)||V'(x_i)|$ term and H term from the divergent integral returning,

$$\begin{aligned} \lim_{H \rightarrow 0} AJ &= \lim_{H \rightarrow 0} \sqrt{4|V''(\alpha)|} \left[\left[H \int_{x_i}^{\alpha-\epsilon} (H + V'(y)^2)^{-\frac{3}{2}} dy \right. \right. \\ &\quad \left. \left. + H \int_{\alpha+\epsilon}^{x_f} (H + V'(y)^2)^{-\frac{3}{2}} dy + 2 \right] \right]^{-\frac{1}{2}}, \\ &= \sqrt{2|V''(\alpha)|}. \end{aligned}$$

This combination of the prefactor and Jacobian cancel out the divergent portion of the integral from both terms. This is a beneficial fact of the Jacobian and shows that the Jacobian and prefactor act together to return a non-infinite probability density function which means that the long-time limit Boltzmann proportionality survives as the action goes like ΔV .

However, an issue still occurs in certain long time situations. If we have a system where the initial position is on an uphill portion of the potential and the final position is on a downhill, we run into a different problem in the long time limit. For example, figure 4.1 shows an example path in which the path will have to linger on the downhill portion of the effective potential to get to infinite time, when it makes more sense that it will travel through the final position and turn around, hovering for a long time near the top of the effective potential.

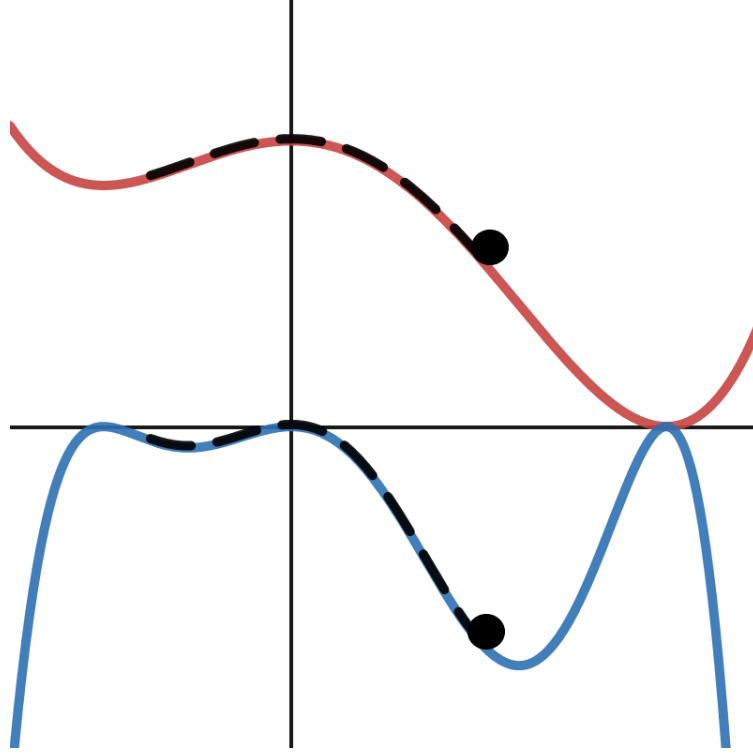


Figure 4.1: Example path that portrays the unintuitive path of ending on a downhill slope for infinite time in both the potential, top in red, and effective potential, bottom in blue.

For $T \rightarrow \infty$ we can equate it to $H \rightarrow 0$, so what happens in the system described for $H \rightarrow 0$, noting that $|V'(x_i)| = V'(x_i)$, $|V'(x_f)| = -V'(x_f)$, is that,

$$\mathcal{J}[x] = \left[\frac{\sqrt{H + V'(x_f)^2} + V'(x_f) \sqrt{H + V'(x_i)^2} - V'(x_i)}{\sqrt{H + V'(x_f)^2} - V'(x_f) \sqrt{H + V'(x_i)^2} + V'(x_i)} \right]^{\frac{1}{4}}$$

$$\mathcal{J}_{H \rightarrow 0} = \left[\frac{|V'(x_f)| + V'(x_f) |V'(x_i)| - V'(x_i)}{|V'(x_f)| - V'(x_f) |V'(x_i)| + V'(x_i)} \right]^{\frac{1}{4}}$$

$$\mathcal{J}_{H \rightarrow 0} = \left[\frac{-V'(x_f) + V'(x_f) V'(x_i) - V'(x_i)}{-V'(x_f) - V'(x_f) V'(x_i) + V'(x_i)} \right]^{\frac{1}{4}}$$

$$\mathcal{J}_{H \rightarrow 0} = \left[\frac{0}{-2V'(x_f) 2V'(x_i)} \right]$$

$$\mathcal{J}_{H \rightarrow 0} = 0.$$

This means that for this particular system and initial and final positions, the Jacobian tends to 0 in the long time limit meaning that the probability density function

will tend to 0; so what is going on here? Intuitively a path cannot end on a downhill and still survive to the long time limit as this makes no physical sense. This issue with the Jacobian is also similar to that of the action term. This is a significant clue that there may be something else going on, and there may be a need for a “*turning path*”; a path that has to travel past the final position, turn around at a maximum of the effective potential and come back to satisfy the relevant long time constraints. This concept also makes more physical sense, as we are investigating paths in the effective potential. We will thoroughly investigate this in chapter 5.

In this chapter, we have seen the introduction of the Jacobian term that arises from the change in variables from the noise function to spatial coordinates. Deriving the full term, describing the differences in interpretations, Ito vs Stratonovich, and how both techniques, Mathematics vs Physics, return the same expression from different scenarios. This has added an extra element to the path integral technique, and its interpretations at long time limits begin to shine a light on the necessity of a turning path which is what the next chapter is all about.

Chapter 5

The concept of the turning path

As mentioned in chapters 2 and 4, the notion of the turning path is needed in order to get the complete picture of a given system. Further, it is necessary to fix the divergent portions of the probability, or the fact that the probability will tend to zero at long time limits incorrectly from our analytical solution. In this chapter, we will explore the necessity for the turning path by looking at the fact that a direct path will have a maximum time it can take before becoming unphysical, and how the turning path can be interpreted as the appearance of a second peak for a double well potential. Finally, we will look at how this further term will allow the correct long time limit to be found, an issue that we have been coming across in the previous chapters.

5.1 Using time to introduce the turn

The best way to show how there is a need for a turning path is to look at the time definition that we have. From the analytical solution in chapter 2 (2.13) we have the definition

$$T = \int_{x_i}^{x_f} \frac{dy}{\sqrt{H + V'(y)^2}}.$$

First, we look at the representation that we have for the energy, $H = \dot{x}^2 - V'(x)^2$, as we can find the minimum amount of energy that a path can have. If we have, for example, a quadratic-shaped potential with $x_i < x_f < 0$, to get the particle up the hill in the effective potential, the minimum energy that the particle can have is when it arrives at x_f with zero velocity. For example, fig 5.1 shows a direct path for the single-well potential, which has come to rest at the final position, so if H is any larger it must travel past the final position and turn around.

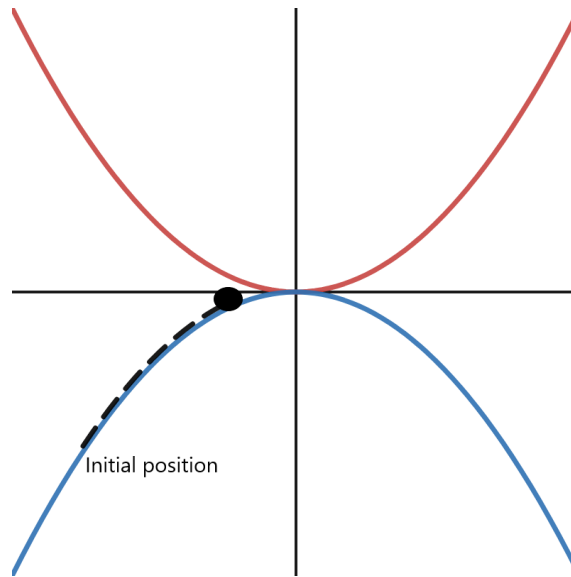


Figure 5.1: An example of the maximum direct path, if H is greater than this critical value, a turning path must exist

We have a critical energy value for this direct path of $H_c = -V'(x_f)^2$ with $\dot{x}_f = 0$, leading to a critical time of

$$T_c = \int_{x_i}^{x_f} \frac{dy}{\sqrt{-V'(x_f)^2 + V'(y)^2}}.$$

This means there is a maximum time for a direct path, and if $H > H_c$, the path must travel past the final position and turn around at a point $x_f < z$. This is the turning path!

So, how does this turning path form change the analytical solution previously found? First, we look at the action. If we have a path $x_i \rightarrow z \rightarrow x_f$, we can split this into three constituent direct parts. The three paths are $x_i \rightarrow x_f$, $x_f \rightarrow z$ and $z \rightarrow x_f$, and we can sum the three actions to return the full action. The portion of (2.9) that we will split up is the time integral into each path's time, $0 \rightarrow \tau_1$, $\tau_1 \rightarrow \tau_2$, $\tau_2 \rightarrow T$ where $T = \tau_1 + (\tau_2 - \tau_1) + (T - \tau_2)$. As we are splitting up a path, the path has the same energy across all paths based on the absolute final position.

$$\begin{aligned}
 S[x] &= S_1[x] + S_2[x] + S_3[x] \\
 &= 2(V(x_f) - V(x_i)) + 2 \int_0^{\tau_1} (2\dot{x}^2 - H) dt \\
 &\quad + 2(V(z) - V(x_f)) + 2 \int_{\tau_1}^{\tau_2} (2\dot{x}^2 - H) dt \\
 &\quad + 2(V(x_f) - V(z)) + 2 \int_{\tau_2}^T (2\dot{x}^2 - H) dt \\
 &= 2V(x_f) - 2V(x_i) - H\tau_1 + 2 \int_{x_i}^{x_f} \dot{x} dx \\
 &\quad + 2V(z) - 2V(x_f) - H(\tau_2 - \tau_1) + 2 \int_{x_f}^z \dot{x} dx \\
 &\quad + 2V(x_f) - 2V(z) - H(T - \tau_2) + 2 \int_z^{x_f} \dot{x} dx
 \end{aligned}$$

In the final line, we have to use the negative square root that comes from the energy definition, $\dot{x} = \pm\sqrt{H + V'^2}$, as described earlier, because we arrive at the final position from the other direction, meaning our velocity is negative.

This means we have,

$$\begin{aligned}
 S[x] &= 2V(x_f) - 2V(x_i) - HT + 2 \int_{x_i}^{x_f} \sqrt{H + V'(y)^2} dy \\
 &\quad + 2 \int_{x_f}^z \sqrt{H + V'(y)^2} dy - 2 \int_z^{x_f} \sqrt{H + V'(y)^2} dy \\
 &= 2V(x_f) - 2V(x_i) - HT + 2 \int_{x_i}^{x_f} \sqrt{H + V'(y)^2} dy + 4 \int_{x_f}^z \sqrt{H + V'(y)^2} dy.
 \end{aligned}$$

This extra integral accounts for the extra paths to the turning point and back. This extra integral also change the other elements of the full probability in the T domain. To find the time, we minimise the action with respect to H as we did in chapter 2, (2.10), giving a T for the turning path, energy value of $H_{\mathcal{T}}$,

$$T = \int_{x_i}^{x_f} \frac{1}{\sqrt{H_{\mathcal{T}} + V'(y)^2}} dy + 2 \int_{x_f}^z \frac{1}{\sqrt{H_{\mathcal{T}} + V'(y)^2}} dy.$$

This follows through for both the prefactor $A[x]$ and the Jacobian $J[x]$ as well, giving a full solution for the turning path probability of

$$\begin{aligned}
 S_{\mathcal{T}}[x_f, x_i, T] &= 2V(x_f) - 2V(x_i) - H_{\mathcal{T}}T \\
 &\quad + 2 \int_{x_i}^{x_f} \sqrt{H_{\mathcal{T}} + V'(y)^2} dy + 4 \int_{x_f}^z \sqrt{H_{\mathcal{T}} + V'(y)^2} dy, \\
 T &= \int_{x_i}^{x_f} \frac{1}{\sqrt{H_{\mathcal{T}} + V'(y)^2}} dy + 2 \int_{x_f}^z \frac{1}{\sqrt{H_{\mathcal{T}} + V'(y)^2}} dy, \\
 A_{\mathcal{T}}[x] &= \left(4\pi D \sqrt{(H_{\mathcal{T}} + V'(x_i)^2)(H_{\mathcal{T}} + V'(x_f)^2)} \right. \\
 &\quad \left. \left[\int_{x_i}^{x_f} \frac{dy}{(H_{\mathcal{T}} + V'(y)^2)^{3/2}} + 2 \int_{x_f}^z \frac{dy}{(H_{\mathcal{T}} + V'(y)^2)^{3/2}} \right] \right)^{-\frac{1}{2}}, \\
 \ln [\mathcal{J}_{\mathcal{T}}(x)] &= \frac{1}{2} \int_{x_i}^{x_f} \frac{V''(y)}{\sqrt{H_{\mathcal{T}} + V'(y)^2}} dy + \int_{x_f}^z \frac{V''(y)}{\sqrt{H_{\mathcal{T}} + V'(y)^2}} dy, \\
 P_{\mathcal{T}}(x_f, T|x_i, 0) &= A_{\mathcal{T}}[x] \mathcal{J}_{\mathcal{T}}(x) \exp \left[-\frac{S_{\mathcal{T}}(x_f, x_i, T)}{4D} \right].
 \end{aligned}$$

5.2 The appearance of a second peak

We can also look further into the critical time when there is a change from the direct to the turning path. Specifically, we can consider the appearance of a second peak in the probability density function for a double well potential. The appearance of this second peak corresponds to the appearance of the turning path because, at times after the direct path critical time, the particle will have enough “energy” to travel over the peak of the potential and make it to the bottom of the other well.

In a tilted double well potential, we can find the critical time for the probability to start settling in the right-hand well if it has begun in the left-hand well. If we select the final position to be the bottom of the right-hand well we can find the relevant energy needed, and as previously, this is the energy required for the longest possible direct path. The emergence of the turning path also relates to the emergence of the rise of the second peak. In order to visualise this, we can use the numerical technique that we have in chapter 3. To do this, we use an extended version of the effective potential, which has the extra $V''(x)$ term from the Stratonovich prescription. This additional term removes the possibility of a divergent portion of the integral when it is numerically integrated. The divergent portion still exists in the numerical path integral solution as there is no Jacobian term to counter it, as shown in the analytical solution in chapter 4. The only effect this has is a manipulation of the effective potential making the peaks that relate to minimums in the real potential taller, and the peaks that relate to the real potential maximums lower, but the turning path argument still holds. The argument makes “physical” sense in this case as the particle can have enough energy to make it over one peak of the effective potential, but then is unable to climb to the peak of the maximum of the effective potential, at x_C . This is what is shown in figure 5.2, and what can be seen in the blue curve is that the effective potential is highest at the right-hand minimum of the real potential at the bottom of the deeper well, where particles would turn around allowing the appearance of the second peak.

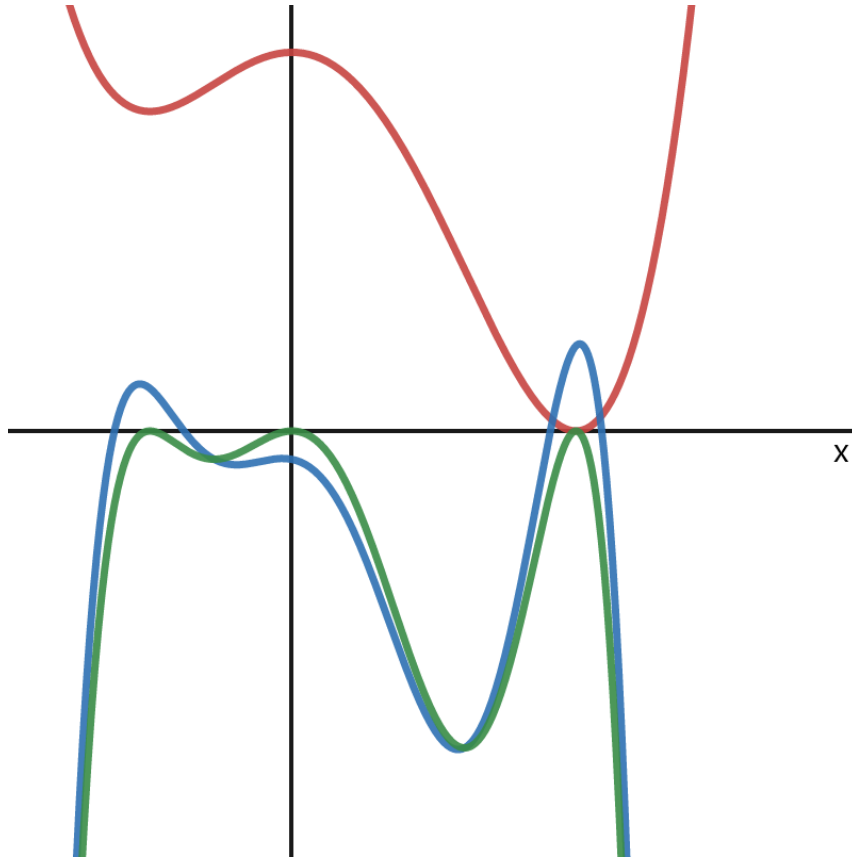


Figure 5.2: The Ito effective potential $\mathcal{V} = -V'(x)^2$, in green —, vs the Stratonovich effective potential $\mathcal{V} = -V'(x)^2 + 2DV''(x)$, in blue —, with the corresponding titled double well potential, in red —.

The critical energy is defined as;

$$\begin{aligned} H_C &= \dot{x}(x_C)^2 - V'(x_C)^2 + 2DV''(x_C), \\ &= 2DV''(x_C) \quad \text{as the velocity is 0, as is the gradient of the potential at C.} \end{aligned}$$

Inputting this into the time definition for the direct path,

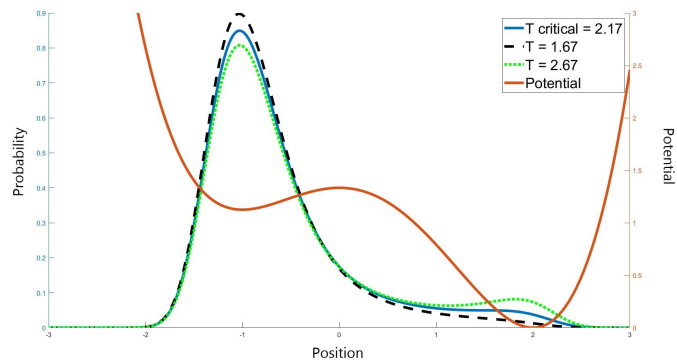
$$\begin{aligned} T_C &= \int_{x_i}^{x_f} \frac{dx}{\sqrt{H_C + V'(x)^2 - 2DV''(x)}}, \\ &= \int_{x_i}^{x_f} \frac{dx}{\sqrt{V'(x)^2 + 2D(V''(x_C) - V''(x))}}. \end{aligned}$$

We can evaluate this numerically and produce a critical time in which the second peak appears. The titled double well potential is the same as in chapter 3, and is

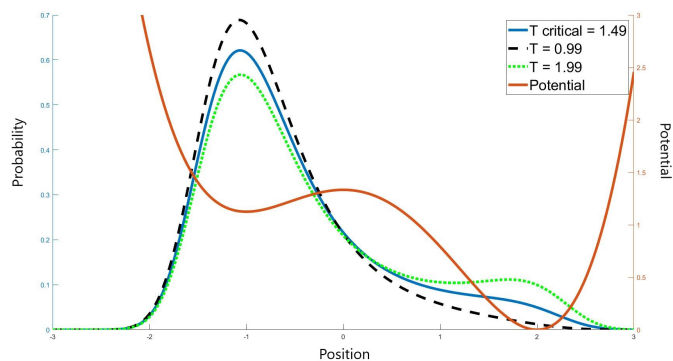
defined as,

$$V(x) = \frac{1}{8}x^4 - \frac{1}{6}x^3 - \frac{1}{2}x^2 + \frac{4}{3}.$$

This numerical integration returns a numerical value for the critical time, so we can use this value to define the time we look at when using the numerical path integral solution. Inputting this critical time as the length of time we run the numerical path integral representation for, and we can look at a few different values of diffusion to see if it returns the expected result for varying D . The results include the results of the numerical path integral representation for 500 time steps before and after to give a comparison to see if the critical time is indeed close to the minimum time required for a second peak to appear.



(a) 500-time steps on either side of T_C , $x_i = -1$, $D = 0.25$



(b) 500-time steps on either side of T_C , $x_i = -1$, $D = 0.5$

Figure 5.3: Probability density function at timesteps either side of the critical time, showing the beginning of the appearance of the second peak, only once the critical time has passed.

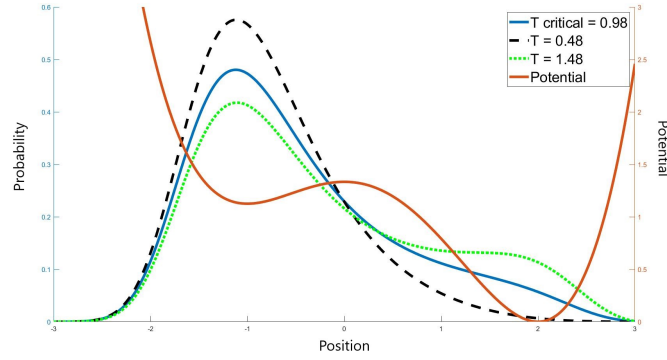
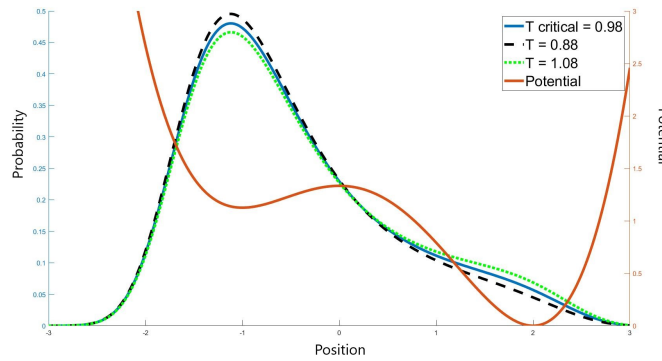
(a) 500-time steps on either side of T_C , $x_i = -1$, $D = 1$ (b) 100-time steps on either side of T_C , $x_i = -1$, $D = 1$

Figure 5.4: Probability density function at timesteps either side of the critical time, showing the beginning of the appearance of the second peak, only once the critical time has passed.

These figures show that the critical time is in the correct region and order of time to be the minimum time for a second peak to start appearing in the second well. They also show that the critical time for the appearance of the second peak, and the longest possible direct path, decreases as we increase the diffusion value, agreeing with intuition as a larger diffusion value means a quicker trip over the barrier.

They show that the second peaks will start to appear only after the critical time is calculated and not before. This shows graphically that the critical time does indeed relate to a change in the behaviour of the system, namely the introduction of the turning path.

5.3 Looking at the long time limit

So, we have found the turning path solution by showing that there must be a turning path past a critical time. However, we can also show that there must be a turning path to return the correct equilibrium probability density function and hopefully solve the issues that occur for both the stochastic action and the jacobian terms in the long time limit. We will now look at how the turning path affects $S(x)$ and $\mathcal{J}(x)$ at long times.

The Harmonic Potential

First, we look at the simplest potential with an interesting solution, where $J \neq 1$; the Harmonic potential. For this system, we know the equilibrium distribution from the Ornstein-Uhlenbeck solution with $T \rightarrow \infty$ [67],

$$P_{eq}(x_f, T|x_i)_{T \rightarrow \infty} = \frac{1}{\sqrt{2\pi D}} \exp\left[-\frac{x_f^2}{2D}\right]. \quad (5.1)$$

So, do we return the same solution from the path integral representation? For the quadratic potential with $x_i < 0$, there are three different systems depending on the final position as this would change the integral limits.

First, we look at $x_f > 0$ in which there is always only a direct path as in the long time limit in the effective potential the particle can spend infinite time at the peak of the effective potential before travelling past to the final position.

The full probability density function for this is

$$P(x_f > 0 > x_i|T) = \frac{\exp\left[\frac{1}{2} \int_{x_i}^{x_f} \frac{V''(y)}{\sqrt{H+V'(y)^2}} dy\right]}{\sqrt{4\pi D \sqrt{H+V'(x_i)^2} \sqrt{H+V'(x_f)^2} \left| \int_{x_i}^{x_f} (H+V'(y)^2)^{-\frac{3}{2}} dy \right|}} \times \exp\left[-\frac{1}{4D} \left(2V(x_f) - 2V(x_i) - HT + 2 \int_{x_i}^{x_f} \sqrt{H+V'(y)^2} dy\right)\right].$$

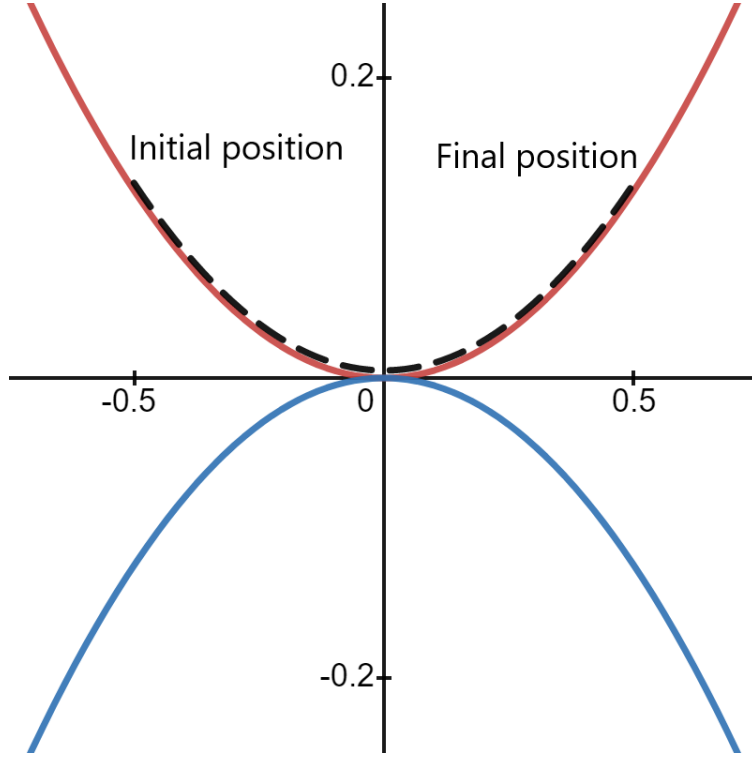


Figure 5.5: A direct path example for $x_i < 0 < x_f$ in the harmonic potential

We can calculate the Jacobian and integral in the prefactor $\mathcal{A} = \left| \int_{x_i}^{x_f} (H + V'(y)^2)^{-\frac{3}{2}} dy \right|$ integrals fully before we take the long time limit, $H \rightarrow 0$. First of all, we calculate the Jacobian integral with $V(x) = \frac{1}{2}x^2$;

$$\begin{aligned}
 \int_{x_i}^{x_f} \frac{1}{\sqrt{H + y^2}} dy &= \frac{1}{2} \log \left[\frac{\sqrt{H + x_f^2} + x_f}{\sqrt{H + x_f^2} - x_f} \right] - \frac{1}{2} \log \left[\frac{\sqrt{H + x_i^2} + x_i}{\sqrt{H + x_i^2} - x_i} \right] \\
 &= \frac{1}{2} \log \left[\frac{\left(\sqrt{H + x_f^2} + x_f \right) \left(\sqrt{H + x_i^2} - x_i \right)}{\left(\sqrt{H + x_f^2} - x_f \right) \left(\sqrt{H + x_i^2} + x_i \right)} \right] \\
 &= \frac{1}{2} \log \left[\frac{\left(\sqrt{H + x_f^2} + x_f \right)^2 \left(\sqrt{H + x_i^2} - x_i \right)^2}{H^2} \right] \\
 &= \log \left[\frac{\left(\sqrt{H + x_f^2} + x_f \right) \left(\sqrt{H + x_i^2} - x_i \right)}{H} \right].
 \end{aligned}$$

We can also calculate \mathcal{A} , which is simpler:

$$\mathcal{A} = \int_{x_i}^{x_f} \frac{1}{(H + y^2)^{\frac{3}{2}}} dy = \frac{x_f}{H\sqrt{H + x_f^2}} - \frac{x_i}{H\sqrt{H + x_i^2}}.$$

Substituting the two integrals into the full form of the probability density function that we have we have a representation,

$$\begin{aligned} P(x_f > 0 > x_i | T) &= \frac{1}{\sqrt{4\pi D \sqrt{H + x_i^2} \sqrt{H + x_f^2}}} \\ &\times \sqrt{\left[\frac{(\sqrt{H + x_f^2} + x_f)(\sqrt{H + x_i^2} - x_i)}{H} \right]} \frac{1}{\sqrt{\frac{x_f}{H\sqrt{H + x_f^2}} - \frac{x_i}{H\sqrt{H + x_i^2}}}} \\ &\times \exp \left[-\frac{1}{4D} \left(x_f^2 - x_i^2 - HT + 2 \int_{x_i}^{x_f} \sqrt{H + y^2} dy \right) \right]. \end{aligned} \quad (5.2)$$

There are some cancellations for H , which means that when we take the long time limit, $H \rightarrow 0$, we do not have an infinite limit. Taking this limit, and remembering that for square roots, we end up with absolute values; $x_i < 0 < x_f \rightarrow x_i = -|x_i|$ and $|x_f| = x_f$. In the long time limit,

$$\begin{aligned} P(x_f > 0 > x_i | T \rightarrow \infty) &= \frac{1}{\sqrt{4\pi D |x_i| |x_f|}} \sqrt{\frac{(2|x_f|)(2|x_i|)}{\frac{x_f}{|x_f|} - \frac{x_i}{|x_i|}}} \\ &\times \exp \left[-\frac{1}{4D} \left(x_f^2 - x_i^2 + 2 \int_{x_i}^{x_f} |y| dy \right) \right], \\ &= \frac{1}{\sqrt{2\pi D}} \exp \left[-\frac{1}{4D} \left(x_f^2 - x_i^2 - 2 \int_{x_i}^0 y dy + 2 \int_0^{x_f} y dy \right) \right], \end{aligned}$$

$$= \frac{1}{\sqrt{2\pi D}} \exp \left[-\frac{x_f^2}{2D} \right],$$

thus returning the correct long-time limit for the harmonic oscillator. The more interesting situation is when the final position is on the same side of the potential as the initial position. This will give the situation in which a turning path is needed after the critical time is reached. For this long time limit investigation we have $x_i < x_f < 0$. Figure 5.6 shows the two paths, direct in black and the extra turning path segments in purple that are needed to travel to $H \rightarrow 0$ corresponding to $T \rightarrow \infty$. The turning path can reach the limit of $T \rightarrow \infty$ by spending infinite time on the top of the effective potential before turning around and travelling back down to the final position.

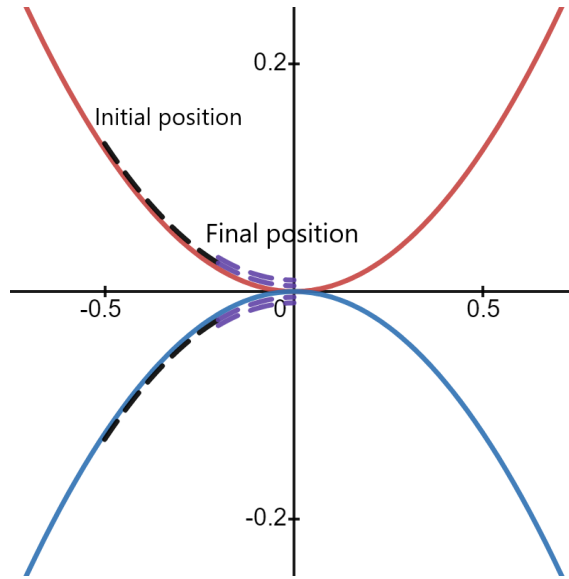


Figure 5.6: The direct path (black) and turning path extra segments (purple), for $x_i < x_f < 0$ in the harmonic potential

First, consider the direct path in a similar set-up to the previous example. The issue that arises here in the long time limit is that the Jacobian and \mathcal{A} integrals dominate the probability and send it to 0.

$$\mathcal{J}[x] = \sqrt{\left[\frac{(\sqrt{H + x_f^2} + x_f)(\sqrt{H + x_i^2} - x_i)}{H} \right]} \frac{1}{\sqrt{\frac{x_f}{H\sqrt{H+x_f^2}} - \frac{x_i}{H\sqrt{H+x_i^2}}}}$$

$$\begin{aligned}\mathcal{J}_{H \rightarrow 0} &= \sqrt{\frac{(|x_f| + x_f)(|x_i| - x_i)}{\frac{x_f}{|x_f|} - \frac{x_i}{|x_i|}}} \\ &= 0.\end{aligned}$$

This is what we expect, however; the direct path can only exist within the short time limit, and the turning path is needed! So, the probability consequently goes to zero in the numerator. This means that the extra integrals that the turning path has must fix this issue and return the equilibrium probability (5.1). The equilibrium probability for the turning path must come from a path that turns at the peak of the effective potential, in order to accumulate infinite time, so the integrals all have $x_T = 0$. The full turning path probability for this situation is,

$$\begin{aligned}P_{\mathcal{T}}(x_i < x_f < 0|T) &= \frac{\exp\left[\frac{1}{2}\int_{x_i}^{x_f} \frac{V''(y)}{\sqrt{H_{\mathcal{T}} + V'(y)^2}} dy + \int_{x_f}^0 \frac{V''(y)}{\sqrt{H_{\mathcal{T}} + V'(y)^2}} dy\right]}{\sqrt{4\pi D \sqrt{H_{\mathcal{T}} + V'(x_i)^2} \sqrt{H_{\mathcal{T}} + V'(x_f)^2} \left|\int_{x_i}^{x_f} (H_{\mathcal{T}} + V'(y)^2)^{-\frac{3}{2}} dy + 2\int_{x_f}^0 (H_{\mathcal{T}} + V'(y)^2)^{-\frac{3}{2}} dy\right|}} \\ &\times \exp\left[-\frac{1}{4D} \left(2V(x_f) - 2V(x_i) - H_{\mathcal{T}}T + 2\int_{x_i}^{x_f} \sqrt{H_{\mathcal{T}} + V'(y)^2} dy + 4\int_{x_f}^0 \sqrt{H_{\mathcal{T}} + V'(y)^2} dy\right)\right].\end{aligned}$$

The integrals for the Jacobian and \mathcal{A} integrals are the same as before, but due to the extra integral, some of the \pm signs change.

$$\begin{aligned}\frac{1}{2}\int_{x_i}^{x_f} \frac{1}{\sqrt{H_{\mathcal{T}} + y^2}} dy + \int_{x_f}^0 \frac{1}{\sqrt{H_{\mathcal{T}} + y^2}} dy \\ = \frac{1}{2} \log \left[\frac{\left(\sqrt{H_{\mathcal{T}} + x_f^2} + x_f\right) \left(\sqrt{H_{\mathcal{T}} + x_i^2} - x_i\right)}{H_{\mathcal{T}}} \right] \\ + \log \left[\frac{\sqrt{H_{\mathcal{T}}} \left(\sqrt{H_{\mathcal{T}} + x_f^2} - x_f\right)}{H_{\mathcal{T}}} \right],\end{aligned}$$

$$\begin{aligned}
 &= \frac{1}{2} \log \left[\frac{\left(\sqrt{H_{\mathcal{T}} + x_f^2} + x_f \right) \left(\sqrt{H_{\mathcal{T}} + x_i^2} - x_i \right) \left(\sqrt{H_{\mathcal{T}} + x_f^2} - x_f \right)^2}{H_{\mathcal{T}}^2} \right], \\
 &= \frac{1}{2} \log \left[\frac{\left(\sqrt{H_{\mathcal{T}} + x_f^2} - x_f \right) \left(\sqrt{H_{\mathcal{T}} + x_i^2} - x_i \right)}{H_{\mathcal{T}}} \right].
 \end{aligned}$$

$$\begin{aligned}
 &\int_{x_i}^{x_f} (H_{\mathcal{T}} + V'(y)^2)^{-\frac{3}{2}} dy + 2 \int_{x_f}^0 (H_{\mathcal{T}} + V'(y)^2)^{-\frac{3}{2}} dy, \\
 &= \frac{x_f}{H_{\mathcal{T}} \sqrt{H_{\mathcal{T}} + x_f^2}} - \frac{x_i}{H_{\mathcal{T}} \sqrt{H_{\mathcal{T}} + x_i^2}} - 2 \frac{x_f}{H_{\mathcal{T}} \sqrt{H_{\mathcal{T}} + x_f^2}}, \\
 &= -\frac{x_f}{H_{\mathcal{T}} \sqrt{H_{\mathcal{T}} + x_f^2}} - \frac{x_i}{H_{\mathcal{T}} \sqrt{H_{\mathcal{T}} + x_i^2}}.
 \end{aligned}$$

Inputting this all into our probability density function representation

$$\begin{aligned}
 P_{\mathcal{T}}(x_i < x_f < 0|T) &= \frac{1}{\sqrt{4\pi D \sqrt{H_{\mathcal{T}} + x_i^2} \sqrt{H_{\mathcal{T}} + x_f^2}}} \\
 &\times \sqrt{\left[\frac{\left(\sqrt{H_{\mathcal{T}} + x_f^2} - x_f \right) \left(\sqrt{H_{\mathcal{T}} + x_i^2} - x_i \right)}{H_{\mathcal{T}}} \right]} \frac{1}{\sqrt{\frac{x_f}{H_{\mathcal{T}} \sqrt{H_{\mathcal{T}} + x_f^2}} + \frac{x_i}{H_{\mathcal{T}} \sqrt{H_{\mathcal{T}} + x_i^2}}}} \\
 &\times \exp \left[-\frac{1}{4D} \left(x_f^2 - x_i^2 - H_{\mathcal{T}}T + 2 \int_{x_i}^{x_f} \sqrt{H_{\mathcal{T}} + y^2} dy \right) \right].
 \end{aligned}$$

For the \mathcal{A} integral, there is a magnitude sign around the integral, so it becomes positive on both terms. Now, taking the long time limit, $H_{\mathcal{T}} \rightarrow 0$,

$$\begin{aligned}
 P_{\mathcal{T}}(x_i < x_f < 0|T \rightarrow \infty) &= \frac{1}{\sqrt{4\pi D |x_i| |x_f|}} \sqrt{\frac{(2|x_f|)(2|x_i|)}{\left| \frac{x_f}{|x_f|} + \frac{x_i}{|x_i|} \right|}} \\
 &\times \exp \left[-\frac{1}{4D} \left(x_f^2 - x_i^2 + 2 \int_{x_i}^{x_f} |y| dy + 4 \int_{x_f}^0 |y| dy \right) \right]
 \end{aligned}$$

$$\begin{aligned}
 &= \frac{1}{\sqrt{2\pi D}} \exp \left[-\frac{1}{4D} \left(x_f^2 - x_i^2 - 2 \int_{x_i}^{x_f} y dy - 4 \int_{x_f}^0 y dy \right) \right] \\
 &= \frac{1}{\sqrt{2\pi D}} \exp \left[-\frac{1}{4D} (x_f^2 - x_i^2 - x_f^2 + x_i^2 + 2x_f^2) \right] \\
 &= \frac{1}{\sqrt{2\pi D}} \exp \left[-\frac{x_f^2}{2D} \right].
 \end{aligned}$$

This shows that the turning path representation returns the correct normalised long-time limit, meaning that the turning path provides information that the direct path cannot. This investigation provides insight into the understanding of the path integral and how we need to construct the probability density function for a given system.

In this chapter, we have shown that the turning path is needed to satisfy long-time limits, and this results from the fact that there is a maximum time for a direct path to make physical sense. Then we looked at how the turning path changes the analytical form we have already found, introducing extra segments of paths and, consequently, extra integrals in each term of the path integral formulation. We then investigated how the turning path relates to the appearance of the second peak in a tilted double-well potential after the maximum direct path time, proving it graphically using the numerical implementation. Finally, we looked at how the turning path returns the correct long-time limit specifically for the Harmonic potential, fixing one of the significant issues that has cropped up in previous chapters.

Chapter 6

The Harmonic Oscillator

In this chapter, we will be looking at the Harmonic Oscillator in detail, and some of the existing methods used to solve for the probability density function. We will then introduce the now full path integral technique solution and show that it will return the same solution. Finally, we will explore the need for turning paths in the given system, and show that there is a necessity for the turning path to return a full physical solution, to find the complete solution for the path integral technique.

We will look at three standard methods that can be used to find the probability density function for the harmonic oscillator, before showing that the path integral returns the same result. We include the following three techniques for solving the harmonic oscillator for a level of completeness in this work, and to be able to compare the path integral directly with existing methods.

6.1 The Eigenfunction expansion

First, we look at the technique described in chapter 5 of Risken's book "The Fokker-Planck Equation" [84], which uses an eigenfunction expansion to solve for $P(x, t)$. It uses the properties and identities of operators to find the eigenfunctions for the Fokker-Planck operator, which can then be related to the ODE solved by the Hermite polynomials [85], and the final probability density function is then calculated by substitution. Starting by looking at the theory for solving the general Fokker-Planck equation, we will then apply the method to the specific problem we are interested in: solving the equation for a quadratic potential.

We are looking for a non-stationary solution to the general Fokker-Planck equation,

$$\frac{\partial W}{\partial t} = L_{FP}W(x, t), \quad (6.1)$$

where L_{FP} is the general differential operator,

$$L_{FP} = -\frac{\partial}{\partial x}D^{(1)}(x) + \frac{\partial^2}{\partial x^2}D^{(2)}(x). \quad (6.2)$$

We begin by using an ansatz to solve this equation, $W(x, t) = \varphi(x)e^{-\lambda t}$, where φ is an eigenfunction with corresponding eigenvalue λ . This means we are now solving the eigenfunction equation after substituting $W(x, t)$ into (6.1),

$$L_{FP}\varphi(x) = -\lambda\varphi(x).$$

In order to solve this equation, it will be useful to provide an alternative form for the operator L_{FP} in terms of solutions that we know. To do this, we now solve for the stationary solution, $\frac{\partial W}{\partial t} = 0$, of the original Fokker-Planck equation (6.1) to find the relationship between $D^{(1)}$ and $D^{(2)}$ in L_{FP} . The stationary solution needs to solve

$$D^{(1)}W_{st}(x, t) = \frac{\partial}{\partial x}D^{(2)}W_{st}(x, t).$$

This is solved with an integrating factor, yielding the solution

$$W_{st} = \frac{A}{D^{(2)}} \exp \left[\int^x \frac{D^{(1)}}{D^{(2)}} \right].$$

We define a function $\Phi(x)$ as the stationary solution, $W_{st} = Ae^{-\Phi(x)}$, where A is a constant, which can be written in a compact form,

$$\Phi(x) = \ln(D^{(2)}) - \int^x \frac{D^{(1)}(y)}{D^{(2)}(y)} dy. \quad (6.3)$$

This function will be used to make the mathematics tidier. Using this representation to modify the operator into a more compact form,

$$\begin{aligned} L_{FP} &= \frac{\partial^2}{\partial x^2}D^{(2)} - \frac{\partial}{\partial x}D^{(1)} \\ &= \frac{\partial}{\partial x} [D^{(2)} - D^{(1)}] \\ &= \frac{\partial}{\partial x}D^{(2)} \left[\frac{D^{(2)}}{D^{(2)}} - \frac{D^{(1)}}{D^{(2)}} \right] \\ &= \frac{\partial}{\partial x}D^{(2)}\Phi' \\ &= \frac{\partial}{\partial x}D^{(2)}e^{-\Phi}\Phi'e^{\Phi} \\ L_{FP} &= \frac{\partial}{\partial x}D^{(2)}e^{-\Phi} \frac{\partial}{\partial x}e^{\Phi}. \end{aligned} \quad (6.4)$$

We now have a more useful form of the differential operator for the Fokker-Planck equation. However, it would be more beneficial if it had the useful property of being a Hermitian operator [86]. This would mean that the operator's eigenvalues are real, and the corresponding eigenfunctions are orthogonal. The property of the

orthogonal eigenfunctions will allow the delta function to be defined in relation to the eigenfunctions, and consequently, the probability density function can then be written as a sum of the eigenfunctions.

First of all, we need to check whether the operator L_{FP} we have just defined is Hermitian [86]. This is done by looking at the inner product, and in order to be Hermitian, it needs to satisfy $\langle W_1, L_{FP}W_2 \rangle = \langle L_{FP}W_1, W_2 \rangle$.

$$\begin{aligned} \langle W_1, L_{FP}W_2 \rangle &= \int_{x_{min}}^{x_{max}} W_1 L_{FP}W_2 dx, \\ &= \int_{x_{min}}^{x_{max}} W_1 \frac{\partial}{\partial x} \left[D^{(2)} e^{-\Phi} \frac{\partial}{\partial x} (e^{\Phi} W_2) \right] dx, \\ &= - \int_{x_{min}}^{x_{max}} \left[\frac{\partial}{\partial x} W_1 \right] D^{(2)} e^{-\Phi} \frac{\partial}{\partial x} [e^{\Phi} W_2] dx + \left[W_1 D^{(2)} e^{-\Phi} \frac{\partial}{\partial x} (e^{\Phi} W_2) \right]_{x_{min}}^{x_{max}}. \end{aligned}$$

At the maximum and minimum, $e^{\Phi} W_{x_{min}} = 0 = e^{\Phi} W_{x_{max}}$, as the probability either decays to 0 if there are infinite boundaries or if there are set boundary conditions the probability is 0 for an absorbing boundary. Meaning that the second term on the right-hand side disappears due to boundary conditions. Consequently,

$$\begin{aligned} \langle W_1, L_{FP}W_2 \rangle &= - \int_{x_{min}}^{x_{max}} \left[\frac{\partial}{\partial x} W_1 \right] D^{(2)} e^{-\Phi} \frac{\partial}{\partial x} [e^{\Phi} W_2] dx, \\ &= \int_{x_{min}}^{x_{max}} e^{\Phi} W_2 \frac{\partial}{\partial x} \left[\left(\frac{\partial}{\partial x} W_1 \right) D^{(2)} e^{-\Phi} \right] dx, \\ &\neq \int_{x_{min}}^{x_{max}} W_2 \frac{\partial}{\partial x} \left[\left(\frac{\partial}{\partial x} e^{\Phi} W_1 \right) D^{(2)} e^{-\Phi} \right] dx = \langle L_{FP}W_1, W_2 \rangle. \end{aligned}$$

This shows that, unfortunately, it is not Hermitian, but we can use a related operator which may be Hermitian, $L = e^{\frac{\Phi}{2}} L_{FP} e^{-\frac{\Phi}{2}}$, as shown below, again using the boundary conditions to simplify.

$$\begin{aligned}
 \langle W_1, LW_2 \rangle &= \int_{x_{min}}^{x_{max}} W_1 LW_2 dx \\
 &= \int_{x_{min}}^{x_{max}} W_1 e^{\frac{\Phi}{2}} \frac{\partial}{\partial x} \left[D^{(2)} e^{-\Phi} \frac{\partial}{\partial x} \left(e^{\Phi} e^{-\frac{\Phi}{2}} W_2 \right) \right] dx \\
 &= \int_{x_{min}}^{x_{max}} W_1 e^{\frac{\Phi}{2}} \frac{\partial}{\partial x} \left[D^{(2)} e^{-\Phi} \frac{\partial}{\partial x} \left(e^{\frac{\Phi}{2}} W_2 \right) \right] dx \\
 \text{Integration by parts} &= - \int_{x_{min}}^{x_{max}} \frac{\partial}{\partial x} \left[W_1 e^{\frac{\Phi}{2}} \right] D^{(2)} e^{-\Phi} \frac{\partial}{\partial x} \left[e^{\frac{\Phi}{2}} W_2 \right] dx \\
 \text{Integration by parts} &= \int_{x_{min}}^{x_{max}} \frac{\partial}{\partial x} \left[D^{(2)} e^{-\Phi} \frac{\partial}{\partial x} \left(e^{\Phi} W_1 e^{-\frac{\Phi}{2}} \right) \right] e^{\frac{\Phi}{2}} W_2 dx \\
 &= \int_{x_{min}}^{x_{max}} e^{\frac{\Phi}{2}} \frac{\partial}{\partial x} \left[D^{(2)} e^{-\Phi} \frac{\partial}{\partial x} \left(e^{\Phi} W_1 e^{-\frac{\Phi}{2}} \right) \right] W_2 dx \\
 &= \langle LW_1, W_2 \rangle.
 \end{aligned}$$

Therefore L is Hermitian. The corresponding eigenfunctions of L are related to the eigenfunctions of L_{FP} via a similar transformation, $\psi_n = e^{\frac{\Phi}{2}} \varphi_n$ with the same corresponding eigenvalues, λ_n . We can now use the eigenfunctions of L to define a completeness relationship for the delta function, which is the initial condition of the system,

$$\begin{aligned}
 \delta(x - x_0) &= \sum_n \psi_n(x) \psi_n(x_0), \\
 &= e^{\frac{\Phi(x)}{2} + \frac{\Phi(x_0)}{2}} \sum_n \varphi_n(x) \varphi_n(x_0), \\
 &= e^{\Phi(x_0)} \sum_n \varphi_n(x) \varphi_n(x_0) = P(x, t = 0 | x_0).
 \end{aligned}$$

Subsequently, we can now define the transition probability in terms of the eigenfunctions for an initial condition,

$$\begin{aligned}
 \frac{\partial}{\partial t} P(x, t | x_0) &= L_{FP} P \\
 \rightarrow P(x, t | x_0) &= e^{L_{FP} t} \delta(x - x_0).
 \end{aligned}$$

The solution can then be expressed in terms of the eigenfunctions,

$$\begin{aligned}
 P(x, t|x_0) &= e^{L_{FP}t} \delta(x - x_0), \\
 &= e^{\Phi(x_0)} \sum_n \varphi_n(x) \varphi_n(x_0) e^{L_{FP}t}, \\
 &= e^{\Phi(x_0)} \sum_n \varphi_n(x) \varphi_n(x_0) e^{-\lambda_n t}, \\
 &= e^{\frac{\Phi(x_0)}{2} - \frac{\Phi(x)}{2}} \sum_n \psi_n(x) \psi_n(x_0) e^{-\lambda_n t}. \tag{6.5}
 \end{aligned}$$

Now that we have a relationship between the transition probability and the eigenfunctions, we need to find what the eigenfunctions are. First of all, we now need the operator L in terms of both $D^{(1)}$ and $D^{(2)}$. We can write L in terms of two further operators,

$$\begin{aligned}
 L &= e^{\frac{\Phi}{2}} L_{FP} e^{-\frac{\Phi}{2}}, \\
 \text{Using (6.4)} \quad &= e^{\frac{\Phi}{2}} \frac{\partial}{\partial x} D^{(2)} e^{-\Phi} \frac{\partial}{\partial x} e^{\frac{\Phi}{2}},
 \end{aligned}$$

$$= -\hat{a}a,$$

$$\text{where } a = \sqrt{D^{(2)}} e^{-\frac{\Phi}{2}} \frac{\partial}{\partial x} e^{\frac{\Phi}{2}}, \tag{6.6}$$

$$\hat{a} = -e^{\frac{\Phi}{2}} \frac{\partial}{\partial x} \sqrt{D^{(2)}} e^{-\frac{\Phi}{2}}. \tag{6.7}$$

Using the solution (6.3), we can relate the operators, a and \hat{a} , to the functions $D^{(1)}$ and $D^{(2)}$.

$$\begin{aligned}
 a &= \sqrt{D^{(2)}} e^{-\frac{\Phi}{2}} \left[e^{\frac{\Phi}{2}} \frac{\partial}{\partial x} + \frac{1}{2} \Phi' e^{\frac{\Phi}{2}} \right] \\
 &= \sqrt{D^{(2)}} \frac{\partial}{\partial x} + \frac{1}{2} \sqrt{D^{(2)}} \Phi' \\
 &= \sqrt{D^{(2)}} \frac{\partial}{\partial x} + \frac{1}{2\sqrt{D^{(2)}}} \left[\frac{dD^{(2)}}{dx} - D^{(1)} \right] \\
 \hat{a} &= -e^{\frac{\Phi}{2}} \frac{\partial}{\partial x} \left[\sqrt{D^{(2)}} e^{-\frac{\Phi}{2}} \right] \\
 &= -\frac{\partial}{\partial x} \sqrt{D^{(2)}} + \frac{1}{2\sqrt{D^{(2)}}} \left[\frac{dD^{(2)}}{dx} - D^{(1)} \right].
 \end{aligned}$$

Specific example: Harmonic Oscillator

We can now apply the techniques described above to a specific example: the harmonic oscillator. This has to satisfy the following Smoluchowski equation,

$$\frac{\partial P}{\partial t} = \frac{\partial}{\partial x} [bxP] + D \frac{\partial^2}{\partial x^2} P, \quad P(x, t = 0 | x_0) = \delta(x - x_0),$$

which when compared to the general operator for the Fokker-Planck equation (6.1) gives, $D^{(1)} = -bx, D^{(2)} = D$. This gives our operators (6.6)(6.7) as,

$$a = \sqrt{D} \frac{\partial}{\partial x} + \frac{b}{2\sqrt{D}} x,$$

$$\hat{a} = -\sqrt{D} \frac{\partial}{\partial x} + \frac{b}{2\sqrt{D}} x.$$

To make the notation more compact, we can introduce a couple of substitutions, $\xi = \sqrt{\frac{b}{2D}} x$ and $a = \sqrt{b}\alpha, \hat{a} = \sqrt{b}\alpha^\dagger$, meaning we have now,

$$\alpha = \frac{1}{\sqrt{2}} \left(\frac{\partial}{\partial \xi} + \xi \right), \tag{6.8}$$

$$\alpha^\dagger = \frac{1}{\sqrt{2}} \left(-\frac{\partial}{\partial \xi} + \xi \right), \tag{6.9}$$

$$\alpha\alpha^\dagger - \alpha^\dagger\alpha = 1, \tag{6.10}$$

$$L = -b\alpha^\dagger\alpha. \tag{6.11}$$

The next step is to work out the eigenvalues of this operator in order to be able to calculate the eigenfunctions. Following the examples and expressions given in [87], we now introduce the operator defined by $N = \alpha^\dagger\alpha$. This operator has the same eigenvalues as L as it is a multiple of $L = -bN$. We can prove it is Hermitian,

$$\begin{aligned} N^\dagger &= (\alpha^\dagger\alpha)^\dagger, \\ &= \alpha^\dagger (\alpha^\dagger)^\dagger, \\ &= \alpha^\dagger\alpha, \\ &= N. \end{aligned}$$

We can also calculate the commutators with α and α^\dagger ,

$$\begin{aligned} [N, \alpha] &= [\alpha^\dagger \alpha, \alpha] = \alpha^\dagger [\alpha, \alpha] + [\alpha^\dagger, \alpha] \alpha = -\alpha, \\ [N, \alpha^\dagger] &= [\alpha^\dagger \alpha, \alpha^\dagger] = \alpha^\dagger [\alpha, \alpha^\dagger] + [\alpha^\dagger, \alpha^\dagger] \alpha = \alpha^\dagger. \end{aligned}$$

These operators are similar in construction to the Ladder operator method used in quantum mechanics, again showing the similarity in techniques between quantum mechanics, classical mechanics and stochastic physics. [88] As defined in [87] an operator with these properties have the corresponding eigenvalues of n , meaning,

$$\begin{aligned} N\psi_n &= n\psi_n, \\ L\psi_n &= -bN\psi_n = -bn\psi_n = -\lambda_n\psi_n, \\ \lambda_n &= bn. \end{aligned}$$

We have worked out the eigenvalues, and we can calculate the ground state eigenfunction corresponding to $n = 0$, meaning we solve $L\psi_0 = 0$. Applying the operators, $\alpha^\dagger(6.9)$ and $\alpha(6.8)$ yields,

$$\begin{aligned} L\psi_0 &= -b\alpha^\dagger\alpha\psi_0 \\ &= -\frac{b}{2} \left(-\frac{\partial}{\partial\xi} + \xi \right) \left(\frac{\partial}{\partial\xi} + \xi \right) \psi_0 \\ &= -\frac{b}{2} \left(-\frac{\partial}{\partial\xi} + \xi \right) \left(\frac{\partial\psi_0}{\partial\xi} + \xi\psi_0 \right) \\ &= -\frac{b}{2} \left[-\frac{\partial^2\psi_0}{\partial\xi^2} - \psi_0 - \xi \frac{\partial\psi_0}{\partial\xi} + \xi \frac{\partial\psi_0}{\partial\xi} + \xi^2\psi_0 \right] \\ &= \frac{b}{2} \left[\frac{\partial^2\psi_0}{\partial\xi^2} - (\xi^2 - 1)\psi_0 \right] \\ \psi_0'' - (\xi^2 - 1)\psi_0 &= 0 \end{aligned}$$

Solving this differential equation is done using an ansatz, $\psi_0 = N_c e^{-k\xi^2}$, where N_c is the normalisation constant.

$$\psi_0' = -2N_c k \xi e^{-k\xi^2}$$

$$\begin{aligned}
 \psi_0'' &= -2N_c k e^{-k\xi^2} + 4N_c k^2 \xi^2 e^{-k\xi^2} \\
 \psi_0'' - (\xi^2 - 1)\psi_0 &= -2N_c k e^{-k\xi^2} + 4N_c k^2 \xi^2 e^{-k\xi^2} - N_c \xi^2 e^{-k\xi^2} + N_c e^{-k\xi^2} = 0 \\
 &\rightarrow k = \frac{1}{2}
 \end{aligned}$$

Now have an ansatz with a normalisation constant that needs calculating. To solve for N_c , we make use of the normalisation of eigenfunctions which means,

$$\begin{aligned}
 \int_{-\infty}^{\infty} \psi_0(x)\psi_0(x)dx &= 1 \\
 &= \int_{-\infty}^{\infty} \psi_0(\xi)\psi_0(\xi)d\xi\sqrt{\frac{2D}{b}} \\
 &= N_c^2 \sqrt{\frac{2D}{b}} \int_{-\infty}^{\infty} e^{-\xi^2} d\xi \\
 &= N_c^2 \sqrt{\frac{2D}{b}} \sqrt{\pi} = 1 \\
 \rightarrow N_c &= \sqrt[4]{\frac{b}{2\pi D}} \\
 \rightarrow \psi_0 &= \sqrt[4]{\frac{b}{2\pi D}} e^{-\frac{\xi^2}{2}} \tag{6.12}
 \end{aligned}$$

We need to work out now a relationship to calculate the other eigenfunctions, using an expression from [87],

$$\psi_n(x) = \frac{(\alpha^\dagger)^n}{\sqrt{n!}} \psi_0(x) = \sqrt[4]{\frac{b}{2\pi D}} \frac{1}{\sqrt{2^n n!}} H_n(\xi) e^{-\frac{\xi^2}{2}}, \tag{6.13}$$

where $H_n(\xi)$ are the Hermite polynomials. We can now start to calculate the probability density function (6.5) using our definitions for the eigenfunctions and $\Phi(x) = \frac{V(x)}{D} = \frac{bx^2}{2D}$.

$$\begin{aligned}
 P(x, t|x_0) &= e^{\frac{\Phi(x_0)}{2} - \frac{\Phi(x)}{2}} \sum_n \psi_n(x)\psi_n(x_0)e^{-\lambda_n t}, \\
 &= e^{\frac{b}{4D}(x_0^2 - x^2)} \sqrt{\frac{b}{2\pi D}} e^{-\frac{1}{2}(\xi_0^2 + \xi^2)} \sum_n \frac{e^{-bnt}}{2^n n!} H_n(\xi) H_n(\xi_0),
 \end{aligned}$$

Note: $\xi = \sqrt{\frac{b}{2D}}x$

$$\begin{aligned}
 P(x, t|x_0) &= \sqrt{\frac{b}{2\pi D}} e^{\frac{b}{4D}(x_0^2-x^2)} e^{-\frac{b}{4D}(x_0^2+x^2)} \sum_n \frac{1}{n!} \left(\frac{e^{-bt}}{2}\right)^n H_n\left(\sqrt{\frac{b}{2D}}x\right) H_n\left(\sqrt{\frac{b}{2D}}x_0\right), \\
 &= \sqrt{\frac{b}{2\pi D}} e^{-\frac{b}{2D}x^2} \sum_n \frac{1}{n!} \left(\frac{e^{-bt}}{2}\right)^n H_n\left(\sqrt{\frac{b}{2D}}x\right) H_n\left(\sqrt{\frac{b}{2D}}x_0\right).
 \end{aligned}$$

Using Mehler's expansion [89], we can calculate the sum,

$$\begin{aligned}
 &\sum_n \frac{1}{n!} \left(\frac{e^{-bt}}{2}\right)^n H_n\left(\sqrt{\frac{b}{2D}}x\right) H_n\left(\sqrt{\frac{b}{2D}}x_0\right) \\
 &= \frac{1}{\sqrt{1-e^{-2bt}}} \exp\left[\frac{2e^{-bt}}{1-e^{-2bt}} \left(\frac{bx_0x}{2D} - \frac{e^{-bt}bx^2}{4D} - \frac{e^{-bt}bx_0^2}{4D}\right)\right] \\
 &= \frac{1}{\sqrt{1-e^{-2bt}}} \exp\left[-\frac{b}{2D(1-e^{-2bt})} (-2xx_0e^{-bt} + x^2e^{-2bt} + x_0^2e^{-2bt})\right].
 \end{aligned}$$

Replacing this in the probability density function yields,

$$\begin{aligned}
 P(x, t|x_0) &= \sqrt{\frac{b}{2\pi D(1-e^{-2bt})}} \exp\left[-\frac{bx^2}{2D}\right] \\
 &\quad \times \exp\left[-\frac{b}{2D(1-e^{-2bt})} (-2xx_0e^{-bt} + x^2e^{-2bt} + x_0^2e^{-2bt})\right] \\
 &= \sqrt{\frac{b}{2\pi D(1-e^{-2bt})}} \exp\left[-\frac{b}{2D(1-e^{-2bt})} (x^2 - 2xx_0e^{-bt} + x_0^2e^{-2bt})\right] \\
 &= \sqrt{\frac{b}{2\pi D(1-e^{-2bt})}} \exp\left[-\frac{b}{2D(1-e^{-2bt})} (x - x_0e^{-bt})^2\right]
 \end{aligned}$$

This is the known PDF for the quadratic potential [90], a long and tricky method to keep up with all of the transformations; hopefully, another technique will be simpler!

6.2 Transformation and separation of variables

The second technique is to use a substitution for the Smoluchowski equation to directly compare with an ordinary differential equation with known solutions, Hermite polynomials [91]. So looking at the Smoluchowski equation,

$$\begin{aligned}\frac{\partial P}{\partial t} &= \frac{\partial}{\partial x} \left[\frac{dV}{dx} P + D \frac{\partial P}{\partial x} \right], \\ &= b \frac{\partial}{\partial x} [xP] + D \frac{\partial^2 P}{\partial x^2}, \\ &= bP + bx \frac{\partial P}{\partial x} + D \frac{\partial^2 P}{\partial x^2},\end{aligned}$$

we want to use substitutions to transform this into the form of the Hermite Equation ODE [85],

$$u'' - 2xu' + 2nu = 0, \quad (6.14)$$

as this would allow us to use known results to find a solution. The first transformation is to transform the Smoluchowski equation to a form of the Schrödinger equation. So, we transform the equation to eliminate the first-order derivative in space, $P(x, t) = F(x)G(x, t)$. The derivatives are,

$$\begin{aligned}\frac{\partial P}{\partial t} &= F \frac{\partial G}{\partial t} \\ \frac{\partial P}{\partial x} &= \frac{dF}{dx} G + F \frac{\partial G}{\partial x} \\ \frac{\partial^2 P}{\partial x^2} &= \frac{d^2 F}{dx^2} G + 2 \frac{dF}{dx} \frac{\partial G}{\partial x} + F \frac{\partial^2 G}{\partial x^2}\end{aligned}$$

Inserting this into the Smoluchowski equation,

$$F \frac{\partial G}{\partial t} = bFG + bx \frac{dF}{dx} G + bx F \frac{\partial G}{\partial x} + D \frac{d^2 F}{dx^2} G + 2D \frac{dF}{dx} \frac{\partial G}{\partial x} + DF \frac{\partial^2 G}{\partial x^2}.$$

So in order to eliminate the first-order derivative in G we require,

$$bx F + 2D \frac{dF}{dx} = 0,$$

$$\frac{dF}{dx} = -\frac{bx}{2D}F,$$

$$F = A \exp\left[-\frac{bx^2}{4D}\right].$$

Substituting this into the equation we find,

$$\frac{\partial G}{\partial t} = \frac{1}{2}bG - \frac{b^2x^2}{4D}G + D\frac{\partial^2 G}{\partial x^2}.$$

This is now in the form of a Schrödinger equation. In order to get to the Hermite equation (6.14), we need to separate the spatial and time derivatives (separation of variables) $G(x, t) = X(x)T(t)$. Substituting this in,

$$X(x)\dot{T}(t) = DX''(x)T(t) + \frac{1}{2}b\left(1 - \frac{bx^2}{2D}\right)X(x)T(t)$$

$$\frac{\dot{T}}{T} = D\frac{X''}{X} + \frac{1}{2}b\left(1 - \frac{bx^2}{2D}\right).$$

As the left-hand side is only time-dependent, and the right-hand side is only space dependent, both sides must equal a constant, λ . The time equation is simple to solve,

$$\dot{T} = -\lambda T$$

$$T = \exp(-\lambda t),$$

whilst also having a spatial equation,

$$DX'' + \frac{1}{2}b\left(1 - \frac{bx^2}{2D}\right)X + \lambda X = 0$$

We use one more transformation to change this spatial equation into the form of the Hermite equation, (6.14). Using the transformation, $y = \sqrt{\frac{b}{2D}}x$, $X(x) = U(y)e^{-\frac{y^2}{2}}$. Calculating the derivatives,

$$X = Ue^{-\frac{y^2}{2}}$$

$$\begin{aligned}
 X' &= -yUe^{-\frac{y^2}{2}} + U'e^{-\frac{y^2}{2}} \\
 X'' &= -Ue^{-\frac{y^2}{2}} - 2yU'e^{-\frac{y^2}{2}} + y^2Ue^{-\frac{y^2}{2}} + U''e^{-\frac{y^2}{2}}.
 \end{aligned}$$

Substituting this into the spatial equation that we have gives

$$\begin{aligned}
 DX'' + \frac{1}{2}b\left(1 - \frac{bx^2}{2D}\right)X + \lambda X &= 0 \\
 \frac{b}{2}X''(y) + \frac{1}{2}b(1 - y^2)X(y) + \lambda X(y) &= 0 \\
 -\frac{b}{2}Ue^{-\frac{y^2}{2}} - byU'e^{-\frac{y^2}{2}} + \frac{b}{2}y^2Ue^{-\frac{y^2}{2}} + \frac{b}{2}U''e^{-\frac{y^2}{2}} + \frac{1}{2}b(1 - y^2)e^{-\frac{y^2}{2}}U + \lambda e^{-\frac{y^2}{2}}U &= 0 \\
 U'' - 2yU' + \frac{2\lambda}{b}U &= 0.
 \end{aligned}$$

So we now have the Hermite equation with eigenvalue $\lambda = bn$, which are real for $n = 0, 1, 2, \dots$ and the solutions $U_n(y)$ are the Hermite polynomials $H_n(y)$. Going all the way back, we have the form of the solution for the probability density function with all the substitutions,

$$\begin{aligned}
 P(x, t) &= AF(x)G(x, t), \\
 &= AF(x)T(t)X(x), \\
 &= Ae^{-\frac{bx^2}{4D}}e^{-\lambda t}U(y)e^{-\frac{y^2}{2}}, \\
 &= \sum_n c_n e^{-\frac{y^2}{2}} e^{-bnt} H_n(y) e^{-\frac{y^2}{2}}; \quad y = \sqrt{\frac{b}{2D}}x \\
 &= e^{-y^2} \sum_n c_n H_n(y) e^{-bnt}.
 \end{aligned}$$

In order to calculate the coefficients c_n we need to use the orthogonality of the Hermite polynomials [91] and the initial condition, $P(x, t = 0) = \delta(x - x_0)$, meaning that,

$$\delta(y - y_0) = \sum_n e^{-y^2} c_n H_n(y).$$

Then using the generalised Fourier series method [92] for calculating the coefficients of a series, with a weight function of the Hermite polynomials of e^{y^2} ,

$$\begin{aligned} c_n &= \frac{\int_{-\infty}^{\infty} dy e^{-y^2} H_n(y) \delta(y - y_0) e^{y^2}}{\int_{-\infty}^{\infty} dy e^{-y^2} H_n(y) e^{-y^2} H_n(y) e^{y^2}}, \\ &= \frac{\int_{-\infty}^{\infty} dy H_n(y) \delta(y - y_0)}{\int_{-\infty}^{\infty} dy e^{-y^2} H_n(y) H_n(y)}. \end{aligned}$$

Using the properties of the delta function, and the orthogonality of the Hermite polynomials,

$$\int_{-\infty}^{\infty} dy e^{-y^2} H_n(y) H_m(y) = \delta_{nm} 2^n n! \sqrt{\pi},$$

we get the coefficients being,

$$c_n = \frac{H_n(y_0)}{2^n n! \sqrt{\pi}}.$$

This means that

$$P(y, t) = N e^{-y^2} \sum_n \frac{H_n(y) H_n(y_0)}{n!} \left(\frac{e^{-bt}}{2} \right)^n,$$

where N is a normalisation constant to be worked out at the end. We can then use Mehler's expansion [89],

$$\sum_n H_n(y) H_n(y_0) \frac{z^n}{n!} = \frac{1}{\sqrt{1-4z^2}} \exp \left[\frac{4z}{1-4z^2} (y_0 y - z y^2 - z y_0^2) \right].$$

Substituting in $y = \sqrt{\frac{b}{2D}} x$,

$$\begin{aligned} P(x, t|x_0) &= N e^{-\frac{bx^2}{2D}} \frac{1}{\sqrt{1-e^{-2bt}}} \exp \left[\frac{2e^{-bt}}{1-e^{-2bt}} \left(\frac{b}{2D} x x_0 - \frac{e^{-bt}}{2} \frac{b}{2D} x^2 - \frac{e^{-bt}}{2} \frac{b}{2D} x_0^2 \right) \right], \\ &= \frac{N}{\sqrt{1-e^{-2bt}}} \exp \left[\frac{b}{2D(1-e^{-2bt})} (-x^2(1-e^{-2bt}) + 2e^{-bt} x x_0 - e^{-2bt} x^2 - e^{-2bt} x_0^2) \right], \\ &= \frac{N}{\sqrt{1-e^{-2bt}}} \exp \left[-\frac{b}{2D(1-e^{-2bt})} (x^2 - 2e^{-bt} x x_0 + e^{-2bt} x_0^2) \right], \\ &= \frac{N}{\sqrt{1-e^{-2bt}}} \exp \left[-\frac{b}{2D(1-e^{-2bt})} (x - e^{-bt} x_0)^2 \right]. \end{aligned}$$

Then normalising, $\int_{-\infty}^{\infty} P(x, t) dx = 1$, using Gaussian identities,

$$\begin{aligned} \int_{-\infty}^{\infty} P(x, t) dx &= \frac{N}{\sqrt{1 - e^{-2bt}}} \int_{-\infty}^{\infty} \exp \left[-\frac{b}{2D(1 - e^{-2bt})} (x - e^{-bt}x_0)^2 \right] dx \\ &= \frac{N}{\sqrt{1 - e^{-2bt}}} \sqrt{\frac{\pi 2D(1 - e^{-2bt})}{b}} \\ &= 1 \\ N &= \sqrt{\frac{b}{2\pi D}}. \end{aligned}$$

Resulting in the result for the probability density function for a quadratic potential,

$$P(x, t|x_0) = \sqrt{\frac{b}{2\pi D(1 - e^{-2bT})}} \exp \left[-\frac{b}{2D(1 - e^{-2bT})} [x - x_0 e^{-bT}]^2 \right]$$

6.3 The WKB approximation

One of the more famous methods to solve certain kinds of differential equation is the WKB approximation [93]. This technique uses a series expansion in D and matching each order. The solution is found by solving the Laplace-transformed Smoluchowski equation for the Harmonic Oscillator,

$$s\bar{P} - \delta(x - x_0) = \bar{P} + x\bar{P}' + D\bar{P}''.$$

Where $\bar{P}(x, s) = \mathcal{L}\{P\}(s) = \int_0^{\infty} P(x, t)e^{-st} dt$ is the Laplace transform of the probability density function. Only looking at $x \neq x_0$, we can try a familiar looking Ansatz $\bar{P} = A[x] \exp \left(-\frac{S[x]}{4D} + J[x] \right)$ where we have a prefactor term and the first two terms in a D expansion. They are functionals, hence the square brackets, to be determined by expansion and equating coefficients to different orders. We need to find the first and second derivatives for our Ansatz to substitute into the Laplace-transformed Smoluchowski equation.

$$\bar{P} = A[x] \exp \left(-\frac{S[x]}{4D} + J[x] \right)$$

$$\bar{P}' = A' \exp\left(-\frac{S}{4D} + J\right) + AJ' \exp\left(-\frac{S}{4D} + J\right) - \frac{1}{4D} AS' \exp\left(-\frac{S}{4D} + J\right)$$

$$\begin{aligned} \bar{P}'' &= A'' \exp\left(-\frac{S}{4D} + J\right) + A'J' \exp\left(-\frac{S}{4D} + J\right) - \frac{1}{4D} A'S' \exp\left(-\frac{S}{4D} + J\right) \\ &+ A'J' \exp\left(-\frac{S}{4D} + J\right) + AJ'' \exp\left(-\frac{S}{4D} + J\right) - \frac{1}{4D} AJ'S' \exp\left(-\frac{S}{4D} + J\right) \\ &+ AJ'^2 \exp\left(-\frac{S}{4D} + J\right) - \frac{1}{4D} A'S' \exp\left(-\frac{S}{4D} + J\right) - \frac{1}{4D} AS'' \exp\left(-\frac{S}{4D} + J\right) \\ &- \frac{1}{4D} AJ'S' \exp\left(-\frac{S}{4D} + J\right) + \frac{1}{16D^2} AS'^2 \exp\left(-\frac{S}{4D} + J\right) \\ &= \exp\left(-\frac{S}{4D} + J\right) \left[A'' + 2A'J' + AJ'' + AJ'^2 \right. \\ &\quad \left. - \frac{1}{4D} [2A'S' + 2AJ'S' + AS''] + \frac{1}{16D^2} AS'^2 \right] \end{aligned}$$

Substituting all these terms into the Smoluchowski equation, we can cancel the exponential terms as they are common throughout. Collecting like terms gives,

$$\begin{aligned} sA &= A + x(A' + AJ') - \frac{1}{4}(2A'S' + 2AJ'S' + AS'') + \frac{1}{D} \left[-\frac{x}{4} AS' + \frac{1}{16} AS'^2 \right] \\ &\quad + D [A'' + 2A'J' + AJ'' + AJ'^2]. \end{aligned}$$

Next, we use dominant balance and equate each order of D as they have to be the same to be correct at each order. Now, with the use of hindsight, if we redefine the Laplace parameter as $s = \frac{H}{4D}$, then when we look at the dominant balance we return a familiar solution. This relationship is needed as s has order of $\frac{1}{D}$ and will become very useful when we make further use of the Laplace-transform in chapter 7. Starting at $\mathcal{O}(\frac{1}{D})$,

$$\begin{aligned} \frac{H}{4} A &= -\frac{x}{4} AS' + \frac{1}{16} AS'^2 \\ S'^2 - 4xS' - 4H &= 0 \\ S' &= \frac{4x \pm \sqrt{16x^2 + 16H}}{2} \end{aligned}$$

$$= 2x \pm 2\sqrt{H+x^2}$$

$$S[x] = x^2 \pm 2 \int \sqrt{H+y^2} dy$$

Now, this looks very similar to the action terms we have previously found using path integrals! Looking at the next order which is the constant terms $\mathcal{O}(1)$,

$$0 = A + xA' + xAJ' - \frac{1}{4} [2A'S' + 2AJ'S' + AS'']$$

$$0 = A + xA' + xAJ' - \frac{1}{4} \left[4A'x \pm 4A'\sqrt{H+x^2} + 4AJ'x \pm 4AJ'\sqrt{H+x^2} + 2A \pm \frac{2Ax}{\sqrt{H+x^2}} \right]$$

$$0 = \frac{1}{2}A \left[1 \mp \frac{x}{\sqrt{H+x^2}} \right] \mp \sqrt{H+x^2} [A' + AJ']$$

We have an equation with two terms that we do not know, but given that the S term returned the action that we have previously found for the Laplace transformed solution, what if we tried a proportional A term that we know? $A = (H+x^2)^{-\frac{1}{4}}$;

$$0 = \frac{1}{2}(H+x^2)^{-\frac{1}{4}} \left[1 \mp x(H+x^2)^{-\frac{1}{2}} \right] \mp (H+x^2)^{\frac{1}{2}} \left[-\frac{x}{2}(H+x^2)^{-\frac{5}{4}} + (H+x^2)^{-\frac{1}{4}}J' \right],$$

$$0 = \frac{1}{2}(H+x^2)^{-\frac{1}{4}} \mp (H+x^2)^{\frac{1}{4}}J',$$

$$J' = \pm \frac{1}{2}(H+x^2)^{-\frac{1}{2}},$$

$$J[x] = \pm \int \frac{dy}{\sqrt{H+y^2}}.$$

So, using the prefactor term that we already have, we returned the Jacobian term! This full probability solves the quadratic form of the Smoluchowski in Laplace space and returns a similar form to path integral formalism that we have found already and will now show that it solves the quadratic potential.

$$\bar{P} = \frac{1}{(H+x^2)^{\frac{1}{4}}} \exp \left[\pm \frac{1}{2} \int \frac{dy}{\sqrt{H+y^2}} - \frac{1}{4D} \left(x^2 \pm 2 \int \sqrt{H+y^2} dy \right) \right]$$

This returns a Laplace domain solution, which in chapter 7 we will find a similar looking solution that can be shown to solve the Laplace transformed Smoluchowski equation and can be inverted back to the time domain solution. For now, we will

stop here and pick up later when looking at the path integral in the Laplace domain.

6.4 Using Path Integrals

We have seen a few different techniques in solving for the Harmonic Oscillator, but what about using path integrals now that we know more about the Jacobian term, which is non-unit for the quadratic, and the concept of turning paths?

The Harmonic Oscillator is a good candidate to see how the path integrals shed new light onto the dynamics of a system because it is the most complex potential that we can solve the integrals for, and we know the analytical solution so we can check that the form is correct. To begin with, we can see if using the basic direct path formalism will return the known Ornstein-Uhlenbeck solution. First, setting up the problem we have,

$$V(x) = \frac{x^2}{2}, \quad (6.15)$$

$$x_i < x_f < 0. \quad (6.16)$$

We can also do the calculations for the other regions that x_f can occupy, which would be a reordering of the integral limits. For $x_f < x_i < 0$, it would mean a swapping of x_f and x_i in all the calculations. In this system, for $x_i < 0 < x_f$, there is only a direct path so the calculations do not change from the method we are first looking at.

As we have found the probability form for a direct path (2.13), now including the Jacobian term;

$$P_{\mathcal{D}}(x_f, T|x_i, 0) = A_{\mathcal{D}}[x, t] \mathcal{J}_{\mathcal{D}}[x, t] \exp\left(-\frac{S_{\mathcal{D}}(x_f, x_i, T)}{4D}\right)$$
$$\mathcal{J}_{\mathcal{D}}[x, t] = \exp\left(\frac{1}{2} \int_0^T V''(x(\tau)) d\tau\right)$$

$$\begin{aligned}
 T &= \int_{x_i}^{x_f} \frac{dx}{\sqrt{H_{\mathcal{D}} + V'^2}} \\
 S_{\mathcal{D}}[x_f, x_i, T] &= 2(V(x_f) - V(x_i)) - H_{\mathcal{D}}T + 2 \int_{x_i}^{x_f} \sqrt{H_{\mathcal{D}} + V'^2} dx \\
 A_{\mathcal{D}}^{-2} &= 4\pi D \sqrt{(H_{\mathcal{D}} + V'(x_i)^2)(H_{\mathcal{D}} + V'(x_f)^2)} \left| \int_{x_i}^{x_f} \frac{dy}{(H_{\mathcal{D}} + V'(y)^2)^{3/2}} \right|.
 \end{aligned}$$

Now, as $V''(x) = 1$, the Jacobian integral is a constant and only depends on time only,

$$\mathcal{J}_{\mathcal{D}}[x, t] = \exp\left(\frac{T}{2}\right). \quad (6.17)$$

To begin finding P , we first calculate the time integral,

$$\begin{aligned}
 T &= \int_{x_i}^{x_f} \frac{1}{\sqrt{H_{\mathcal{D}} + x^2}} dx \\
 &= \frac{1}{2} \ln \left[\frac{x + \sqrt{H_{\mathcal{D}} + x^2}}{\sqrt{H_{\mathcal{D}} + x^2} - x} \right] \Big|_{x_i}^{x_f} \\
 &= \frac{1}{2} \ln \left[\frac{x_f + \sqrt{H_{\mathcal{D}} + x_f^2}}{\sqrt{H_{\mathcal{D}} + x_f^2} - x_f} \right] - \frac{1}{2} \ln \left[\frac{x_i + \sqrt{H_{\mathcal{D}} + x_i^2}}{\sqrt{H_{\mathcal{D}} + x_i^2} - x_i} \right] \\
 \text{Rationalising the denominator} \quad &= \frac{1}{2} \ln \left[\frac{[x_f + \sqrt{H_{\mathcal{D}} + x_f^2}]^2}{H_{\mathcal{D}}} \right] - \frac{1}{2} \ln \left[\frac{[x_i + \sqrt{H_{\mathcal{D}} + x_i^2}]^2}{H_{\mathcal{D}}} \right] \\
 T &= \ln \left[\frac{\sqrt{H_{\mathcal{D}} + x_f^2} + x_f}{\sqrt{H_{\mathcal{D}} + x_i^2} + x_i} \right] \\
 &= \operatorname{arcsinh} \frac{x_f}{\sqrt{H_{\mathcal{D}}}} - \operatorname{arcsinh} \frac{x_i}{\sqrt{H_{\mathcal{D}}}}.
 \end{aligned}$$

In order to find the other quantities we need for the probability density function, we need to rearrange this to find $H_{\mathcal{D}}$. This can be done by using double-angle formulae for the inverse hyperbolic functions and expanding the square roots resulting in a quartic function in $H_{\mathcal{D}}$. The solutions to this quartic are

$$H_{\mathcal{D}} = \frac{x_f^2 + x_i^2 \pm 2x_f x_i \cosh(T)}{\sinh(T)^2} \quad \text{and} \quad H_{\mathcal{D}} = 0. \quad (6.18)$$

The question now is, which solution do we use going forward? With the benefit of hindsight, the correct solution is to use the $-$ value from the $H_{\mathcal{D}}$ solution. Both the

+ and 0 solutions do not satisfy the normalisation condition for the probability, but we will see that later. We can then calculate the action integrals

$$\begin{aligned}
 S_{\mathcal{D}} &= 2V(x_f) - 2V(x_i) - H_{\mathcal{D}}T + 2 \int_{x_i}^{x_f} \sqrt{H_{\mathcal{D}} + x^2} dx \\
 &= (x_f^2 - x_i^2) - H_{\mathcal{D}}T + x_f \sqrt{H_{\mathcal{D}} + x_f^2} - x_i \sqrt{H_{\mathcal{D}} + x_i^2} + H_{\mathcal{D}} \ln \left[\frac{\sqrt{H_{\mathcal{D}} + x_f^2} + x_f}{\sqrt{H_{\mathcal{D}} + x_i^2} + x_i} \right] \\
 S_{\mathcal{D}} &= (x_f^2 - x_i^2) + x_f \sqrt{H_{\mathcal{D}} + x_f^2} - x_i \sqrt{H_{\mathcal{D}} + x_i^2}, \tag{6.19}
 \end{aligned}$$

where we used the logarithmic relationship between T and $H_{\mathcal{D}}$ to cancel two terms.

The substitution for our $H_{\mathcal{D}}$ can then be done and the action simplifies down to

$$S_{\mathcal{D}} = x_f \left(x_f + \sqrt{(x_f \coth(T) - x_i \operatorname{cosech}(T))^2} \right) - x_i \left(x_i + \sqrt{(x_i \coth(T) - x_f \operatorname{cosech}(T))^2} \right). \tag{6.20}$$

The next step is to calculate the prefactor $A_{\mathcal{D}}$ for the system, and again, using the relationship for $H_{\mathcal{D}}$, we arrive at the form

$$\begin{aligned}
 A_{\mathcal{D}}^{-2} &= 4\pi D \sqrt{H_{\mathcal{D}} + x_f^2} \sqrt{H_{\mathcal{D}} + x_i^2} \left| \int_{x_i}^{x_f} (H_{\mathcal{D}} + x^2)^{-\frac{3}{2}} dx \right| \\
 &= \left| \frac{4\pi D}{H_{\mathcal{D}}} \left[x_f \sqrt{H_{\mathcal{D}} + x_i^2} - x_i \sqrt{H_{\mathcal{D}} + x_f^2} \right] \right| \tag{6.21} \\
 &= \left| \frac{4\pi D \sinh(T)^2 \left[-x_i \sqrt{(x_f \coth(T) - x_i \operatorname{cosech}(T))^2} + x_f \sqrt{(x_i \coth(T) - x_f \operatorname{cosech}(T))^2} \right]}{x_i^2 + x_f^2 - 2x_i x_f \cosh(T)} \right|
 \end{aligned}$$

As this is the Harmonic Oscillator, we know the solution we are after and can see how the path integral approach returns the correct result. Starting with the Ornstein-Uhlenbeck process [67], we can separate out the factors that we have calculated

$$\begin{aligned}
 P_{\text{O-U}}(x_f, T | x_i, 0) &= \sqrt{\frac{1}{2\pi D(1 - e^{-2T})}} \exp \left(-\frac{1}{2D(1 - e^{-2T})} (x_f - x_i e^{-T})^2 \right), \\
 &= \sqrt{\frac{e^T}{2\pi D(e^T - e^{-T})}} \exp \left(-\frac{1}{2D(1 - e^{-2T})} (x_f - x_i e^{-T})^2 \right),
 \end{aligned}$$

$$\begin{aligned}
&= \sqrt{\frac{1}{4\pi D \sinh(T)}} \exp\left(\frac{T}{2}\right) \exp\left(-\frac{1}{2D(1-e^{-2T})} (x_f - x_i e^{-T})^2\right), \\
&= A[x, t] \mathcal{J}[x, t] \exp\left(-\frac{S(x_f, x_i, T)}{4D}\right).
\end{aligned}$$

Comparing the path integral elements with the final line above means that we can identify the elements that we have,

$$\begin{aligned}
A_{\mathcal{D}}[x, t]^{-2} &= 4\pi D \sinh(T), \\
\mathcal{J}_{\mathcal{D}}[x, t] &= \exp\left(\frac{T}{2}\right), \\
S_{\mathcal{D}}[x_f, x_i, T] &= \frac{2(x_f - x_i e^{-T})^2}{D(1 - e^{-2T})}, \\
&= (x_i - e^T x_f)^2 (\coth(T) - 1).
\end{aligned}$$

We know what we are after, so does our path integral representation return the same results? The Jacobian is already sorted for this system (6.17), so how can we find the relevant prefactor and action terms? For both the prefactor (6.21) and action (6.20), we have brackets that are squared and then square rooted, meaning there are magnitude signs for both that we must deal with. Are these factors positive or negative? We can simplify this by using the assumptions that we gave as we set up the system (6.15), $x_i < x_f < 0$, and the fact that $T > 0$ as it is the representation for time. Using these inequalities, we can simplify the prefactor to find the form that we desire, but with a time constraint

$$A_{\mathcal{D}}[x, t]^{-2} = 4\pi D \sinh(T) \quad \text{for } x_i < x_f \cosh(T).$$

Using this third constraint along with the two initial assumptions for the action again returns the known Ornstein-Uhlenbeck solution

$$S_{\mathcal{D}} = (x_i - e^T x_f)^2 (\coth(T) - 1) \quad \text{for } x_i < x_f \cosh(T).$$

So the path integral approach returns the known Ornstein-Uhlenbeck solution but for a constraint on the time! This constraint illustrates that for a path there is a time limit for it to be a direct path, and beyond this time constraint we need to introduce a *turning path* as there is a maximum energy value H . We have seen in chapter 5 the turning path introduction means an extra integral that covers the path travelling to the turning point and back, in this case at $V'(x) = 0$ meaning $x = 0$. Calculating the turning path action and prefactor is very similar to the direct path, as the integrals are all the same, just an additional cancellation. Starting with the time integral calculation

$$\begin{aligned}
 T &= \int_{x_i}^{x_f} \frac{1}{\sqrt{H_{\mathcal{T}} + x^2}} dx + 2 \int_{x_f}^0 \frac{1}{\sqrt{H_{\mathcal{T}} + x^2}} dx \\
 &= \ln \left[\frac{\sqrt{H_{\mathcal{T}} + x_f^2} + x_f}{\sqrt{H_{\mathcal{T}} + x_i^2} + x_i} \right] + 2 \ln \left[\frac{\sqrt{H_{\mathcal{T}}}}{\sqrt{H_{\mathcal{T}} + x_f^2} + x_f} \right] \\
 &= \ln \left[\frac{H_{\mathcal{T}}}{\left[\sqrt{H_{\mathcal{T}} + x_f^2} + x_f \right] \left[\sqrt{H_{\mathcal{T}} + x_i^2} + x_i \right]} \right] \\
 &= -\arcsin \frac{x_f}{\sqrt{H_{\mathcal{T}}}} - \arcsin \frac{x_i}{\sqrt{H_{\mathcal{T}}}} \tag{6.22}
 \end{aligned}$$

Solving for the resultant quartic in $H_{\mathcal{T}}$;

$$H_{\mathcal{T}} = \frac{x_f^2 + x_i^2 \pm 2x_f x_i \cosh(T)}{\sinh(T)^2} \quad \text{and} \quad H_{\mathcal{T}} = 0$$

It returns the same form of the energy, and again we chose the $-$ solution for the energy. This does mean that the energy form is the same for the direct and turning path, but there is a point at critical T where we change from one to the other in A and S to keep the final probability solution consistent. Calculating the turning path action

$$\begin{aligned}
 S_{\mathcal{T}} &= 2V(x_f) - 2V(x_i) - H_{\mathcal{T}}T + 2 \int_{x_i}^{x_f} \sqrt{H_{\mathcal{T}} + x^2} dx + 4 \int_{x_f}^0 \sqrt{H_{\mathcal{T}} + x^2} dx \\
 &= (x_f^2 - x_i^2) - H_{\mathcal{T}}T - x_f \sqrt{H_{\mathcal{T}} + x_f^2} - x_i \sqrt{H_{\mathcal{T}} + x_i^2}
 \end{aligned}$$

$$\begin{aligned}
 & + H_{\mathcal{T}} \ln \left[\frac{\sqrt{H_{\mathcal{T}} + x_f^2} + x_f}{\sqrt{H_{\mathcal{T}} + x_i^2} + x_i} \right] + 2H_{\mathcal{T}} \ln \left[\frac{\sqrt{H_{\mathcal{T}}}}{\sqrt{H_{\mathcal{T}} + x_f^2} + x_f} \right] \\
 & = (x_f^2 - x_i^2) - x_f \sqrt{H_{\mathcal{T}} + x_f^2} - x_i \sqrt{H_{\mathcal{T}} + x_i^2} \tag{6.23}
 \end{aligned}$$

$$S_{\mathcal{T}} = x_f \left(x_f - \sqrt{(x_f \coth(T) + x_i \operatorname{cosech}(T))^2} \right) - x_i \left(x_i + \sqrt{(x_i \coth(T) + x_f \operatorname{cosech}(T))^2} \right).$$

Then calculating the turning path prefactor again using the $H_{\mathcal{T}}$ solution

$$\begin{aligned}
 |A_{\mathcal{T}}^{-2}| & = 4\pi D \sqrt{H_{\mathcal{T}} + x_f^2} \sqrt{H_{\mathcal{T}} + x_i^2} \left| \int_{x_i}^{x_f} (H_{\mathcal{T}} + x^2)^{-\frac{3}{2}} dx + 2 \int_{x_f}^0 (H_{\mathcal{T}} + x^2)^{-\frac{3}{2}} dx \right| \\
 & = \frac{4\pi D}{H_{\mathcal{T}}} \left| -x_f \sqrt{H_{\mathcal{T}} + x_i^2} - x_i \sqrt{H_{\mathcal{T}} + x_f^2} \right| \tag{6.24}
 \end{aligned}$$

$$|A_{\mathcal{T}}^{-2}| = \left| -\frac{\sinh(T)^2 \left[x_i \sqrt{(x_f \coth(T) + x_i \operatorname{cosech}(T))^2} + x_f \sqrt{(x_i \coth(T) + x_f \operatorname{cosech}(T))^2} \right]}{x_i^2 + x_f^2 + 2x_i x_f \cosh(T)} \right|$$

Again, using the initial conditions that we have, $x_i < x_f < 0$ and $T > 0$, we can simplify these action and prefactor terms to the Ornstein-Uhlenbeck solution only for $x_i \geq x_f \cosh(T)$. Meaning that at this condition, the dominant path transitions from the direct to the turning path,

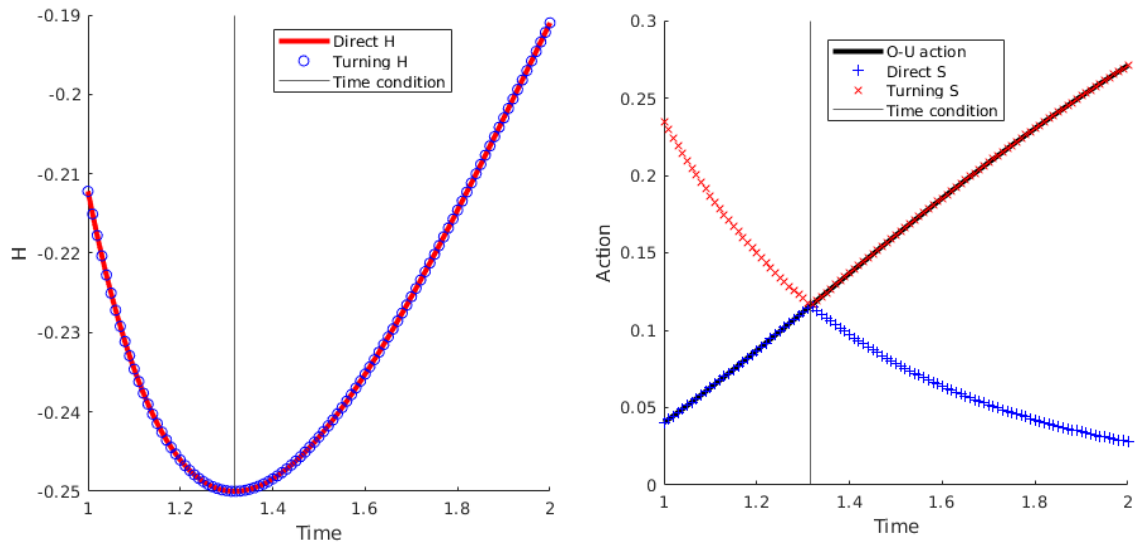
$$|A_{\mathcal{T}}[x, t]^{-2}| = 4\pi D \sinh(T) \quad \text{for } x_i \geq x_f \cosh(T).$$

Using this third constraint along with the two assumptions from the beginning for the action again returns the known Ornstein-Uhlenbeck solution,

$$S_{\mathcal{T}} = (x_i - e^T x_f)^2 (\coth(T) - 1) \quad \text{for } x_i \geq x_f \cosh(T).$$

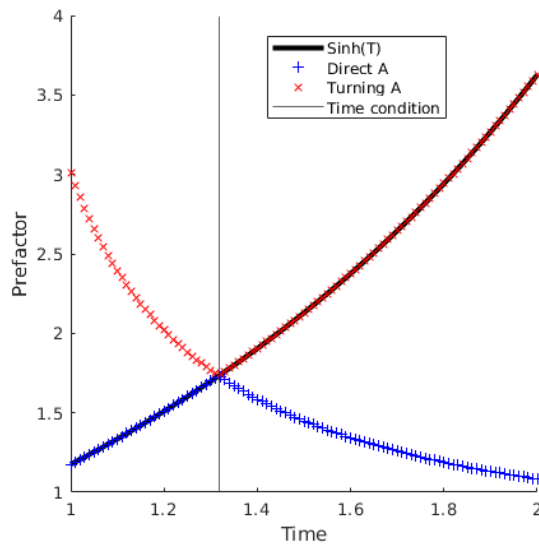
So, we have a solution for the Harmonic Oscillator using path integrals for which we have to switch from a direct to a turning path at a given time, a phenomenon of the system that is not found if we use the other methods described. This provides an insight into the system's dynamics that are not previously seen. We can see this

change from direct to turning path by graphing the prefactor and action terms over time.



(a) Energy over time

(b) Action over time



(c) Prefactor over time

Figure 6.1: Graphs showing the elements for the path integral formalism over time with the time constraint imposed, detailing the change between the direct path and the turning path at the critical time.

What figure (6.1a) shows are the forms for both the direct and turning path energies, which are the same (6.18), (6.22) over time. The interesting factor is that the energy becomes minimum at the point when it will change from the direct to the turning path. This is because the longest direct path time is when the “particle” stops at

the final position resulting in a minimum H for the direct path; any $H > H_C$ results in a direct path reaching x_f with $\dot{x} > 0$. Figure (6.1b) shows the action over time for the direct and turning path action (6.19) and (6.23) respectively. We use the forms of the actions that include the energy terms mainly because it is fewer terms in the code, but it returns the same solution as using the full final form before we included the assumptions. This fact means that the actions actually automatically have the assumptions built in before we simplify the equations. Both figure (6.1b) and figure (6.1c) also have the relevant Ornstein-Uhlenbeck solutions for comparison, and they line up perfectly on either side of the time condition as they should. The path integral only matches the known solution when the time constraint is valid, which shows that the solution is correct.

Aside: The other energy values

Now, when we calculated the energy for the direct path (6.18), we chose the $-$ from the \pm choice with hindsight. In this aside, we will explore what happens if we choose the other energy values. First, if we had chosen $H_{\mathcal{D}} = 0$, we would do all the integrals again but substitute in our $H_{\mathcal{D}}$ value at the beginning. Starting with the T integral,

$$\begin{aligned} T &= \int_{x_i}^{x_f} \frac{dx}{\sqrt{H_{\mathcal{D}} + x^2}}, \\ &= \int_{x_i}^{x_f} \frac{dx}{x}, \\ &= \ln \frac{x_f}{x_i}, \\ x_f &= x_i e^T. \end{aligned}$$

To calculate the action integral, we have to consider the square root of a squared x . In this case, the integral takes place entirely in the negative x domain, so we pick up an extra minus sign

$$S_{\mathcal{D}} = x_f^2 - x_i^2 - H_{\mathcal{D}}T + 2 \int_{x_i}^{x_f} dx \sqrt{H_{\mathcal{D}} + x^2},$$

$$\begin{aligned}
 &= x_f^2 - x_i^2 + 2 \int_{x_i}^{x_f} |x| dx, \\
 &= (x_f^2 - x_i^2) - (x_f^2 - x_i^2), \\
 S_{\mathcal{D}} &= 0.
 \end{aligned}$$

And finally the prefactor,

$$\begin{aligned}
 A_{\mathcal{D}}^{-\frac{1}{2}} &= 4\pi D \sqrt{H_{\mathcal{D}} + x_f^2} \sqrt{H_{\mathcal{D}} + x_i^2} \left| \int_{x_i}^{x_f} (H_{\mathcal{D}} + x^2)^{-\frac{3}{2}} dx \right|, \\
 &= 4\pi D |x_i| |x_f| \left| \int_{x_i}^{x_f} dx \frac{1}{x^3} \right|, \\
 &= -4\pi D |x_i| |x_f| \frac{1}{2} \left(\frac{1}{x_f^2} - \frac{1}{x_i^2} \right), \\
 &= 4\pi D |x_i| |x_f| \left(\frac{1}{x_i^2} - \frac{1}{x_f^2} \right), \\
 &= 2\pi D \begin{pmatrix} x_f & x_i \\ x_i & x_f \end{pmatrix},
 \end{aligned}$$

Using the T definition $A_{\mathcal{D}} = \sqrt{\frac{1}{2\pi D(e^T - e^{-T})}}$.

We can now input this into the definition of the probability to get what it is for $H_{\mathcal{D}} = 0$,

$$\begin{aligned}
 P(x_f, T | x_i, 0; H_{\mathcal{D}} = 0) &= \sqrt{\frac{1}{2\pi D(e^T - e^{-T})}} \exp\left(\frac{T}{2}\right) \exp\left(-\frac{(x_f^2 - x_i^2)}{2D}\right), \\
 &= \sqrt{\frac{1}{2\pi D(1 - e^{-2T})}} \exp\left(-\frac{(x_f^2 - x_i^2)}{2D}\right).
 \end{aligned}$$

The issue with this selection of energy value is only apparent when we have to check the normalisation condition of this probability form.

Previously with the $-$ choice, it is already normalised for all values of T , but here

it is not as shown below;

$$\begin{aligned} \int_{-\infty}^{\infty} P(x, T | x_i, 0; H_{\mathcal{D}} = 0) dx &= \int_{-\infty}^{\infty} dx \sqrt{\frac{1}{2\pi D(1 - e^{-21T})}} \exp\left(-\frac{(x^2 - x_i^2)}{2D}\right), \\ &= \sqrt{\frac{1}{2\pi D(1 - e^{-21T})}} \exp\left(\frac{x_i^2}{2D}\right) \int_{-\infty}^{\infty} dx \exp\left(-\frac{x^2}{2D}\right). \end{aligned}$$

Using Gaussian Integral identities [94];

$$\begin{aligned} &= \sqrt{\frac{1}{2\pi D(1 - e^{-2T})}} \exp\left(\frac{x_i^2}{2D}\right) \sqrt{2\pi D}, \\ &= \sqrt{\frac{1}{1 - e^{-2T}}} \exp\left(\frac{x_i^2}{2D}\right). \end{aligned}$$

The only way this equals 1 and is normalised is if it is in the long time limit, $T \rightarrow \infty$ and the initial position is at $x_i = 0$, so this is only valid for specific conditions. This does make sense for this particular system as if we think about the effective potential for the harmonic oscillator, $H = 0$ corresponds to the path having to start at the top of the effective potential and stay there for an infinite time as the particle has no energy to move.

Now looking at the + sign of the $H_{\mathcal{D}}$ quadratic, we can check the normalisation to see if it is valid. The difference is only in the action calculation, as the T and $A_{\mathcal{D}}$ calculations have no dependence on which $H_{\mathcal{D}}$ value we take. The $A_{\mathcal{D}}$ form uses an identity from the T calculation before we form the quartic that gives the relevant $H_{\mathcal{D}}$ equations. Meaning that it will always give us the correct $\sinh(T)$ solution that we need. Starting at the point in the previous derivation (6.20) when we took the negative value only affects the action derivation, which simplifies down to,

$$S_{\mathcal{D}} = \frac{2}{e^T - e^{-T}} [x_f^2 e^T + x_f x_i e^{-2T} - x_i^2 e^{-T}].$$

When we input into the function for P ,

$$\begin{aligned}
 P(x_f, T|x_i, 0) &= \sqrt{\frac{e^{-T}}{2\pi D(1 - e^{-2T})}} \\
 &\quad \times \exp \left[-\frac{1}{2D(e^T - e^{-T})} [x_f^2 e^T + x_f x_i e^{-2T} - x_i^2 e^{-T}] - 2DT \right], \\
 &= \sqrt{\frac{1}{2\pi D(1 - e^{-2T})}} \exp \left[-\frac{1}{2D(1 - e^{-2T})} [x_f^2 + x_f x_i e^{-3T} - x_i^2 e^{-2T}] \right].
 \end{aligned}$$

Normalising this shows the issue with this representation at short times,

$$\begin{aligned}
 \int_{-\infty}^{\infty} P(x_f, T|x_i, 0) dx &= \sqrt{\frac{1}{2\pi D(1 - e^{-2T})}} \\
 &\quad \times \int_{-\infty}^{\infty} \exp \left[-\frac{1}{2D(1 - e^{-2T})} [x^2 + x x_i e^{-3T} - x_i^2 e^{-2T}] \right] dx, \\
 &= \sqrt{\frac{1}{2\pi D(1 - e^{-2T})}} \exp \left[\frac{x_i^2 e^{-2T}}{2D(1 - e^{-2T})} \right] \\
 &\quad \times \int_{-\infty}^{\infty} \exp \left[-\frac{1}{2D(1 - e^{-2T})} [x^2 + x x_i e^{-3T}] \right] dx.
 \end{aligned}$$

Using Gaussian Integral identities [94];

$$\begin{aligned}
 &= \sqrt{\frac{1}{2\pi D(1 - e^{-2T})}} \exp \left[\frac{x_i^2 e^{-2T}}{2D(1 - e^{-2T})} \right] \\
 &\quad \times \sqrt{2\pi D(1 - e^{-2T})} \exp \left[\frac{x_i^2 e^{-6T}}{8D(1 - e^{-2T})} \right], \\
 &= \exp \left[\frac{x_i^2}{8D(1 - e^{-2T})} [e^{-6T} + 4e^{-2T}] \right].
 \end{aligned}$$

This shows that the probability density function for taking the + value of the G quadratic is only normalised when $T \rightarrow \infty$, and not at small time scales like the – choice.

We have now looked at various techniques to solve the Harmonic oscillator, all returning the same solution in many different ways. The path integral technique allows

a new interpretation of the stochastic evolution in terms of an effective Hamiltonian system however and the necessary introduction of the turning path to return the correct long-time limit.

Chapter 7

The use of the Laplace Transform

In this chapter, we will transform to the *Laplace domain* as a method to provide other useful insights into the use of path integrals in solving for certain systems. This transformation removes the time dependence of the solution and allows the explicit summation of the paths, allowing an easier route to the full solution. The use of Laplace also allows the introduction of *boundary conditions* to make the probability density function into a more usable state, as many systems are more interested in first passage times, in which boundaries are needed, as explored in chapter 1. This transformation will allow further interpretation in terms of the energy of the effective Hamiltonian system, from the relationship between the *Laplace parameter* and the *energy*, $s = \frac{H}{4D}$.

So far, we have seen the use of path integrals in solving only the simplest potentials. The most complex potential that it is possible to have an analytical solution for is the quadratic potential; with anything more complicated the integrals become unsolvable analytically, mainly the action integral. One of the significant issues with working in the time domain is the fact that each path will have a different energy at a fixed time T , and there is difficulty in combining contributions from the most dominant paths, as there is not necessarily one single dominant path.

One technique to remove some of the issues is to use the Laplace transform method [95], which removes the time dependence of the Smoluchowski equation, subsequently removing the time dependence in the approximate probability density function that we have found. The transference will also allow explicit summation of the dominant path weights that appear in a given system, something that we will see later in this chapter allows the return of correct results when dealing with systems with boundaries and the subsequent calculation of first passage time densities and moments of the FPT.

The standard Laplace transform [95] is as follows

$$\mathcal{L}[f(t)](s) = \bar{f}(s) = \int_0^{\infty} e^{-st} f(t) dt.$$

However, what is the $\bar{f}(s)$ function in our path integral formalism? The way to find this is to do a similar derivation that we did for the WKB approximation for the Harmonic Oscillator. Suppose we assume that the Laplace-transformed probability density function has the same form as the time domain probability. In that case, we can try to solve the Laplace-transformed Smoluchowski equation to varying orders in D . We still are solving a differential equation, but it has changed from a partial differential equation to an ordinary differential equation in the Laplace domain. The other thing that we can interpret is that there are $e^{\pm st}$ terms in the Laplace transform equations, and there is a $e^{\frac{HT}{4D}}$ term in our T domain action, so we can

interpret our energy value also as our Laplace transform parameter, $s = \frac{H}{4D}$. This interpretation can be justified by looking at the WKB approximation and can be seen as the appearance of conjugate variables, which arises in classical physics where time and “energy” is related. A further mathematical technique that we can use to see how the Laplace parameter is defined in this way is Legendre transforms [96]. If we define \mathcal{W} to be

$$\mathcal{W} = HT + \mathcal{S},$$

this is a Legendre transform, taking us from time t to energy H . \mathcal{W} is Hamilton’s characteristic function, and \mathcal{S} is Hamilton’s principal function, action functional evaluated along the extremal path. If we write the exponential in P as $\exp(Ht/4D)\exp(-\mathcal{W}/4D)$ and identify the Laplace parameter $s = H/4D$, we can see the integrand of an inverse Laplace transform. The inverse Laplace transform will be an integral over the path energies, H , and would be dominated by the values of H where $\frac{\partial(HT-\mathcal{W})}{\partial H} = 0$, which returns the dominant paths, $\frac{\partial \mathcal{S}}{\partial H} = 0$. Starting with the Laplace-transformed Smoluchowski equation,

$$\frac{H}{4D}\bar{P} - \delta(x - x_0) = V''(x)\bar{P} + V'(x)\bar{P}' + D\bar{P}'', \quad (7.1)$$

if we assume a form of $\bar{P} = A[x]\mathcal{J}[x]e^{-\frac{S[x]}{4D}}$ we can solve it order-by-order in D . Calculating the derivatives first of all gives,

$$\begin{aligned} \bar{P} &= A[x]\mathcal{J}[x]e^{-\frac{S[x]}{4D}}, \\ \bar{P}' &= e^{-\frac{S[x]}{4D}} \left[A'\mathcal{J} + A\mathcal{J}' - \frac{1}{4D}A\mathcal{J}S' \right], \\ \bar{P}'' &= e^{-\frac{S[x]}{4D}} \left[A''\mathcal{J} + 2A'\mathcal{J}' + A\mathcal{J}'' - \frac{1}{4D}(2A'\mathcal{J}S' + 2A\mathcal{J}'S' + A\mathcal{J}S'') + \frac{1}{16D^2}A\mathcal{J}S'^2 \right]. \end{aligned}$$

Substituting all this into (7.1) and beginning with $\mathcal{O}(D^{-1})$,

$$\begin{aligned} \frac{H}{4}A\mathcal{J} &= -\frac{1}{4}V'A\mathcal{J}S' + \frac{1}{16}A\mathcal{J}S'^2, \\ 0 &= S'^2 - 4V'S' - 4H, \end{aligned}$$

$$S' = 2V' \pm 2\sqrt{H + V'^2},$$

$$S[x] = 2V(x_i) - 2V(x_f) \pm \int_{x_i}^{x_f} \sqrt{H + V'(y)^2} dy.$$

This is very similar to our time domain action, minus the time dependence, as is expected in the Laplace domain as the time dependence was removed when we transformed. Next we can look at $\mathcal{O}(D^0)$,

$$0 = \frac{1}{2}V''A\mathcal{J} + V'A'\mathcal{J} + V'A\mathcal{J}' - \frac{1}{2}A'\mathcal{J}S' - \frac{1}{2}A\mathcal{J}'S' - \frac{1}{4}A\mathcal{J}S'',$$

$$0 = \frac{1}{2}V''A\mathcal{J} \mp \frac{V'V''}{2\sqrt{H + V'^2}}A\mathcal{J} \mp \sqrt{H + V'^2}(A'\mathcal{J} + A\mathcal{J}').$$

Now, if we managed to return the action-like term, what if the \mathcal{J} term is similar to the time domain Jacobian? Using the x -dependent version of the Jacobian:

$$\mathcal{J} = \exp\left(\pm \frac{1}{2} \int \frac{V''}{\sqrt{H + V'^2}} dy\right)$$

$$\mathcal{J}' = \pm \frac{1}{2} \frac{V''}{\sqrt{H + V'^2}} \mathcal{J}.$$

Substituting this into our $\mathcal{O}(D^0)$ equation,

$$0 = \frac{1}{2}V''A\mathcal{J} \mp \frac{V'V''}{2\sqrt{H + V'^2}}A\mathcal{J} \mp \sqrt{H + V'^2}A'\mathcal{J} - \frac{1}{2}V''A\mathcal{J},$$

$$0 = \mp \frac{V'V''}{2\sqrt{H + V'^2}}A \mp \sqrt{H + V'^2}A',$$

$$\pm \frac{A'}{A} = \mp \frac{V'V''}{2\sqrt{H + V'^2}},$$

$$\pm \ln(A) = \mp \frac{1}{4} \ln(H + V'^2),$$

$$A = (H + V'^2)^{-\frac{1}{4}}.$$

This returns the time-independent portion of the prefactor calculation. The major non- T dependent difference between the time domain and the Laplace domain is the absence of the $\frac{3}{2}$ integral in the prefactor.

A spooky aside

The $\frac{3}{2}$ integral actually can come about from the inverse Laplace transform, instead of the technique with the quantum fluctuations or next order \mathcal{S} expansion that we have already looked at in chapter 2. When calculating the inverse Laplace transform, it will have the form,

$$\begin{aligned}
 P(x, t) &= \frac{1}{2\pi i} \lim_{\gamma \rightarrow \infty} \int_{-i\gamma}^{i\gamma} \exp(+st) \bar{P} ds \\
 &= \frac{1}{2\pi i} \lim_{\gamma \rightarrow \infty} \int_{-i\gamma}^{i\gamma} \exp(+st) A[x] \mathcal{J}[x] \exp\left(-\frac{S[x, s]}{4D}\right) ds,
 \end{aligned}$$

where the integration is done along the vertical line at $Re(s) = 0$ in the complex plane, such that all the real parts of all the singularities of \bar{P} are to the right of 0. This is then a contour integral, using the Bromwich integral, figure (7.1).

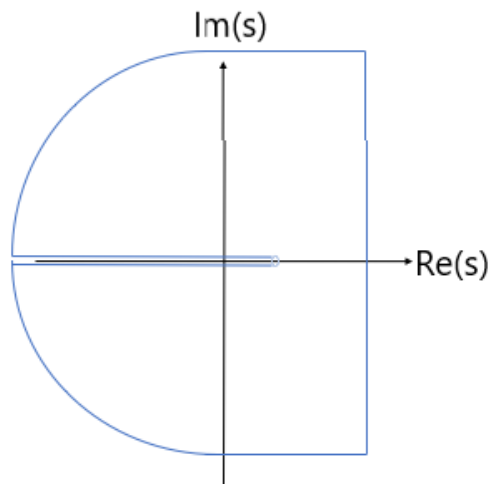


Figure 7.1: Bromwich Contour to calculate the inverse Laplace transform [97], deformed around the poles on the real axis.

For evaluating integrals of the form of the inverse Laplace transform we can draw connections to Laplace's method [93],

$$\int_a^b \exp(Mf(x)) dx = \sqrt{\frac{2\pi}{Mf''(x_0)}} \exp(Mf(x_0)), \quad M \text{ large.} \quad (7.2)$$

This technique is closely related to both Stationary phase and the Method of steepest descent, but as there is no imaginary portion of the integrand, we can deform the complex contour to be able to use Laplace's method to evaluate the inverse Laplace transform integral. Relating the function $f(x)$ in Laplace's method to $S[x, s] - st$ in the exponential with $\frac{1}{D}$ large. This means that the $f''(x_0)$ term in the denominator of equation, (7.2) will become

$$\begin{aligned} f''(x_0) &= \frac{1}{4D} \frac{\partial^2 S}{\partial s^2}, \\ &= 4D \frac{\partial^2 S}{\partial H^2}, \\ &= 4D \int_{x_i}^{x_f} \frac{1}{(H + V'(y))^{\frac{3}{2}}} dx. \end{aligned}$$

This returns the $\frac{3}{2}$ integral, the same as the stochastic fluctuations, from the analogy with quantum mechanical quadratic fluctuations. This in itself is a spooky phenomenon as it is saying that the combination of an approximation solution in the Laplace domain followed by an approximate inversion using Laplace's method returns the full exact analytical solution in the T-domain that we did not need to approximate for! This is just weird that somehow the two errors cancel out.

Returning to the Laplace domain, we have the full single path, γ , probability of;

$$\bar{P}(H) = \frac{\exp \left[\frac{1}{2} \int_{\gamma} \frac{V''}{\sqrt{H+V'^2}} dy \right]}{(H + V'(x_f)^2)^{\frac{1}{4}} (H + V'(x_i)^2)^{\frac{1}{4}}} \exp \left[-\frac{1}{4D} \left(2V(x_f) - 2V(x_i) + 2 \int_{\gamma} \sqrt{H + V'^2} dy \right) \right]. \quad (7.3)$$

The main advantage of using the Laplace transform technique, other than removing the time dependence, is that when we have multiple paths we can sum them to get the full probability because they all have the same H . But what multiple paths can there be in a system? We have the direct path or the turning path, which can reverse at the turning points of $V(x)$, but what about further paths? This is where the introduction of boundaries comes in and allows the summation of all paths.

7.1 Introduction of Boundary Conditions

If there is only one boundary, there will only be two possible paths, the direct path and the turning path that goes to the boundary and returns. If there are two boundaries, then there are actually infinitely many paths. The four base paths are the direct path, the bounce of one boundary, one bounce off the other boundary and the path that bounces off both boundaries. Each of these paths has increasing energy values in the T domain, and a path with an energy larger than the double boundary path will complete a full cycle path before completing one of the four base paths. In the Laplace domain, we can sum these paths and it starts looking something like,

$$\begin{aligned} \bar{P}(H) = & \bar{P}_{\text{Direct}} + \bar{P}_{\text{Turn at a}} + \bar{P}_{\text{Turn at b}} + \bar{P}_{\text{Two turns}} \\ & + \bar{P}_{\text{Full cycle}} * [\bar{P}_{\text{Direct}} + \bar{P}_{\text{Turn at a}} + \bar{P}_{\text{Turn at b}} + \bar{P}_{\text{Two turns}}] \\ & + \bar{P}_{\text{Full cycle}} * \bar{P}_{\text{Full cycle}} * [\bar{P}_{\text{Direct}} + \bar{P}_{\text{Turn at a}} + \bar{P}_{\text{Turn at b}} + \bar{P}_{\text{Two turns}}] + \dots \end{aligned}$$

The full cycle paths, including the relevant base path multiply, as they are integrals in the exponent, and add on extra integrals in a similar way to the turning path. This means we can write this as a summation:

$$\bar{P}(H) = \sum_{n=0}^{\infty} (\bar{P}_{\text{Full cycle}})^n * [\bar{P}_{\text{Direct}} + \bar{P}_{\text{Turn at a}} + \bar{P}_{\text{Turn at b}} + \bar{P}_{\text{Two turns}}].$$

The summation only works for a constant H across all paths. This is just a *geometric series* [98], $\sum_{k=0}^{\infty} ar^k = \frac{a}{1-r}$, so we can write a form for the full probability of a two boundary system,

$$\bar{P}(H) = \frac{\bar{P}_{\text{Direct}} + \bar{P}_{\text{Turn at a}} + \bar{P}_{\text{Turn at b}} + \bar{P}_{\text{Two turns}}}{1 - \bar{P}_{\text{Full cycle}}}. \quad (7.4)$$

Each path has its own action and subsequent Jacobians, which are just sums of integrals of each section of the path. The other element that we need for a general system is how the probability will interact with a boundary and if any specific

additional terms are needed to satisfy the relevant boundary conditions.

There are two different boundaries that the system can have. One is the absorbing boundary, and the other is the reflecting boundary. The absorbing boundary is one where the “particle” will be removed from the system when it interacts with it; the reflecting boundary stops the “particle” from escaping the system. In order to solve for the possible constants that are needed we can set up a dummy system with a general potential $V(x)$ and an absorbing boundary at $x = a$ and a reflecting boundary at $x = b$ which have conditions,

$$\begin{aligned}\bar{P}(H; x = a) &= 0, \\ V'(b)\bar{P}(H; x = b) + D\bar{P}'(H; x = b) &= 0.\end{aligned}$$

The absorbing boundary condition comes from the fact that “particles” are removed at the boundary meaning the probability is zero. The reflecting boundary condition comes from zero flux over the boundary. Flux $j[x]$ is related to probability by,

$$\begin{aligned}\frac{dj}{dx} &= \frac{\partial P}{\partial t} \\ \text{Using Smoluchowski} &= \frac{\partial}{\partial x} \left[V'(x)P + D \frac{\partial P}{\partial x} \right] \\ j[x] &= V'(x)P + D \frac{\partial P}{\partial x} \\ \text{Taking Laplace transform} & \quad \bar{j}[x] = V'(x)\bar{P} + D\bar{P}'.\end{aligned}$$

Then at the reflecting boundary, $\bar{j}[x = b] = 0$ gives the correct boundary condition. The full probability for this dummy system with the two constants, A for the boundary condition at $x = a$, and B for the boundary condition for $x = b$ is

$$\bar{P}(H) = \frac{\bar{P}_{\text{Direct}} + A\bar{P}_{\text{Turn at a}} + B\bar{P}_{\text{Turn at b}} + AB\bar{P}_{\text{Two turns}}}{1 - AB\bar{P}_{\text{Full cycle}}}.$$

The absorbing boundary constant is the easier of the two to solve for. When the final position is at the boundary $x = a$, it means that the base paths come in two

pairs as $\bar{P}_{\text{Direct}} = \bar{P}_{\text{Turn at a}}$ and $\bar{P}_{\text{Turn at b}} = \bar{P}_{\text{Two turns}}$. We need them to cancel in pairs, which can be achieved by simply setting $A = -1$, regardless of what B will equal.

Now, to solve for the reflecting boundary constant. In this case, we will need the derivative of the probability with respect to the final position, and then take that to the boundary. The full cycle path is not x dependent, so we only have to take the derivative of the four possible base paths. Starting with the possible direct path for $a < x_i < x_f < b$, we can write the derivative in terms of the full probability as two of the terms are exponential terms

$$\begin{aligned}\bar{P}_{\text{Direct}}(H) &= \frac{\exp\left[\frac{1}{2}\int_{x_i}^{x_f}\frac{V''}{\sqrt{H+V'^2}}dy\right]}{(H+V'(x_f)^2)^{\frac{1}{4}}(H+V'(x_i)^2)^{\frac{1}{4}}} \\ &\quad \times \exp\left[-\frac{1}{4D}\left(2V(x_f)-2V(x_i)+2\int_{x_i}^{x_f}\sqrt{H+V'^2}dy\right)\right], \\ \bar{P}'_{\text{Direct}}(H) &= -\frac{V''(x_f)V'(x_f)}{2(H+V'(x_f)^2)}\bar{P}_{\text{Direct}}(H) \\ &\quad + \left[\frac{V''(x_f)}{2\sqrt{H+V'(x_f)^2}} - \frac{V'(x_f)+\sqrt{H+V'(x_f)^2}}{2D}\right]\bar{P}_{\text{Direct}}(H).\end{aligned}$$

The derivatives of the paths that have a turning portion are the same, just with an extra couple of terms from the extra integrals that appear from the extra pieces of the path. For example, the turn at boundary $x = b$

$$\begin{aligned}\bar{P}_{\text{Turn at b}} &= \frac{\exp\left[\frac{1}{2}\int_{x_i}^{x_f}\frac{V''}{\sqrt{H+V'^2}}dy + \int_{x_f}^b\frac{V''}{\sqrt{H+V'^2}}dy\right]}{(H+V'(x_f)^2)^{\frac{1}{4}}(H+V'(x_i)^2)^{\frac{1}{4}}} \\ &\quad \times \exp\left[-\frac{1}{4D}\left(2V(x_f)-2V(x_i)+2\int_{x_i}^{x_f}\sqrt{H+V'^2}dy + 4\int_{x_f}^b\sqrt{H+V'^2}dy\right)\right]\end{aligned}$$

$$\bar{P}'_{\text{Turn at b}}(H) = -\frac{V''(x_f)V'(x_f)}{2(H+V'(x_f)^2)}\bar{P}_{\text{Turn at b}}$$

$$+ \left[\frac{V''(x_f)}{2\sqrt{H + V'(x_f)^2}} - \frac{V''(x_f)}{\sqrt{H + V'(x_f)^2}} - \frac{V'(x_f) + \sqrt{H + V'(x_f)^2} - 2\sqrt{H + V'(x_f)^2}}{2D} \right] \bar{P}_{\text{Turn at b}}$$

$$\begin{aligned} \bar{P}'_{\text{Turn at b}}(H) &= -\frac{V''(x_f)V'(x_f)}{2(H + V'(x_f)^2)} \bar{P}_{\text{Turn at b}} \\ &+ \left[-\frac{V''(x_f)}{2\sqrt{H + V'(x_f)^2}} - \frac{V'(x_f) - \sqrt{H + V'(x_f)^2}}{2D} \right] \bar{P}_{\text{Turn at b}}. \end{aligned}$$

As the extra factors for the turn at $x = a$ are not dependent on the final position, the terms are similar between the direct and the turn at $x = a$, and the turn at $x = b$ and turn at both. Subsequently, we have a full set of derivatives, also setting $G(x_f) = \sqrt{H + V'(x_f)^2}$;

$$\bar{P}'_{\text{Direct}}(H) = \left[-\frac{V'(x_f)V''(x_f)}{2G(x_f)^2} + \frac{V''(x_f)}{2G(x_f)} - \frac{V'(x_f) + G(x_f)}{2D} \right] \bar{P}_{\text{Direct}}(H)$$

$$\bar{P}'_{\text{Turn at a}}(H) = \left[-\frac{V'(x_f)V''(x_f)}{2G(x_f)^2} + \frac{V''(x_f)}{2G(x_f)} - \frac{V'(x_f) + G(x_f)}{2D} \right] \bar{P}_{\text{Turn at a}}(H)$$

$$\bar{P}'_{\text{Turn at b}}(H) = \left[-\frac{V'(x_f)V''(x_f)}{2G(x_f)^2} - \frac{V''(x_f)}{2G(x_f)} - \frac{V'(x_f) - G(x_f)}{2D} \right] \bar{P}_{\text{Turn at b}}(H)$$

$$\bar{P}'_{\text{Two turns}}(H) = \left[-\frac{V'(x_f)V''(x_f)}{2G(x_f)^2} - \frac{V''(x_f)}{2G(x_f)} - \frac{V'(x_f) - G(x_f)}{2D} \right] \bar{P}_{\text{Two turns}}(H)$$

Substituting this into the boundary condition for the reflecting boundary and evaluating at the boundary we can collect like terms together as $\bar{P}_D(x = b) = \bar{P}_{Tb}(x = b)$ and $\bar{P}_{Ta}(x = b) = \bar{P}_{TB}(x = b)$;

$$0 = V'(b)\bar{P}(H; b) + D\bar{P}'(H; b)$$

$$0 = V'(b)\bar{P}_{\text{Direct}}(H; b) [1 + B] + V'(b)\bar{P}_{\text{Turn at a}}(H; b) [A + AB]$$

$$+ D\bar{P}_{\text{Direct}}(H; b) \left[\frac{V'(b)V''(b)}{2G(b)^2} (1 + B) + \frac{V''(b)}{2G(b)} (1 - B) - \frac{V'(b)}{2D} (1 + B) - \frac{G(b)}{2D} (1 - B) \right]$$

$$+ D A \bar{P}_{\text{Turn at a}}(H; b) \left[\frac{V'(b)V''(b)}{2G(b)^2} (1+B) + \frac{V''(b)}{2G(b)} (1-B) - \frac{V'(b)}{2D} (1+B) - \frac{G(b)}{2D} (1-B) \right].$$

The best way to try and solve for B is to look at all the constants multiplying the probabilities individually, and see if the large bracket equals zero. Looking at everything that multiplies \bar{P}_D ,

$$\frac{V'(b)}{2} (1+B) - \frac{G(b)}{2} (1-B) + D \left[-\frac{V'(b)V''(b)}{2G(b)^2} (1+B) + \frac{V''(b)}{2G(b)} (1-B) \right] = 0.$$

If we look at the orders of D we can see if it returns the same value of B ;

$$\begin{aligned} \mathcal{O}(D^0) \quad V'(b) + V'(b)B - G(b) + G(b)B &= 0, \\ B &= \frac{G(b) - V'(b)}{G(b) + V'(b)}, \end{aligned}$$

$$\begin{aligned} \mathcal{O}(D) \quad -\frac{V'(b)V''(b)}{2G(b)^2} (1+B) + \frac{V''(b)}{2G(b)} (1-B) &= 0, \\ -V'(b) - V'(b)B + G(b) - G(b)B &= 0, \\ B &= \frac{G(b) - V'(b)}{G(b) + V'(b)}. \end{aligned}$$

Both of these orders of D return the same answer for the reflecting boundary constant. This means we have found the reflecting boundary's constant to satisfy the boundary condition. So we now have a full solution for a probability density function for a system with two boundaries at $x = a$ and $x = b$, $b > a$;

$$\bar{P}(H) = \frac{\bar{P}_{\text{Direct}} + A\bar{P}_{\text{Turn at a}} + B\bar{P}_{\text{Turn at b}} + AB\bar{P}_{\text{Two turns}}}{1 - AB\bar{P}_{\text{Full cycle}}} \quad (7.5)$$

$$\bar{P}_\gamma(H) = \frac{\exp\left[\frac{1}{2} \int_\gamma \frac{V''}{\sqrt{H+V'^2}} dy\right]}{(H + V'(x_f)^2)^{\frac{1}{4}} (H + V'(x_i)^2)^{\frac{1}{4}}} \exp\left[-\frac{1}{4D} \left(2V(x_f) - 2V(x_i) + 2 \int_\gamma \sqrt{H + V'^2} dy\right)\right]$$

$$\bar{P}_{\text{Full cycle}} = \exp \left[-\frac{1}{D} \int_a^b \sqrt{H + V'^2} dy \right]$$

$$\text{Absorbing boundary } A = -1; \quad \text{Reflecting boundary } B = \frac{G(b) - V'(b)}{G(b) + V'(b)}$$

Note: if the reflecting boundary is to the left of the absorbing boundary, $b < a$, then the only difference is that the boundary condition is inverted. This can be found by following a similar derivation as above, the major difference being the order of the integral limits. Meaning that for $b < a$,

$$B = \frac{G(b) + V'(b)}{G(b) - V'(b)}.$$

In this chapter, we have investigated the use of the Laplace domain in advancing the path integral formulation to provide a fuller solution for a given system. We constructed \bar{P} by solving the transformed Smoluchowski equation and introducing the concept of absorbing and reflecting boundaries, as we need multiple turning paths to calculate the correct long-time limit. These tools will allow the exploration of the first passage time density and further moments of a given system in chapter 8, a key area of interest in many areas of science.

Chapter 8

First Passage Times

In section 1.2, the importance of first passage times is described within all areas of science. In this chapter, we will explore the use of path integrals in solving for the FPT densities in the Laplace domain. Deriving how the density is formed for the simplest of systems, the flat and linear potentials, each with a mixture of boundaries and then give a general form for the FPT density for a general potential $V(x)$. We will also calculate the relevant value of the mean FPT for the flat and linear potentials and show that this quantity agrees with the value found using definitions described in section 1.2.1. Then looking at the numerical solution from chapter 3, and its use in calculating the FPT of a system. Finally, we will look at the further moments of the first passage time density, and compare the solutions we find to the widely used exponential distribution and how the path integral can provide a more complete solution. What is new in this chapter is the fact that the path integral can provide a full solution for FPT density curves, allowing a more accurate calculation of further moments for the given system, which can then be used in numerical simulations like kMC and FPTkMC [48]. As far as we are aware, analytical expressions for non-zero potentials have not been obtained before.

8.1 The flat potential

From first principles

First, we can solve the flat potential from first principles using standard techniques, solving the Smoluchowski equation directly and then showing that the path integral approach agrees. The simplest of systems we can explore is the flat potential where $V(x) = 0$. In this system, the Smoluchowski equation is defined as the heat equation, [36]

$$\frac{\partial P}{\partial t} = D \frac{\partial^2 P}{\partial x^2}. \quad (8.1)$$

The first system that we will look at is when there are two absorbing boundaries which have the boundary conditions for an interval (a, b) , where $a < x_i < b$, and the initial condition,

$$P(a, t) = P(b, t) = 0, \quad P(x, 0) = \delta(x - x_i).$$

Taking the Laplace transform in t , the Smoluchowski equation becomes the differential equation

$$s\bar{P} - \delta(x - x_i) = D \frac{\partial^2 \bar{P}}{\partial x^2}.$$

This ordinary differential equation has two solutions, one increasing and one decreasing, on either side of the initial position x_i . The general solution with translations to satisfy the boundary conditions are,

$$\bar{P}_L(x < x_i) = A_L \sinh \left[\sqrt{\frac{s}{D}}(x - a) \right],$$

$$\bar{P}_R(x > x_i) = A_R \sinh \left[\sqrt{\frac{s}{D}}(b - x) \right].$$

To find the constants, we can make use of the fact that the probability density function is continuous everywhere, meaning it must be continuous over the initial

position,

$$\bar{P}_L(x = x_i) = \bar{P}_R(x = x_i).$$

There is also a jump in the derivative across the initial position, which arises from integrating the Laplace-transformed Smoluchowski equation across the initial position,

$$\int_{x_i-\epsilon}^{x_i+\epsilon} s\bar{P}dx - \int_{x_i-\epsilon}^{x_i+\epsilon} \delta(x - x_i)dx = \int_{x_i-\epsilon}^{x_i+\epsilon} \frac{\partial^2 \bar{P}}{\partial x^2} dx,$$

$$\text{as } \epsilon \rightarrow 0 \quad -1 = D \left[\frac{\partial \bar{P}}{\partial x} \right]_{x_i^-}^{x_i^+}.$$

The first integral equals zero as the continuity of the probability density function means that $\lim_{\epsilon \rightarrow 0} \bar{P}(x_i + \epsilon) = \lim_{\epsilon \rightarrow 0} \bar{P}(x_i - \epsilon)$. Using these two conditions gives us two simultaneous equations for A_L and A_R ;

$$\bar{P}_L(x < x_i; x_i) = \bar{P}_R(x > x_i; x_i),$$

$$A_L \sinh \left[\sqrt{\frac{s}{D}}(x_i - a) \right] = A_R \sinh \left[\sqrt{\frac{s}{D}}(b - x_i) \right],$$

$$\bar{P}'_R(x > x_i; x_i) - \bar{P}'_L(x < x_i; x_i) = -\frac{1}{D},$$

$$-A_R \sqrt{\frac{s}{D}} \cosh \left[\sqrt{\frac{s}{D}}(b - x_i) \right] - A_L \sqrt{\frac{s}{D}} \cosh \left[\sqrt{\frac{s}{D}}(x_i - a) \right] = -\frac{1}{D}.$$

These can easily be solved and return the probability density function for either side of the initial position,

$$\bar{P}_L = \frac{1}{\sqrt{Ds}} \frac{\sinh \left[\frac{s}{D}(b - x_i) \right] \sinh \left[\frac{s}{D}(x - a) \right]}{\sinh \left[\frac{s}{D}(b - a) \right]} \quad a < x < x_i,$$

$$\bar{P}_R = \frac{1}{\sqrt{Ds}} \frac{\sinh \left[\frac{s}{D}(x_i - a) \right] \sinh \left[\frac{s}{D}(b - x) \right]}{\sinh \left[\frac{s}{D}(b - a) \right]} \quad x_i < x < b.$$

Now we can find the first passage time density in the Laplace domain using equation (1.14), calculated easily with hyperbolic derivatives,

$$\begin{aligned}\bar{f}(s) &= D\bar{P}'_L(a) - D\bar{P}'_R(b), \\ &= \frac{\sinh\left[\sqrt{\frac{s}{D}}(b-x_i)\right] + \sinh\left[\sqrt{\frac{s}{D}}(x_i-a)\right]}{\sinh\left[\sqrt{\frac{s}{D}}(b-a)\right]}.\end{aligned}\quad (8.2)$$

The other useful quantity found using this solution to the Laplace transformed Smoluchowski equation is the mean first passage time. This value is the expected time for the event to occur, the particle crossing one of the boundaries. This value can be found using integration (1.23) [37], but certain Laplace properties can be used to find the mean FPT without needing to integrate;

$$\begin{aligned}\bar{\tau} &= \lim_{t \rightarrow \infty} \int_0^t \tau f(\tau) d\tau, \\ \text{Using final value theorem} &= \lim_{s \rightarrow 0} s \mathcal{L} \left[\int_0^t \tau f(\tau) d\tau \right], \\ \text{Using Laplace transform identities} &= \lim_{s \rightarrow 0} s \left[-\frac{1}{s} \frac{d\bar{f}(s)}{ds} \right], \\ \bar{\tau} &= -\lim_{s \rightarrow 0} \frac{d\bar{f}(s)}{ds}.\end{aligned}$$

To find the mean first passage time, all we need to find is the derivative of the first passage time density. This derivative is a simple calculation and simplified to,

$$\begin{aligned}\frac{d\bar{f}}{ds} &= \frac{\operatorname{cosech}\left[\sqrt{\frac{s}{D}}(b-a)\right]}{2\sqrt{Ds}} \left[(b-x_i) \cosh\left[\sqrt{\frac{s}{D}}(b-x_i)\right] + (x_i-a) \cosh\left[\sqrt{\frac{s}{D}}(x_i-a)\right] \right. \\ &\quad \left. - (b-a) \coth\left[\sqrt{\frac{s}{D}}(b-a)\right] \left[\sinh\left[\sqrt{\frac{s}{D}}(b-x_i)\right] + \sinh\left[\sqrt{\frac{s}{D}}(x_i-a)\right] \right] \right].\end{aligned}$$

To find the limit, we expand each hyperbolic function around s small and only use the first two terms in each Taylor series expansion as when the limit is taken anything higher is zero,

$$\sinh[x] \approx x + \frac{x^3}{3!}, \quad \cosh[x] \approx 1 + \frac{x^2}{2!}, \quad \coth[x] \approx \frac{1}{x} - \frac{x}{3}, \quad \operatorname{cosech}[x] \approx \frac{1}{x} - \frac{x}{6}.$$

We must take at least two terms in each expansion to find every term that will have a constant value once the brackets have been expanded. Using these hyperbolic expansions, we can find the mean first passage time density to be,

$$\bar{\tau} = \frac{1}{2D} [x_i(b+a) - ab - x_i^2]. \quad (8.3)$$

So we can find the probability density function, first passage time density, and the mean first passage time by solving the Laplace transformed Smoluchowski equation directly. This technique is a significant amount of algebra, so path integrals may be more accessible.

Using Path Integrals

In this system, we have four possible “base” paths that a particle can take from the initial position to the final position, the direct path, in orange —, the turning path at $x = b$, in red —, the turning path at $x = a$, in green — and the turning path at both $x = b$ and $x = a$, in blue —.

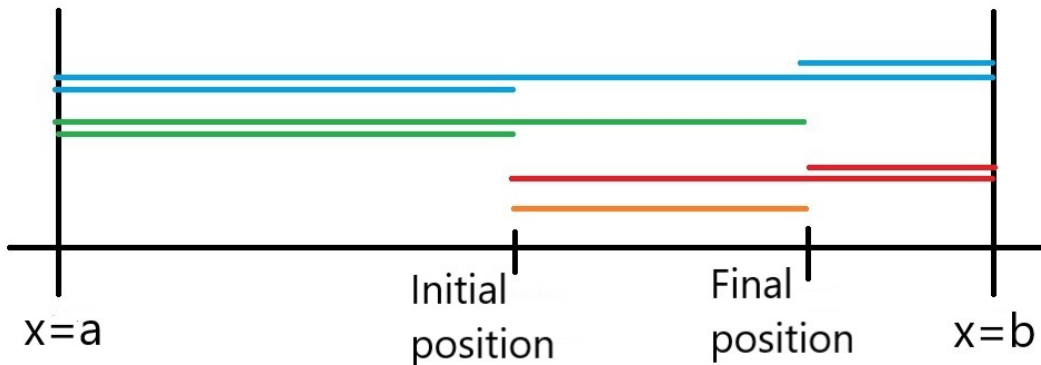


Figure 8.1: The four “base” paths for this flat potential system.

We can use the general form for the path integral (7.5) for each path with $V'(x) = 0$ meaning the full probability has the form,

$$\bar{P}(H) = \frac{1}{\sqrt{H} [1 - \exp(-\frac{S_0}{4D})]} \left[e^{-\frac{S_D}{4D}} - e^{-\frac{S_{Ta}}{4D}} - e^{-\frac{S_{Tb}}{4D}} + e^{-\frac{S_{TB}}{4D}} \right],$$

where the \pm signs are there to satisfy the relevant boundary conditions, similar to the “method of images” technique used in other areas of science like electrostatics [99]. There are strictly two probability density functions on either side of the initial position x_i that have different actions for each path due to the integral limits in the action being dependent on whether the final position is greater than or less than the initial position.

We can also use these representations of probability in Laplace space to find the probability density function in the time domain by numerically inverting the probability. We can do this by using Matlab Laplace inversion techniques, specifically, the Talbot inversion [100], and we can build up a picture of how the probability density function acts in this system over time. This is what figure 8.2 shows, a delta function style peak at the initial position, $x_i = 0.5$, then over time the probability spreads out and disappears over the boundaries at ± 1 , as expected. The probability density is not normalised in this case as the probability is “leaking” out of the system due to the absorbing boundaries.

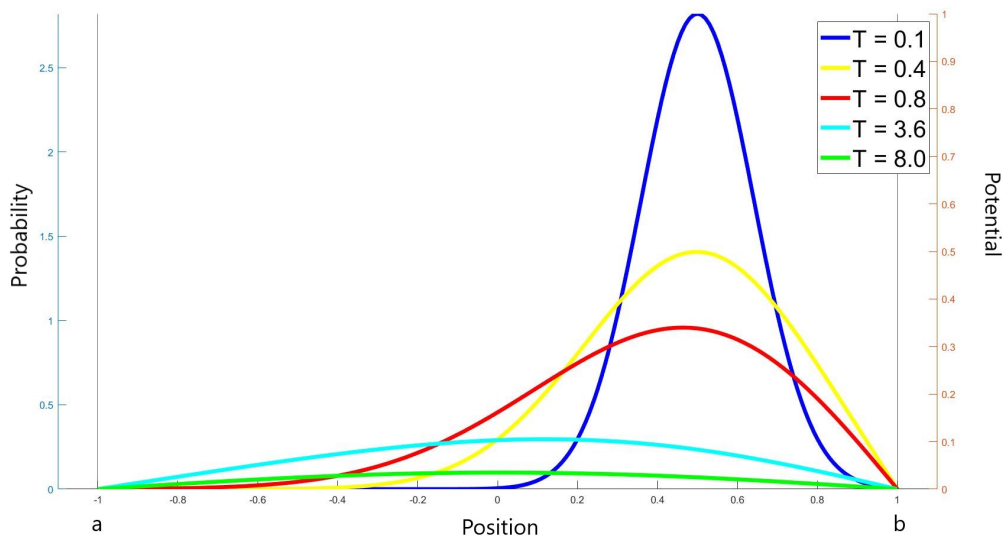


Figure 8.2: PDF at different time steps for the flat potential with double absorbing boundaries, $x_i = 0.5$, $D = 0.25$

We can then use (1.14) to calculate the first passage time density. To find the FPT density, we need the derivatives of the probability, specifically the derivatives of the actions on either side of the initial position, calculated as;

$$\begin{aligned}
 & \underline{x_f > x_i} \\
 S_{\mathcal{D}} &= 2V(x_f) - 2V(x_i) + 2 \int_{x_i}^x \sqrt{H} dy & S_{Tb} &= S_{\mathcal{D}} + 4 \int_{x_f}^b \sqrt{H} dy \\
 &= 2\sqrt{H}(x_f - x_i) & S'_{Tb} &= -2\sqrt{H} \\
 S'_{\mathcal{D}} &= 2\sqrt{H} & S_{TB} &= S_{\mathcal{D}} + 4 \int_a^{x_i} \sqrt{H} dy + 4 \int_{x_f}^b \sqrt{H} dy \\
 S_{Ta} &= S_{\mathcal{D}} + 4 \int_a^{x_i} \sqrt{H} dy & S'_{TB} &= -2\sqrt{H} \\
 S'_{Ta} &= 2\sqrt{H}
 \end{aligned}$$

$$\begin{aligned}
 & \underline{x_f < x_i} \\
 S_{\mathcal{D}} &= 2V(x_f) - 2V(x_i) + 2 \int_{x_f}^{x_i} \sqrt{H} dy & S_{Tb} &= S_{\mathcal{D}} + 4 \int_{x_i}^b \sqrt{H} dy \\
 &= -2\sqrt{H}(x_f - x_i) & S'_{Tb} &= -2\sqrt{H} \\
 S'_{\mathcal{D}} &= -2\sqrt{H} & S_{TB} &= S_{\mathcal{D}} + 4 \int_a^{x_f} \sqrt{H} dy + 4 \int_{x_i}^b \sqrt{H} dy \\
 S_{Ta} &= S_{\mathcal{D}} + 4 \int_a^{x_f} \sqrt{H} dy & S'_{TB} &= 2\sqrt{H} \\
 S'_{Ta} &= 2\sqrt{H}
 \end{aligned}$$

Now that we have the action derivatives calculated, and all the relevant actions calculated, we can look at the derivative of the probability density function:

$$\overline{P}'(H) = \frac{1}{4D\sqrt{H} [1 - \exp(-\frac{S_0}{4D})]} \left[-S'_{\mathcal{D}} e^{-\frac{S_{\mathcal{D}}}{4D}} + S'_{Ta} e^{-\frac{S_{Ta}}{4D}} + S'_{Tb} e^{-\frac{S_{Tb}}{4D}} - S'_{TB} e^{-\frac{S_{TB}}{4D}} \right].$$

This needs to be evaluated at each boundary to calculate the FPT density, and using the definitions above for the actions and their derivatives we have,

$$\begin{aligned}
 D\overline{P}'(H; x = a) &= \frac{1}{[1 - \exp(-\frac{S_0}{4D})]} \left[e^{-\frac{S_{\mathcal{D}}(a)}{4D}} - e^{-\frac{S_{Tb}(a)}{4D}} \right], \\
 D\overline{P}'(H; x = b) &= \frac{1}{[1 - \exp(-\frac{S_0}{4D})]} \left[-e^{-\frac{S_{\mathcal{D}}(b)}{4D}} + e^{-\frac{S_{Ta}(b)}{4D}} \right],
 \end{aligned}$$

resulting in an FPT density for the flat potential with two absorbing boundaries of,

$$\bar{f}(H) = \frac{1}{\left[1 - \exp\left(-\frac{\sqrt{H}(b-a)}{D}\right)\right]} \left[e^{-\frac{\sqrt{H}(x_i-a)}{2D}} - e^{-\frac{\sqrt{H}(2b-x_i-a)}{2D}} + e^{-\frac{\sqrt{H}(b-x_i)}{2D}} - e^{-\frac{\sqrt{H}(b-x_i-2a)}{2D}} \right]. \quad (8.4)$$

Using the hyperbolic double angle formulae $1 - e^{-2a} = 2e^{-a} \sinh(a)$, we can rearrange this form to show that it agrees with the form found by solving the Smoluchowski equation directly (8.2), remembering $s = \frac{H}{4D}$,

$$\bar{f}(H) = \frac{\sinh\left[\frac{\sqrt{H}}{2D}(b-x_i)\right] + \sinh\left[\frac{\sqrt{H}}{2D}(x_i-a)\right]}{\sinh\left[\frac{\sqrt{H}}{2D}(b-a)\right]}.$$

That also means that the same derivation can be followed in finding the mean FPT. So, we have shown that for the simplest of systems with two absorbing boundaries, the path integral approach returns the same results for the FPT density and the mean FPT value. As with the probability density function, we can numerically invert this form for the Laplace FPT into the time domain. Figure 8.3 shows the FPT density, the flux over each boundary and the cumulative FPT density. What occurs is that the FPT density spikes for a short time for the boundary closest to the initial position as the particles have not had time to reach the other boundary. At a long time, as the probability density function spreads out the flux over each boundary becomes equal as the particle has an equal probability of going over each boundary. The areas under the curve also highlight some of the dynamics of the system, with the area under the full FPT curve, in yellow, being normalised when T is large enough, whilst the area under the red curve is larger than the blue curve as the flux over the closer boundary at $x = b$ is much larger than the flux over the boundary at $x = a$.

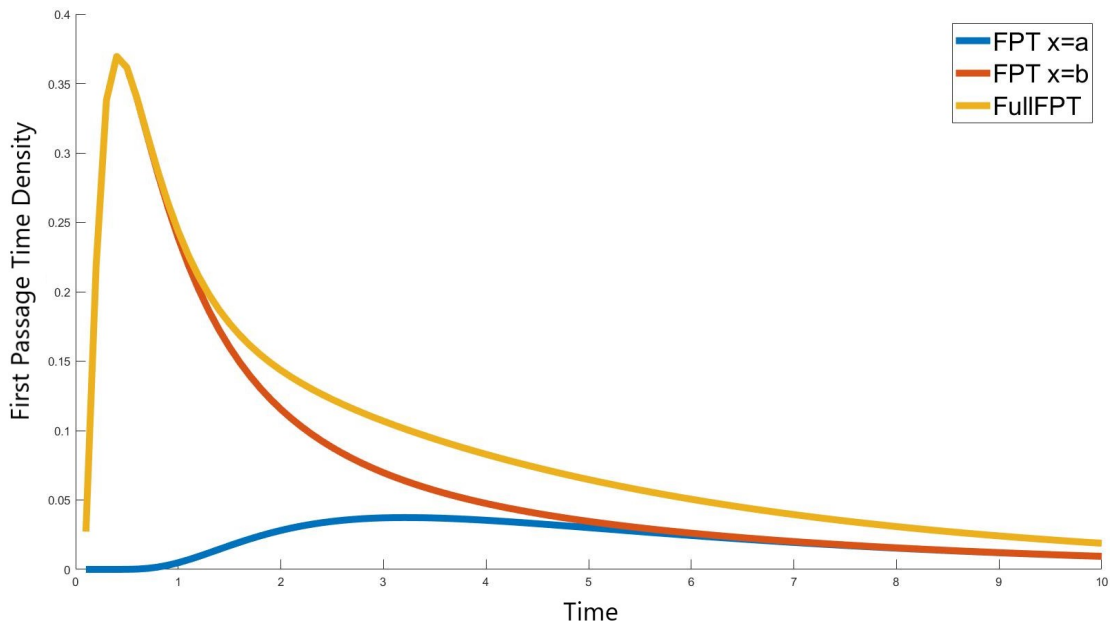


Figure 8.3: FPT density for the double absorbing boundary in the flat potential, for $D = 0.25$.

There is one other check for the first passage time densities that we can calculate to make sure that our representation is correct, and that is to use the *initial* and *final value theorems* [101]. These are the limits to both 0 and ∞ , $H \rightarrow 0/\infty$, in the Laplace domain correspond with the limit to ∞ and 0, $T \rightarrow \infty/0$, in the time domain respectively.

Generally, they are defined as, where $F(s) = \mathcal{L}[f(t)]$,

$$\lim_{H \rightarrow 0} sF(s) = \lim_{T \rightarrow \infty} f(t),$$

$$\lim_{H \rightarrow \infty} sF(s) = \lim_{T \rightarrow 0} f(t).$$

To relate this to the FPT density representation that we have calculated, we use the cumulative density function definition in the time domain, which is defined as,

$$\text{CDF} = \int_0^{\infty} f(t)dt,$$

$$\lim_{T \rightarrow \infty} \text{CDF} = 1,$$

$$\lim_{T \rightarrow 0} \text{CDF} = 0,$$

where $f(t)$ is the FPT density in the time domain. Taking the Laplace transform of the CDF integral returns a relationship with $\bar{f}(s)$,

$$\begin{aligned} \mathcal{L}[\text{CDF}] &= \mathcal{L} \left[\int_0^\infty f(t) dt \right], \\ &= \frac{1}{s} \mathcal{L}[f(t)], \\ &= \frac{1}{s} \bar{f}(s). \end{aligned}$$

Inputting this into the initial and final value theorems returns the limits that we will need our representation to satisfy,

$$\lim_{T \rightarrow \infty} \text{CDF} = \lim_{T \rightarrow \infty} \mathcal{L}[\text{CDF}] = \lim_{s \rightarrow 0} s \frac{1}{s} \bar{f}(H) = \lim_{H \rightarrow 0} \bar{f}(H) = 1,$$

$$\lim_{T \rightarrow 0} \text{CDF} = \lim_{T \rightarrow 0} \mathcal{L}[\text{CDF}] = \lim_{s \rightarrow \infty} s \frac{1}{s} \bar{f}(H) = \lim_{H \rightarrow \infty} \bar{f}(H) = 0.$$

So, we have two limits that the FPT density must satisfy to be able to be related to the time domain FPT density. We can use (8.4) to investigate the limits as it makes the limits themselves easier to deal with exponentials instead of hyperbolics. First we look at $H \rightarrow \infty$ in which all the exponential terms $\rightarrow 0$ as $\lim_{x \rightarrow \infty} e^{-ax} = 0$, so the numerator is 0 and the denominator is 1, so $\bar{f}(H) \rightarrow 0$. The trickier one is the $H \rightarrow 0$ limit, as the numerator and denominator tend to 0 with all the exponential terms becoming 1. In order to calculate the limit we will need to use L'Hopital's rule, taking the derivative of the numerator and denominator,

$$\lim_{H \rightarrow 0} \bar{f}(H) = \lim_{H \rightarrow 0} \frac{X(H)}{Y(H)} = \lim_{H \rightarrow 0} \frac{X'(H)}{Y'(H)}.$$

Taking these derivatives with respect to H , we have

$$X(H) = e^{-\frac{\sqrt{H}(x_i-a)}{2D}} - e^{-\frac{\sqrt{H}(2b-x_i-a)}{2D}} + e^{-\frac{\sqrt{H}(b-x_i)}{2D}} - e^{-\frac{\sqrt{H}(b-x_i-2a)}{2D}},$$

$$\begin{aligned}
 X'(H) &= -\frac{x_i - a}{4D\sqrt{H}}e^{-\frac{\sqrt{H}(x_i - a)}{2D}} + \frac{2b - x_i - a}{4D\sqrt{H}}e^{-\frac{\sqrt{H}(2b - x_i - a)}{2D}} \\
 &\quad - \frac{b - x_i}{4D\sqrt{H}}e^{-\frac{\sqrt{H}(b - x_i)}{2D}} + \frac{b - x_i - 2a}{4D\sqrt{H}}e^{-\frac{\sqrt{H}(b - x_i - 2a)}{2D}}, \\
 Y(H) &= 1 - \exp\left(-\frac{\sqrt{H}(b - a)}{D}\right), \\
 Y'(H) &= \frac{b - a}{2D\sqrt{H}}e^{-\frac{\sqrt{H}(b - a)}{D}}.
 \end{aligned}$$

Now we can take the limit of the numerator and denominator derivatives. Doing this gives the final value theorem,

$$\begin{aligned}
 \lim_{H \rightarrow 0} X'(H) &= \frac{1}{4D\sqrt{H}}(-x_i + a + 2b - x_i - a - b + x_i + b - x_i - 2a), \\
 &= \frac{1}{4D\sqrt{H}}(2(b - a)), \\
 \lim_{H \rightarrow 0} Y'(H) &= \frac{1}{2D\sqrt{H}}(b - a), \\
 \\
 \lim_{H \rightarrow 0} \bar{f}(H) &= \frac{\frac{1}{4D\sqrt{H}}(2(b - a))}{\frac{1}{2D\sqrt{H}}(b - a)}, \\
 &= 1 = \lim_{T \rightarrow \infty} f(t).
 \end{aligned}$$

This shows that our representation for the first passage time density agrees with the initial and final value theorems, further evidence that our representation is correct. An addition that occurs from the path integral approach is the ability to explicitly see how the paths construct the dynamics of the system, possibly allowing a fuller explanation and understanding of how a specific system evolves over time.

8.2 Linear potential

8.2.1 Two absorbing boundaries

Using path integrals

We can extend this solution to a linear potential with two absorbing boundaries. This is an easy change as for a potential $V(x) = \alpha x$ the gradient is just $V'(x) = \alpha$ instead of $V'(x) = 0$ for the flat potential. The system is defined as,

$$V(x) = \alpha x; \quad \bar{P}(x = a) = 0 = \bar{P}(x = b)$$

This means that all that is needed is the substitution $\sqrt{H} \rightarrow \sqrt{H + \alpha^2}$ and the addition to the action of the $2V(x) - 2V(x_i)$ term,

$$\bar{P}(H) = \frac{1}{\sqrt{H + \alpha^2} [1 - \exp(-\frac{S_0}{4D})]} \left[e^{-\frac{S_D}{4D}} - e^{-\frac{S_{Ta}}{4D}} - e^{-\frac{S_{Tb}}{4D}} + e^{-\frac{S_{TB}}{4D}} \right]$$

$$\begin{aligned} & \underline{x_f > x_i} \\ S_D &= 2V(x_f) - 2V(x_i) + 2 \int_{x_i}^{x_f} \sqrt{H} dy & S_{Tb} &= S_D + 4\sqrt{H + \alpha^2}(b - x_f) \\ &= 2\alpha(x_f - x_i) + 2\sqrt{H + \alpha^2}(x_f - x_i) & S_{TB} &= S_D + 4\sqrt{H + \alpha^2}(x_i - a) + 4\sqrt{H + \alpha^2}(b - x_f) \\ S_{Ta} &= S_D + 4\sqrt{H + \alpha^2}(x_i - a) \\ & \underline{x_f < x_i} \\ S_D &= 2V(x_f) - 2V(x_i) + 2 \int_{x_i}^{x_f} \sqrt{H} dy & S_{Tb} &= S_D + 4\sqrt{H + \alpha^2}(b - x_i) \\ &= 2\alpha(x_f - x_i) + 2\sqrt{H + \alpha^2}(x_f - x_i) & S_{TB} &= S_D + 4\sqrt{H + \alpha^2}(x_f - a) + 4\sqrt{H + \alpha^2}(b - x_i) \\ S_{Ta} &= S_D + 4\sqrt{H + \alpha^2}(x_f - a) \end{aligned}$$

As with the flat potential, we can numerically invert the Laplace-transformed probability density functions to see how they behave over time, figure (8.4). It follows a

similar behaviour to the flat potential, with a slight shift to the left as the potential affects the spread of the probability.

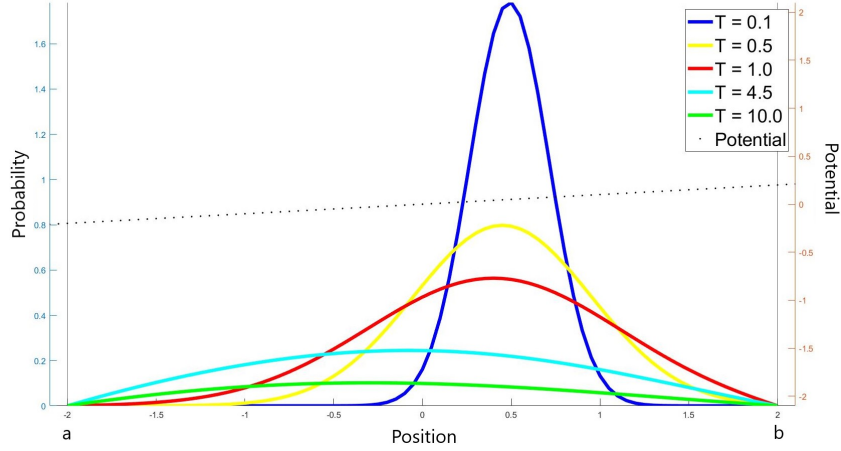


Figure 8.4: PDF at different timesteps for a sloped potential, $V(x) = \frac{x}{10}$ with two absorbing boundaries

This substitution and addition of the $\Delta V(x)$ term follows through the calculations of the first passage time density as well, which gives the solution noting that $G = \sqrt{H + \alpha^2}$,

$$\begin{aligned} \bar{f}(H) = & \frac{1}{\left[1 - \exp\left(-\frac{G(b-a)}{D}\right)\right]} \left[\exp\left(\frac{(G-\alpha)(a-x_i)}{2D}\right) \left[1 - \exp\left(-\frac{G(b-x_i)}{D}\right)\right] \right. \\ & \left. + \exp\left(-\frac{(G+\alpha)(b-x_i)}{2D}\right) \left[1 - \exp\left(\frac{G(a-x_i)}{D}\right)\right] \right] \end{aligned}$$

Similarly, we can also check the initial and final value theorems to see if it satisfies the short and long-time limits of the FPT density,

$$\begin{aligned} \lim_{H \rightarrow 0} f(H) &= \lim_{t \rightarrow \infty} \text{CDF}(t) = 1, \\ \lim_{H \rightarrow \infty} f(H) &= \lim_{t \rightarrow 0} \text{CDF}(t) = 0. \end{aligned}$$

The $H \rightarrow \infty$ limit corresponds to $G \rightarrow \infty$ and is satisfied at the exponential terms dominate sending $\lim_{H \rightarrow \infty} f(H) = 0$. For the $H \rightarrow 0$ limit we can use the fact that

$G \rightarrow \alpha$ as $\alpha > 0$,

$$\begin{aligned} \bar{f}(H \rightarrow 0) &= \frac{1}{N} \left[\exp \left(-\frac{\alpha(a-x_i)}{2D} - \frac{\alpha(x_i-a)}{2D} \right) \left[1 - \exp \left(-\frac{\alpha(b-x_i)}{D} \right) \right] \right. \\ &\quad \left. + \exp \left(-\frac{\alpha(b-x_i)}{2D} - \frac{\alpha(b-x_i)}{2D} \right) \left[1 - \exp \left(-\frac{\alpha(x_i-a)}{D} \right) \right] \right], \\ &= \frac{1}{N} \left[1 - \exp \left(-\frac{\alpha(b-a)}{D} \right) \right], \\ &= 1. \end{aligned}$$

So, the FPT density satisfies the initial and final value theorems. Subsequently, we can numerically invert the Laplace FPT density to see its behaviour. Figure 8.5 shows the FPT density from both boundaries and the full density. It shows that the flux over the boundary closest to the initial position peaks early, as the diffusion is strong enough to get particles over that boundary, but as time goes on the lower boundary takes over as dominant as the linear potential organically leads the particles to escape over the left-hand boundary peaking at a slightly longer time than for the upper boundary. This is also reflected in the distribution of area, with the red curve, $x = b$, having more at small times whilst at longer times there is more area under the blue curve, $x = a$ per unit time as more of the probability escapes over that barrier.

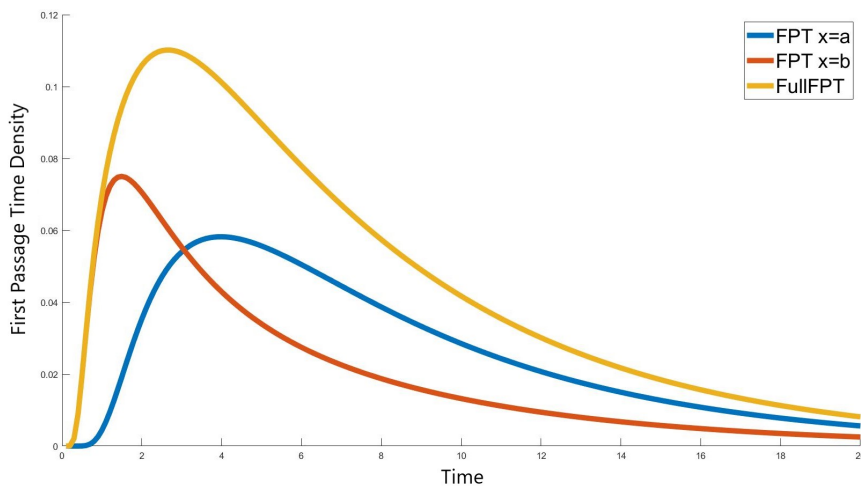


Figure 8.5: FPT density for the sloped potential, $V(x) = \frac{x}{10}$, with two absorbing boundaries, $D = 0.25$

Calculating the mean FPT is a simple task of calculating the derivative of the FPT density and taking the limit $H \rightarrow 0$. We can use a more compact form of the mean FPT expression,

$$\tau = -\lim_{s \rightarrow 0} \frac{d\bar{f}}{ds} = -\frac{2D}{\alpha} \lim_{G \rightarrow \alpha} \frac{d\bar{f}}{dG}.$$

First of all, calculating the derivative,

$$\begin{aligned} \lim_{G \rightarrow \alpha} \frac{\partial \bar{f}}{\partial G} \left[1 - \exp\left(-\frac{\alpha(b-a)}{D}\right) \right] &= -\frac{b-a}{D} e^{-\frac{\alpha(b-a)}{D}} - \frac{x_i-a}{2D} + \frac{x_i-a}{2D} e^{-\frac{\alpha(b-x_i)}{D}} \\ &+ \frac{b-x_i}{D} e^{-\frac{\alpha(b-x_i)}{D}} - \frac{b-x_i}{2D} e^{-\frac{\alpha(b-x_i)}{D}} + \frac{b-x_i}{2D} e^{-\frac{\alpha(b-x_i)}{D} - \frac{\alpha(x_i-a)}{D}} \\ &+ \frac{x_i-a}{D} e^{-\frac{\alpha(b-x_i)}{D} - \frac{\alpha(x_i-a)}{D}}, \\ &= -\frac{x_i-a}{2D} - \frac{1}{2D} e^{-\frac{\alpha(b-a)}{D}} (b-x_i) - \frac{1}{2D} e^{-\frac{\alpha(b-x_i)}{D}} (a-b). \end{aligned}$$

We then substitute this into the mean FPT expression that we have given the final solution

$$\bar{\tau} = \frac{\left[x_i - a + e^{-\frac{\alpha(b-a)}{D}} (b-x_i) - e^{-\frac{\alpha(b-x_i)}{D}} (b-a) \right]}{\alpha \left[1 - \exp\left(-\frac{\alpha(b-a)}{D}\right) \right]}$$

8.2.2 A mixture of boundaries

From first principles

Now to make it more complex. The logical next step is to introduce a non-zero potential with a combination of different boundaries, so we will now look at a linear potential with one absorbing boundary and one reflecting boundary. The difference in the boundary condition is that for the reflecting boundary, we have the flux equal to zero for the reflecting boundary instead of the probability being zero. The potential is $V(x) = \alpha x$, and we have the Smoluchowski equation

$$\frac{\partial P}{\partial t} = \alpha \frac{\partial P}{\partial x} + D \frac{\partial^2 P}{\partial x^2}. \quad (8.5)$$

This has the boundary conditions and initial condition for the interval (a, b) where $a < x_i < b$,

$$P(b, t) = 0, \quad \alpha P(a, t) + DP'(a, t) = 0, \quad P(x, 0) = \delta(x - x_i).$$

We follow a similar method in the flat potential to find the probability density function by solving the Laplace-transformed Smoluchowski equation directly using standard techniques. The Laplace transformed equation is,

$$s\bar{P} - \delta(x - x_i) = \alpha\bar{P}' + D\bar{P}''.$$

The easiest method to solve this differential equation is to use an ansatz of the form $\bar{P} = Ae^{\gamma x}$ which results in a characteristic equation with solutions for γ ,

$$\begin{aligned} \gamma^2 + \frac{\alpha}{D}\gamma - \frac{s}{D} &= 0 \\ \gamma &= -\frac{\alpha}{2D} \pm \frac{\sqrt{\alpha^2 + 4Ds}}{2D}. \end{aligned}$$

Note: to make later calculations neater we define $G = \sqrt{\alpha^2 + 4Ds}$. The solution to the characteristic equation gives the probability density function solution of

$$\bar{P}(s) = e^{-\frac{\alpha x}{2D}} \left[A \cosh\left(\frac{Gx}{2D}\right) + B \sinh\left(\frac{Gx}{2D}\right) \right].$$

As with previous probabilities, this has separate solutions on either side of the initial position, and we can use the boundary conditions along with the continuity and discontinuity conditions to find the constants. For $x > x_i$,

$$\bar{P}(x > x_i) = e^{-\frac{\alpha x}{2D}} \left[A_R \cosh\left(\frac{G(b-x)}{2D}\right) + B_R \sinh\left(\frac{G(b-x)}{2D}\right) \right],$$

using the boundary condition $\bar{P}(b) = 0 \rightarrow A_R = 0$,

$$\bar{P}(x > x_i) = e^{-\frac{\alpha x}{2D}} B_R \sinh\left(\frac{G(b-x)}{2D}\right).$$

For $x < x_i$,

$$\bar{P}(x < x_i) = e^{-\frac{\alpha x}{2D}} \left[A_L \cosh \left(\frac{G(x-a)}{2D} \right) + B_L \sinh \left(\frac{G(x-a)}{2D} \right) \right],$$

using the boundary condition $\alpha \bar{P}(a) + D \bar{P}' = 0 \rightarrow B_L = -\frac{\alpha}{G} A_L$,

$$\bar{P}(x < x_i) = A_L e^{-\frac{\alpha x}{2D}} \left[\cosh \left(\frac{G(x-a)}{2D} \right) - \frac{\alpha}{G} \sinh \left(\frac{G(x-a)}{2D} \right) \right].$$

Going through the same continuity and discontinuity equations as in the flat potential we can find the simultaneous equations to solve for the constants.

$$\begin{aligned} \bar{P}(x < x_i; x_i) &= \bar{P}(x > x_i; x_i) \\ A_L \left[\cosh \left(\frac{G(x_i-a)}{2D} \right) - \frac{\alpha}{G} \sinh \left(\frac{G(x_i-a)}{2D} \right) \right] &= B_R \sinh \left(\frac{G(b-x_i)}{2D} \right) \\ \bar{P}'(x > x_i; x_i) - \bar{P}'(x < x_i; x_i) &= -\frac{1}{D} \\ -B_R \left[\alpha \sinh \left(\frac{G(b-x_i)}{2D} \right) - G \cosh \left(\frac{G(b-x_i)}{2D} \right) \right] &+ \\ A_L \left[\alpha \left[\cosh \left(\frac{G(x_i-a)}{2D} \right) - \frac{\alpha}{G} \sinh \left(\frac{G(x_i-a)}{2D} \right) \right] \right] &+ \\ A_L \left[G \left[\sinh \left(\frac{G(x_i-a)}{2D} \right) - \frac{\alpha}{G} \cosh \left(\frac{G(x_i-a)}{2D} \right) \right] \right] &= -2e^{\frac{\alpha x_i}{2D}} \end{aligned}$$

These continuity conditions return the equations,

$$A_L \left[\cosh \left(\frac{G(x_i-a)}{2D} \right) - \frac{\alpha}{G} \sinh \left(\frac{G(x_i-a)}{2D} \right) \right] = B_R \sinh \left(\frac{G(b-x_i)}{2D} \right),$$

$$B_R e^{-\frac{\alpha x_i}{2D}} \cosh \left(\frac{G(b-x_i)}{2D} \right) + A_L e^{-\frac{\alpha x_i}{2D}} \left[\sinh \left(\frac{G(x_i-a)}{2D} \right) - \frac{\alpha}{G} \cosh \left(\frac{G(x_i-a)}{2D} \right) \right] = \frac{2}{G}.$$

Using these simultaneous equations to solve for the two constants we find the full probability density function is,

$$\bar{P}(x > x_i) = \frac{2}{G} e^{-\frac{\alpha(x-x_i)}{2D}} \sinh\left(\frac{G(b-x)}{2D}\right) \left[\frac{G \cosh\left(\frac{G(x_i-a)}{2D}\right) - \alpha \sinh\left(\frac{G(x_i-a)}{2D}\right)}{G \cosh\left(\frac{G(b-a)}{2D}\right) - \alpha \sinh\left(\frac{G(b-a)}{2D}\right)} \right],$$

$$\bar{P}(x < x_i) = \frac{2}{G} e^{-\frac{\alpha(x-x_i)}{2D}} \sinh\left(\frac{G(b-x_i)}{2D}\right) \left[\frac{G \cosh\left(\frac{G(x-a)}{2D}\right) - \alpha \sinh\left(\frac{G(x-a)}{2D}\right)}{G \cosh\left(\frac{G(b-a)}{2D}\right) - \alpha \sinh\left(\frac{G(b-a)}{2D}\right)} \right].$$

Now that we have found the linear potential PDF, the next step is to calculate the first passage time density. In this system, we only have one absorbing boundary, meaning there is only one term in the FPT definition as there is no flux over the boundary at $x = a$,

$$\begin{aligned} \bar{f}(H) &= -D\bar{P}'(x > x_i; x = b), \\ &= e^{-\frac{\alpha(b-x_i)}{2D}} \left[\frac{G \cosh\left(\frac{G(x_i-a)}{2D}\right) - \alpha \sinh\left(\frac{G(x_i-a)}{2D}\right)}{G \cosh\left(\frac{G(b-a)}{2D}\right) - \alpha \sinh\left(\frac{G(b-a)}{2D}\right)} \right]. \end{aligned} \quad (8.6)$$

This then leads to the calculation of the mean first passage time, and we can use the same equation as in the flat potential (8.3). After some algebra and using Mathematica's help with the limit expansion gives a mean FPT,

$$\bar{\tau} = \frac{D}{\alpha^2} \left[e^{\frac{\alpha(b-a)}{D}} - e^{\frac{\alpha(x_i-a)}{D}} \right] - \frac{b-x_i}{\alpha}.$$

The other standard technique in finding the mean first passage time when we have one absorbing boundary is to use the derivation shown in 1.2.1. Using equation (1.23),

$$\begin{aligned} \bar{\tau} &= \frac{1}{D} \int_{x_i}^b e^{\frac{V(y)}{D}} \int_a^y e^{-\frac{V(x)}{D}} dx dy, \\ &= \frac{1}{D} \int_{x_i}^b e^{\frac{\alpha y}{D}} \int_a^y e^{-\frac{\alpha x}{D}} dx dy, \end{aligned}$$

$$\begin{aligned}
 &= -\frac{1}{\alpha} \int_{x_i}^b e^{\frac{\alpha y}{D}} \left[e^{-\frac{\alpha y}{D}} - e^{-\frac{\alpha a}{D}} \right] dy, \\
 &= -\frac{1}{\alpha} \int_{x_i}^b \left[1 - e^{\frac{\alpha y}{D}} e^{-\frac{\alpha a}{D}} \right] dy, \\
 &= \frac{D}{\alpha^2} \left[e^{\frac{\alpha(b-a)}{D}} - e^{\frac{\alpha(x_i-a)}{D}} \right] - \frac{b-x_i}{\alpha}.
 \end{aligned}$$

We have an agreement between the two standard techniques for calculating the mean first passage time.

Using Path Integrals

We then can look at the path integral derivation to see if it returns the same solution for the FPT density and mean FPT. For this system, we have a similar setup as we did for the flat potential. There are the four “base” paths and a normalisation constant which absorbs all the full cycle paths from the geometric series as shown in chapter 7. The “base” paths, the direct path, in orange —, the turning path at $x = b$, in red —, the turning path at $x = a$, in green — and the turning path at both $x = b$ and $x = a$, in blue —, (7.4).

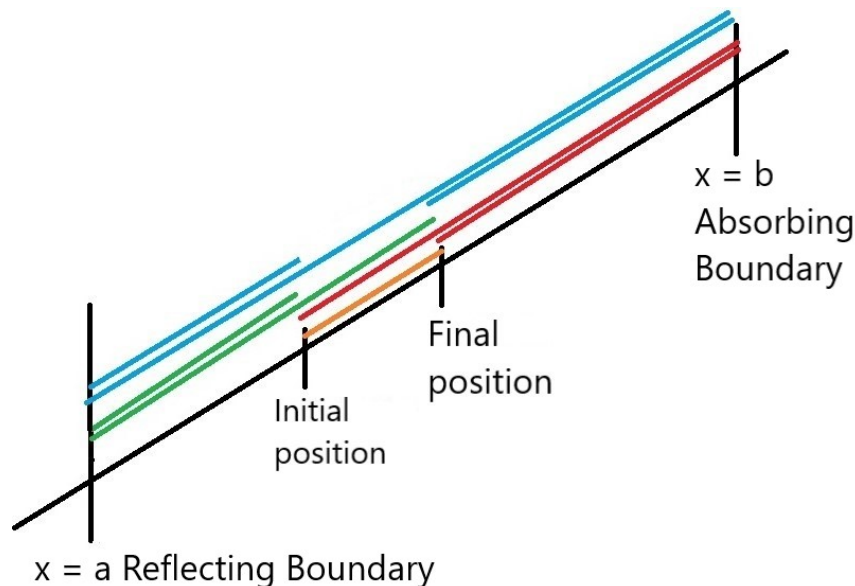


Figure 8.6: The “base” paths for the linear potential

The major difference is the constant required to satisfy the boundary condition at the reflecting boundary. For a reflecting boundary, there is zero flux over the

boundary, so the constant required for the boundary condition at $x = a$ is $\frac{G(a)+V'(a)}{G(a)-V'(a)}$ (7.5). This gives a full probability density function solution of,

$$\bar{P}(H) = \frac{1}{NG} \left[\exp \left[-\frac{S_{\mathcal{D}}}{4D} \right] + \frac{G + \alpha}{G - \alpha} \exp \left[-\frac{S_{Ta}}{4D} \right] - \exp \left[-\frac{S_{Tb}}{4D} \right] - \frac{G + \alpha}{G - \alpha} \exp \left[-\frac{S_{TB}}{4D} \right] \right],$$

$$N = 1 + \frac{G + \alpha}{G - \alpha} \exp \left[-\frac{G(b-a)}{D} \right],$$

$$G = \sqrt{H + \alpha^2}.$$

We can use this form for the probability to form the probability density function over time. Using a Matlab function [100] to calculate the Laplace inversion at different time steps, we can check that the PDF acts like we think it should. It begins as a delta function style peak at $x_i = 0$ and starts to slide down the potential hill collecting at the left-hand boundary as it cannot escape to the left due to the reflecting boundary. The PDF acts like it should, which is helpful to check.

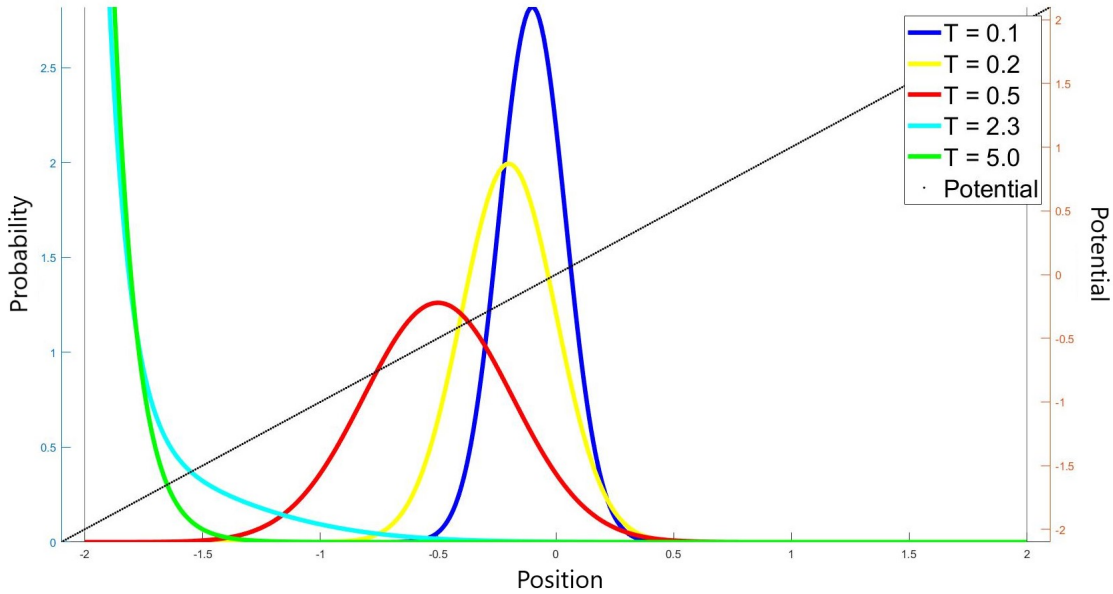


Figure 8.7: PDF over time for the sloped potential $V = 0.1x$ with diffusion $D = 0.1$ and mixed boundaries, reflecting on the left, absorbing on the right

As in the other examples, to find the first passage time density, we need to find the derivatives of the actions of each base path. In this system, we only need to find

the derivatives for when x_f is near the absorbing boundary, meaning we only need to find the action derivatives for when $x_f > x_i$,

$$\begin{aligned}
 S_{\mathcal{D}} &= 2V(x_f) - 2V(x_i) + 2 \int_{x_i}^{x_f} G dy \\
 &= 2\alpha(x_f - x_i) + 2G(x_f - x_i) \\
 S'_{\mathcal{D}} &= 2(\alpha + G) \\
 S_{T_a} &= S_{\mathcal{D}} + 4 \int_a^{x_i} G dy \\
 S'_{T_a} &= 2(\alpha + G) \\
 S_{T_b} &= S_{\mathcal{D}} + 4 \int_{x_f}^b G dy \\
 S'_{T_b} &= 2(\alpha - G) \\
 S_{T_B} &= S_{\mathcal{D}} + 4 \int_a^{x_i} G dy + 4 \int_{x_f}^b G dy \\
 S'_{T_B} &= 2(\alpha - G).
 \end{aligned}$$

The first passage time density is defined for one absorbing boundary as the flux over that boundary, with the fact that the boundary is at the upper limit,

$$\bar{f}(H) = -D\bar{P}'(H, x_f = b).$$

Differentiating the probability density function,

$$\begin{aligned}
 \bar{P}'(H; x_f > x_i) &= -\frac{1}{4DNG} \left[S'_{\mathcal{D}} \exp\left[-\frac{S_{\mathcal{D}}}{4D}\right] + \frac{G + \alpha}{G - \alpha} S'_{T_a} \exp\left[-\frac{S_{T_a}}{4D}\right] \right. \\
 &\quad \left. - S'_{T_b} \exp\left[-\frac{S_{T_b}}{4D}\right] - \frac{G + \alpha}{G - \alpha} S'_{T_B} \exp\left[-\frac{S_{T_B}}{4D}\right] \right], \\
 &= -\frac{1}{2DNG} \left[(G + \alpha) \exp\left[-\frac{S_{\mathcal{D}}}{4D}\right] + \frac{(G + \alpha)^2}{G - \alpha} \exp\left[-\frac{S_{T_a}}{4D}\right] \right. \\
 &\quad \left. + (G - \alpha) \exp\left[-\frac{S_{T_b}}{4D}\right] + (G + \alpha) \exp\left[-\frac{S_{T_B}}{4D}\right] \right].
 \end{aligned}$$

At the boundary, $x_f = b$, we can evaluate the actions which have equality relationships $S_{\mathcal{D}}(b) = S_{T_b}(b)$ and $S_{T_a}(b) = S_{T_B}(b)$.

$$\bar{P}'(H; x > x_i; x = b) = -\frac{1}{2DNG} \left[\exp\left[-\frac{S_{\mathcal{D}}(b)}{4D}\right] (2G) + \exp\left[-\frac{S_{T_a}(b)}{4D}\right] \left[\frac{(G + \alpha)^2}{G - \alpha} + G + \alpha \right] \right]$$

$$\begin{aligned}
&= -\frac{1}{ND} \left[\exp \left[-\frac{S_{\mathcal{D}}(b)}{4D} \right] + \frac{G + \alpha}{G - \alpha} \exp \left[-\frac{S_{T_a}(b)}{4D} \right] \right] \\
N &= 1 + \frac{G + \alpha}{G - \alpha} \exp \left[-\frac{G(b-a)}{D} \right] \\
&= \frac{1}{G - \alpha} \left[G - \alpha + (G + \alpha) \exp \left[-\frac{G(b-a)}{D} \right] \right]
\end{aligned}$$

This gives a first passage time density,

$$\bar{f}(H) = \frac{1}{G - \alpha + (G + \alpha) \exp \left[-\frac{G(b-a)}{D} \right]} \left[(G - \alpha) \exp \left[-\frac{S_{\mathcal{D}}(b)}{4D} \right] + (G + \alpha) \exp \left[-\frac{S_{T_a}(b)}{4D} \right] \right] \quad (8.7)$$

$$S_{\mathcal{D}}(b) = 2(G + \alpha)(b - x_i)$$

$$S_{T_a}(b) = 2\alpha(b - x_i) + 2G(b + x_i - 2a)$$

As with the other examples, we can numerically invert this form to see if it behaves as we think it should, as shown in figure 8.8. The FPT density spikes early as some of the probability is able to diffuse up the potential and escape over the absorbing boundary, flattening quickly as all the probability settles down near the reflecting boundary as expected, not being able to travel up the potential to the other boundary. This is also reflected in the area under the curve, which is not equal to 1 as some of the probability has not escaped the system.

In a similar method to the flat potential, this form can be transformed to be the same as equation (8.6). This is done by using the double-angle formulae for hyperbolic functions. Again we can also check whether our representation satisfies the initial and final value theorems. The initial value theorem is satisfied as all the exponential terms tend to 0, and by the same reasoning as for the flat potential, the numerator tends to 0 while the denominator tends to 1.

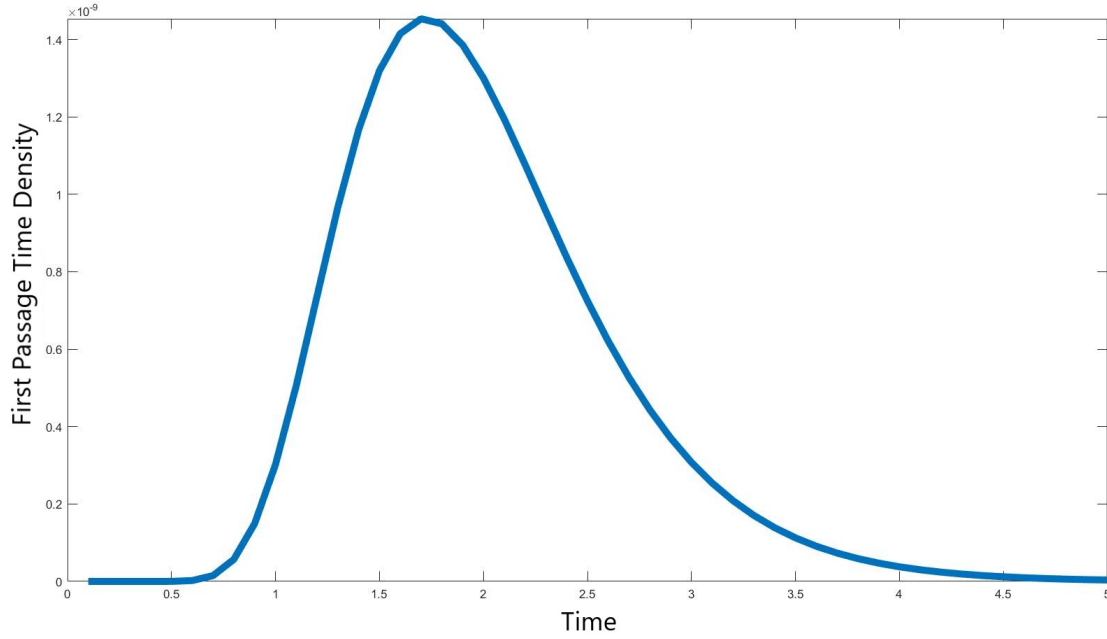


Figure 8.8: FPT density for the sloped potential $y = x$ with mixed boundaries, meaning only one curve with the one absorbing barrier, $D = 0.1$.

The final value theorem is the more interesting one, and we can substitute in $G = \sqrt{H + \alpha^2}$ to make the mathematics simpler, so,

$$\begin{aligned} \lim_{H \rightarrow 0} \bar{f}(H) &= \lim_{G \rightarrow \alpha} \bar{f}(H), \\ &= \frac{2\alpha \exp\left[-\frac{S_{T_a}(b; G=\alpha)}{4D}\right]}{2\alpha \exp\left[-\frac{\alpha(b-a)}{D}\right]}, \end{aligned}$$

$$\begin{aligned} S_{T_a}(b; G = \alpha) &= 2\alpha(b - x_i) + 2\alpha(b + x_i - 2a), \\ &= \alpha(b - a), \end{aligned}$$

$$\lim_{H \rightarrow 0} \bar{f}(H) = \frac{2\alpha \exp\left[-\frac{\alpha(b-a)}{D}\right]}{2\alpha \exp\left[-\frac{\alpha(b-a)}{D}\right]} = 1.$$

So, the path integral representation for the sloped potential also satisfies the initial and final value theorems.

In order to find the mean first passage time, the derivative is needed as is the $s \rightarrow 0$

limit. The equation for the mean FPT can be changed by changing the derivative using the chain rule to be with respect to G as $G = \sqrt{4Ds + \alpha^2}$. $\bar{\tau}$ transforms as previously,

$$\begin{aligned}\bar{\tau} &= -\lim_{s \rightarrow 0} \frac{d\bar{f}}{ds}, \\ &= -\frac{2D}{\alpha} \lim_{G \rightarrow \alpha} \frac{d\bar{f}}{dG}.\end{aligned}$$

In the calculation using the path integral form for the first passage time, there is no need to expand terms to a certain order in s or H and after some algebra using,

$$\lim_{G \rightarrow \alpha} S_{\mathcal{D}}(b) = 4\alpha(b - x_i); \quad \lim_{G \rightarrow \alpha} S_{T_a}(b) = 4\alpha(b - a),$$

we arrive at the same definition of the mean first passage time for a linear potential

$$\bar{\tau} = \frac{D}{\alpha^2} \left[e^{\frac{\alpha(b-a)}{D}} - e^{\frac{\alpha(x_i-a)}{D}} \right] - \frac{b - x_i}{\alpha}. \quad (8.8)$$

So we have again shown that the path integral technique returns the same expression for both first passage time densities and the resultant mean first passage time densities.

8.3 General potential

We have seen that the path integral approach returns the correct result for the simplest of potentials, so we now extend this to a general potential form (7.5). A general potential form cannot be found using standard techniques, which is the extension possibility for the path integral technique. For a system which again has a mixture of boundaries similar to the linear potential,

$$\begin{aligned}\bar{P}(H; x_f = b) &= 0, \\ V'(a)\bar{P}(H; x_f = a) + D\bar{P}'(H; x_f = a) &= 0.\end{aligned}$$

This has a full probability density function, where the reflecting boundary prefactor is evaluated on the boundary. Note that this is an approximation as it is in the weak noise limit, meaning the diffusion value is small compared to the boundary height, which we need to use the technique of minimising the action. The full PDF is,

$$\bar{P}(H) = \frac{1}{N\sqrt{G(x_f)G(x_i)}} \left[\mathcal{J}_{\mathcal{D}} \exp \left[-\frac{S_{\mathcal{D}}}{4D} \right] + A\mathcal{J}_{Ta} \exp \left[-\frac{S_{Ta}}{4D} \right] \right. \\ \left. - \mathcal{J}_{Tb} \exp \left[-\frac{S_{Tb}}{4D} \right] - A\mathcal{J}_{TB} \exp \left[-\frac{S_{TB}}{4D} \right] \right]$$

$$N = 1 + AJ_0 \exp \left[-\frac{S_0}{D} \right]$$

$$G = \sqrt{H + V'(x)^2}$$

$$A = \frac{G(a) + V'(a)}{G(a) - V'(a)}.$$

The actions S and Jacobians \mathcal{J} are defined as:

$$\begin{array}{ll} \underline{x > x_i} & \\ S_{\mathcal{D}} = 2V(x_f) - 2V(x_i) + 2 \int_{x_i}^{x_f} G(y)dy & \mathcal{J}_{\mathcal{D}} = \exp \left[\frac{1}{2} \int_{x_i}^{x_f} \frac{V''(y)}{G(y)} dy \right] \\ S_{Ta} = S_{\mathcal{D}} + 4 \int_a^{x_i} G(y)dy & \mathcal{J}_{Ta} = \mathcal{J}_{\mathcal{D}} \exp \left[\int_a^{x_i} \frac{V''(y)}{G(y)} dy \right] \\ S_{Tb} = S_{\mathcal{D}} + 4 \int_{x_f}^b G(y)dy & \mathcal{J}_{Tb} = \mathcal{J}_{\mathcal{D}} \exp \left[\int_{x_f}^b \frac{V''(y)}{G(y)} dy \right] \\ S_{TB} = S_{\mathcal{D}} + 4 \int_a^{x_i} G(y)dy + 4 \int_{x_f}^b G(y)dy & \mathcal{J}_{TB} = \mathcal{J}_{\mathcal{D}} \exp \left[\int_a^{x_i} \frac{V''(y)}{G(y)} dy + \int_{x_f}^b \frac{V''(y)}{G(y)} dy \right] \end{array}$$

$$\begin{array}{ll} \underline{x_f < x_i} & \\ S_{\mathcal{D}} = 2V(x) - 2V(x_i) + 2 \int_{x_f}^{x_i} G(y)dy & \mathcal{J}_{\mathcal{D}} = \exp \left[\frac{1}{2} \int_{x_f}^{x_i} \frac{V''(y)}{G(y)} dy \right] \\ S_{Ta} = S_{\mathcal{D}} + 4 \int_a^{x_f} G(y)dy & \mathcal{J}_{Ta} = \mathcal{J}_{\mathcal{D}} \exp \left[\int_a^{x_f} \frac{V''(y)}{G(y)} dy \right] \\ S_{Tb} = S_{\mathcal{D}} + 4 \int_{x_i}^b G(y)dy & \mathcal{J}_{Tb} = \mathcal{J}_{\mathcal{D}} \exp \left[\int_{x_i}^b \frac{V''(y)}{G(y)} dy \right] \\ S_{TB} = S_{\mathcal{D}} + 4 \int_a^{x_f} G(y)dy + 4 \int_{x_i}^b G(y)dy & \mathcal{J}_{TB} = \mathcal{J}_{\mathcal{D}} \exp \left[\int_a^{x_f} \frac{V''(y)}{G(y)} dy + \int_{x_i}^b \frac{V''(y)}{G(y)} dy \right] \end{array}$$

Meaning that we can construct a full probability density function for a general potential using a method of images style construction. The usual applications of the method of images are in fields such as electrostatics or two-dimensional fluids, where the function in question, f , is harmonic, meaning it solves Laplace's equation $\nabla^2 f = 0$ [102]. Whereas what we have here is the use of the method of images in the construction of a PDF for a general equation, and can approximately solve the Smoluchowski equation. To calculate the FPT density, we need to find the derivative of the general $\bar{P}(H)$ and then evaluate it at the absorbing boundary, $x_f = b$. In its general form,

$$\begin{aligned} \bar{P}'(H) = & -\frac{G'(x_f)}{2G}\bar{P}(H) \\ & + \frac{1}{\sqrt{G(x_f)G(x_i)}\left[1 - J_0 e^{\frac{s_0}{4D}}\right]} \left[e^{-\frac{s_D}{4D}} \left(J'_D - \frac{1}{4D} J_D S'_D \right) + A e^{-\frac{s_{Ta}}{4D}} \left(J'_{Ta} - \frac{1}{4D} J_{Ta} S'_{Ta} \right) \right. \\ & \left. - e^{-\frac{s_{Tb}}{4D}} \left(J'_{Tb} - \frac{1}{4D} J_{Tb} S'_{Tb} \right) - A e^{-\frac{s_{TB}}{4D}} \left(J'_{TB} - \frac{1}{4D} J_{TB} S'_{TB} \right) \right]. \end{aligned}$$

The derivatives of the actions and Jacobians are then needed, and using the definitions above for $x > x_i$, as we only need the upper boundary,

$$\begin{aligned} S'_D &= 2(V' + G) & J'_D &= \frac{V''}{2G} J_D \\ S'_{Ta} &= 2(V' + G) & J'_{Ta} &= \frac{V''}{2G} J_{Ta} \\ S'_{Tb} &= 2(V' - G) & J'_{Tb} &= -\frac{V''}{2G} J_{Tb} \\ S'_{TB} &= 2(V' - G) & J'_{TB} &= -\frac{V''}{2G} J_{TB} \end{aligned}$$

Using these derivatives, along with the fact that at the boundary $S_D(b) = S_{Tb}(b)$, $J_D(b) = J_{Tb}(b)$ along with similar for the action and Jacobian with turns at a we can write,

$$\begin{aligned} \bar{P}'(H; x = b) = & \frac{1}{\sqrt{G(b)G(x_i)}N} \left[J_D(b) \exp \left[-\frac{S_D(b)}{4D} \right] \left[\frac{V''(b)}{G(b)} - \frac{G(b)}{D} \right] \right. \\ & \left. + A J_{Ta}(b) \exp \left[-\frac{S_{Ta}(b)}{4D} \right] \left[\frac{V''(b)}{G(b)} - \frac{G(b)}{D} \right] \right]. \end{aligned}$$

Subsequently, we can find the first passage time density for the general potential, using the fact that both the action and Jacobian for the turn at a , a direct path can be factored out

$$\bar{f}(H) = -\frac{J_{\mathcal{D}}(b) \exp\left[-\frac{S_{\mathcal{D}}(b)}{4D}\right]}{\sqrt{G(b)G(x_i)}N} \left[\frac{DV''(b)}{G(b)} - G(b)\right] \left[1 + A \exp\left[\int_a^{x_i} \left(\frac{V''(y)}{G(y)} - \frac{G(y)}{D}\right) dy\right]\right],$$

$$N = 1 + AJ_0 \exp\left[-\frac{S_0}{D}\right], \quad G = \sqrt{H + V'(x)^2}, \quad A = \frac{G(a) + V'(a)}{G(a) - V'(a)}.$$

8.4 A Barrier Escape problem

We have seen how the path integral formalism can provide the first passage time density for a general potential. Still, we can look at how it compares to some known approximations, specifically the *Kramers rate* in the generic barrier escape problem [49]. This method describes a particle that is caught in a potential hole and, through Brownian motion, can escape over a potential barrier, which is a suitable model for calculating transitions of the rate of chemical reactions.

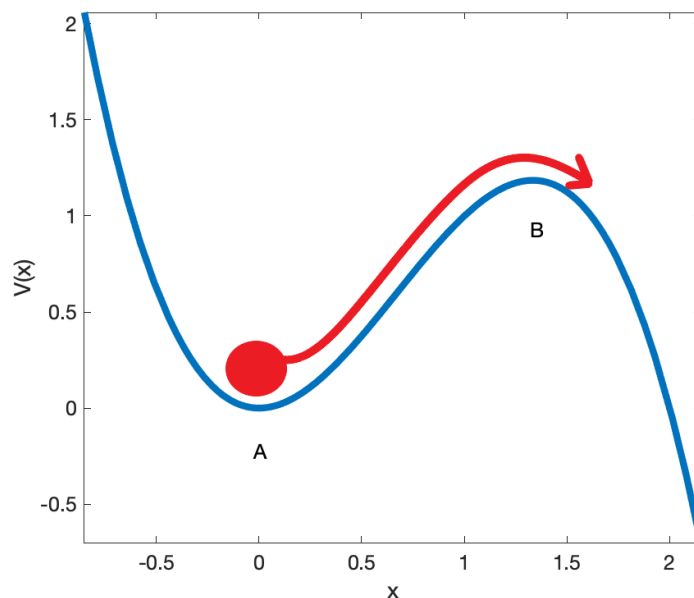


Figure 8.9: A generic barrier escape potential

In this system, we calculate the first passage time density for a particle to escape from near the bottom of the well at $x = A = 0$ over the barrier at $x = B$. This is approximated using the Kramers rate as the rate of the system in the exponential distribution used to model the FPT density at equilibrium, i.e. the long time limit,

$$\Gamma_{\text{Kramers}} \propto |V_B''| \exp(-V_B/D)$$
$$f(t) \rightarrow \Gamma \exp(-\Gamma t) \quad \text{as } t \rightarrow \infty.$$

It is assumed that the system follows exponentially distributed wait times, similar to a Poisson process representation. The rate Γ is the inverse of the mean first passage time value, $\Gamma = \frac{1}{\tau}$, and this is similar in form to the Arrhenius equation [51] which relates the rate of the system to the activation energy, in Kramers is the height of the potential barrier. So, how does this relate to the path integral representation? Well, suppose we can show that in the long time limit, the path integral returns a result proportional to the Kramers rate solution. In that case, we can say that our result has the same behaviour as the current numerical methods, with the prefactor of the Kramers' rate arising from the normalisation of the probability density function. The only difference is that the path integral result also holds the information for short time, non-equilibrated, crossing of the potential barrier, a possible improvement on using the Kramers rate as an approximation. We have previously discussed this potential benefit in section 1.2, where we looked at short-time discrepancies between a full FPT density and the exponential distribution approximation.

In the Laplace domain, we wish to look at paths that travel from an initial position at $x = A$ and to a point x near the peak of the barrier at B ; then, we will calculate the relevant first passage time density at the point $x = B$. We can construct the probability density function in the same way that we have done previously by having two possible paths, the direct path and the path that turns at $x = B$. We have to remember all the terms, including the Jacobian term and also that the construction includes the boundary condition that at the peak of the barrier there is an absorbing

barrier at $x = B$, i.e. $\bar{P}(x = B) = 0$. This means we have the Laplace-transformed probability density,

$$\bar{P}(x; H) = \lambda \left[N J_D \exp\left(-\frac{S_D}{4D}\right) - N J_T \exp\left(-\frac{S_T}{4D}\right) \right],$$

where there is a factor of λ which is a function of H that we can use to fix any normalisation that might be required. This is because we are comparing this probability density function and subsequent first passage time density to the exponential approximation with the Kramer's rate, which itself is an approximation. This means that to equate to the approximation, an extra factor may be needed to equate the two.

The actions and Jacobians that we have are written in their full form, with $V(A) = 0$,

$$\begin{aligned} N &= \left((H + V'(A)^2) (H + V'(x)^2) \right)^{-\frac{1}{4}} \\ S_D &= 2V(x) + 2 \int_A^x \sqrt{H + V'^2} dy \\ S_T &= 2V(x) + 2 \int_A^x \sqrt{H + V'^2} dy + 4 \int_x^B \sqrt{H + V'^2} dy \\ J_D &= \exp\left(\frac{1}{2} \int_A^x \frac{V''(y)}{G(y)} dy\right) \\ J_T &= \exp\left(\frac{1}{2} \int_A^x \frac{V''(y)}{G(y)} dy + \int_x^B \frac{V''(y)}{G(y)} dy\right). \end{aligned}$$

To then calculate the first passage time, we do what we have done a few times already, calculate the derivative of the probability density and then evaluate it at the boundary. This is the same method as what we have just done in the general potential solution, instead, we do not have a second boundary. This results in the PDF derivative:

$$\bar{P}'(H; x = B) = \lambda \frac{1}{\sqrt{H}} J_D \exp\left(-\frac{S_D}{4D}\right) \left[\frac{V''(x)}{G} - \frac{G}{D} \right] \Bigg|_B$$

So, for the Laplace-transformed first-passage time density we have:

$$\begin{aligned}\bar{f}(H) &= -D\bar{P}(H; x = B) \\ &= \lambda \frac{1}{\sqrt{H}} \left[\frac{D|V''(B)|}{\sqrt{H}} + \sqrt{H} \right] \exp \left(\frac{1}{2} \int_A^B \frac{V''(y)}{G(y)} dy - \frac{2V(B) + 2 \int_A^B \sqrt{H + V'^2} dy}{4D} \right).\end{aligned}$$

The Jacobian term can be calculated directly, as we have a non-integral form for it already. The non-integral form will make the expression simpler, because it depends on the gradient of the potential at the endpoints of the integrand, and in this system, this is 0. This means that,

$$\begin{aligned}J_{\mathcal{D}}|_B &= \exp \left(\frac{1}{2} \int_A^B \frac{V''(y)}{G(y)} dy \right) \\ &= \sqrt{\left. \frac{\left[\sqrt{H + V'(x)^2} + V'(x) \right]}{\left[\sqrt{H + V'(x)^2} - V'(x) \right]} \right|_A^B} \\ &= 1\end{aligned}$$

This results in the form of the first passage time density of,

$$\bar{f}(H) = \frac{\lambda}{H} [D|V''(B)| + H] \exp \left(-\frac{2V(B) + 2 \int_A^B \sqrt{H + V'^2} dy}{4D} \right)$$

So, we have a first passage time density for the standard barrier problem, but how does it relate to Kramer's rate? First, we need to transform the exponential distribution used in the time domain as the approximation for this particular system into the Laplace domain to see what we are trying to find. Note that as this is the exponential approximation, this is only valid in the long time limit, or the small H limit. Transforming the exponential approximation, $f_k(t)$, with rate Γ ,

$$\begin{aligned}f_k(t) &\rightarrow \Gamma \exp(-\Gamma t) \quad \text{as } t \rightarrow \infty \\ \bar{f}_k &= \frac{\Gamma}{\Gamma + s}\end{aligned}$$

$$\begin{aligned}
 s &= \frac{H}{4D}; &= \frac{\frac{4D\Gamma}{H}}{1 + \frac{4D\Gamma}{H}} \\
 & &= \frac{4D|V_B''| \exp(-V_B/D)}{H + 4D|V_B''| \exp(-V_B/D)}.
 \end{aligned}$$

This means that we now have a small H solution that we can match our FPT representation to, as we know that in the long time limit, the exponential approximation is a good representation of the first passage time density. This is also how we will find our λ constant, as we can equate the $H \rightarrow 0$ limit of the FPT expression to the Kramers rate solution. Remembering that $\lim_{H \rightarrow 0} S_{\mathcal{D}} = 4V_B$,

$$\begin{aligned}
 \lim_{H \rightarrow 0} \bar{f}(H) &= \bar{f}_k, \\
 \frac{\lambda DV_B''}{H} \exp\left(-\frac{V_B}{D}\right) &= \frac{4D|V_B''| \exp(-V_B/D)}{H + 4D|V_B''| \exp(-V_B/D)}, \\
 \lambda &= \frac{4H}{H + 4DV_B'' \exp(-\frac{V_B}{D})}, \\
 &= \frac{4}{1 + \frac{4DV_B''}{H} \exp(-\frac{V_B}{D})}.
 \end{aligned}$$

This value of λ has a relationship with our notion of the full cycle paths, that we used when we constructed the flat and linear FPT densities with two boundaries from the geometric series. This λ expression corresponds to the sum over the paths that travel up and down the potential hill, before reaching the peak properly for the first time, figure (8.10). It is related to the alternating geometric series because there is a -1 from the hard bounce off the absorbing barrier, with a $+1$ from a soft bounce off the origin.

Returning a full FPT density expression for the barrier crossing,

$$\bar{f}(H) = \frac{[4DV_B'' + 4H] \exp\left(-\frac{2V(B)+2 \int_A^B \sqrt{H+V'^2} dy}{4D}\right)}{H + 4DV_B'' \exp\left(-\frac{V_B}{D}\right)}.$$

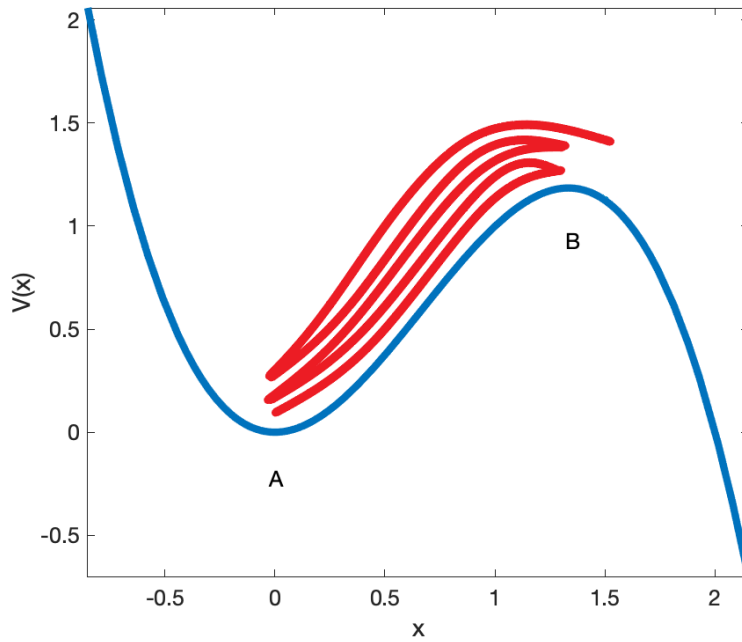


Figure 8.10: An example path, that travels to the peak multiple times before crossing

This expression does satisfy the initial and final value theorems as expected as the exponential dominates for the $H \rightarrow \infty$ limit, $\lim_{H \rightarrow \infty} \bar{f}(H) = 0$, whilst the $H \rightarrow 0$ limit is obvious, $\lim_{H \rightarrow 0} \bar{f}(H) = 1$.

To get a good idea of the added bonus of the path integral representation over the exponential approximation, we will need to see the solution in the time domain. This can be achieved by using a numerical inversion algorithm in Matlab's functions, called the Talbot inversion [103] [100]. Figure 8.11 shows the comparison between the two techniques over a given time frame, with the two values being equal at $T \rightarrow \infty$ as that is how it has been constructed.

Whilst the two methods will agree at long time, $T \rightarrow \infty$, we can see that at short time the exponential approximation breaks down and will not return the correct form, typically when the system is non-equilibrated. This can also be seen if we look at the log graph for the two representations, showing the growing difference between the two techniques, shown in figure (8.12).

This is where the path integral representation becomes more powerful, filling in the missing information and allowing the system to be in a non-equilibrated state, removing an assumption currently made in the vast majority of computer simulations.

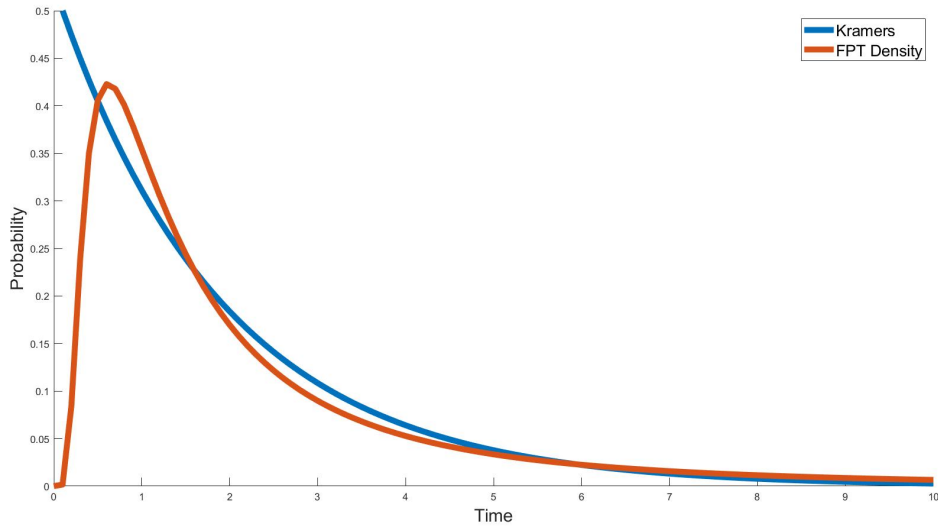


Figure 8.11: Kramers Exponential Distribution, in blue, vs the path integral FPT density, in red, with $D = 1$ and $V(x) = -\frac{x^3}{3} + x^2$.

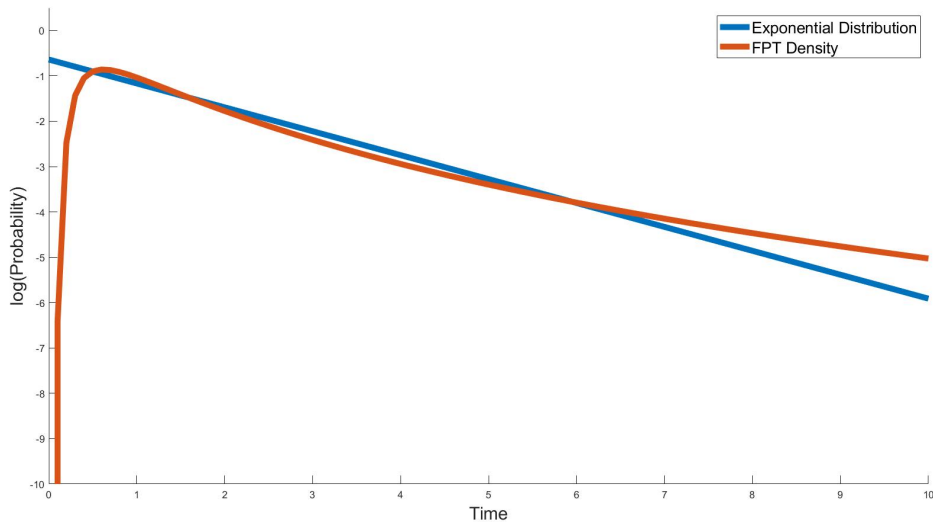


Figure 8.12: Comparison between the natural logarithm of the FPT density and the Kramers exponential approximation, with $D = 1$.

8.5 Numerical solution

As seen in chapter 3, we can also use a numerical path integral representation to find the probability density function for a particle in a given potential. So can this numerical solution be used to find the first passage time for a given system?

8.5.1 Boundary conditions

For all the findings in chapter 3 we used “soft” boundaries where we stopped calculating when the probability became insignificant, $P(\pm\infty) = 0$, $\left. \frac{\partial P}{\partial x} \right|_{\pm\infty} \approx 0$. The more useful case for first passage times would be if the method derived in chapter 3 was able to still give a good approximation to the solution but with “hard” boundaries, $P = 0$, $\frac{\partial P}{\partial x} \neq 0$. This means that we force the problem to truncate at a given point, not when the probability is sufficiently small, enabling the numerical path integral formulation of the probability density function to be used in systems with absorbing boundaries. The absorbing boundary is the same as the other systems in this chapter, where $P(x, t) = 0$ when x is at the boundary. Due to the versatility of the numerical path integral representation of the probability density function, this was achieved by simply applying hard boundaries to the area in which the probability was calculated by setting $P = 0$ for any final positions outside the desired range.

The problem we are dealing with is fundamentally different from the one stated in (3.1). It is solving the Smoluchowski equation but with different boundary conditions,

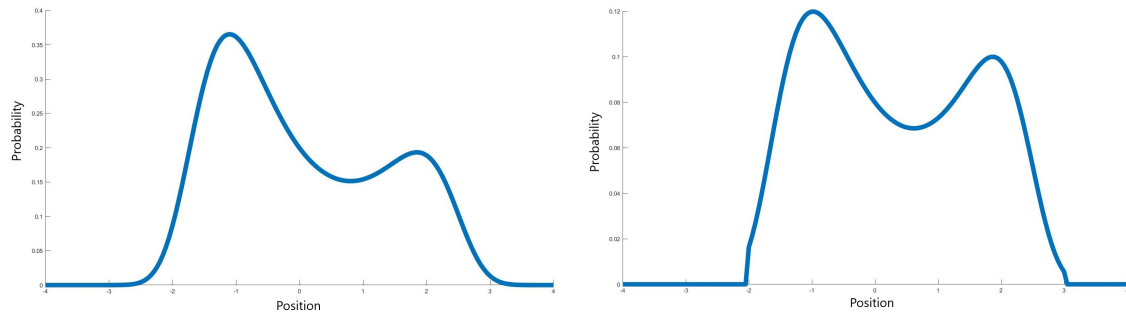
$$\frac{\partial P(x, t)}{\partial t} = \frac{\partial}{\partial x} \left[\frac{dV(x)}{dx} P(x, t) + D \frac{\partial P(x, t)}{\partial x} \right],$$

$$\text{with initial condition } P(x, 0|x_i) = \delta(x - x_i),$$

$$\text{and boundary conditions } P(a, t) = 0 = P(b, t).$$

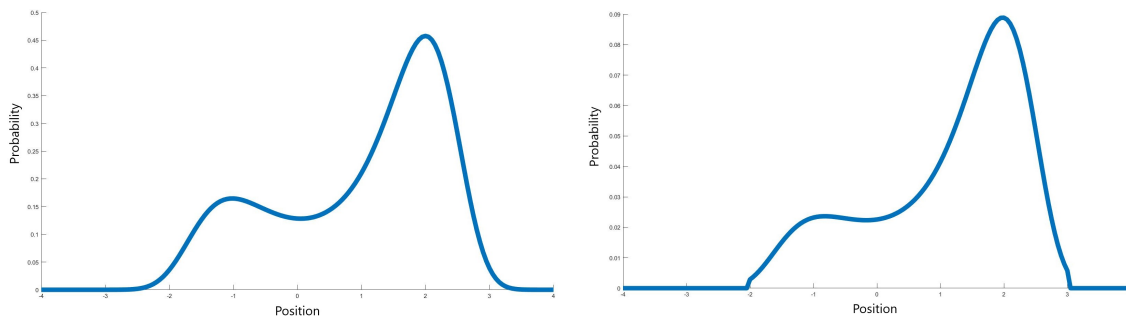
Figures 8.13a, 8.14b, 8.14a and 8.14b show the difference between the two systems,

one without hard boundaries, one with. Figures 8.13a and 8.14a show the normal probability density function, calculated until the probability is small enough to ignore, whilst figures 8.13b and 8.14b shows the probability density function calculated with hard boundaries. At the boundaries, the probability tends to a zero with a non-zero slope, as expected. The nature of the boundaries forces the probability to be 0 outside the limits, which is what we are after as we need $P' \neq 0$ at the boundaries to have a non-zero first passage time density. Note that the scales of the PDF are drastically different. This is because the introduction of hard boundaries means that some of the probability is “leaking” out of the system at the absorbing boundaries.



(a) With no hard boundary conditions, only when the probability is negligible (b) With hard boundary conditions at $x = -2$ and $x = 3$.

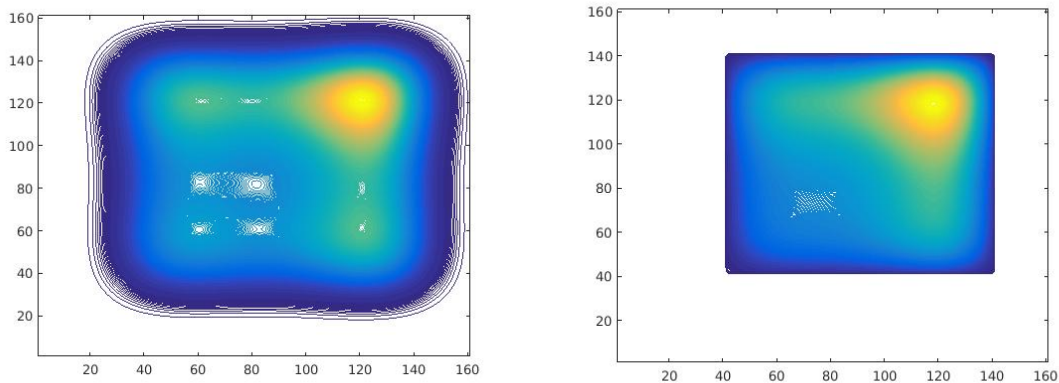
Figure 8.13: The probability density function for a tilted potential for $T = 2.5$, showing the probability being 0 outside the boundaries.



(a) With no hard boundary conditions, only when the probability is negligible (b) With hard boundary conditions at $x = -2$ and $x = 3$.

Figure 8.14: The probability density function for a tilted potential for $T = 10$, showing the probability being 0 outside the boundaries.

The visual difference can also be seen by graphing the stationary f_{ij} propagator matrix, which contains all of the system's evolution, for the tilted potential as a surface plot, shown in figures 8.15a and 8.15b. The surface plot in figure 8.15a shows the general f matrix with no boundary conditions. It shows how the matrix used in calculating the probability density function decays towards zero as the probability of staying up on the slopes, and not falling into one of the two potential wells becomes increasingly small the further away from the bottom of the wells. Figure 8.15b shows that when hard boundaries are introduced, the probability of travelling outside the defined region is instantly zero, as the matrix is not defined outside the boundaries. This means that, as shown in figure 8.14b, the probability is zero, and there is a sharp drop-off from just inside the boundaries to just outside them.



(a) With no hard boundary conditions, only when the probability is negligible. (b) With hard boundary conditions at $i = 41$, $i = 141$, $j = 41$ and $j = 141$.

Figure 8.15: A surface plot of the f_{ij} matrix for a tilted potential for $T = 6$, showing the hard boundaries imposed cuts forces 0 outside the boundaries.

These visual representations show that the density matrix and probability density function are acting as expected, but we can also use the Matlab partial differential equation solver with narrower boundaries to check that the results are comparable. This is much like we did to check the initial results in chapter 3. Figure 8.16 shows the probability density function at three different times against the partial differential equation solver at the same time intervals, showing good agreement between the two representations.

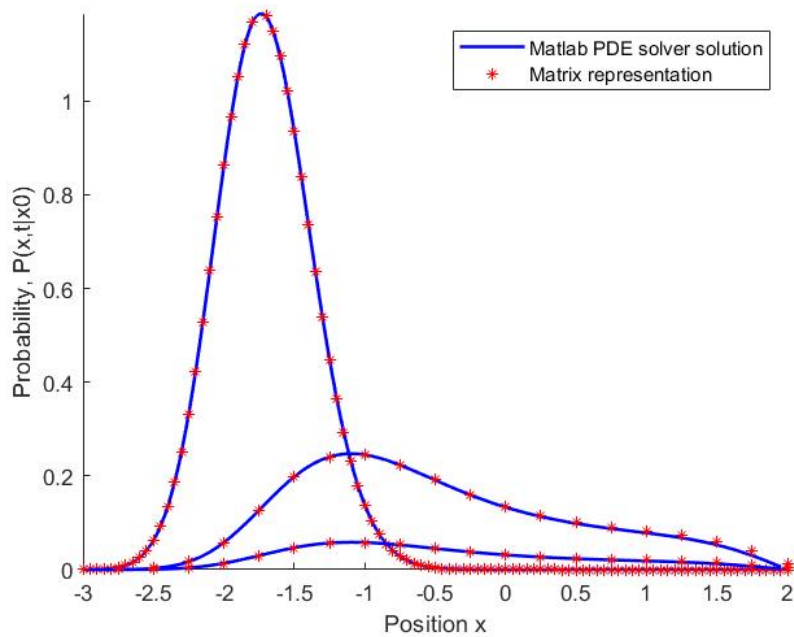


Figure 8.16: Matlab partial differential equation solver vs the numerical path integral with hard boundary conditions, showing the comparable nature of the numerical path integral technique.

Now that we know that our representation of the probability is accurate with hard boundary conditions, we can use it to calculate the first passage time for a particle in a system between two absorbing boundaries.

8.5.2 Calculation of the flux at the boundaries

The calculation of the first passage time comes from calculating the flux at the boundaries. The flux $j(x)$ over a boundary is defined with the relationship to the probability as [104]

$$\frac{\partial P(x, t)}{\partial t} + \frac{\partial j(x, t)}{\partial x} = 0. \quad (8.9)$$

(8.9) is also used in quantum mechanics, as a conservation equation, and can be used for the definition of the conservation of energy, among other things. In our case, it will be able to give the distribution of the probability flux over time, and we will be able to extract the mean first passage time. We can rearrange equation

(8.9) to give an integral form for the flux,

$$j(x, t) = - \int_a^b \frac{\partial P(x, t)}{\partial t} dx,$$

where we can use the Smoluchowski equation to substitute in for $\frac{\partial P}{\partial t}$ (3.1) and identify a and b as our two boundaries we have confined the particle to. So the flux becomes

$$j(x, t) = - \int_a^b \frac{\partial}{\partial x} \left[V'(x)P(x, t) + D \frac{\partial P(x, t)}{\partial x} \right] dx$$

$$j(x, t) = - \left[V'(x)P(x, t) + D \frac{\partial P(x, t)}{\partial x} \right]_a^b$$

$$j(x, t) = -V'(b)P(b, t) - D \frac{\partial P(b, t)}{\partial x} + V'(a)P(a, t) + D \frac{\partial P(a, t)}{\partial x}.$$

Due to the definition of the boundary conditions, the probability at a and b is zero leaving us with the calculation of the flux,

$$j(x, t) = -D \left[\frac{\partial P(x, t)}{\partial x} \Big|_{x=b} - \frac{\partial P(x, t)}{\partial x} \Big|_{x=a} \right]. \quad (8.10)$$

Note: $j(x, t) = f(t)$ the inverse Laplace transformed $\bar{f}(H)$.

(8.10) shows that the flux can be calculated from the gradient of the probability density function at the boundaries. As it is a measure of how much probability is escaping from the area in question it has to be a positive value, as nothing is being put into the system. Looking at figure 8.14b, the gradient at the upper boundary, b , is clearly negative, while at the lower boundary, a , it is positive, meaning from (8.10) the value of $j(x, t)$ will always be positive, which is what is required for this relationship to be true.

There is a second way to calculate the flux at the boundaries without using the gradient at the boundaries. That is to use the cumulative density function, CDF [105], a measure of how much probability is left in the region, and see how that

changes over time, also known as the survival probability, i.e. the probability that a particle survives to a certain time t in the bounded region. The CDF is defined as one minus the area under the probability density function and can be shown to give the same result as the gradient of the probability at the boundaries.

$$\text{CDF}(t) = 1 - \text{Area} = 1 - \int_a^b P(x, t) dx$$

Note that $\int_a^b P(x, t) dx \neq 1$, as the “particles” are being removed from the system at the boundaries.

Taking the derivative of the CDF with respect to time will give a measure of how it changes as the system evolves, and reveals the link to the flux and the first passage time density:

$$\begin{aligned} \frac{\partial \text{CDF}(t)}{\partial t} &= - \int_a^b \frac{\partial P(x, t)}{\partial t} dx \\ \text{Using (8.9)} \quad \frac{\partial \text{CDF}}{\partial t} &= - \int_a^b \left[- \frac{\partial j(x, t)}{\partial x} \right] dx \\ \frac{\partial \text{CDF}}{\partial t} &= j(x, t) = f(t). \end{aligned}$$

This derivation shows that we have two ways of calculating the first passage time of a particle in the system by two completely separate techniques. The results from these two representations are shown in 8.17, and show the similarity between the two methods. Both methods peak at the same time value, meaning they will have the same mean first passage time; the only discrepancy is in the height, which is negligible. It shows how the numerical path integral technique can calculate the full FPT density.

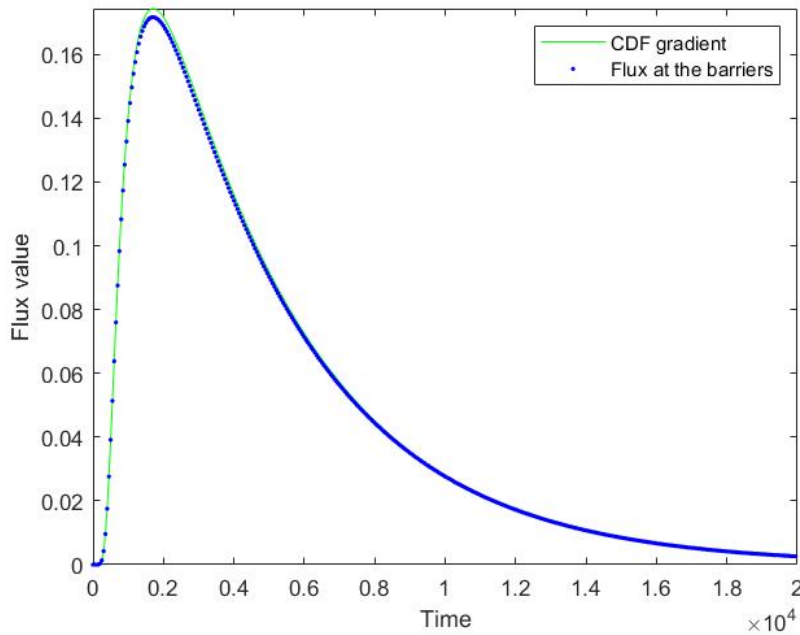


Figure 8.17: The flux over time, calculated using the gradient of the probabilities and the change in the cumulative density function over time.

8.6 Moments of the FPT density

We have looked at the first passage time density and the first moment, the mean first passage time, but we can go further to find *higher moments*. The first moment is the mean or expected value; the second is the variance, a measure of the spread of the probability density function; and the third is the skewness, a measure of the asymmetry of the function. There are higher moments, but these three are the most commonly used, and the ones that we will look at.

The comparison we will be looking at is between the path integral technique and the exponential distribution, which we looked at briefly back in chapter 1 and section 8.4. We mentioned that the exponential and FPT density will disagree under certain circumstances, and we can see here that they disagree further when looking at the higher moments, and not just the full FPT density. To begin, we define the exponential distribution,

$$f(t) = \lambda e^{-\lambda t},$$

where λ is the rate parameter and is defined as $E[t] = \tau = \frac{1}{\lambda}$, so it is one over the mean value of the probability density function. Typically, the mean FPT value of a system is known, e.g. Kramers' rate, and used to construct an exponential distribution approximation for the full FPT density, for an equilibrated system.

We show that, although this approximation can be valid for long times, an issue occurs at short times. Suppose we calculate an FPT density for a linear potential with a mixture of boundary conditions. In that case, we can use the path integral technique to find both the full FPT density (8.7) and the subsequent mean FPT value (8.8). Using this known mean FPT value, we can construct the exponential distribution. Figure 8.18 shows the comparison between the two. As can be seen, the long time limits of the functions are converging on the same value of 0, meaning the exponential distribution is a good approximation to the full FPT density; however, the small time values diverge dramatically, and a lot of information is subsequently lost by using the exponential distribution.

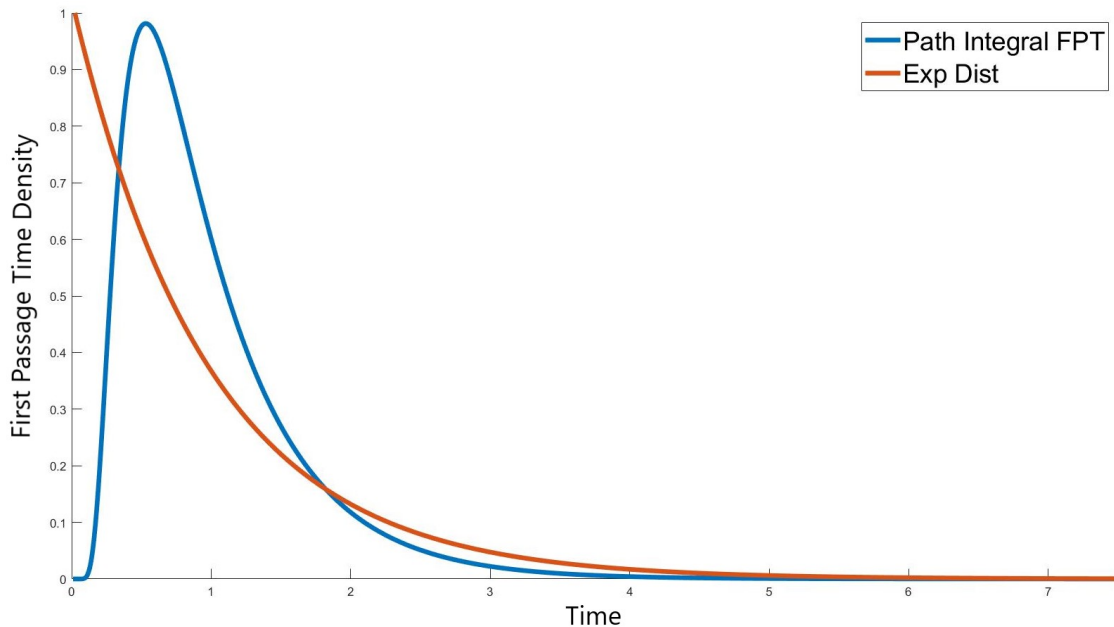


Figure 8.18: FPT density comparison between the exponential distribution and the full FPT solution for a sloped potential with a mixture of boundaries. Showing the discrepancy at short time, with the path integral technique providing a fuller solution.

We can look at this comparison further by looking at the higher moments of the system. To do this, we first look at how the moments are constructed for the exponential distribution, which is known as, for $n \in \mathbb{N}$,

$$E[t^n] = \frac{n!}{\lambda^n} = \tau^n n!.$$

We can also calculate the further moments using the path integral technique by again appealing to Laplace inversion facts as we did for the mean FPT earlier. The moments are defined using an integral form,

$$E[t^n] = \lim_{t \rightarrow \infty} \int_0^t \tau^n f(\tau) d\tau.$$

Using a similar technique to find the mean FPT value, we can Laplace transform this to find the related expression in the Laplace domain,

$$E[t^n] = \lim_{t \rightarrow \infty} \int_0^t \tau^n f(\tau) d\tau,$$

$$\text{Using final value theorem} \quad = \lim_{s \rightarrow 0} s \mathcal{L} \left[\int_0^t \tau^n f(\tau) d\tau \right],$$

$$\text{Using Laplace transform identities} \quad = \lim_{s \rightarrow 0} s \left[(-1)^n \frac{1}{s} \frac{d^n \bar{f}(s)}{ds^n} \right],$$

$$\bar{\tau} = (-1)^n \lim_{s \rightarrow 0} \frac{d^n \bar{f}(s)}{ds^n}.$$

This means that we have expressions for all the moments of the first passage time density,

$$E[t^2] = \text{Var}(t) = \lim_{s \rightarrow 0} \frac{d^2 \bar{f}}{ds^2}; \quad E[t^3] = - \lim_{s \rightarrow 0} \frac{d^3 \bar{f}}{ds^3}.$$

We can compare these values with the exponential distribution by calculating the mean FPT using the known solution, and using that value for the exponential distribution. This means that the mean FPT will be the same, but how do the second and third moments compare? The derivatives for the full FPT solution can be cal-

culated, and to compare fully we can calculate the second and third moments for a range of diffusion values. This enables a good comparison between the two techniques for different values of D . Figure 8.19 this comparison, and we see that, as the diffusion value becomes smaller and smaller, the divergence between the two techniques becomes larger. This is because as D gets smaller the FPT density becomes a better representation than the exponential distribution.

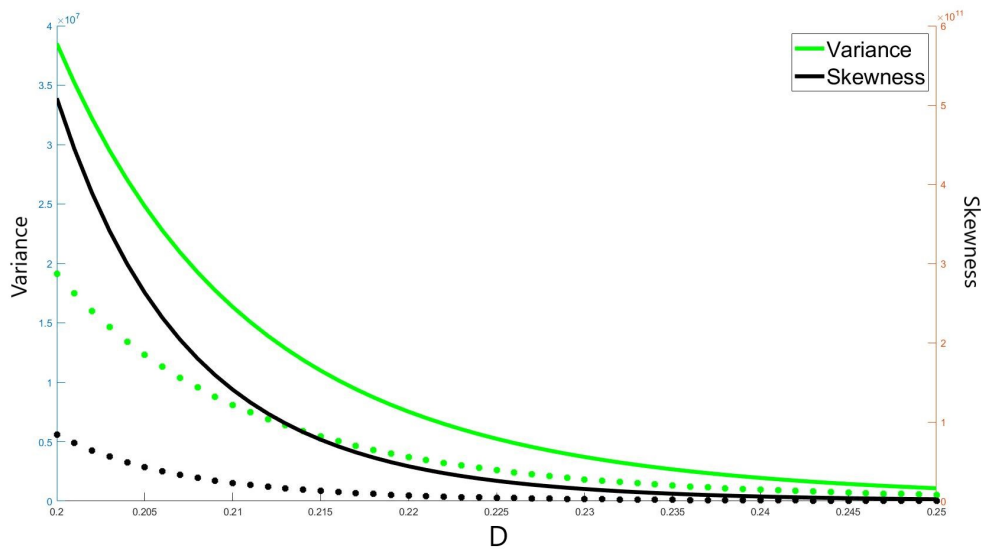


Figure 8.19: Comparison between second and third moments for the exponential distribution (*) and the full FPT solution (—)

As previously, the exponential distribution is an excellent comparison to the full FPT density in many situations, but not with all, and the accuracy can begin to break down for short times and small diffusion values. This is an advantage of the path integral representation, as it provides the full expression meaning the full expression for the moments of the first passage time density.

In this chapter, we have seen the calculation of both FPT densities and mean FPT values for the flat and linear potential with a variety of boundaries, showing that they agree with known solutions that are analytically calculable. What the path integral technique allows is the next step, calculating a full FPT density in the Laplace domain for a general potential $V(x)$, allowing just a simple numerical inversion to

find the full density in the T -domain. This allows more information about a given system to be kept and is more accurate than the exponential approximation currently used. The use of the path integral formalism also allows a greater understanding of the dynamics of the system and the dominant paths that the particles may take. We then investigated this comparison between the full FPT density and the exponential approximation through further moments and found that they agree at long times when a system may be at equilibrium, but disagree at short times. This is the main advantage of the path integral technique: providing accurate short-time, non-equilibrated solutions.

Chapter 9

Multi Dimensional Path Integrals

We have found the probability density function and first passage time densities in one dimension, but how will this translate to higher dimensions? This chapter will examine how all the functions translate into a general-dimension form, specifically the Jacobian and prefactor terms. We will finally look at the formation of the full probability density function and the first passage time density for the free diffusion case, and the probability density function for the symmetric harmonic oscillator. This is a far more complicated problem than what has been seen in the rest of this work, and here we sketch out a possible route for the beginning of further studies.

In order to find the multi-dimensional form of the probability density function, we need to investigate each element of the formulation: the action, the Jacobian and the prefactor, and how they change when more dimensions are introduced. The system that we are now solving has the Langevin equation,

$$dx_i = -\nabla V_i(x)dt + d\xi_i, \quad (9.1)$$

The action term is the easiest of the three to change to the multi-dimensional case, as it is just a change from a one-dimensional gradient to the general version,

$$\begin{aligned} S[x] &= 2V(x) - 2V(x_0) - 2HT + 2 \int_{\gamma} \sqrt{H + V'(y)^2} dy, \\ \Rightarrow S[\underline{x}] &= 2V(\underline{x}) - 2V(\underline{x}_0) - 2HT + 2 \int_{\gamma} \sqrt{H + (\nabla|V(\underline{y})|)^2} dy. \end{aligned}$$

This is because the potential gradient when squared, becomes the dot product of two unit vectors, with the scalar factor being the derivative vector of each element of the potential. The interesting thing is that the integral in the action is still a one-dimensional integral along the length of the path that the particle takes through a multi-dimensional space.

The Jacobian term can be calculated in the same way as we did in chapter 4, by discretising the Langevin equation and finding the determinant of the relevant matrix. Discretising (9.1) over N time steps of length Δt , and note that,

$$\mathcal{J} = \left| \frac{\delta \xi}{\delta x} \right| = \lim_{N \rightarrow \infty} \det \frac{d\xi_i}{dx_j}.$$

Equation (9.1) becomes (adding spatial indices α and time step indices i),

$$x_i^\alpha - x_{i-1}^\alpha = -(\lambda \partial^\alpha V(\mathbf{x}_i) + (1 - \lambda) \partial^\alpha V(\mathbf{x}_{i-1})) \Delta t + \xi_i^\alpha - \xi_{i-1}^\alpha.$$

The parameter λ again controls the discretisation protocol like in one dimension; $\lambda = 0$ corresponds to Ito calculus, and $\lambda = 1/2$ Stratonovich. Let's take $\lambda = 0$. It is

clear that $d\xi_i/dx_j = \delta_{ij}$ and $\mathcal{J} = 1$, but the time integrals in the action would need to be interpreted in the Ito sense, gaining the extra factor using the Ito integral, again like in the one-dimensional case gaining the same term as below from the Stratonovich prescription. Setting $\lambda = 1/2$, we can use the Stratonovich calculus with the usual interpretation of the integrals at the cost of introducing a non-unit Jacobian:

$$\frac{d\xi_i}{dx_j} = 1 \cdot \delta_{ij}^{\alpha\beta} + (\lambda \partial^\alpha \partial^\beta V(\mathbf{x}_i) + (1 - \lambda) \partial^\alpha \partial^\beta V(\mathbf{x}_{i-1})) \Delta t$$

$$\frac{d\xi_i}{dx_j} = \begin{cases} \delta^{\alpha\beta} + \frac{\Delta t}{2} \partial^\alpha \partial^\beta V(\mathbf{x}_i), & j = i \\ -\delta^{\alpha\beta} + \frac{\Delta t}{2} \partial^\alpha \partial^\beta V(\mathbf{x}_{i-1}), & j = i - 1 \\ 0 & \text{otherwise.} \end{cases}$$

This is an upper-triangular block matrix and has the following form similar to the one-dimensional case,

$$\frac{d\xi_i}{dx_j} = \begin{pmatrix} \delta^{\alpha\beta} + \frac{\Delta t}{2} \partial^\alpha \partial^\beta V(\mathbf{x}_i) & -\delta^{\alpha\beta} + \frac{\Delta t}{2} \partial^\alpha \partial^\beta V(\mathbf{x}_{i-1}) & 0 & \dots \\ 0 & \delta^{\alpha\beta} + \frac{\Delta t}{2} \partial^\alpha \partial^\beta V(\mathbf{x}_i) & -\delta^{\alpha\beta} + \frac{\Delta t}{2} \partial^\alpha \partial^\beta V(\mathbf{x}_{i-1}) & \dots \\ 0 & 0 & \delta^{\alpha\beta} + \frac{\Delta t}{2} \partial^\alpha \partial^\beta V(\mathbf{x}_i) & \dots \\ \vdots & \vdots & \vdots & \dots \end{pmatrix}.$$

To calculate this determinant, we use the fact that for a triangular matrix, the determinant is just the product of the determinants of the diagonal entries,

$$\left| \frac{\delta\xi}{\delta x} \right| = \prod_n \det \left(\delta^{\alpha\beta} + \frac{\Delta t}{2} \partial^\alpha \partial^\beta V(\mathbf{x}_i) \right).$$

To find the determinants, we can use the fact that,

$$\det(\mathbf{I} + \epsilon \mathbf{M}) = 1 + \epsilon \operatorname{tr} \mathbf{M} + \mathcal{O}(\epsilon^2),$$

to expand the brackets and use the fact that for second derivatives, the trace of the

resultant matrix of second derivatives is just the Laplace operator. This results in the product:

$$\begin{aligned} \left| \frac{d\xi_i}{dx_j} \right| &= \left(1 + \frac{\Delta t}{2} \nabla^2 V(\mathbf{x}_0) \right) \left(1 + \frac{\Delta t}{2} \nabla^2 V(\mathbf{x}_1) \right) \dots \left(1 + \frac{\Delta t}{2} \nabla^2 V(\mathbf{x}_N) \right) + \mathcal{O}(\Delta t^2) \\ &\rightarrow \exp \sum_i \frac{\Delta t}{2} \nabla^2 V(\mathbf{x}_i) \text{ as } \Delta t \rightarrow 0, \end{aligned}$$

and $\mathcal{J} = \exp \left(\frac{1}{2} \int_0^T \nabla^2 V(\mathbf{x}(t)) dt \right)$.

So, we have found the Jacobian for general dimensions; now, the final piece of the puzzle is to find out how the prefactor behaves in higher dimensions. To achieve this, we will use the van Vleck determinant form of the prefactor from the quantum mechanics' analogy, which will have a multi-dimensional form [2],

$$A = [4\pi D]^{-\frac{n}{2}} \left[\left| \frac{\partial x_f^i}{\partial x_0^j} \right| \right]^{-\frac{1}{2}},$$

where the only difference is the addition of indices to the derivative. See chapter 2 for a fuller discussion of this expression. This will need to be calculated for the specific system, but the technique will remain the same, so we can first see how it works for the simplest of systems, the free diffusion case, specifically in three dimensions.

9.1 Three-dimensional free diffusion

We begin by calculating the probability density function before calculating the first passage time density for the system. We have a free diffusion system, in a region B , which has a barrier at R that the particle travels to in time T . We begin by looking at the equation of motion for this system, which as $V = 0$, is $\ddot{r} = 0$. To solve this, we need to know some of the conditions the system must satisfy to find $r(t)$. For a

free diffusion system where there is a barrier at $r = R$ and begins at $r = 0$, we have,

$$r(0) = 0; \quad r(T) = R,$$

$$\ddot{r} = 0 \Rightarrow r(t) = \frac{Rt}{T}.$$

We can relate this to the initial position and velocity vectors of the system with a unit directional vector;

$$x_i(t) = r(t)\hat{n}_i = \frac{Rt}{T}\hat{n}_i,$$

$$v_j^0(t) = \dot{r}(t)\hat{n}_j = \frac{R}{T}\hat{n}_j,$$

$$\rightarrow x_i(t) = v_i^0 t,$$

where v_i^0 is the initial velocity in the \hat{n}_i direction. The expression for the position is equivalent to $speed = \frac{distance}{time}$. Now, to find the prefactor we can replace the numerator with the expression for the position vector,

$$\frac{\partial x^i}{\partial \dot{x}_0^j} = t \frac{\partial v_0^i}{\partial v_0^j} = t \delta_{ij},$$

$$\left| \frac{\partial x_f^i}{\partial \dot{x}_0^j} \right| = T^3,$$

$$A = (4\pi DT)^{-\frac{3}{2}}.$$

We now have the prefactor for the flat diffusion case in three dimensions, so let us see if the full probability returns the correct solution. In full, we have,

$$S = -HT + 2 \int_{x_i}^{x_f} \sqrt{H} dy,$$

$$\mathcal{J} = 1,$$

$$A = (4\pi DT)^{-\frac{3}{2}},$$

$$P = A\mathcal{J} \exp\left(-\frac{S}{4D}\right).$$

We can see that this is the correct form by the fact that it solves the three-dimensional free diffusion Smoluchowski equation,

$$\frac{\partial P}{\partial t} = D\nabla^2 P.$$

To find the full probability form, we first need to calculate the relationship between time and “energy” by using the relationship that we have in the free diffusion case, $V(r) = 0$,

$$\begin{aligned} T &= \int_0^r \frac{d\mathcal{R}}{\sqrt{H}}, \\ &= \frac{r}{\sqrt{H}}, \end{aligned}$$

inserting this into the action equation,

$$\begin{aligned} S &= -HT + 2\sqrt{H} \int_0^r d\mathcal{R}, \\ &= -HT + 2\sqrt{H}r, \\ &= \frac{r^2}{T}, \\ &= \frac{x^2 + y^2 + z^2}{T}. \end{aligned}$$

This gives a full probability density function for the free diffusion,

$$P(x, y, z, T) = \frac{1}{(4\pi DT)^{\frac{3}{2}}} \exp\left(-\frac{x^2 + y^2 + z^2}{4DT}\right).$$

So, does this solve the Smoluchowski equation? For the free diffusion case, this is the three-dimensional heat equation;

$$\frac{\partial P}{\partial t} = \nabla^2 P(x, y, z, t)$$

To find this, we need the time derivative and the second derivative with respect to the spatial coordinates.

$$\frac{\partial P}{\partial T} = D \left(\frac{\partial^2 P}{\partial x^2} + \frac{\partial^2 P}{\partial y^2} + \frac{\partial^2 P}{\partial z^2} \right),$$

$$\frac{\partial P}{\partial T} = -\frac{3}{2T}P + \frac{x^2 + y^2 + z^2}{4DT^2}P,$$

$$\frac{\partial P}{\partial x} = -\frac{x}{2DT}P,$$

$$\frac{\partial^2 P}{\partial x^2} = \left(\frac{x^2}{4D^2T^2} - \frac{1}{2DT} \right) P.$$

Inputting this all into the Smoluchowski equation, the spatial derivatives are the same with interchanges of x , y and z . This gives,

$$\begin{aligned} -\frac{3}{2T}P + \frac{x^2 + y^2 + z^2}{4DT^2}P &= D \left(\frac{x^2}{4D^2T^2} - \frac{1}{2DT} \right) P + D \left(\frac{y^2}{4D^2T^2} - \frac{1}{2DT} \right) P \\ &\quad + D \left(\frac{z^2}{4D^2T^2} - \frac{1}{2DT} \right) P \end{aligned}$$

$$-\frac{3}{2T}P + \frac{x^2 + y^2 + z^2}{4DT^2}P = -\frac{3}{2T}P + \frac{x^2 + y^2 + z^2}{4DT^2}P.$$

This shows that it solves the Smoluchowski equation, meaning that our representation for the free diffusion case is correct. Next, we can use our definition of the first passage time density to calculate the value for the three-dimensional free diffusion case. First, we construct the probability density function which includes the terms required to satisfy the boundary condition at $r = R$, $P(R) = 0$, by appealing to the method of images techniques,

$$P(r; T) = \frac{1}{(4\pi DT)^{\frac{3}{2}}} \exp\left(-\frac{r^2}{4DT}\right) - \frac{1}{(4\pi DT)^{\frac{3}{2}}} \exp\left(-\frac{(r - 2R)^2}{4DT}\right).$$

This construction is similar in technique to the adding of paths that we constructed for the one-dimensional case, with a turning path that turns around at the barrier. In the method of images terminology, this is like having an imaginary path that arrives from the other side of the barrier. Figure 9.1 shows the two paths we have used to construct, with the imaginary path coming from a region R' , which translates to the path that bounces off of the barrier.

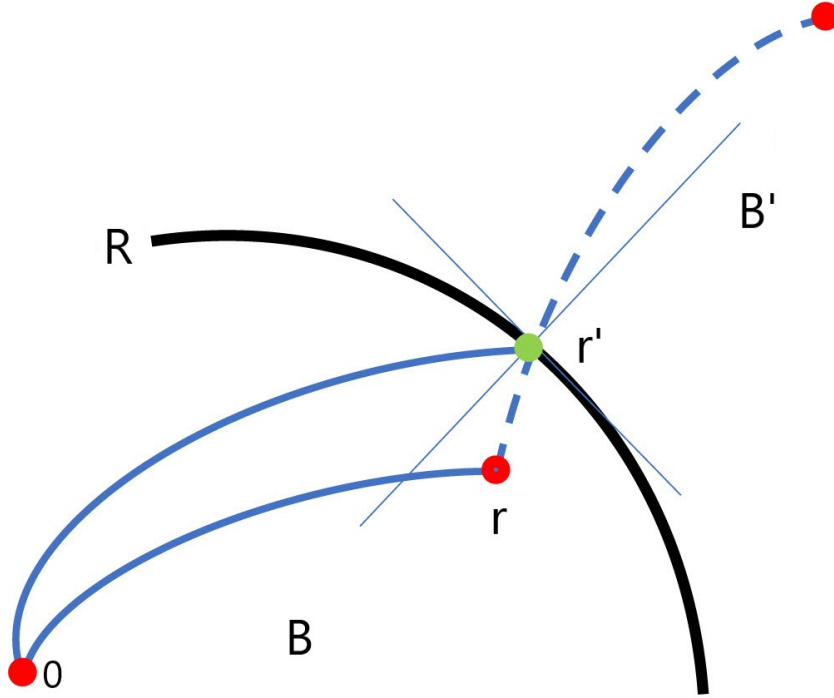


Figure 9.1: Two paths from 0 to $r \in B$: one direct and the other bouncing off R at r' , with a mirror direct path from B' .

Calculating the first passage time density is similar to the one-dimensional, one-boundary case where we evaluate the derivative of the probability on the boundary;

$$\begin{aligned}
 f(T) &= -D \left. \frac{\partial P}{\partial r} \right|_R, \\
 &= -\frac{D}{(4\pi DT)^{\frac{3}{2}}} \left[-\frac{2r}{4DT} \exp\left(-\frac{r^2}{4DT}\right) + \frac{2(r-2R)}{4DT} \exp\left(-\frac{(r-2R)^2}{4DT}\right) \right] \Big|_R, \\
 &= \frac{R \exp\left(-\frac{R^2}{4DT}\right)}{(4\pi D)^{\frac{3}{2}} T^{\frac{5}{2}}}.
 \end{aligned}$$

This is very similar to the one-dimensional Brownian motion FPT density [106], just with an extra factor of $\frac{1}{T}$, which is apparent as there is the same extra factor in the representation of P . We can also show that this free diffusion FPT density satisfies the correct short and long-time limits, as the FPT density curve should tend to 0 for both $T \rightarrow 0$ and $T \rightarrow \infty$. For the $T \rightarrow 0$ limit, the exponential tends to 0, as does the denominator, but by using L'Hopital's rule multiple times, the T on the denominator is differentiated enough times to move to the numerator, and the limit is satisfied. The $T \rightarrow \infty$ limit is easier as the exponential tends to 1 because the exponent tends to 0, meaning the denominator dominates, sending the function to 0.

9.2 Three-dimensional Harmonic oscillator

We have seen that the path integral formulation works for the free diffusion case in three dimensions, but does it work for the harmonic oscillator case? For this system, we have a similar set-up, with an initial position at the origin with an absolute boundary at $r = R$, and the particle reaches the boundary at time T , $r(0) = 0$, $r(T) = R$. For this system, we deal with a symmetric potential, $V(r) = \frac{1}{2}\alpha r^2$, in spherical coordinates. First, we can calculate the Jacobian term,

$$\begin{aligned} \mathcal{J} &= \exp\left(\frac{1}{2}\int_0^T \nabla^2 V(x(t))dt\right) \\ \nabla^2 V &= \frac{1}{r^2} \frac{\partial}{\partial r} \left(r^2 \frac{\partial V}{\partial r} \right) \\ &= \frac{2}{r} \frac{\partial V}{\partial r} + \frac{\partial^2 V}{\partial r^2} \\ &= 3\alpha \end{aligned}$$

$$\mathcal{J} = \exp\left(\frac{3}{2}\alpha T\right).$$

This is actually just the one-dimensional Harmonic oscillator Jacobian term cubed, which makes sense for a jump from 1-D to 3-D. Now to calculate the prefactor, using the same method as the free diffusion case, beginning at the equation of motion.

$$\begin{aligned}\ddot{\underline{r}} &= \nabla (|\nabla V|^2) \\ &= \nabla (\alpha^2 r^2) \\ &= 2\alpha^2 r \hat{\underline{r}} \\ \ddot{r} &= 2\alpha^2 r\end{aligned}$$

Solving this with the initial conditions, $r(0) = 0$ and $r(T) = R$,

$$\begin{aligned}r(t) &= A \cosh \sqrt{2}\alpha t + B \sinh \sqrt{2}\alpha t \\ &= \frac{R \sinh \sqrt{2}\alpha t}{\sinh \sqrt{2}\alpha T}\end{aligned}$$

As in the free diffusion case, we now want to find the initial velocity, to be able to calculate the van Vleck determinant,

$$\begin{aligned}\dot{r}(t) &= \frac{\sqrt{2}\alpha R \cosh \sqrt{2}\alpha t}{\sinh \sqrt{2}\alpha T} \\ v^0 &= \frac{\sqrt{2}\alpha R}{\sinh \sqrt{2}\alpha T} \\ r(t) &= \frac{v^0 \sinh \sqrt{2}\alpha t}{\sqrt{2}\alpha}.\end{aligned}$$

Inserting this into the van Vleck determinant,

$$\begin{aligned}x_i(t) &= \frac{v_i^0 \sinh \sqrt{2}\alpha t}{\sqrt{2}\alpha} \\ \frac{\partial x^i}{\partial \dot{x}_0^j} &= \frac{\delta_{ij} \sinh \sqrt{2}\alpha t}{\sqrt{2}\alpha} \\ \left| \frac{\partial x_f^i}{\partial \dot{x}_0^j} \right| &= \left(\frac{\sinh \sqrt{2}\alpha t}{\sqrt{2}\alpha} \right)^3.\end{aligned}$$

This gives a full probability for the 3-D harmonic oscillator with $|\nabla V|^2 = \nabla V \cdot \nabla V = \alpha^2 r^2$,

$$S = \alpha r^2 - HT + 2 \int_0^r \sqrt{H + \alpha^2 y^2} dy$$

$$P = \left[\frac{\sqrt{2}\alpha e^{\alpha T}}{4\pi D \sinh \sqrt{2}\alpha T} \right] \exp \left(-\frac{\alpha r^2 - HT + 2 \int_0^r \sqrt{H + \alpha^2 y^2} dy}{4D} \right)$$

This shows a use of the path integral formalism in solving for probability density functions and first passage time densities in three dimensions, and begins the steps towards using the path integral in solving for higher dimensional systems. The ability to solve for the PDF and FPT density in these higher dimensions might allow the possibility of the advancement of techniques such as FPT kinetic Monte Carlo that we have discussed previously, which is only valid for free diffusion cases because a full FPT density curve is not available for more than a zero-potential. This is where this technique shown through this work could become applicable.

Conclusion

Stochastic processes appear throughout science, and the importance of both fundamental understanding, and practical numerical implementations, can hardly be overstated. We hope the path integral techniques studied in this work contribute to both. While current techniques focus on long-time average approximations for barrier-crossing rates [50], and first passage time densities at near-equilibrium, we have attempted to build a semi-closed form for all timeframes and general potentials in one dimension. The long-time, near-equilibrium assumption discards some potentially crucial information which our approach retains.

Previous investigations using stochastic path integrals [28] [29] were also confined to the investigation of mean rates (albeit with more complicated, correlated noise). This work has gone beyond that previous work by demonstrating the ability of the path integral formalism to construct a full probability density function, subsequent first passage time densities, and mean first passage times for a general potential in one dimension with only a weak noise assumption.

The remarkable correspondence between the most probable stochastic trajectories through a potential V , and the conservative, Hamiltonian dynamics in an effective potential $-|\nabla V|^2$ has shed more light on overdamped stochastic processes in general. First noticed in [19], our work significantly extends those observations. In particular, the necessity of turning paths to recover the correct long-time limit, even in the

simplest case of the harmonic oscillator, exposes the limitations of previous work, and reveals how to generalize to more complicated systems.

This work reviews how the path integral can be built from standard stochastic differential equations, culminating in an expression that solves the Smoluchowski equation for particles diffusing in a potential. Whilst formally correct, the integral cannot be exactly evaluated for all but the simplest potentials (up to quadratic). This is consistent with the fact that no analytical solution for the Smoluchowski equation exists for potentials other than these.

In the weak noise limit, however, analytic progress can be made by concentrating on the paths that dominate the integral. The actions of these extremal paths, together with small fluctuations around them, and the functional Jacobian arising from the change of variables from noise to coordinate, were used to construct an approximate solution. We also compared our solution with a formal WKB expansion, and identified the action and pre-exponential factor emerging order-by-order. This solution was shown to be exact for the explicitly-soluble case of the harmonic oscillator, but only when the subtleties of the turning path were included. Previous work [1] did not consider these, and arrived at the correct Ornstein-Uhlenbeck form by a fortunate cancellation.

The move to the Laplace domain then allowed the construction of the first passage time density, and its moments, by introducing absorbing and reflecting boundaries. These boundary conditions increase the scope of potential applications, since many physical, chemical, and biological systems can be modelled by a first passage process. The boundary conditions were enforced by considering another form of turning path, one with a “hard bounce” off the absorbing boundary. Multiple paths can be easily summed over in the Laplace domain, allowing the correct long-time limit to be recovered with short- and intermediate-time densities being recoverable by a simple (one-dimensional) numerical inversion of the transform. A truncated WKB expan-

sion does not achieve the correct long-time limit. The fact that infinite sums over turning paths are required reflects the tension between the weak noise and long-time limits. These do not commute, as was noticed in [107], and the path integral approach provides the insight needed to deal with this.

The FPT and mean FPT solutions gained from path integrals agree with first principles derivations for the simplest systems, which can also be solved by elementary means. As far as we are aware, none of these solutions appear in the literature. Indeed, the first passage literature, e.g. [39], focuses on free diffusion in a variety of complicated domains. Very little work previously existed on first passage densities in nonzero potentials.

We have also revisited the ubiquitous Kramers problem of particle escape over a potential barrier, recovering the standard rate. Moreover, our approach delivered the full first passage density, rather than simply the mean, which was all that was available previously. The exponential escape time distribution, used by assumption in kinetic Monte Carlo simulations, was recovered at long times. Whilst an accurate representation of the tail of the density, the exponential distribution cannot be correct at short times, as it has mode zero. Our results are valid at all times.

Throughout this work, we also saw the ability of the path integral to be used numerically as well as analytically. We followed the methods of [71] and coded a Smoluchowski solver that outperformed the commercial implementation available in MATLAB. We also extended the methodology to determine first passage densities numerically. Whilst highly efficient in one dimension, the approach (like other numerical solutions of parabolic PDEs) quickly becomes computationally intractable in higher dimensions. The action integral for the dominant path, however, is always one-dimensional.

Finally, we began the exploration of applying the path integral to higher-dimensional systems. The correct results for the simplest systems were recovered, which suggests that this is a promising avenue for future research.

All this shows that the path integral formulation can offer valuable insights not available from standard techniques, which could potentially contribute to larger-scale stochastic simulation methods. There is also the capability for the path integral to be used for general non-equilibrated systems in more than one dimension, extending the possible insights available. The work should continue towards this goal by looking at higher-order WKB expansion terms to find terms such as Γ from chapter 8 “organically”, with the ultimate aim of constructing solutions in multiple dimensions for use in real-world modelling applications.

These real-world applications are a possible next step for this research into areas of science that we have discussed throughout this work. The logical next steps for this work would be to look at the extension of first passage kinetic Monte Carlo techniques, described by Ooppelstrup et. al. [48]. The path integral formulation derived in this work could allow this method to be extended to nontrivial potentials. This would represent a major generalisation of the technique, and greatly enhance its range of applicability.

There are many areas of science that could benefit from practical applications of this work. Examples include the diffusion of impurities through a crystal and analytical results for first passage problems for polymer chains. Concerning impurity diffusion, the path integral technique could allow a reduction in the computational power requirements required to fully understand the dynamics of how an impurity travels throughout the structure. Path integrals would allow the ability to encompass the entire potential landscape in the crystal, including other microstructures in the crystal, e.g. dislocations.

For polymer chains, the application of the first passage time density results in this work, namely in higher dimensions, could provide fuller solutions to densities than previously found [108] along with the possible application to accelerating Brownian dynamics simulations [109].

All these possible applications show the many directions this work could continue to pursue and the range of insights that the path integral technique could provide for those who wish to continue with this work.

Bibliography

- [1] Horacio Wio. *Path Integrals for stochastic processes: An introduction*. World Scientific Publishing Co. Pte. Ltd, 2013 (cit. on pp. vii, 4, 27, 28, 30, 44, 55, 206).
- [2] L. S. Schulman. *Techniques and Applications of Path Integration*. Dover Publications Inc, New York, 2005 (cit. on pp. vii, 29, 38, 40, 45, 197).
- [3] Emanuel Parzen. *Stochastic processes*. Holden-Day series in probability and statistics. San Francisco: Holden-Day, 1962 (cit. on p. 2).
- [4] Murray. Rosenblatt. New York: Springer-Verlag, 1974. ISBN: 0387900853 (cit. on p. 2).
- [5] P.C. Bressloff. *Stochastic Processes in Cell Biology*. Interdisciplinary Applied Mathematics. Springer International Publishing, 2014. ISBN: 9783319084886. URL: <https://books.google.co.uk/books?id=SwZYBAAAQBAJ> (cit. on p. 2).
- [6] Joseph L. Doob. *Stochastic processes*. eng. Wiley series in probability and mathematical statistics. New York: Wiley, 1953 (cit. on p. 2).
- [7] J.M. Steele. *Stochastic Calculus and Financial Applications*. Stochastic Modelling and Applied Probability. Springer New York, 2012. ISBN: 9781468493054. URL: <https://books.google.co.uk/books?id=fsgkBAAAQBAJ> (cit. on p. 2).
- [8] W. Paul and J. Baschnagel. *Stochastic Processes: From Physics to Finance*. Springer International Publishing, 2013. ISBN: 9783319003276. URL: <https://books.google.co.uk/books?id=0WANAAAAQBAJ> (cit. on p. 2).

- [9] R. Lande, S. Engen, and B.E. Sæther. *Stochastic Population Dynamics in Ecology and Conservation*. Oxford series in ecology and evolution. Oxford University Press, 2003. ISBN: 9780198525257. URL: <https://books.google.co.uk/books?id=6KClauq80ekC> (cit. on p. 2).
- [10] F. Baccelli and B. Błaszczyszyn. *Stochastic Geometry and Wireless Networks*. Foundations and trends in networking v. 1. Now Publishers, 2010. URL: <https://books.google.co.uk/books?id=H3ZkTN2pYS4C> (cit. on p. 2).
- [11] Oliver C. Ibe. *Chapter 12 - Special Random Processes*. Second Edition. Academic Press, 2014, pp. 369–425. ISBN: 978-0-12-800852-2 (cit. on p. 2).
- [12] Peter Morters. *Brownian motion*. Cambridge University Press, 2010 (cit. on p. 2).
- [13] J.F.C. Kingman. *Poisson Processes*. Oxford Studies in Probability. Clarendon Press, 1992. ISBN: 9780191591242. URL: <https://books.google.co.uk/books?id=VEiM-0twDHkC> (cit. on p. 2).
- [14] A.M.O. de Almeida. *Hamiltonian Systems: Chaos and Quantization*. Cambridge Monographs on Mathematical Physics. Cambridge University Press, 1990. ISBN: 9780521386708. URL: <https://books.google.co.uk/books?id=nNeNSEJUEHUC> (cit. on p. 2).
- [15] D. ter. Haar. *Elements of Hamiltonian mechanics*. eng. Second edition. International series of monographs in natural philosophy ; v. 34. Oxford: Pergamon, 1971. ISBN: 0080167268 (cit. on p. 2).
- [16] Hebert Goldstein. *Classical mechanics*. Addison-Wedley publishing company inc, 1980 (cit. on pp. 2, 44, 45).
- [17] Paul Adrien M Dirac. “The Lagrangian in quantum mechanics”. In: *Physikalische Zeitschrift der Sowjetunion* 3 (1933), pp. 312–320 (cit. on p. 2).
- [18] Richard P Feynman, Albert R Hibbs, and Daniel F Styer. *Quantum mechanics and path integrals*. Courier Corporation, 2010 (cit. on p. 2).

- [19] Hao Ge and Hong Qian. “Analytical mechanics in stochastic dynamics: most probable path, large-deviation rate function and Hamilton–Jacobi equation”. In: *International Journal of Modern Physics B* 26.24 (2012), p. 1230012. DOI: 10.1142/s0217979212300125. URL: <https://doi.org/10.1142%5C%2Fs0217979212300125> (cit. on pp. 2, 6, 205).
- [20] Rosalind J Allen, Chantal Valeriani, and Pieter Rein ten Wolde. “Forward flux sampling for rare event simulations”. In: *Journal of Physics: Condensed Matter* 21.46 (2009), p. 463102. DOI: 10.1088/0953-8984/21/46/463102. URL: <https://dx.doi.org/10.1088/0953-8984/21/46/463102> (cit. on pp. 3, 63).
- [21] Rosalind J. Allen, Daan Frenkel, and Pieter Rein ten Wolde. “Simulating rare events in equilibrium or nonequilibrium stochastic systems”. In: *The Journal of Chemical Physics* 124.2 (2006), p. 024102. DOI: 10.1063/1.2140273 (cit. on pp. 3, 63).
- [22] R. P. Feynman. “Space-Time Approach to Non-Relativistic Quantum Mechanics”. In: *Rev. Mod. Phys.* 20 (2 1948), pp. 367–387. DOI: 10.1103/RevModPhys.20.367. URL: <https://link.aps.org/doi/10.1103/RevModPhys.20.367> (cit. on p. 3).
- [23] Scott Ferson. “What Monte Carlo methods cannot do”. In: *Human and Ecological Risk Assessment: An International Journal* 2.4 (1996), pp. 990–1007. DOI: 10.1080/10807039609383659. eprint: <https://doi.org/10.1080/10807039609383659>. URL: <https://doi.org/10.1080/10807039609383659> (cit. on p. 3).
- [24] Dirk P. Kroese et al. “Why the Monte Carlo method is so important today”. In: *WIREs Computational Statistics* 6.6 (2014), pp. 386–392. DOI: <https://doi.org/10.1002/wics.1314> (cit. on p. 3).
- [25] Don S. Lemons and Anthony Gythiel. “Paul Langevin’s 1908 paper “On the Theory of Brownian Motion” [“Sur la théorie du mouvement brownien,” C. R. Acad. Sci. (Paris) 146, 530–533 (1908)]”. In: *American Journal of Physics*

- 65.11 (1997), pp. 1079–1081. DOI: 10.1119/1.18725. eprint: <https://doi.org/10.1119/1.18725>. URL: <https://doi.org/10.1119/1.18725> (cit. on pp. 3, 30).
- [26] L.P. Kadanoff. *Statistical Physics: Statics, Dynamics and Renormalization*. Statistical Physics: Statics, Dynamics and Renormalization. World Scientific, 2000. ISBN: 9789810237646. URL: <https://books.google.co.uk/books?id=22dadF5p6gYC> (cit. on p. 3).
- [27] Daniel W Stroock. *An introduction to Markov processes*. Vol. 230. Springer Science & Business Media, 2013 (cit. on p. 5).
- [28] A. J. McKane. “Noise-induced escape rate over a potential barrier: Results for general noise”. In: *Phys. Rev. A* 40 (7 1989), pp. 4050–4053. DOI: 10.1103/PhysRevA.40.4050. URL: <https://link.aps.org/doi/10.1103/PhysRevA.40.4050> (cit. on pp. 5, 205).
- [29] A. J. Bray, A. J. McKane, and T. J. Newman. “Path integrals and non-Markov processes. II. Escape rates and stationary distributions in the weak-noise limit”. In: *Phys. Rev. A* 41 (2 1990), pp. 657–667. DOI: 10.1103/PhysRevA.41.657. URL: <https://link.aps.org/doi/10.1103/PhysRevA.41.657> (cit. on pp. 5, 205).
- [30] T. C. Gard. *Introduction to stochastic differential equations*. eng. Monographs and textbooks in pure and applied mathematics ; 114. New York: M. Dekker, 1988. ISBN: 082477776X (cit. on p. 7).
- [31] *Ito’s lemma*. 2012. URL: <https://www.quantstart.com/articles/Ito-Lemma/> (cit. on pp. 7, 88).
- [32] Kyle Siegrist. *Probability, Mathematical Statistics, Stochastic Processes, chap: 4.9*. 2017 (cit. on p. 8).
- [33] Marian Smoluchowski. “Drei Vorträge über Diffusion, Brownsche Molekularbewegung und Koagulation von Kolloidteilchen”. ger. In: *Pisma Mariana Smoluchowskiego* 2.1 (1927), pp. 530–594. URL: <http://eudml.org/doc/215805> (cit. on pp. 9, 50).

- [34] K.A. Dill, S. Bromberg, and D. Stigter. *Molecular Driving Forces: Statistical Thermodynamics in Chemistry and Biology*. Garland Science, 2003. URL: <https://books.google.co.uk/books?id=hde0Dhjp1bUC> (cit. on pp. 9, 32).
- [35] Herbert B. Callen and Theodore A. Welton. “Irreversibility and Generalized Noise”. In: *Phys. Rev.* 83 (1 1951), pp. 34–40. DOI: 10.1103/PhysRev.83.34. URL: <https://link.aps.org/doi/10.1103/PhysRev.83.34> (cit. on p. 9).
- [36] J.R. Cannon and F.E. Browder. *The One-Dimensional Heat Equation*. Encyclopedia of Mathematics and its Applications. Cambridge University Press, 1984. ISBN: 9780521302432. URL: <https://books.google.co.uk/books?id=XWSnBZxbz2oC> (cit. on pp. 10, 151).
- [37] Drs S.P. Fitzgerald & R. M. L. Evans with thanks to Prof D.J. Read. *Advanced Entropy in the Physical World Lecture Notes, University of Leeds*. 2021 (cit. on pp. 10, 21, 153).
- [38] P. Atkins and J. de Paula. *Physical Chemistry for the Life Sciences*. OUP Oxford, 2011. ISBN: 9780199564286. URL: <https://books.google.co.uk/books?id=HX0cAQAQBAJ> (cit. on p. 11).
- [39] S. Redner. *A Guide to First-Passage Processes*. A Guide to First-passage Processes. Cambridge University Press, 2001. ISBN: 9780521652483. URL: <https://books.google.co.uk/books?id=xtsqMh3VC98C> (cit. on pp. 12, 207).
- [40] James L. Melsa. *An introduction to probability and stochastic processes*. eng. Prentice-Hall information and system sciences series. Englewood Cliffs ; Prentice-Hall, 1973. ISBN: 0130348503 (cit. on p. 15).
- [41] George. Arfken. *Mathematical methods for physicists*. eng. Sixth edition. Boston ; Elsevier, 2005 (cit. on p. 15).
- [42] Di Zhang and Roderick V. N. Melnik. “First passage time for multivariate jump-diffusion processes in finance and other areas of applications”. In: *Applied Stochastic Models in Business and Industry* 25.5 (2009), pp. 565–582. DOI: <https://doi.org/10.1002/asmb.745> (cit. on p. 16).

- [43] Tomasz R Bielecki and Marek Rutkowski. *Credit risk: modeling, valuation and hedging*. Springer Science & Business Media, 2004 (cit. on p. 16).
- [44] Abraham Nitzan. *Chemical dynamics in condensed phases : relaxation, transfer, and reactions in condensed molecular systems*. eng. Oxford ; Oxford University Press, 2006. ISBN: 0198529791 (cit. on p. 16).
- [45] Aleksandar Donev et al. “A First-Passage Kinetic Monte Carlo algorithm for complex diffusion–reaction systems”. In: *Journal of Computational Physics* 229.9 (2010), pp. 3214–3236. ISSN: 0021-9991. DOI: <https://doi.org/10.1016/j.jcp.2009.12.038> (cit. on p. 16).
- [46] Susanne Ditlevsen and Petr Lansky. “Estimation of the input parameters in the Ornstein-Uhlenbeck neuronal model”. In: *Physical review E* 71.1 (2005), p. 011907 (cit. on p. 16).
- [47] Attila Szabo, Klaus Schulten, and Zan Schulten. “First passage time approach to diffusion controlled reactions”. In: *The Journal of Chemical Physics* 72.8 (1980), pp. 4350–4357. DOI: 10.1063/1.439715 (cit. on p. 16).
- [48] Tomas Opplestrup et al. “First-Passage Monte Carlo Algorithm: Diffusion without All the Hops”. In: *Physical review letters* 97 (Jan. 2007), p. 230602. DOI: 10.1103/PhysRevLett.97.230602 (cit. on pp. 16, 18, 19, 150, 208).
- [49] H.A. Kramers. “Brownian motion in a field of force and the diffusion model of chemical reactions”. In: *Physica* 7.4 (1940), pp. 284–304. ISSN: 0031-8914. DOI: [https://doi.org/10.1016/S0031-8914\(40\)90098-2](https://doi.org/10.1016/S0031-8914(40)90098-2). URL: <https://www.sciencedirect.com/science/article/pii/S0031891440900982> (cit. on pp. 17, 176).
- [50] Peter Hänggi, Peter Talkner, and Michal Borkovec. “Reaction-rate theory: fifty years after Kramers”. In: *Reviews of modern physics* 62.2 (1990), p. 251 (cit. on pp. 17, 205).
- [51] Keith J. Laidler. “The development of the Arrhenius equation”. In: *Journal of Chemical Education* 61.6 (1984), p. 494. DOI: 10.1021/ed061p494. eprint:

- <https://doi.org/10.1021/ed061p494>. URL: <https://doi.org/10.1021/ed061p494> (cit. on pp. 17, 177).
- [52] S. P. Fitzgerald et al. “Stochastic transitions: Paths over higher energy barriers can dominate in the early stages”. In: *The Journal of Chemical Physics* 158.12 (2023), p. 124114. DOI: 10.1063/5.0135880. URL: <https://doi.org/10.1063/5.0135880> (cit. on p. 18).
- [53] Valerio Magnasco. “3 - The Particle in the Box”. In: *Elementary Methods of Molecular Quantum Mechanics*. Ed. by Valerio Magnasco. Amsterdam: Elsevier Science B.V., 2007, pp. 103–116 (cit. on p. 25).
- [54] C. W. Gardiner. *Handbook of Stochastic Methods: for Physics, Chemistry and the natural sciences. Third Edition*. Springer-Verlag, Berlin, 2004 (cit. on p. 28).
- [55] F. Langouche, D. Roekaerts, and E. Tirapegui. “Functional Integral Methods in Fokker-Planck Dynamics”. In: *Functional Integration and Semiclassical Expansions*. Dordrecht: Springer Netherlands, 1982, pp. 139–166. DOI: 10.1007/978-94-017-1634-5_7. URL: https://doi.org/10.1007/978-94-017-1634-5_7 (cit. on p. 29).
- [56] Lars Onsager and Stefan Machlup. “Fluctuations and irreversible processes”. In: *Physical Review* 91.6 (1953), p. 1505 (cit. on p. 31).
- [57] Gavin E Crooks. “Entropy production fluctuation theorem and the nonequilibrium work relation for free energy differences”. In: *Physical Review E* 60.3 (1999), p. 2721 (cit. on p. 32).
- [58] Christian P Robert, George Casella, and George Casella. *Monte Carlo statistical methods*. Vol. 2. Springer, 1999 (cit. on p. 32).
- [59] A. O’Hagan. *Kendall’s Advanced Theory of Statistic 2B*. Wiley, 2010. URL: <https://books.google.co.uk/books?id=ewyYAAAAQBAJ> (cit. on p. 32).
- [60] L.D. Landau and E.M. Lifshitz. *Statistical Physics: Volume 5*. v. 5. Elsevier Science, 2013. ISBN: 9780080570464. URL: <https://books.google.co.uk/books?id=VzgJN-XPTRsC> (cit. on pp. 32, 50).

- [61] Robert Graham. “Path integral formulation of general diffusion processes”. In: *Zeitschrift für Physik B Condensed Matter* 26.3 (1977), pp. 281–290 (cit. on p. 34).
- [62] *Hamiltonian mechanics*. July 20, 2022. URL: https://en.wikipedia.org/wiki/Hamiltonian_mechanics (visited on 07/20/2022) (cit. on p. 34).
- [63] Charles Fox. *An introduction to the calculus of variations*. eng. London: Oxford University Press, 1950 (cit. on p. 34).
- [64] Douglas Cline. *Variational principles in classical mechanics*. University of Rochester River Campus Librarie, 2017 (cit. on p. 36).
- [65] A. (Antonio) Fasano. *Analytical mechanics : an introduction*. eng. Oxford: Oxford University Press, 2006. ISBN: 0198508026 (cit. on p. 37).
- [66] Ruslan Leontievich Stratonovich. “On the probability functional of diffusion processes”. In: *Selected Trans. in Math. Stat. Prob* 10 (1971), pp. 273–286 (cit. on p. 38).
- [67] G. E. Uhlenbeck and L. S. Ornstein. “On the Theory of the Brownian Motion”. In: *Phys. Rev.* 36 (5), pp. 823–841. DOI: 10.1103/PhysRev.36.823. URL: <https://link.aps.org/doi/10.1103/PhysRev.36.823> (cit. on pp. 40, 69, 102, 128).
- [68] Israel M Gel’fand and Akiva M Yaglom. “Integration in functional spaces and its applications in quantum physics”. In: *Journal of Mathematical Physics* 1.1 (1960), pp. 48–69 (cit. on p. 40).
- [69] L.C. Evans. *Partial Differential Equations*. Graduate studies in mathematics. American Mathematical Society, 2010. ISBN: 9780821849743. URL: https://books.google.co.uk/books?id=Xnu0o%5C_EJrCQC (cit. on p. 48).
- [70] H. C. Luckock and A. J. McKane. “Path integrals and non-Markov processes. III. Calculation of the escape-rate prefactor in the weak-noise limit”. In: *Phys. Rev. A* 42 (4 1990), pp. 1982–1996. DOI: 10.1103/PhysRevA.42.1982. URL: <https://link.aps.org/doi/10.1103/PhysRevA.42.1982> (cit. on p. 55).

- [71] A.N. Drozdov V.F. Baibuz V.Yu. Zitserman. “Diffusion in a potential field: Path-Integral approach”. In: *Physica A: Statistical Mechanics and its Applications* (1984), pp. 173–193 (cit. on pp. 56–58, 68, 84, 207).
- [72] Kyle Siegrist. *Probability, Mathematical Statistics, Stochastic Processes, chap: 8.2*. 2017 (cit. on p. 58).
- [73] Eric W Weisstein. ”Riemann Sum.” *From MathWorld—A Wolfram Web Resource*. URL: <http://mathworld.wolfram.com/RiemannSum.html> (visited on 01/18/2022) (cit. on p. 61).
- [74] Lipschutz Seymour and Marc Lipson. *Schaum’s Outline of Linear Algebra Fourth Edition (Schaum’s Outline Series)*. McGraw-Hill. ISBN: 007154352X (cit. on p. 61).
- [75] Mads R. So/rensen and Arthur F. Voter. “Temperature-accelerated dynamics for simulation of infrequent events”. In: *The Journal of Chemical Physics* 112.21 (2000), pp. 9599–9606. DOI: 10.1063/1.481576 (cit. on p. 63).
- [76] Arthur F. Voter. “Hyperdynamics: Accelerated Molecular Dynamics of Infrequent Events”. In: *Phys. Rev. Lett.* 78 (20 1997), pp. 3908–3911. DOI: 10.1103/PhysRevLett.78.3908. URL: <https://link.aps.org/doi/10.1103/PhysRevLett.78.3908> (cit. on p. 63).
- [77] *Diagonalizable matrix*. July 20, 2022. URL: https://en.wikipedia.org/wiki/Diagonalizable_matrix (visited on 07/20/2022) (cit. on p. 64).
- [78] Kane Yee. “Numerical solution of initial boundary value problems involving Maxwell’s equations in isotropic media”. In: *IEEE Transactions on antennas and propagation* 14.3 (1966), pp. 302–307 (cit. on p. 74).
- [79] B. Guo. *Spectral Methods and Their Applications*. World Scientific, 1998. ISBN: 9789810233334. URL: <https://books.google.co.uk/books?id=soaoQJMtcYMC> (cit. on p. 74).
- [80] I. S. Gradshteyn. *Tables of integrals, series and products*. eng. Fourth edition / prepared by Yu. V. Geronimus [and] M. Yu. Tseytlin. New York: Academic, 1965 (cit. on p. 86).

- [81] Kiyosi Itô. “109. stochastic integral”. In: *Proceedings of the Imperial Academy* 20.8 (1944), pp. 519–524 (cit. on p. 86).
- [82] “Conditional Markov processes and their application to the theory of optimal control”. In: (1968) (cit. on p. 86).
- [83] Bernt Oksendal. *Stochastic Differential Equations: An Introduction with Applications*. Universitext. Springer Berlin / Heidelberg, 2014. ISBN: 9783540047582 (cit. on p. 88).
- [84] Hannes Risken. *Fokker-planck equation*. Springer, 1996, pp. 63–95 (cit. on p. 110).
- [85] Jon. Mathews. *Mathematical methods of physics*. eng. New York: W.A. Benjamin, 1964 (cit. on pp. 110, 119).
- [86] Eric W. Weisstein. “Hermitian Operator.” *From MathWorld—A Wolfram Web Resource*. 2022. URL: <https://mathworld.wolfram.com/HermitianOperator.html> (visited on 11/29/2022) (cit. on pp. 111, 112).
- [87] *Quantum Mechanics Volume One*. Wiley and Sons, New York, 1977 (cit. on pp. 115–117).
- [88] P. A. M. (Paul Adrien Maurice) Dirac. *The principles of quantum mechanics*. Fourth edition (revised). International series of monographs on physics ; 27. Clarendon Press, 1981. ISBN: 0198520115 (cit. on p. 116).
- [89] *Mehler kernel*. July 20, 2022. URL: https://en.wikipedia.org/wiki/Mehler_kernel (visited on 07/20/2022) (cit. on pp. 118, 122).
- [90] V. (Venkataraman) Balakrishnan. *Elements of nonequilibrium statistical mechanics*. eng. New Delhi: Ane Books, 2008. ISBN: 9781420074192 (cit. on p. 118).
- [91] Eric W. Weisstein. *Hermite Polynomial – from Wolfram MathWorld*. 2022. URL: <https://mathworld.wolfram.com/HermitePolynomial.html> (visited on 07/20/2022) (cit. on pp. 119, 121).

- [92] Eric W. Weisstein. *Generalized Fourier Series from Wolfram Mathworld*. 2022. URL: <https://mathworld.wolfram.com/GeneralizedFourierSeries.html> (visited on 11/29/2022) (cit. on p. 122).
- [93] Carl M Bender, Steven Orszag, and Steven A Orszag. *Advanced mathematical methods for scientists and engineers I: Asymptotic methods and perturbation theory*. Vol. 1. Springer Science & Business Media, 1999 (cit. on pp. 123, 142).
- [94] Eric W. Weisstein. *Gaussian Integral – from Wolfram MathWorld*. 2022. URL: <https://mathworld.wolfram.com/GaussianIntegral.html> (visited on 07/20/2022) (cit. on pp. 135, 136).
- [95] “Laplace transform.” *Wikimedia Foundation*. Last modified October 22, 2022. 2022. URL: https://en.wikipedia.org/wiki/Laplace_transform (visited on 11/29/2022) (cit. on p. 139).
- [96] Royce KP Zia, Edward F Redish, and Susan R McKay. “Making sense of the Legendre transform”. In: *American Journal of Physics* 77.7 (2009), pp. 614–622 (cit. on p. 140).
- [97] G.A. Evans. “Numerical inversion of laplace transforms using contour methods”. In: *International Journal of Computer Mathematics* 49.1-2 (1993), pp. 93–105. DOI: 10.1080/00207169308804220 (cit. on p. 142).
- [98] Eric W. Weisstein. “Geometric Series.” *From MathWorld—A Wolfram Web Resource*. 2022. URL: <https://mathworld.wolfram.com/GeometricSeries.html> (visited on 11/29/2022) (cit. on p. 144).
- [99] D.J. Griffiths. *Introduction to Electrodynamics*. v. 2. Cambridge University Press, 2017. ISBN: 9781108420419 (cit. on p. 155).
- [100] Tucker McClure. *Numerical Inverse Laplace Transform*. 2023. URL: <https://www.mathworks.com/matlabcentral/fileexchange/39035-numerical-inverse-laplace-transform> (visited on 03/09/2023) (cit. on pp. 155, 169, 181).
- [101] *Fourier and Laplace transforms*. eng;dut. Cambridge: Cambridge University Press, 2003. ISBN: 0521534410 (cit. on p. 158).

- [102] Y.T. Chou, C.S. Pande, and R.A. Masumura. “The role of harmonic functions in dislocation–boundary interactions by the method of images”. In: *Materials Science and Engineering: A* 452-453 (2007), pp. 99–102. ISSN: 0921-5093. DOI: <https://doi.org/10.1016/j.msea.2006.10.103>. URL: <https://www.sciencedirect.com/science/article/pii/S0921509306022878> (cit. on p. 175).
- [103] Joseph Abate and Ward Whitt. “A unified framework for numerically inverting Laplace transforms”. In: *INFORMS Journal on Computing* 18.4 (2006), pp. 408–421 (cit. on p. 181).
- [104] G. M. Wysin. “Probability Current and Current Operators in Quantum Mechanics”. In: (2011) (cit. on p. 186).
- [105] *Engineering Statistics handbook*. 2022. URL: <https://www.itl.nist.gov/div898/handbook/eda/section3/eda362.htm> (visited on 12/20/2019) (cit. on p. 187).
- [106] M. C. K. Tweedie. “Statistical Properties of Inverse Gaussian Distributions. I”. In: *The Annals of Mathematical Statistics* 28.2 (1957), pp. 362–377. URL: <https://doi.org/10.1214/aoms/1177706964> (cit. on p. 202).
- [107] Lukas Kikuchi et al. “Ritz method for transition paths and quasipotentials of rare diffusive events”. In: *Phys. Rev. Research* 2.3 (2020), p. 033208 (cit. on p. 207).
- [108] Jing Cao et al. “Large deviations of Rouse polymer chain: First passage problem”. In: *The Journal of Chemical Physics* 143.20 (2015), p. 204105. DOI: 10.1063/1.4936130 (cit. on p. 209).
- [109] Alyssa Travitz and Ronald G. Larson. “Brownian Dynamics Simulations of Telechelic Polymers Transitioning between Hydrophobic Surfaces”. In: *Macromolecules* 54.18 (2021), pp. 8612–8621. DOI: 10.1021/acs.macromol.1c01540 (cit. on p. 209).